INFORMATION TO USERS

This manuscript has been reproduced from the microfilm master. UMI films the text directly from the original or copy submitted. Thus, some thesis and dissertation copies are in typewriter face, while others may be from any type of computer printer.

The quality of this reproduction is dependent upon the quality of the copy submitted. Broken or indistinct print, colored or poor quality illustrations and photographs, print bleedthrough, substandard margins, and improper alignment can adversely affect reproduction.

In the unlikely event that the author did not send UMI a complete manuscript and there are missing pages, these will be noted. Also, if unauthorized copyright material had to be removed, a note will indicate the deletion.

Oversize materials (e.g., maps, drawings, charts) are reproduced by sectioning the original, beginning at the upper left-hand corner and continuing from left to right in equal sections with small overlaps. Each original is also photographed in one exposure and is included in reduced form at the back of the book.

Photographs included in the original manuscript have been reproduced xerographically in this copy. Higher quality 6" x 9" black and white photographic prints are available for any photographs or illustrations appearing in this copy for an additional charge. Contact UMI directly to order.

UMI

A Bell & Howell Information Company
300 North Zeeb Road, Ann Arbor MI 48106-1346 USA
313/761-4700 800/521-0600

SYNTHESIS OF BIOLOGICALLY ACTIVE MOLECULES: NOVEL ANTIFUNGALS AND RETINAL ANALOGS.

by

LANGU PENG

A dissertation submitted to the Graduate Faculty in Chemistry in partial fulfillment of the requirements for the degree of Doctor of Philosophy, The City University of New York.

1998

This manuscript has been read and accepted by the Graduate Faculty in Chemistry in satisfaction of the dissertation requirement for the degree of Doctor of Philosophy.

September 16, 1998
Date

Chair of Examining Committee

Sept 17, 1998
Date

Executive Officer

Dr. Valeria Balogh-Nair

Dr. John R. Lombardi

Dr. Maria Tomasz

Dr. Xiangning Chen

Supervisory Committee

THE CITY UNIVERSITY OF NEW YORK

ABSTRACT

SYNTHESIS OF BIOLOGICALLY ACTIVE MOLECULES: NOVEL ANTIFUNGALS AND RETINAL ANALOGS.

by

LANGU PENG

Advisor: Professor Valeria Balogh-Nair

PART I.

Syntheses of spacer-armed retinal analogs were undertaken to serve as tools to investigate the tertiary structures of retinal proteins, and to serve as models in the design of biopolymer based devices. A common key intermediate was prepared in a multi-step synthesis. Derivatizations of this intermediate afforded three analogs with functionalized spacer-arms attached to a seco-ring. The first analog contains an 11-carbon spacer-arm. In the second analog, the spacer is of twelve carbon length and contains a polar carboxyl terminus. In the third analog, designed to generate orderly arrays of bacteriorhodopsin on gold, a disulfide bond joins two spacer-armed retinyl moieties.

PART II.

Syntheses of oxaziridines, metallomacrocycles and nitronyl nitroxides were undertaken to demonstrate the antifungal potential

of these novel pharmacophores. Three bisoxaziridines, the first example of a trisoxaziridine, a macrobicyclic hexaoxaziridine, a Ni(II)-macrocyclic amide complex, and a dendrimer-based tris(nitronyl nitroxide) were synthesized efficiently. The antifungal activity of the compounds synthesized was evaluated in collaborative studies. These studies established that at least three oxaziridine units per molecule are necessary to achieve high levels of antifungal activity, and they demonstrated the usefulness of metallomacrocycles as antifungals. The tris(nitronylnitroxide) had antifungal activity against *P. carinii* equivalent to that of the current drug, thereby strongly supporting the oxidoredox pharmacophore hypothesis.

Dedicated to my parents and my wife

Acknowledgment

I would like to express my thanks to Professor Valeria Balogh-Nair for her guidance, inspiration and encouragement.

I would like to thank Professor Marilyn S. Bartlett, Indiana University Medical School for the evaluation of the compounds in antifungal assays, and Dr. Cunxiang Chen for his generous help with my research work.

Finally, I would like to thank my parents for their constant support and encouragement. During all of these years my wife always stood by me, no matter how hard life was. This dissertation is dedicated to her.

Table of contents

List of figures:

PART II. SYNTHESIS OF ANTIFUNGALS CONTAINING NOVEL PHARMACOPHORES.

List of figure and table:

Part I. SYNTHESIS OF THE SPACER-ARMED RETINALS.

1. INTRODUCTION

Halobacterium salinarium, a member of Archaebacteria, thrives in highly saline environments and produces purple patches in its cell membrane under intense illumination in anaerobic conditions. Bacteriorhodopsin (bR), the sole protein component of these membrane patches,[1] was isolated from lysed cells of *H. salinarium* by sucrose density gradient centrifugation.[2] The purple membrane, which consist of 75% bR and 25% phospholipids, provides an alternate source of energy to the bacterium by converting the light energy absorbed by bR to a proton gradient accross the cell membrane that in turn drives ATP synthesis and other cellular processes.[3] The protein-bound retinal chromophore in bR is responsible for the purple color of the membrane. Light absorption by the chromophore triggers the photocycling of bR. During the photocycle, which contains several spectroscopically distinct intermediates, the structure of the protein-bound chromophore and the tertiary structure of the protein change in concert to facilitate proton translocation.

The elucidation of bR's tertiary structure is of great challenge and is of widespread interest because bR, a small (ca. 26,000 D) integral membrane protein, has photochemistry resembling that of more complex sensory rhodopsins found in animals. Further, because

bR is the simplest member of an extended family of seven-helix trans-membrane proteins, elucidating its tertiary structure is of fundamental importance to our understanding of biological structure and function. Moreover, owing to its long-term stability to thermal and photochemical degradation, high efficiency as an energy converter, and its relatively simple structure in which the seven membrane-spanning helices are organized in a rigid two-dimensional hexagonal protein array, bR is of great interest in the construction of biopolymer-based photosensors[4] and artificial receptors,[5] optoelectronic devices, and molecular devices such as spatial light modulators, light switches, and holographic storage media.[6,7]

Prominent among the approaches employed to gain information on the tertiary structure of bR are diffraction studies, site-directed mutagenesis experiments, and studies employing synthetic bR analogs.[8] Synthetic retinal analogs can be combined with the apoprotein to yield artificial bRs, and studies of these bR analogs can serve as useful pointers towards elucidation of the tertiary structure. Synthetic bR analogs can also be endowed with properties to enhance their usefulness in bR-based biomaterials. The objective of the present study was to synthesize retinal analogs based on the spacer-arm concept.[9] The spacer arm-derivatized retinals are uniquely suited to investigate the tertiary structure of bR.[10-12] Thus, when the spacer-arm of the retinal is fluorescent-, spin-, or photoaffinity label-derivatized, the retinal analogs can be employed to probe the tertiary structure of bR at sites removed from the immediate vicinity of the natural retinal's binding site. Analogs in which the spacer-

arm's terminus is derivatized with thiols have the potential to generate highly ordered structures of bR on gold, suitable for diffraction studies.

1.1. Bacteriorhodopsin in the purple membrane.

Bacteriorhodopsin consists of a two-dimensional hexagonal crystal lattice of bR-trimers in a lipid bilayer, that has a thickness of about 5 nm and an average diameter of 500 nm. Seminal electron diffraction studies by Henderson and Unwin[13] at 7Å resolution revealed that each bacteriorhodopsin molecule consists of seven transmembrane α-helical segments oriented nearly perpendicular to the plane of the membrane.

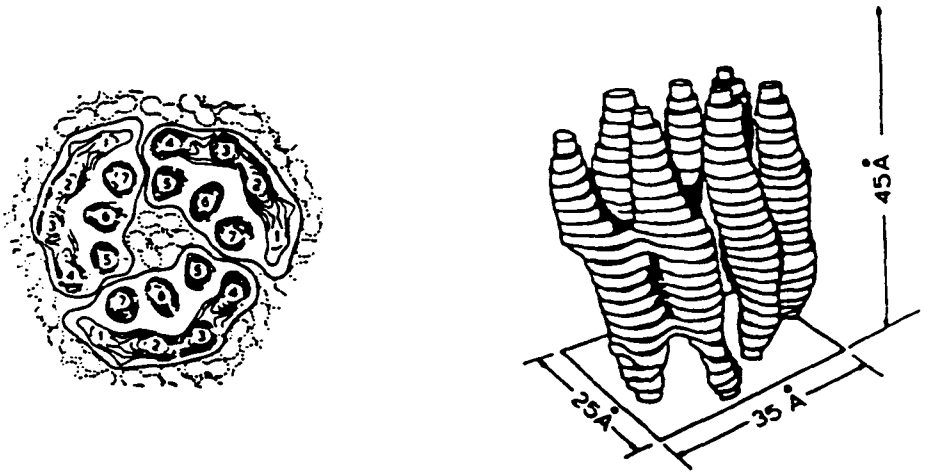

Figure 1. Structure of the purple membrane from *H. salinarium*.[13]

When the primary sequence of the polypeptide chain of 248 amino acids in bR was established by both amino acid[14-15] and DNA sequencing,[16] models were proposed to determine the amino acid segments which form the seven α-helices based on their accessibility

to proteolytic cleavage, and hydrophobicity/hydrophilicity considerations. In all the models the hydrophobic sides of the α-helices face the nonpolar lipids whereas the hydrophilic moieties are oriented towards the interior of the molecule and the protein is oriented in the membrane with its C-terminus facing the cytoplasmic side and the N-terminus at the exterior of the cell membrane. Later studies aimed at the assignment of amino acid sequences to α-helical segments based on data from neutron diffraction[17a-e] and crosslinking using *m*-diazirinophenylretinal[18] led Khorana to propose a different model for the secondary structure.

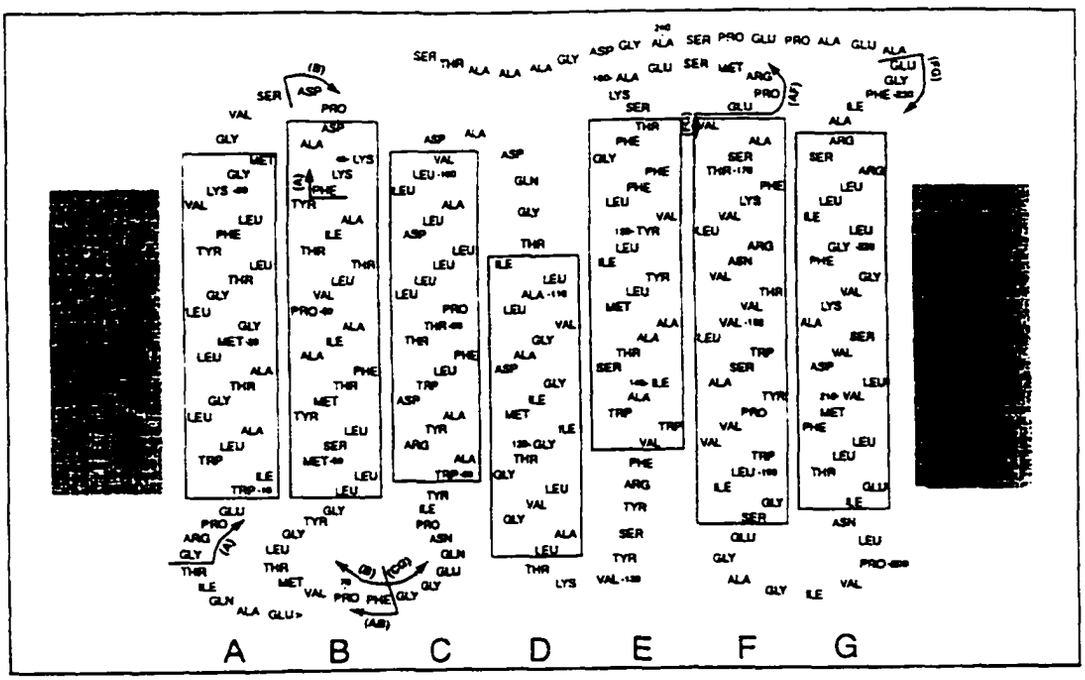

Figure 2. The sequence of bR, showing the secondary structure.[19] The boxed-in regions are helical, the shaded areas show the approximate location of the hydrophobic region of the membrane.

However, more recent protein folding studies by Khan and Engelman[19] demonstrated that the secondary structure (Figure 2)

arises from the side-to-side association of independently stable helices, yielding a model for bR. This is also in agreement with the data from Henderson's electron cryo-microscopic studies[20] that yielded a three-dimensional electron-density map for bR with 3.5 Å resolution parallel and 10 Å resolution perpendicular to the plane of the membrane.

1.2. Chromophore structure in bacteriorhodopsin.

The light absorbing entity, the all-*trans* retinal chromophore in bR, is attached to the ε-amino group of Lysine-216[21a-c] on helix G of the protein, bacterio-opsin, through a protonated Schiff base linkage.[22] Illuminated purple membrane contains light-adapted bacteriorhodopsin (bR^{LA}) that undergoes a photocycle, during which protons are translocated from the inside to the outside of the cell. In the absence of light, bR exists in a dark adapted state (bR^{DA}) that does not translocate protons.

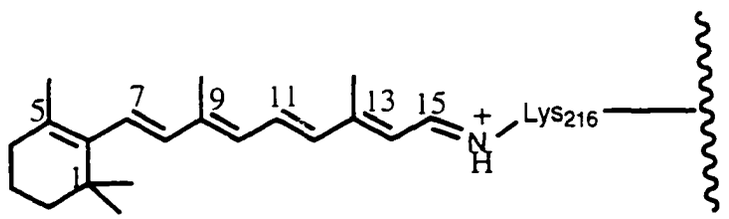

bR^{LA}_{568}

The bR^{LA} has a long wavelength absorption maximum at 568 nm and contains an all-*trans* retinal Schiff base, whereas bR^{DA} has λ_{max} at 558 nm and is an equilibrium mixture of two proteins, one

containing an all-*trans*, the other the 13-*cis* isomer. The isomeric nature of the retinal in bR^{LA} as being all-*trans* has never been questioned, but bR^{DA} was reported by several authors to contain roughly equal amounts of the all-*trans* and 13-*cis* retinal Schiff bases. However, a carefully controlled extraction technique combined with quantitation employing high performance liquid chromatography demonstrated a 13-*cis* to all-*trans* isomeric ratio of 2:1.[23] The role this isomeric ratio plays in dark-adapted purple membrane is not yet understood, but it is believed that different conformational states of the protein may be involved.

The exact nature of the Schiff base linkage in bR has been controversial for over two decades. The strongest evidence for a protonated Schiff base linkage was derived from Resonance Raman experiments,[24] later confirmed by FTIR[25a-b] measurements as well as by studies which employed synthetic retinal analogs.[26] The proposal by Sandorfy,[27] based on IR and UV studies of model protonated Schiff bases of retinal in organic solvents of varying polarity, that the Schiff base is not only protonated, but is also weakly hydrogen bonded, was confirmed by solid state NMR measurements on a ε-^{15}N-labeled bR analog.[28] The presence of water molecules acting as bridge between charged and hydrogen bonded groups at the Schiff base site has also been proposed.[29] Employing [14-^{13}C]-retinal labeled bR in solid state nmr studies, Harbison *et al.*[30] determined that dark-adapted bR contains the all-*trans*, 15-*anti* and the 13-*cis*, 15-*syn* isomers of the retinal Schiff base, whereas the functional,

light-adapted form, contains only the all-*trans*, 15-*anti* isomer. Moreover, solid state magic angle spinning nmr studies on a [5-^{13}C]-labeled bR analog indicated that the conformation of the retinal in bR is 6-s-*trans*.[31-32] The validity of the proposed 6-s-*trans* form in bR was confirmed unequivocally by measurements on a double ^{13}C-labeled [8,18-$^{13}C_2$]retinal-bR, using a novel rotationally resonant magnetization exchange technique,[33] suitable to measure internuclear distances between like spins in solids. The early linear dichroism studies by Heyn *et al.*,[34] indicating that the long axis of the retinal is tilted ~20° from the membrane plane towards the external surface of the membrane has now been confirmed by neutron diffraction studies,[35] diffusion enhanced energy transfer measurements[36] and second-harmonic interference experiments.[37]

Based on the data summarized above, Figure 3 shows the general structure of the binding pocket of the retinal chromophore in light-adapted bR.[38] The Schiff base group of the chromophore separates the cytoplasmic and extracellular proton pathways. The ionone ring end of the retinal is tilted toward the extracellular side and the vector from the Schiff base nitrogen to its proton is also oriented towards the cell exterior.

The UV/VIS and biphasic CD spectra of bR is strongly red-shifted compared to that of the retinal chromophore. Association of three bR molecules in clusters close enough for their retinal transition dipole moments to interact among each other could explain

the exciton splitting seen in the CD spectrum,[39] but it could not account for the significant red-shift of the absorption maximum.

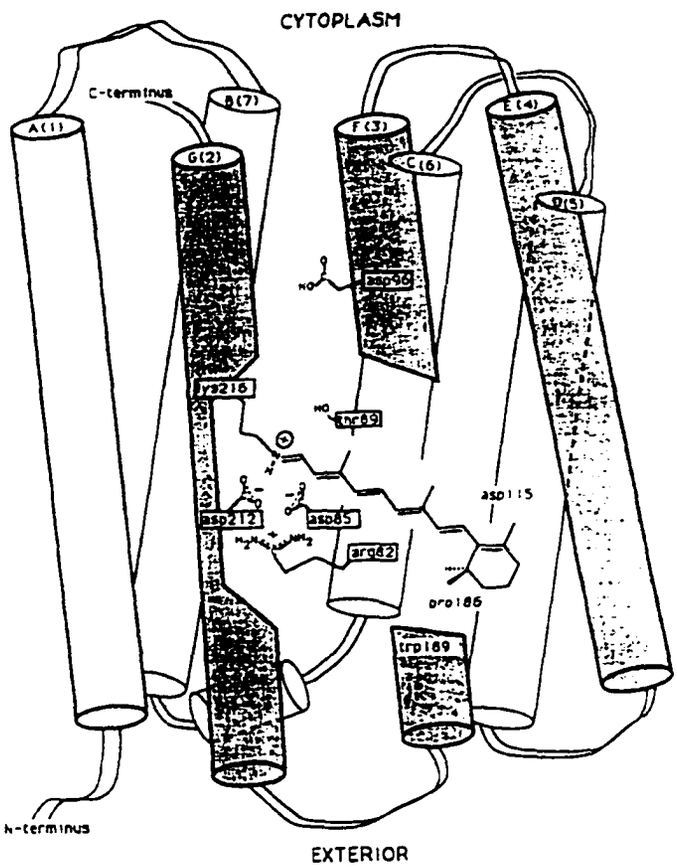

Figure 3. The Schiff base site, retinal geometry and orientation of the retinal chromophore in bR^{LA}. Key residues Asp-85, Asp-96, Asp-212, Lys-216 and Arg-82, Tyr-81, Tyr-182, , Tyr-185, Tyr-189 and Pro-186, that form the binding pocket and/or participate in proton transport are boxed.[38]

Protonation of the retinal Schiff base alone also could not account for the magnitude of the observed red-shift. Therefore, highly specific

interactions of the protonated Schiff base with the protein segments at the vicinity of the binding site were held responsible for providing a microenvironment conducive to these shifts. The red-shift, i.e., the difference in the absorption maxima of the protonated Schiff base compared to the rhodopsin, expressed in cm^{-1}, has been defined as the opsin shift, amounting to 5,100 cm^{-1} in bR.[40] To account for this large value, the first "point-charge model" was proposed, based on the study of the absorption spectra of a homologous series of dihydrorhodopsins and their respective protonated Schiff bases.[41] This point charge model has since been revised (Figure 4) to include the effect of a protein dipole at the ring binding site[42-43] as well as the effect of the weak hydrogen bonding of the Schiff base's counterion. The revised model also takes into account the contribution of the 6-s-*trans* conformation[44] of the retinal.

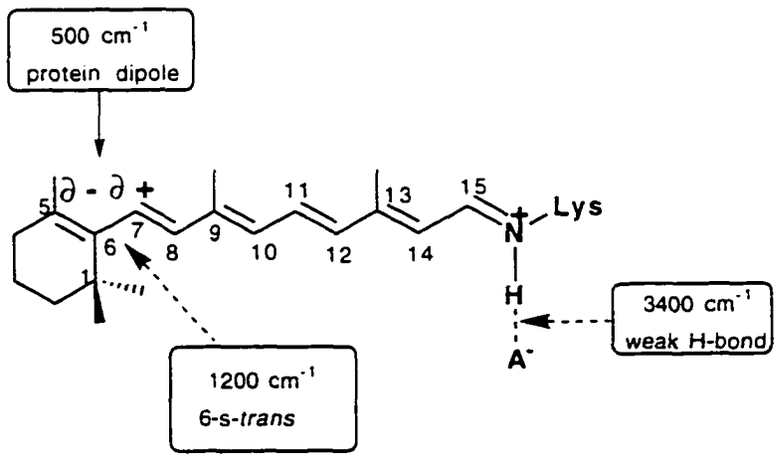

Figure 4. The 5,100 cm^{-1} opsin shift in bR^{LA}, showing the most important contributions: the hydrogen-bonding interaction at the Schiff base site and the 6-s-*trans* conformation at the ring binding site.[44]

1.3. The bacteriorhodopsin photocycle.

Only the light-adapted form of bacteriorhodopsin, bR^{LA}, pumps protons across the cell membrane. Upon photon absorption, retinal isomerizes around the C13-C14 bond then thermally reverts to the initial all-*trans* state, thereby passing a series of intermediates termed K_{590}, L_{550}, M_{410}, N_{550} and O_{640} (Figure 5).[45]

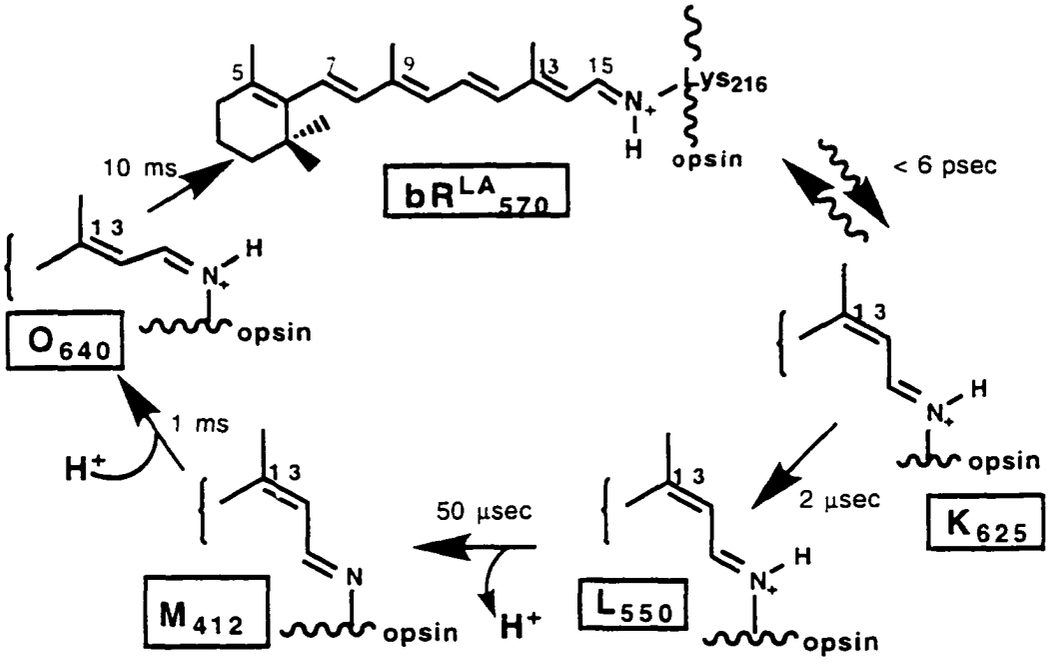

Figure 5. The photocycle of bR. The absorption maxima of the intermediates are indicated by subscripts, the bonds undergoing isomerization/conformational changes and the proton uptake/release are shown by the partial structures and curved arrows respectively.

There is general consensus that the photoproduct, K_{590}, formed in the so called primary event, involves the change of all-*trans*, 6-s-*trans*, C=N *anti* chromophore to a 13-*cis*, 6-s-*trans*, C=N *anti* form with concomitant movement of the Schiff base away from its Asp-212 counterion in bR towards Asp-85 which can accept the proton from the Schiff base in the L_{550} to M_{412} step. However, more complex,

branched and parallel photocycles have also been proposed as well as additional intermediates, multiple forms of bR, and multiple forms of intermediates L, M, and O. A further simplification in Figure 5 is that the transient species formed prior to K_{590}, i.e., the excited state of bR (lifetime *ca.* 500 fs) and intermediate J_{625} (a groundstate species, but which is stable only at liquid helium temperatures) are not shown.

The photocycle is tightly coupled to proton transport. During the L-M transition step, Asp-85 is protonated by the Schiff base,[46] and a proton is released to the extracellular membrane surface,[47] followed by reprotonation of the Schiff base from Asp-96 (M-N step),[48] and subsequent proton uptake from the cytoplasm/reprotonation of Asp-96 (during the N-O step at physiological pH).[49] There is a consensus that at least 11.6 Kcal/mol of the absorbed quantum's energy is stored in the primary step. However, from the chemical point of view, much remains to be done since the isomeric nature of the retinal is fully ascertained only in the cases of bR and M_{412} intermediate. Thus, even the very nature of the primary photoisomerization reaction in the photocycle has been reinvestigated recently using molecular dynamics simulations.[50,51] Water molecules also appear to play a crucial role in the proton pump cycle, thus dehydration of the membranes slows down the decay of the M_{412} intermediate,[52] and water molecules are apparently necessary for the reprotonation of the retinal Schiff

base[53] from Asp-96. However, even the best 3D structure model of bR presently available[20] does not permit assigning the location of water molecules within the tertiary structure.

1.4. "Classical" and spacer-armed bacteriorhodopsin analogs.

1.4.1. The "classical" analogs of bR.

Studies employing synthetic analogs of the retinal chromophore were useful not only to explain the purple color of the membrane by the external point charge model, but the hundreds of analogs prepared, mainly during the past two decades helped to elucidate many structural and functional aspects of BR.[8] For instance, photoaffinity label bearing retinal analogs synthesized with radiolabel[10,18,54-57] permitted identification of specific amino acid residues likely to be present in the retinal's binding domain on the opsin. However, these labeling experiments were not without difficulties. Thus, the earliest photoaffinity labeling studies of bR employed a *m*-diazirinophenyl analog of retinal tritiated at the aldehyde carbon.[18] The crosslinking experiments indicated Ser-193 and Glu-194 to be the predominant sites of crosslinking, and the model derived for bR based on these studies had the retinal chromophore inclined towards helix 6 and oriented towards the external surface of the membrane. These results had to be revised later, mainly because the bR analog could only be obtained in low yield (10%), and it was likely that the analog did not occupy the natural binding site.

Recently, synthetic retinals were also employed not for structural studies of BR, but to improve the properties of BR to make it more useful in molecular electronics applications. On June 25, 1992 the space shuttle flight Columbia carried on board a "smart" protein, bR, to test the viability of bR in a new optical three-dimensional computer memory device. According to Dr. Robert R. Birge, Director of Syracuse University Center for Molecular Electronics: *"The three-dimensional memory operates by using two laser beams to activate a tiny irradiated volume inside a transparent rectangular solid that contains the protein. Because the size of this irradiated volume is only 30 cubic millionth of a meter -one thousandth the size of a grain of sand- a small rectangular solid can store an enormous amount of information. For example, a rectangular solid with a volume of only 5 cubic centimeters can store 18 billion bytes of information - the content of some 4,000 college textbooks - including error correcting bits.* --- Birge explains that *"the protein generates an electrical signal upon its absorption of light from the lasers, and that this signal is used to assign the state of individual bits of information within the optical memory--- The key issue in converting the marsh-grown protein to a commercially viable substance for use in computers, is the preparation of volumes of protein samples with a high degree of homogeneity in terms of light absorbance as well as a good orientation of the protein within the transparent rectangular solid."* The intrinsic properties of native bR which make it an ideal candidate in molecular electronic applications are: 1) Long-term stability to thermal and photochemical degradation 2) Picosecond photochemical reaction times 3) High forward and reverse quantum yields that permit the

use of low light levels for switching 4) Wavelenght-independent quantum yields 5) A large shift in the absorption spectrum accompanying photochemistry that permits accurate and reproducible assignment of state 6) High two-photon cross sections that permit activation in the IR and higher storage densities in digital optical memory applications 7) High second order hyperpolarizabilities that open up nonlinear optical applications and 8) The ability to form thin films of bR with excellent optical properties by using the Langmuir-Blodgett or polymer matrix spin coating techniques. Each of these properties of bR can be further modulated by using bR analogs reconstituted from synthetic retinals and the apoprotein bacterio-opsin.

1.4.2. The spacer-armed analogs of bR.

The concept of using spacer-armed retinal analogs to investigate the tertiary structures of membrane proteins was proposed in 1987.[9] The domain of the tertiary structure that can be elucidated with the help of spacer-armed retinal analogs is both spatially and conceptually different from the one investigated employing the " classical analogs". In the latter case, the domain of interest is relevant mainly to the photochemical event (that yields photocycle intermediate K_{590}), since the structure of this domain is geared towards optimization of the selective and efficient light absorption by the retinal chromophore. In the former, another domain of the tertiary structure, spatially removed from the first, is involved. Thus, the spacer-arms are attached to a seco-ring to permit conformational mobility, but the 1,1'- and 5-methyl groups are

preserved in the probes' structure to assure the recognition of the chromophore by the binding site (Figure 6.)

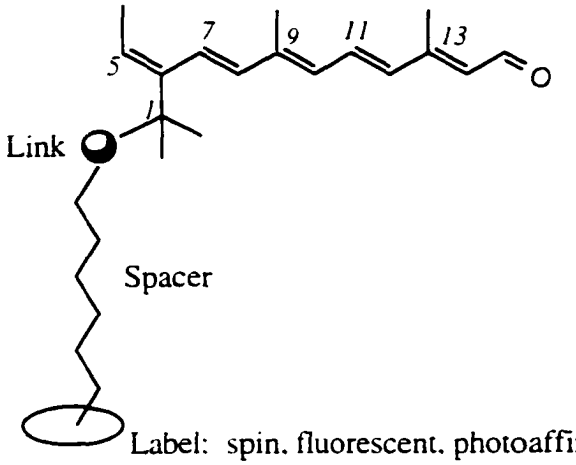

Figure 6. Schematic representation of the spacer-arm concept.[9]

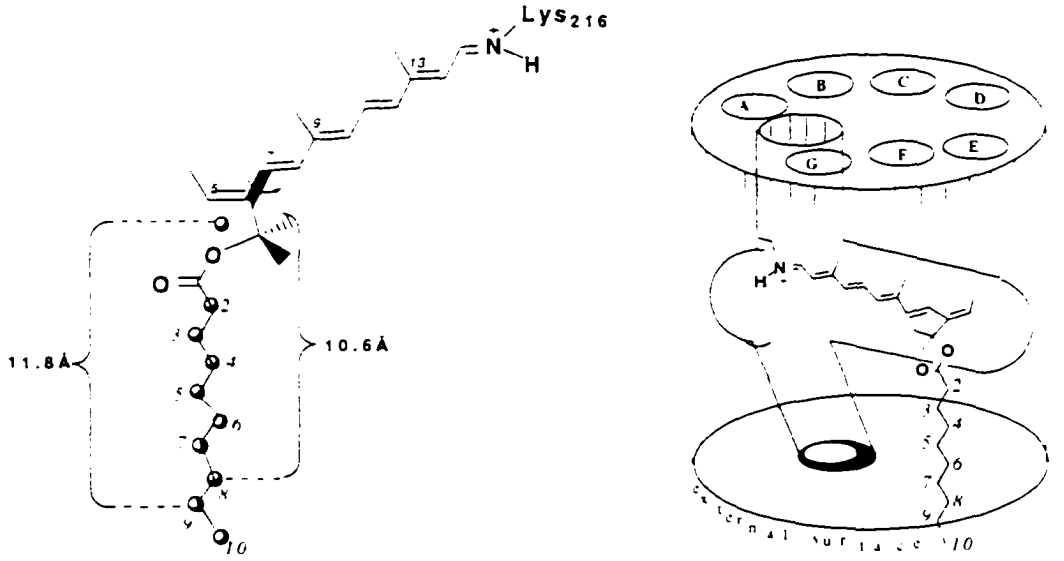

Figure 7. Alkyl-spacer-armed retinals as molecular rulers.[12]

Synthesis and binding studies with a series of alkyl spacer-armed retinals[12] revealed a channel-like space, extending from the retinal's ring towards the membrane surface between the seven helices, where spacer-arms can be inserted into bacteriorhodopsin. Figure 7 illustrates the use of spacer-arms as molecular rulers;[12] the Schiff

base site is on helix G, and the four helices C, D, E, and F surround the spacer-arm. Taking into account the known orientation of the retinal's transition moment in the membrane, the binding of up to nine carbon length spacers, but not of the ten carbon ones, indicated that the retinal's ring is oriented towards the external surface of the membrane. The retinal's ring appears to be situated less than 12 Å distance from the membrane surface. A precise value, assuming an extended conformation of the alkyl chain, is between 10.6-11.8 Å, corresponding to the perfectly binding 8-carbon and fine-structure yielding 9-carbon spacer lengths. This data is excellent agreement with the distance obtained both from neutron diffraction and energy transfer experiments.

1.4.3 Spacer-armed retinals to immobilize bR on gold.

Following the work of Nuzzo and Allara in 1983,[58] showing that dialkyldisulfides form oriented monolayers on gold surfaces, the phenomena of molecular self-assembly, in which thio compounds (Figure 8) adsorb spontaneously onto metallic surfaces to form self-assembled monolayers (SAMs), has been an area of intense research for molecular immobilization.[59-61] SAMs are formed spontaneously

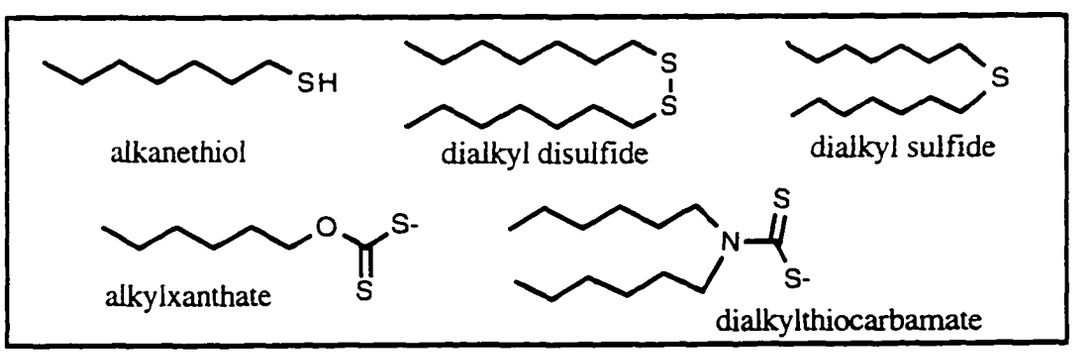

Figure 8. Surface-active organosulfur compounds.

by immersion of an ultraflat gold surface, Au (111), epitaxially grown on mica, into a dilute solution of a thio compound in an appropriate solvent (Figure 9).

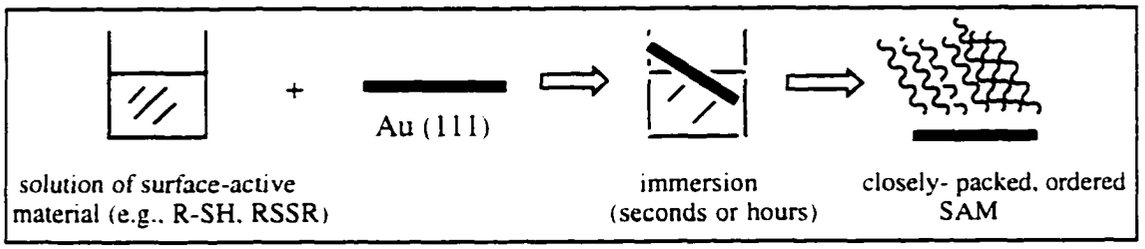

Figure 9. Formation of self-assembled monolayers (SAMs).[59-61]

Through variation of the thio compounds' terminal group, the surface properties exhibited by the SAM may be modified to obtain various properties, such as hydrophobicity/hydrophilicity, or acidity/basicity. Further, functionalities may be introduced that allows the SAM to be coupled to a range of biomolecules, e.g., proteins, thereby immobilizing them.[62] Even mammalian cells can be adhered to surfaces using SAMs of alkanethiolates on gold.[63] Therefore, it should be possible to form SAMs from a protein such as bR, site-specifically functionalized with a thiol or disulfide group at the spacer-arm's terminus. The highly ordered, rigid bR assemblies obtained should display unique properties enabling studies of the tertiary structure using a variety of sophisticated diffraction and microscopic imaging techniques. Moreover, if successful, these studies employing the thiolated spacer-armed retinal analogs can be extended to the investigation of the tertiary structures of other retinal proteins. Prime candidates for these studies will be the visual rhodopsins embedded in highly fluid natural membranes, precluding

investigation of their tertiary structures by diffraction techniques. Another benefit of the bR-based SAMs might be their potential use as novel materials in a variety of applications, such as biosensor and optical memory devices and nanoscale electronics.

2. RESULTS AND DISCUSSION

2.1 Structural design of spacer-armed retinal analogs.

Prior to our studies with spacer-armed retinals, all of the synthetic retinal analogs employed in conjunction with bR studies contained modifications only of the retinal's ring and/or side chain in the immediate proximity of the retinal's binding site. Based on the hypothesis that the interhelical spaces in bR may be able to accommodate various chemical structures, a conceptually novel family of retinal analogs, called spacer-armed probes, were designed to test this hypothesis (Figure 10a).[9]

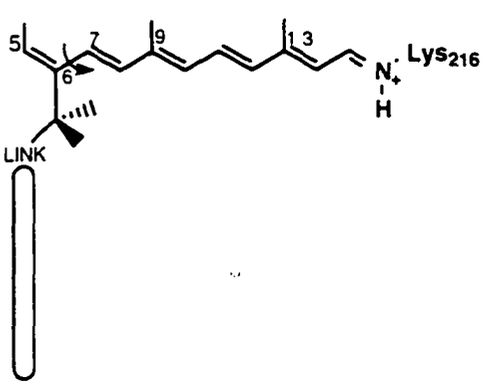

Figure 10a.

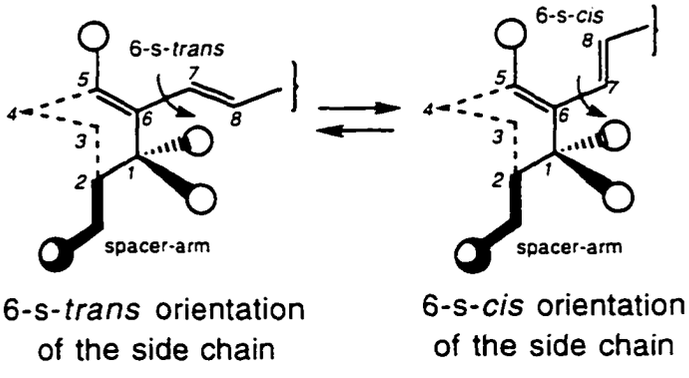

Figure 10b.

The spacer-armed probes consist of three structurally distinct parts: The polyene side chain from carbons 7-15, the truncated, seco-ring that replaces the natural cyclohexenylidene ring of the

retinal, and the spacer-arm. The full polyene side chain of the retinal is preserved in the spacer-armed probes so as to assure binding to the protein that results in bR analogs with absorption maxima close to the native bR, at *ca.* 570 nm. The cyclohexenylidene ring of the natural retinal is not preserved in the spacer-armed probes, in which a truncated, seco-ring, is employed instead. The importance of the seco-ring in the design of the spacer-armed probes needs to be further emphasized. The enhanced rotational freedom of the seco-ring, as compared to the rigid cyclohexene ring, allows the spacer-armed retinal to assume a 6-s-*trans* conformation on binding, without affecting the orientation of the spacer-arm towards the external surface (Figure 10b). In contrast, spacer-arms attached to an intact cyclohexene ring cannot assume conformations for binding in a natural (6-s-*trans*) orientation. The nature of the link (Scheme 10a), that attaches the spacer-arm to the seco-ring of the retinal in the probes, must be a functionality that will not interfere with efficient binding of the spacer-armed probe. In addition, it must be stable, and its precursor should be facile to derivatize allowing the introduction of a variety of spacer-arms differing in chemical structure. A hydroxyl group, that by derivatization allows introduction of the spacer-arms, via formation of ester linkages, was employed in the syntheses leading to the target compounds.

The length and structure of the spacer-arm is another critical factor to assure efficient reconstitution of a bR analog from the probe and bacterio-opsin. Thus, our previous studies[10-12] have shown that retinals with alkyl spacer-arms of up to 12Å length could be introduced into the interhelical spaces of bR, but longer alkyl spacer-arms precluded formation of bR analogs. When spacer-arms

containing rigid conjugated double bonds or aromatic rings were employed (Figure 11), only the retinal shown in 11C, in which the phenyl ring is attached with a flexible one carbon spacer, formed a bR analog. This indicated that any structure designed to fit the interhelical spaces must have flexibility, i.e., bond(s) that allow free rotation in the proximity (ca. 3.5 Å distance) of the ring binding site. We believe that at such distance from the retinal's ring binding site, the interhelical channel is narrower or more discriminating towards electron rich moieties. In the case of retinal shown in 11B, the spacer-arm extends too far with the aromatic ring clashing into the α-helical segments of the protein which surround the interhelical spaces. In the case of retinal shown in Figure 11A, which has two conjugated double bonds preventing free rotation of the spacer, minute adjustments to the interhelical space are not possible, hence a situation similar to that observed with retinal shown in Figure 11B arises.

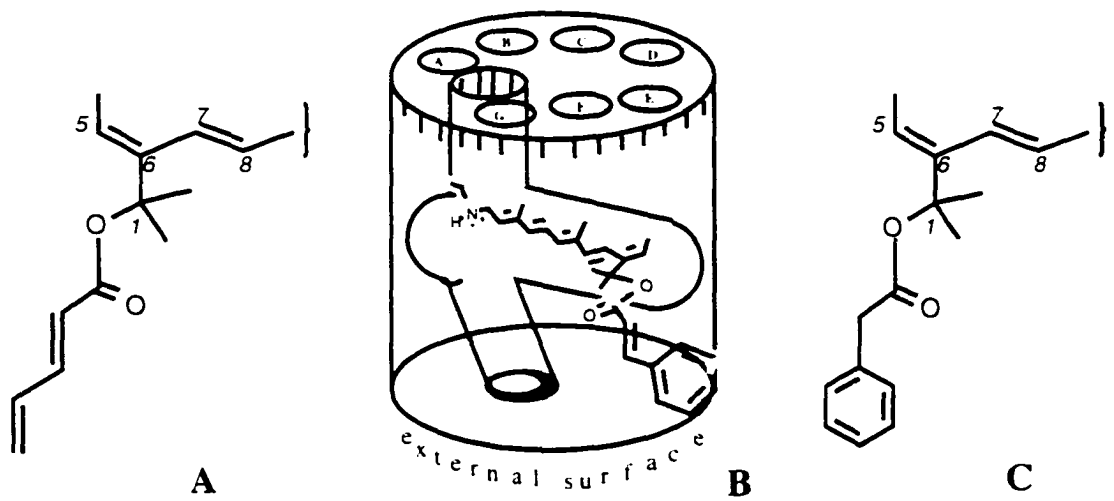

Figure 11. Retinal analogs with electron-rich spacer-arms.

Therefore, it appears that flexibility of the spacer-arm at a distance of ca. 3.5 Å (as in case of 11A) and less than 6 Å (as in case of 11B)

from the retinal's ring binding site is crucial for generating bR analogs, and structures designed to fit the interhelical spaces must satisfy this requirement. In agreement with the electron diffraction studies, this suggests that Trp-185, may be situated at *ca.* 5-6Å distance below the retinal's ring. The presence of this tryptophan's aromatic side chain would narrow the interhelical space, and would also hinder the binding of electron-rich moieties at 3.5Å - 6Å distance below the retinal's ring.

Considering the properties of the interhelical spaces, together with the goals set forth, namely to elicit information on bR's tertiary structure and to generate bR-based novel materials, a set of three spacer-armed retinals were designed and synthesized as described vide infra.

2.2. Synthesis of spacer-armed retinal analogs.

The rational for the synthesis of retinal analogs **11-13** is as follows: Retinal **11** with the eleven carbon length alkyl spacer-arm has been synthesized previously.[64] This compound would be of interest because its spacer-arm, if fully extended, should reach beyond the α-helical domain formed by helices C, D, E, and F. However, the first synthesis of **11** yielded submilligram amounts of the material, adequate only for characterization of the compound and for preliminary binding studies with opsin. Because of the paucity of the material available these binding studies were not conclusive; the analog had to be synthesized again, more efficiently, to obtain adequate amounts for in depth biochemical/biophysical studies.

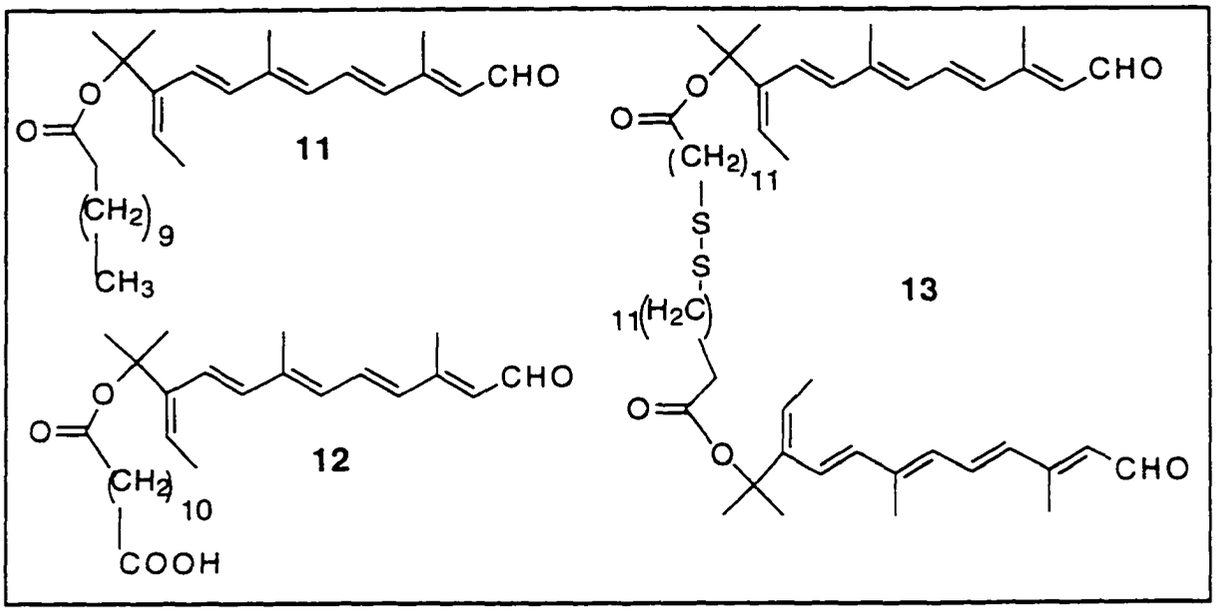

Analogs **12** and **13** are novel compounds. Analog **12**, in which the spacer arms have a polar terminus, will be employed, subsequent to further functionalization, for the investigation of bR's tertiary structure. Retinal analog **13** in which a disulfide bond joins two spacer-armed retinyl moieties, will serve not only in studies geared towards elucidation of the tertiary structure, it will also be employed to obtain bR-based SAMs useful in materials science applications, as described in section 1.4.1.

2.2.1. Synthesis of the common key intermediate.

The synthetic strategy we developed provides the opportunity to generate structurally diverse series of retinal analogs using the same intermediate, compound **10**. Thus, all three target compounds,

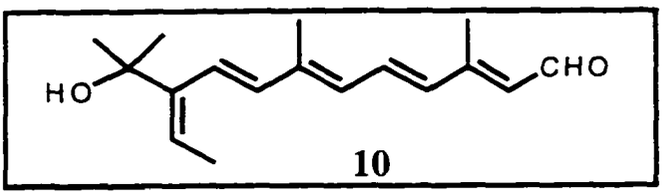

10

11-13, were derived from a single precursor **10**, by straightforward derivatizations with the appropriate spacer-arms.

The most desirable starting material for the synthesis of the key intermediate **10** is Heathcock's ketone **4**.[65] a prototype member of a series of α–trimethylsilyloxy ketones that are useful for stereoselective aldol addition reactions. Compound **4** can be prepared in four steps according to Scheme 1. Thus, addition of acetone to protected propionaldehyde cyanohydrin followed by hydrolysis and base-induced dehydrocyanation converted the diastereomeric nitriles to the hydroxyketone **3**. The tertiary hydroxyl group was then protected as trimethylsilyl ether to allow elaboration of the polyene side chain.

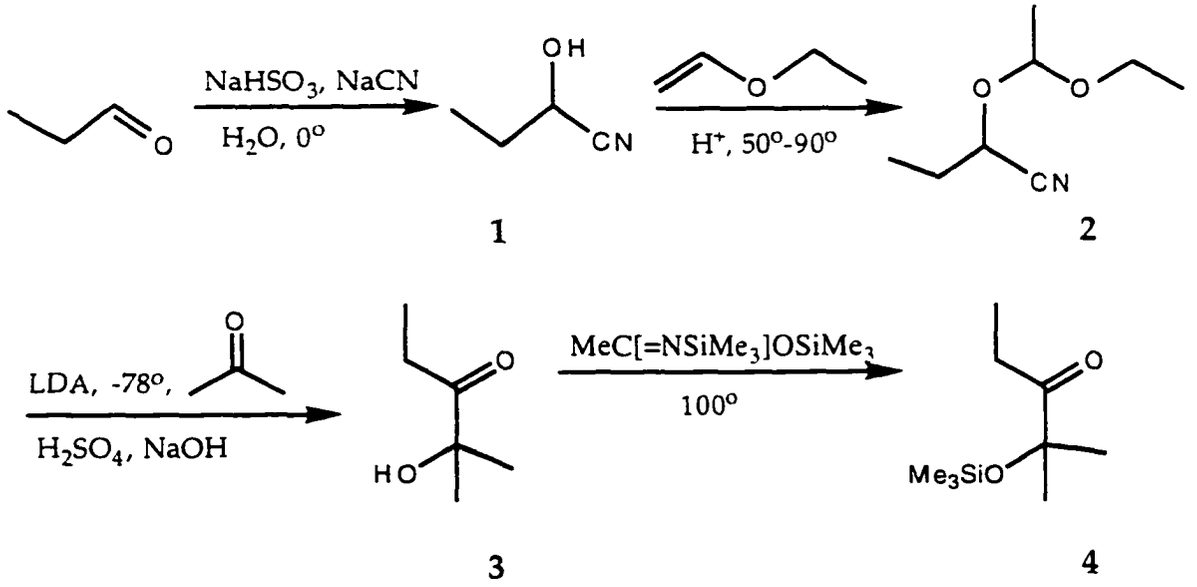

Scheme 1.

Protected hydroxyketone, **4**, was converted to the seco-β-ionone, **6**, in two steps according to Scheme 2. In the first step, the regiospecifically generated enolate was trapped with N-phenyltrifluorometanesulfonimide[66,67] to give enol triflate **5** which was then submitted to a palladium-catalyzed Heck-type olefination[68-69] with methyl vinyl ether to afford the seco-β-ionone **6**, in good yield.

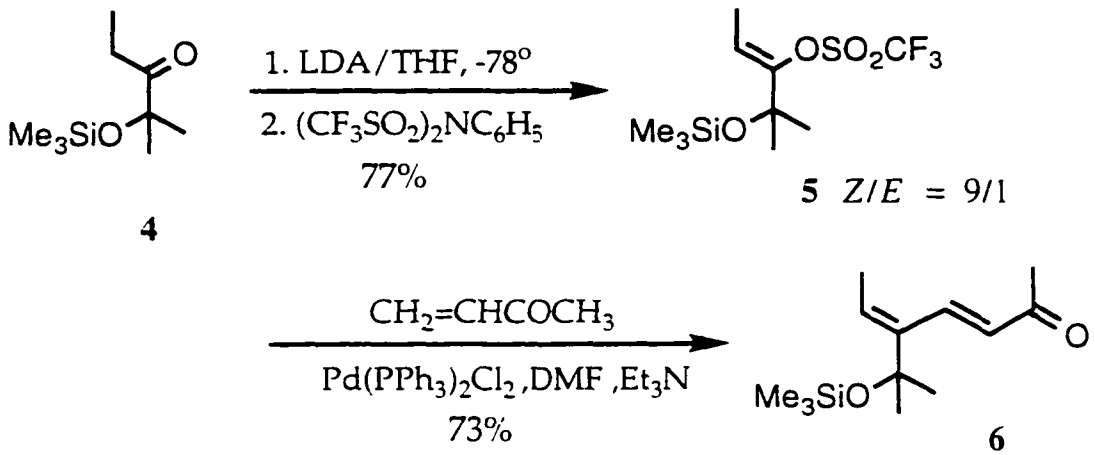

Scheme 2.

The reaction conditions to generate the enolate of **4** regiospecifically, i.e., with a high *Z/E* ratio of 9/1, are critical to the success of the entire synthesis because the key intermediate **10** derived from the *E*-enolate does not bind with the apoprotein. The size of the substituent group plays an important role in the stereochemical outcome of the deprotonation, as illustrated by the transition state structures leading to the **(Z)-5** and **(*E*)-5** isomers.

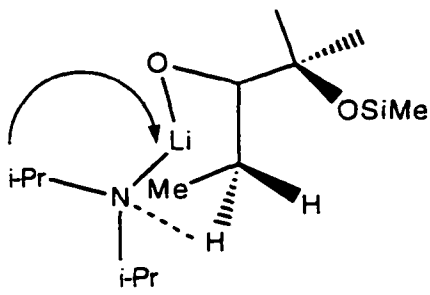

(*Z*)-enolate TS

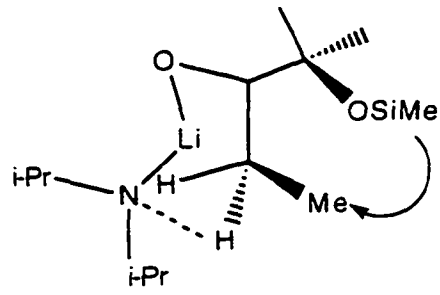

(*E*)-enolate TS

Because the repulsion is less between the methyl and isopropyl groups in the *Z*-isomer TS than between the methyl and Me3SiO- groups in the *E*-isomer TS, the *Z*-isomer TS is more stable, hence formation of (*Z*)-triflate is preferred.

It is important to notice that the enol triflates (***Z/E***)-**5** can and must be separated and purified by vacuum distillation prior to employing the (***Z***)-isomer in the Heck olefination. The triflates tend to decompose on silica gel, thus their purification by flash column chromatography leads to poor yields. The triflates can be easily distinguished by their ^{1}H nmr spectra shown in Figure 12.

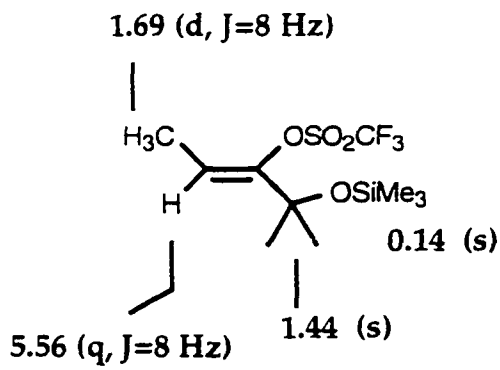

(*Z*)-5

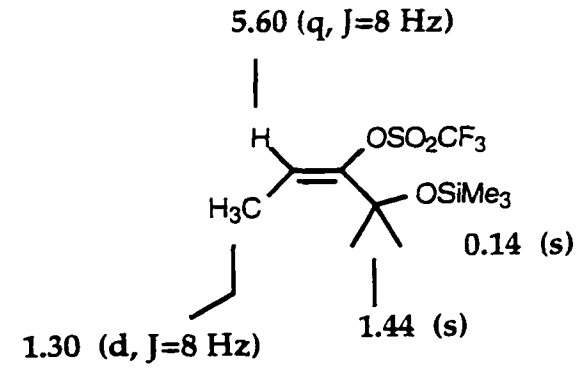

(*E*)-5

Figure 12. ^{1}H nmr of isomeric triflates (***Z***)-**5** and (***E***)-**5**.

Heck reaction of (*Z*)-**5** with methyl vinyl ketone mediated by Pd(0) species proceeded smoothly to give **6** in 73% yield. The highest yields are obtained in the Heck reaction when the alkene reactant is stabilized by an electron withdrawing, e.g., ketone or ester group. Steric hindrance in the enol triflate (as in **5**) has no significant effect on the reaction rate, and the double bond stereochemistry in the final product results from palladium-catalyzed equilibration. hence the most stable, *E* product is obtained in the reaction with methyl vinyl ketone. Chain extension by a two carbon unit was effected by reacting **6** with a Corey type of silylated aldimine[70] (Scheme 3). The product was obtained as a 4.5 : 1 mixture of 9-*trans* : 9-*cis* isomers that after separation by FCC afforded the pure, 9-*trans* isomer of **7**.

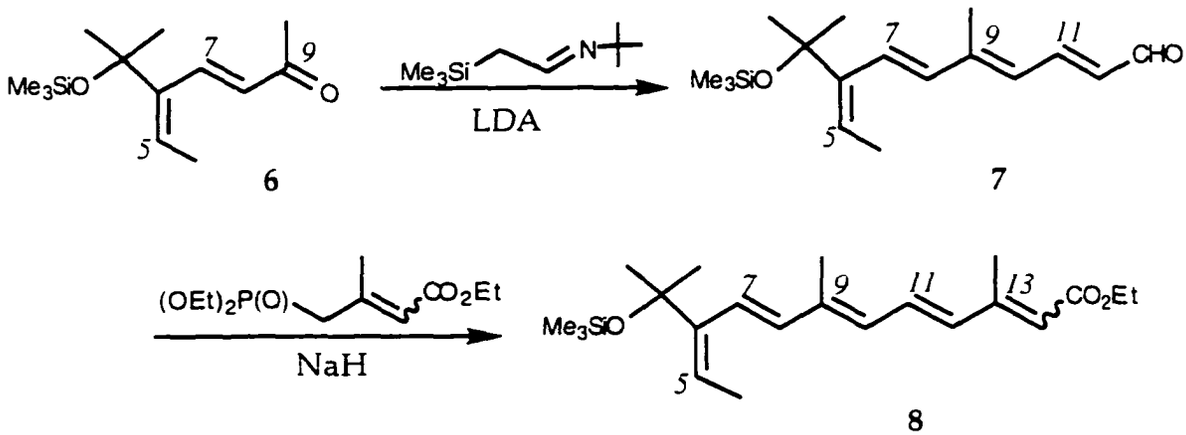

Scheme 3.

The 9-*trans* isomer of tetraenal **7** was subjected to a Horner-Wadsworth-Emmons reaction to obtain ester **8** in 94% yield as a mixture of 13-(*E*)/(*Z*) isomers (Scheme 3). Deprotection of **8** with fluoride to **9**, followed by reduction of the ester with DIBAH and subsequent CAMOX[71] oxidation afforded a mixture of the 13-*cis*/13-*trans* isomers of the key intermediate **10** (Scheme 4). Pure **10** was

obtained by FCC separation of the mixture and its structure was confirmed by ^{1}H and ^{13}C nmr, and CI-MS.

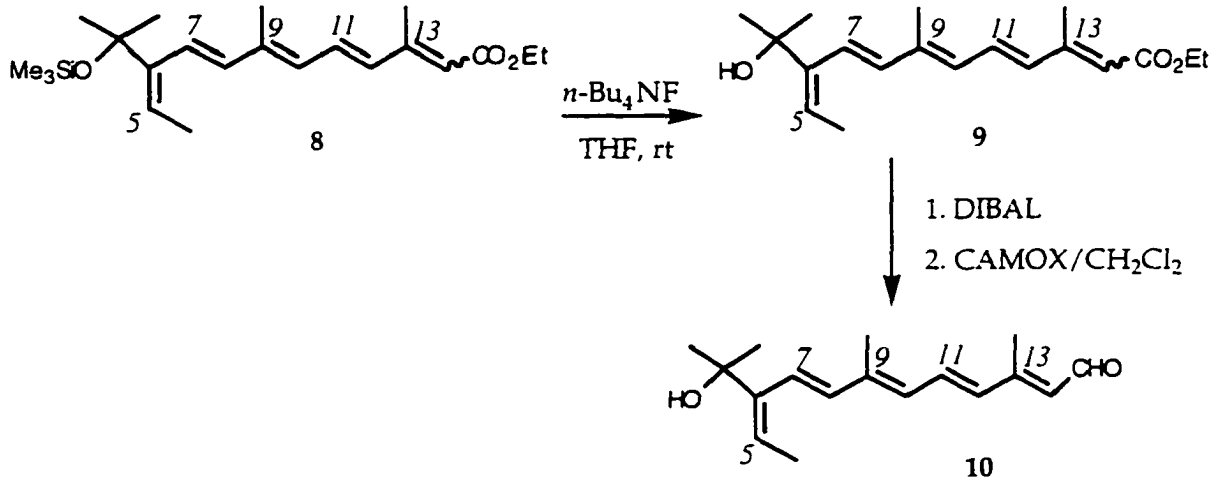

Scheme 4.

2.2.2 Synthesis of the spacer-armed retinals.

Three spacer-armed retinal analogs, **11-13**, were synthesized by derivatizations of their common precursor, key intermediate **10**. All spacer-arms were attached to the key intermediate **10** by esterification with carboxylic acids or acid chlorides of the tertiary alcohol in **10**.

Although many useful and reliable methods for the esterification of carboxylic acids have been reported in the literature, a great need still exists for a versatile and simple process whereby esters may be formed under very mild conditions, especially in case of the retinal analogs which are very sensitive to acids, bases and heat. Pyridine is one of the traditional catalysts for acylation reactions, but 4-N,N-dialkylaminopyridines, are approximately four powers of ten more reactive compared to pyridine when used as

acylation catalysts (Scheme 5).[72] In consequence, they are used with increasing regularity for acylation reactions which proceed either incompletely or not at all in pyridine. Generally, 0.05-0.2 mole of catalyst is employed per mole of substrate with either acids, anhydrides, or acyl chlorides. The acid which is released may be bound with an equivalent amount of pyridine or triethylamine. Reactions may be conducted in various media: hexane, toluene, benzene, dichloromethane, ethyl acetate, THF, triethylamine, or pyridine.

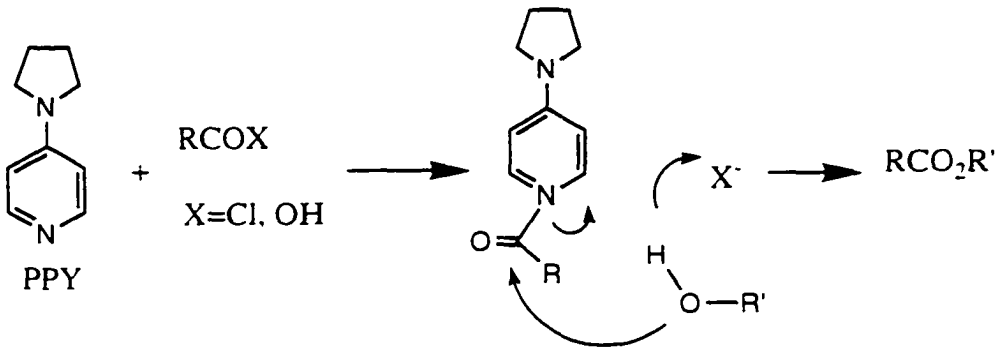

Scheme 5.

This type of acylation proceeds under mild conditions, at room temperature, but half of the carboxylic acid is not converted to ester.[73] Hassner and Alexanian[74] have shown how the problem may be solved by the incorporation of dicyclohexyl carbodiimide (DCC) into the reaction (Scheme 6). We used their method to synthesize retinal analogs **11-13.** The key intermediate, **10**, was esterified with the appropriate carboxylic acids or acid chlorides at room temperature in CH_2Cl_2, in the presence of PPY and DCC as the catalysts. The yields ranged from 70% to 85%.

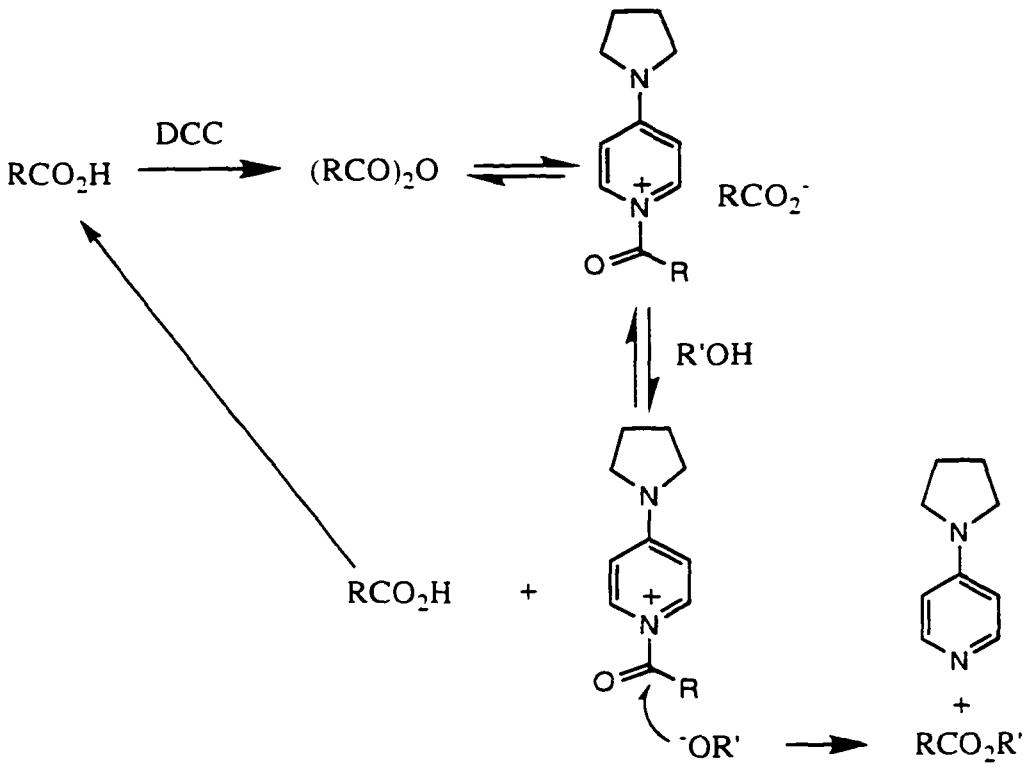

Scheme 6.

Retinal analog **13** with the disulfide bond containing spacer-arm, designed to form a monolayer on gold, was synthesized by esterification of the key intermediate **10** with 12,12'-dithio-bis(dodecanoic acid), according to Scheme 7. The disulfide was prepared by converting 12-bromododecanoic acid to the Bunte salt with thiosulfate ion, followed by *in situ* reaction of the Bunte salt with iodine.

In collaborative work, the gold film, Au(111) will be immersed into a dilute CH_2Cl_2 solution of compound **13**. If the retinals form a monolayer on the gold's surface, the retinal analog **13** fixed to the gold surface via the thiol-derivatized spacer arm, will be also bound to the protein via the Schiff base linkage. We expect that in this

manner the protein molecules will be organized, and their mobility will be reduced because they will be "fixed" on the gold film. Orderly arrays of the protein will be generated suitable for diffraction studies.

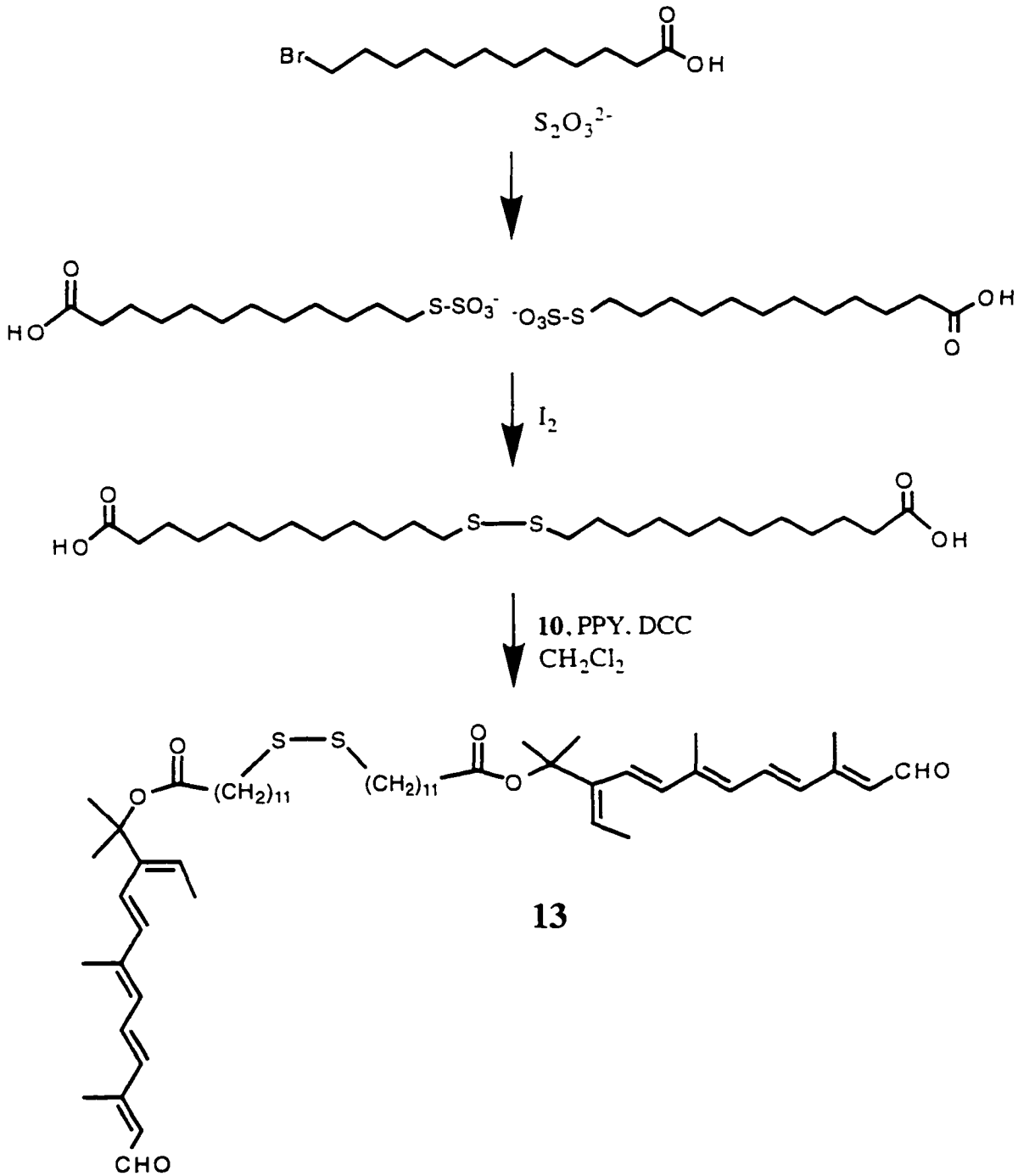

13

Scheme 7.

2.3. Conclusion

A common, key synthetic intermediate was prepared that by derivatizations led to spacer-armed retinal analogs of diverse structures. This intermediate was employed to synthesize three spacer-armed retinal analogs: The first, compound **11**, contains an 11-carbon aliphatic spacer-arm. In the second analog, **12**, the spacer is of 12-carbon length and contains a polar carboxyl terminus. In retinal analog **13** a disulfide bond joins two spacer-armed retinyl moieties. The first two analogs will be employed to investigate the tertiary structure of bacteriorhodopsin. The third analog, designed to generate orderly arrays of bacteriorhodopsin adsorbed on gold will facilitate analysis of its tertiary structure by diffraction techniques. In addition, orderly arrays of bR generated by syntheses, will have high potential in modulating the properties of bR-based molecular devices, and will represent a novel approach to modify the properties of biopolymer-based materials.

3. EXPERIMENTAL

General techniques.

Nuclear magnetic resonance (^{1}H and ^{13}C) spectra were recorded on a Bruker NR300 MHz instrument in $CDCl_3$ solutions. Chemical shifts are reported as δ values from tetramethylsilane. Numbering of the carbons for the ^{13}C NMR spectra follows retinal numbering instead of the IUPAC system. Ultraviolet-visible spectra were recorded on a Hewlett-Packard HP8452A fast-scan UV/VIS diode array spectrophotometer. Infrared spectra were measured on a Nicolet Magna 750 FT-IR spectrophotometer as KBr pellets. Electron impact, chemical ionization and fast atom bombardement mass spectra (EI-MS, CI-MS, and FAB-MS) were obtained with a Finnegan Mat SSQ70 instrument.

All air and/or moisture-sensitive reactions were carried out in flame-dried glassware under nitrogen atmosphere, using standard syringe/septum techniques. All operations involving compounds carrying chromophoric groups longer than a triene moiety were carried out in a dark room under dim red light ($\lambda > 620$ nm). Retinal analogs and other sensitive compounds were stored under nitrogen at -70°C in the dark. Anhydrous solvents and air-sensitive reagents used were purchased from Sigma-Aldrich Inc. Reactions were monitored by thin layer chromatography (TLC) on Polygram Sil G UV-254 plates and preparative TLC was carried out on Analtech silica gel GF glass plates. The spots were visualized by UV light at 254 and/or 365 nm, or by dipping the plate in vanillin reagent (1.5 g vanillin, 0.5 mL conc. sulfuric acid, 100 mL ethanol) followed by

heating. Flash column chromatography (FCC) was carried out on silica gel (Merck, grade 60, 230-400 mesh), and high performance liquid chromatography (HPLC) was performed by using using a Hewlett-Packard 1100 chromatograph equipped with Chem Station and a DAD UV/VIS detector. The columns used were as follows: Analytical column: μ-Porasil, 3.9 mm x 30 cm; Semi-preparative column: Altex Lichrosorb Si60/5, 10 mm x 25 cm.

2-Hydroxybutyronitrile (1).

A 1000 ml, three-necked, round-bottomed flask fitted with a mechanical stirrer and thermometer and charged with 104 g (1.0 mol) of sodium bisulfite dissolved in 350 ml of water, was placed in an ice-water bath. A solution of sodium cyanide (49 g, 1 mol) in water (150 ml) and propionaldehyde (58 g, 1 mol) were separately cooled to 0°C in an ice-salt bath. When the temperature of the vigorously-stirring sodium bisulfite solution has stabilized at 0°C the cold solution of propionaldehyde was added in one portion. The temperature of the solution immediately increased to *ca.* 35°C, then returned to *ca.* 0°C. After 30 min, the cold sodium cyanide solution was added in one portion. This mixture was stirred for 2 h at 0°C, during which time a thick white precipitate of sodium sulfite formed. The supernatant liquid was decanted into a separatory funnel and the precipitate was washed with 350 ml of ice-water. The combined aqueous layers were extracted with ether (3 x 330 ml), and the extracts were washed with brine (350 ml). After drying ($MgSO_4$) and filtering, the ether was removed by means of a rotary evaporator at rt. After the pH of the residue was adjusted to 5, with a few drops of

concentrated hydrochloric acid, the residue was distilled to give 42.73 g (74%) of 2-hydroxybutyronitrile, bp 108-110 °C (30 mm), as a colorless liquid.

^{1}H NMR ($CDCl_3$): δ 1.07 (t, 3H, J=9 Hz, CH_3), 1.86 (m, 2H, CH_2), 2.87 (br, 1H, OH), and 4.40 (dd, 1H, J= , Hz, CH).

2-[(1'-ethoxy)-1-ethoxy]butyronitrile (2).

In a 100 ml three-necked, round-bottomed flask equipped with a condenser topped with a calcium chloride drying tube, a magnetic stirring bar, a pressure-equalizing dropping funnel, and a thermometer, 2-hydroxybutyronitrile (40 g, 0.47 mol) and 0.5 ml concentrated hydrochloric acid were introduced. Ethyl vinyl ether (50.8 g, 0.7 mol) was then added dropwise to the stirred cyanohydrin maintaining the temperature at 50°C. When the addition was complete, the mixture was heated to 90°C for 4 h. The condenser was then replaced with a distillation head, and the dropping funnel and thermometer were replaced with stoppers. Direct distillation of the gold-yellow solution from the reaction flask gave 71.1 g (96%) of 2-[(1'-ethoxy)-1-ethoxy]butyronitrile, bp 55-60°C (15 mm), as a colorless liquid.

^{1}H nmr ($CDCl_3$) (major diastereomer): δ 1.08 (t, 3H, J=7 Hz, CH_3), 1.20 (tt, 3H, J= 7,8 Hz, CH_3), 1.36 (dd, 3H, J= 8 Hz, CH_3), 1.86 (m, 2H, CH_2), 3.53, 3.67 (m,m, 2H, CH_2), 4.24, 4.41 (t, t, 1H, J= 7,8 Hz, CN-CH), 4.85 4.93 (q, q, 1H, J= 8 Hz, O-CH-O).

2-Hydroxy-2-methylpentan-3-one (3).

A flame-dried, 250 mL three-necked round-bottomed flask was equipped with a magnetic stirring bar, low temperature thermometer, nitrogen inlet, rubber septum, and a pressure-equalizing dropping funnel that was sealed with a rubber septum. The flask was charged with dry isopropylamine (7.6 ml. 54 mmol) and anhydrous THF (36.0 ml), cooled to -10°C and 1.6 M butyllithium in hexane (33.9 ml, 54 mmol) was added dropwise at a rate which maintained the temperature at -10°C. After the addition was complete, the solution of lithium diisopropylamide (LDA) obtained was cooled to -75 °C and 2-[(1'-ethoxy)-1-ethoxy]butyronitrile (5 g, 32 mmol) was slowly added to the stirred solution at such a rate that the temperature of the reaction mixture does not exceed -70°C. The mixture was stirred for 10 min then anhydrous acetone (4.2 g, 72 mmol) was added over a 35 min period at -70°C. When the addition was complete the cooling bath was removed and the reaction mixture was allowed to warm to 0°C. The solution was poured into 30 ml of water and the resulting mixture was concentrated at aspirator pressure with a rotary evaporator (30 °C water bath) to remove the volatile organic compounds. The aqueous residue was extracted with methylene chloride (3 x 30 ml). The combined organic layers were washed with water (2 x 25 ml), then concentrated with a rotary evaporator to obtain a yellow, syrupy residue. This material was stirred with methanol (14 ml) and aqueous 5% sulfuric acid (7.0 ml) overnight at rt. The methanol was evaporated with a rotary evaporator (30°C water bath) at aspirator pressure and the yellow residue was extracted with ether (3 x 30 ml). The combined extracts were shaken in a 500 ml of separatory funnel with 10 N aqueous

sodium hydroxide (5 ml) for 15 min. The layers were separated, and the ether layer was washed with brine (25 ml) and dried ($MgSO_4$) for 2 h. The drying reagent was removed by filtration through a coarse, sintered-glass funnel, and the ether was removed with a rotary evaporator (water bath below 40°C) at aspirator pressure. The crude product was distilled at 57-58°C (15 mm) to give 9.42 g (83% yield) of **3**, a pale yellow oil.

^{1}H nmr ($CDCl_3$): δ 1.09 (t, 3H, J=8Hz, 5-CH_3), 1.63 (s, 6H, 1,1'-Me), 2.60 (q, 2H, J= 8Hz, 5-CH_2), and 3.86 (br. 1H, OH).

2-Methyl-2-trimethylsilyloxypentan-3-one, (4).

A dry, 100 ml three necked round-bottomed flask equipped with a magnetic stirrer, reflux condenser, a nitrogen inlet, and a thermometer was charged with 2-hydroxy-2-methylpentan-3-one (7.0 g, 63 mmol) and *N,O*-bis(trimethylsilyl)acetamide (4.6 g, 32 mmol). The mixture was heated at 100°C for 16 h with stirring and then cooled to rt, at which point the mixture becomes a semisolid as the acetamide crystallizes. The semisolid was diluted with 12.5 ml of water and stirred for 1 h. After the stirring was stopped, 50 ml of hexane was added and the layers were separated. The aqueous layer was extracted with hexane (25 ml). The combined hexane extracts were washed with water (4 x 25 ml) and then dried ($MgSO_4$) for 2 h. After removing the drying reagent by filtration through a coarse, sintered-glass funnel, the hexane was evaporated on a rotary evaporator (25°C water bath) at aspirator pressure. The crude, pale yellow oil was distilled to afford 9.24 g (83%) of 2-methyl-2-trimethylsilyloxypentan-3-one, bp 71-73°C (15 mm), as a colorless liquid.

^{1}H nmr ($CDCl_3$): δ 0.14 (s, 9H, $SiMe_3$), 1.03 (t, 3H, J=7Hz, 5-CH_3), 1.34 (s, 6H, 1,1'-CH_3), 2.66 (q, 2H, J=7 Hz, 5-CH_2).

3-trifluoromethanesulfonyloxy-4-methyl-4-trimethylsilyl-oxy-2-pentane (5).

Lithium diisopropylamide (LDA) was prepared by adding to a solution of diisopropylamide (4.1 g, 0.04 mmol) in anhydrous THF (54 ml) 1.6 M butyllithium in *n*-hexane (25 ml, 0.04 mmol) at -10°C under inert atmosphere and stirring the solution for 10 min. To this solution of LDA, cooled to -75°C, a solution of 2-methyl-2-trimethylsilyloxypentan-3-one (5 g, 27 mmol) in anhydrous THF (34 ml) was added. Stirring was continued for an additional 1.5 h, then a solution of N-phenyl trifluoromethanesulfonimide (15 g, 40 mmol) in anhydrous THF (34 ml) was added. The resulting brown solution was warmed to rt and stirred for a further 48 h at rt. The reaction mixture was diluted with *n*-pentane (30 ml) and the organic layer was washed with saturated aqueous sodium bicarbonate (2 x 20 ml). After drying ($MgSO_4$) and filtering, the solvents were removed at rt using a rotary evaporator at aspirator pressure. The crude product was distilled to give 4.51 g (77%) of the enol triflate (*Z*)-**5** as a colorless liquid, bp. 50-52°C (15 mm).

^{1}H nmr ($CDCl_3$): δ 0.14 (s, 9H, $SiCH_3$), 1.44 (s, 6H, 1,1'-CH_3), 1.69 (d, 3H, J=8 Hz, 5-CH_3), and 5.56 (q, 1H, J=8 Hz, =CH).

5-[1'-(trimethylsilyloxy)-1'-methylethyl]-3(E),5(E)-hepten-2-one (6).

A 100 ml three-necked round-bottomed flask, equipped with a condenser, magnetic stirrer, and a thermometer, was charged with bis(triphenylphosphine)palladium(II) dichloride (0.43 g, 2.2 mol%) triethylamine (7.1 g, 70 mmol), methyl vinyl ketone (4.1 g, 59 mmol) in DMF (45 ml), and enol triflate **(Z)-5** (9 g, 28 mmol) and the mixture was heated to 75°C for 9 h. The mixture was cooled to rt, diluted with water (25 ml) and extracted with CH_2Cl_2 (3 x 25 ml). The combined extracts were washed with water (4 x 10 ml), dried ($MgSO_4$) and concentrated. The residue was purified by FCC on Si gel (300 g), eluting with 25% ether in hexane to obtain 3.48 g of the ketone **6** (73% yield).

R_f: 0.78, ether/hexane=1:3

^1H nmr ($CDCl_3$): 0.07 (s, 9H, $SiCH_3$), 1.44 (s, 6H, 1,1'-CH_3), 1.78 (d, J=7.3 Hz, 3H, 5-CH_3), 2.29 (s, 3H, 9-CH_3), 5.59 (q, J=7.3 Hz,1H, 5-H), 6.64 (d, J=16 Hz, 1H, 7-H), δ 7.31 (d, J=16 Hz, 1H, 8-H).

3-methyl-6-(1'-trimethylsilyloxy-1'-methylethyl)-octa-2(E/Z),4(E),6(E)-trienal (7a/7b).

In a flame dried three-necked round-bottom flask, equipped with a low temperature thermometer, magnetic stirrer, nitrogen inlet, and pressure-equalized adding funnel, lithium diisopropylamide (LDA) was prepared by adding to a stirred solution of diisopropylamine (1.12 g, 15 mmol) in anhydrous THF (5.2 ml) 1.6 M butyllithium in hexane (10 ml, 15 mmol) at -10°C and stirring the mixture for 10 min. The solution of LDA was cooled to -75°C and silylated acetaldehyde *t*-butylimine (3.2 g, 18 mmol) in THF (5 ml) was added over a period of 10 min followed by addition of **6** (2.0 g, 7 mmol) in

THF (3 ml). The reaction mixture was warmed to -20°C over a 4 h period, quenched with 60 ml of water, and was extracted with 2 x 60 ml ether. The organic layers were washed with brine (2 x 60 ml), dried ($MgSO_4$), and were concentrated. The crude product was purified by FCC on Si gel (100 g), eluting with 25% ether in hexane to give 1.29 g of **7a** (*trans*), 1.00 g of **7b** (*cis*), and 0.30 g of *trans/cis* mixture of **7a** and **7b**, (84 % overall yield).

R_f: 0.42 (*trans*), 0.5 (*cis*), ether/hexane=1:3

λ_{max} (hexane): 290, 306, and 320 (fine structure) (*trans*)

^1H nmr ($CDCl_3$):

Trans: δ 0.08 (s, 9H, $SiCH_3$), 1.39 (s, 6H, 1,1'-CH_3), 1.78 (d, J=7.2 Hz, 3H, 5-CH_3), 2.3 (s, 3H, 9-CH_3), 5.8 ppm (q, J=7 Hz, 1H, 5-H), 5.9 (d, J=8 Hz, 1H, 10-H), 6.6 (d, J=16 Hz, 1H, 8-H), 6.8 (d, J=16 Hz, 1H, 7-H), 10.1 (d, J=8 Hz, 1H, 11-H).

3,7-dimethyl-10-(1'-trimethylsilyloxymethylethyl)-dodeca-2(E/Z),4(E),6(E),10(E)-pentaenoic acid ethyl ester (8a/8b).

A 60% mineral oil dispersion of NaH (0.3 g, 7.5 mmol) was freed from mineral oil by washing with dry THF and was resuspended in THF (8 ml). To this stirred suspension, a solution of triethyl phosphonosenecioate (1.1 g, 6.3 mmol) in dry THF (20 ml) was added dropwise at 0°C under inert atmosphere. The mixture was stirred 30 min at 0°C, another 30 min at rt, then cooled to 0°C and a solution of **7a** (1.50 g, 6.3 mmol) in THF (5 ml) was added slowly, over a period of 30 min. The reaction mixture was was stirred for 4.5 h at rt then was quenched with 20 ml of water/ether (1/1). The organic layer was separated and the aqueous layer was extracted

with ether (100 ml). The combined organic layers were washed with brine (100 ml), dried ($MgSO_4$), concentrated, and the product was purified by FCC on Si gel (200 g), eluting with 20% ether in hexane to give 1.43 g of the ester **8a and 8b** (overall yield 92%). (1 g*Trans* and 0.43 g *cis*).

R_f: 0.67(*Trans*), 0.72 (*Cis*), ether/hexane=.1/3

λ_{max} (hexane): 358, 262 nm (**8a**, *trans*),

λ_{max} (hexane): 354, 262 nm (**8b**, *cis*).

^1H nmr ($CDCl_3$):

Trans: δ 0.08 (s, 9H, $SiCH_3$), 1.26 (t, J=7 Hz, 3H, ester-CH_3), 1.39 (s, 6H, 1,1'-CH_3), 1.78 (d, J=7 Hz, 3H, 5-CH_3), 2.0 (s, 3H, 9-CH_3), 2.33 (s, 3H, 13-CH_3), 4.13 (q, J=7 Hz, 2H, ester-CH_2), 5.75 (q, J=7 Hz, 1H, 5-H), 5.76 (s, 1H, 14-H), 6.17 (d, J=11 Hz, 1H, 10-H), 6.27 (d, J=15 Hz, 1H, 12-H), 6.3 (d, J=16 Hz, 1H, 8-H), 6.51 (d, J=16 Hz, 1H, 7-H), 6.97 (dd, J=15, 11 Hz, 1H, 11-H).

3,7-dimethyl-10-(1'-hydrooxy-1'-methylethyl)-dodeca-2(E/Z), 4(E),6(E),8(E),10(E)-pentaenoic acid ethyl ester (9a/9b).

To a solution of the ester **8a** (2.7 g, 6 mmol) in THF (40 ml), 1 M tetrabutylammonium fluoride (10 ml, 10 mmol) in THF was added and the mixture is stirred for 45 min at rt. The reaction mixture was diluted with ether (100 ml), the organic layer was separated, dried ($MgSO_4$), and the solvents were removed. The crude oil obtained was purified by FCC on Si gel (200 g), eluting with 20% ether in hexane to give **9a/9b** (*trans* :1.516 g, 91% overall yield).

R_f: 0.25 (trans), 0.33 (cis), hexane/ether=4:1.

λ_{max}(hexane): 265, 360 nm

^{1}H nmr ($CDCl_3$):

Trans: δ 1.26 (t, J=7 Hz, 3H, ester-CH_3), 1.39 (s, 6H, 1,1'-CH_3), 1.78 (d, J=7 Hz, 3H, 5-CH_3), 1.99 (s, 3H, 9-CH_3), 2.33 (s, 3H, 13-CH_3), 4.13 (q, J=7 Hz, 2H, ester-CH_2), 5.75 (s, 1H, 14-H), 5.76 (q, J=7 Hz, 1H, 5-H), 6.17 (d, J=11 Hz, 1H, 10-H), 6.27 (d, J=15 Hz, 1H, 12-H), 6.30 (d, J=16 Hz, 1H, 8-H), 6.51 (d, J=16 Hz, 1H, 7-H), 6.97 (dd, J=15, 11 Hz, 11-H).

3,7-dimethyl-10-(1'-hydroxyl-1'-methylethanyl)-dodeca-2-(E/Z),4(E),6(E),8(E),10(E)-pentaenal (10a/10b).

1 M solution of DIBAL (20 ml, 20 mmol) in hexane was added dropwise at -70°C under inert atmosphere to a solution of ester **9 a** (2.32 g, 7.65 mmol) in anhydrous ether (120 ml). The solution was stirred for a further 5 min at -70°C, quenched with ethyl acetate (15 ml), allowed to warm to 0°C, then 10 ml of water was added. The mixture was warmed to rt, diluted with ether (30 ml), and filtered. The white solid was washed with 10 ml of ether. The organic phases were combined, washed with brine (20 ml), dried ($MgSO_4$), and the solvents were removed to yield 1.26 g of an oily residue. The residue was redissolved in CH_2Cl_2 (50 ml) and cooled to 0°C, 16.3 g of CAMOX (MnO_2 on celite) was added slowly and the suspension was stirred 1h at rt. The slurry was filtered through a celite pad on a sintered-glass funnel, washed with CH_2Cl_2, and the filtrate concentrated *in vacuo*. The product was separated and purified by FCC on Si gel (100 g), eluting with 25% ether in hexane, to yield 0.97 g of **10a** (13-*trans isomer)* and 0.58 **10b** (13-*cis* isomer), 84% overall yield.

R_f: 0.196 (*trans*), 0.23(*cis*), hexane/ether=4:1

^{1}H nmr ($CDCl_3$): δ 1.38 (s, 6H, 1.1'-CH_3), 1.77 (d, J=7 Hz, 3H, 5-CH_3), 2.0 (s, 3H, 9-CH_3), 2.31 (s, 3H, 13-CH_3), 5.81 (q, J=7 Hz, 1H, 5-H), 5.96 (d, J=8 Hz, 1H, 14-H), 6.23 (d, J=11Hz, 1H, 10-H), 6.36 (d, J=16 Hz, 1H, 8-H), 6.37 (d, J=15 Hz, 1H, 12-H), 6.47 (d, J=16 Hz, 1H,7-H), 7.11 (dd, J=15,11 Hz, 1H, 11-H), 10.09 (d, J=8 Hz, 1H, 15-H).

^{13}C nmr ($CDCl_3$): 12.8 (9-Me), 13.1 (13-Me), 14.7(5-Me), 28.5(1.1'-Me) 73.2 (10-C), 212.1(7,14-C), 126.0(5-C), 129.3(12-C), 130.6(8,11-C), 132.2(6-C), 135.2(9-C), 137.6(13-C) and 191.6(CHO).

FAB-MS (nitrobenzylalcohol): *m/z* = 260 (M^+).

Spacer-armed retinal analog (11).

A flame-dried two-necked flask equipped with a nitrogen inlet was charged with compound **10a** (26 mg, 0.1 mmol), 4-pyrrolidinopyridine (15 mg, 0.1 mmol), and triethylamine (0.25 ml, 1.8 mmol) in 15 ml anhydrous CH_2Cl_2. Undecanoyl chloride (2 ml, 14.4 mmol) in 2 ml of anhydrous CH_2Cl_2 was then added and the mixture was stirred at rt for 2 h. The reaction mixture was diluted with CH_2Cl_2 (2.5 ml), washed with water (2 x 2.5 ml), the organic phase dried ($MgSO_4$), and concentrated. The product was separated and purified by preparative TLC on Si gel, eluting with 50% ether in hexane, to yield 34 mg of an isomeric (all-*trans*/13-*cis*) mixture of spacer-armed retinals **11a/11b** (84% yield). The isomers were separated by HPLC on a Lichrosorb semi-preparative column, eluting with 10% ether in hexane at 3 ml/min flow rate. Retention times were 19 min for the all-*trans*, and 14 min. for the 13-*cis* isomer.

R_f: 0.44 (all-*trans*), 0.48 (13*cis*), ether/hexane=1:1

λ_{max} (MeOH): 356 nm (all-*trans* isomer)

^{1}H NMR ($CDCl_3$): δ 0.85 (q, 2H, J= 6Hz, 9'H), 1.15-1.22 (m, 14H, 2'-8'H), 1.37 (s, 6H, 1,1'-C H_3), 1.75 (d, 3H, J=7Hz, 5-CH_3), 2.02 (s, 3H, 9-CH_3), 2.33 (s, 3H, 13-CH_3), 3.21(t, 2H, J=7Hz, 1'H), 5.79 (q, J=7 Hz, 1H, 5-H), 5.93 (d, J=8 Hz, 1H, 14-H), 6.22 (d, J=10 Hz, 1H, 10-H), 6.36 (d, J=17 Hz, 1H, 8-H), 6.37 (d, J=17 Hz, 1H, 12-H), 6.45 (d, J=17 Hz, 1H, 7-H), 7.11 (dd, J=10,17 Hz, 1H, 11-H), 10.09 (d, J=8 Hz, 1H, 15-H).

CI-MS (NH_3): *m/z*= 441(M^+), 457($M + NH_4$)$^+$

λ_{max}(hexane): 370, 356, 336, 320, 275 nm (fine structure)

Spacer-armed retinal analog (12).

The anhydride, prepared from 1,11-undecanedicarboxylic acid (22.4 mg, 0.086 mmol) and dicyclohexylcarbodiimide (17.4 mg, 0.086 mmol) in anhydrous CH_2Cl_2 (2 ml) was added, via a microsyringe, to a mixture of **10a** (22 mg, 85 mmol), 4-pyrrolidinopyridine (12 mg, 86 mmol), triethylamine (1.5 ml, 0.09 mmol) and 2 ml anhydrous CH_2Cl_2 (2ml) under an inert atmosphere. The reaction mixture was stirred at rt for 12 h and then was diluted with ether (5 ml). The organic phase was washed with brine (5 ml), water (5 ml), dried ($MgSO_4$), and the solvent removed. The oily residue was separated by FCC on Si gel, eluting with 50% ether in hexane, to give 32.5 mg of semisolid mixture of all-*trans* and 13-*cis* isomers of **12.** The isomeric mixture was separated by HPLC on a Lichrosorb semi-preparative column, eluting with 10% ether in hexane at 3 ml/min flow rate. The retention time of the all*trans*-**12** was 20 min.

R_f: 0.8 (all-*trans*), ether/hexane=1:1)

λ_{max}(hexane): 375 nm (*trans*)

^{1}H nmr ($CDCl_3$): δ 0.85 (q, 2H, J=6Hz, 9'H), 1.25 (br, 14H, 3-8'H), 1.37(s, 6H, 1,1'-Me), 2.02 (s, 3H, 9-CH_3), 2.33 (s, 3H, 13-CH_3), 2.38(t,

2H, J=7Hz, 10'H), 3.21 (t, 2H, J=5Hz, 1'H), 5.79 (q, 1H, J=7 Hz, 5-H), 5.93 (d, 1H, J=8 Hz, 14-H), 6.22 (d, 1H, J=10 Hz, 10-H), 6.36 (d, 1H, J=17 Hz, 8-H), 6.37 (d, 1H, J=17 Hz, 12-H), 6.45 (d, 1H, J=17 Hz, 7-H), 7.11 (dd, 1H, J=10,17 Hz, 11-H), 10.09 (d, 1H J=8 Hz, 15-H).

CI-MS (NH_3): *m/z* =474(M+1)$^+$.

12, 12'-dithio-bis(dodecanoic acid).

Sodium thiosulfate (1.7 g, 7 mmol) was added to a suspension of 12-bromododecanoic acid (2 g, 7 mmol) in 50% aqueous 1,4-dioxane (20 ml). The mixture was heated at reflux (90°C) for 2 h until the reaction to the intermediate Bunte salt was complete (clear solution). The oxidation to the corresponding disulfide was carried out *in situ* by adding iodine in portions until the solution retained a yellow to brown color. The excess iodine was retitrated with 15% sodium pyrosulfite in water. After removal of the dioxane by rotary evaporation the creamy suspension was filtered to yield the crude product. Recrystallization from ethyl acetate/THF gave 1.25 g (77 %) 12, 12'-dithio-bis(dodecanoic acid) as a white solid.

mp: 94°C

^{1}H NMR ($CDCl_3$): δ 1.26 (br, 32H, 2,2'-9,9' CH_2), 1.62 (br, 4H, 10,10'CH_2), 2.43 (t, 4H, J= 7Hz, 1,1'-CH_2), 2.66 (t, 4H, J=7Hz, 11,11'-CH_2). 11.33 (br, 2H, COOH).

FAB-MS (nitrobenzylalcohol): *m/z*=434 (M^+)

Spacer-armed retinal analog (13).

The anhydride, prepared from 12,12'-dithio-bis(dodecanoic acid) (37 mg, 0.08 mmol) and dicyclohexylcarbodiimide (33 mg, 0.16 mmol) in anhydrous CH_2Cl_2 (1 ml) was added, via a microsyringe, to a mixture of **10a** (40 mg, 0.15 mmol), 4-pyrrolidinopyridine (1.5 mg, 0.01

mmol), triethylamine (0.5 ml, 0.16 mmol) and anhydrous CH_2Cl_2 (2ml) under an inert atmosphere and the mixture was stirred at rt overnight. The reaction mixture was diluted with CH_2Cl_2 (5 ml) and was washed with brine (5 ml) and water (5 ml). The organic layer was dried ($MgSO_4$), concentrated, and the residue was purified by FCC on Si gel (20 g), eluting with 50% ether in hexane to give 25 mg (45%) of the semisolid, crude product **13**.

R_f: 0.9, eluting with ether/hexane=1:1

^1H NMR ($CDCl_3$): δ 0.89 (t, 4H, J=8Hz, spacer-arm1 1'-H), 0.98-1.35 (m, 32H, spacer-arm 2'-10'-H), 1.37 (s, 12H, 1,1'- CH_3), 1.76 (d, 6H, J=7 Hz, 5-CH_3), 2.02 (s, 6H, 9-CH_3), 2.31 (s, 6H, 13-CH_3), 3.10(q, 4H, spacer-arm 1'-H), 5.81 (q, J=7 Hz, 2H, 5-H), 5.95 (d, J=9 Hz, 2H, 14-H), 6.22 (d, 2H, J=10 Hz, 10-H), 6.36 (d, 2H, J=17 Hz, 8-H), 6.37 (d, 2H, J=17 Hz, 12-H), 6.45 (d, 2H, J=17 Hz, 7-H), 7.11 (dd, 2H, J=10,17 Hz, 11-H), and 10.09 (d, 2H, J=9 Hz, 15-H).

λ_{max}(hexane): 365 nm.

CI-MS (NH_3): *m/z*=946(M^+)

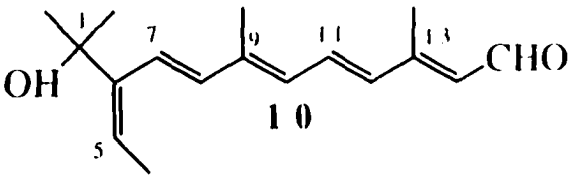

10

1,1'-Me=1.37(s, 3H)
5-Me=1.75(d, 2H, J=7 Hz)
9-Me=2.02(s, 3H)
13-Me=2.33(s, 3H)
H_5=5.79(q, 1H, J=7 Hz)
H_{14}=5.93(d, 1H, J=8 Hz)
H_{10}=6.22(d, 1H, J=10 Hz)
H_{12}=6.36(d, 1H, J=17 Hz)
H_8=6.36(d, 1H, J=17 Hz)
H_7=6.45(d, 1H, J=17 Hz)
H_{11}=7.11(dd, 1H, J=10,17 Hz)
CHO=10.07(d, 1H, J=8 Hz)

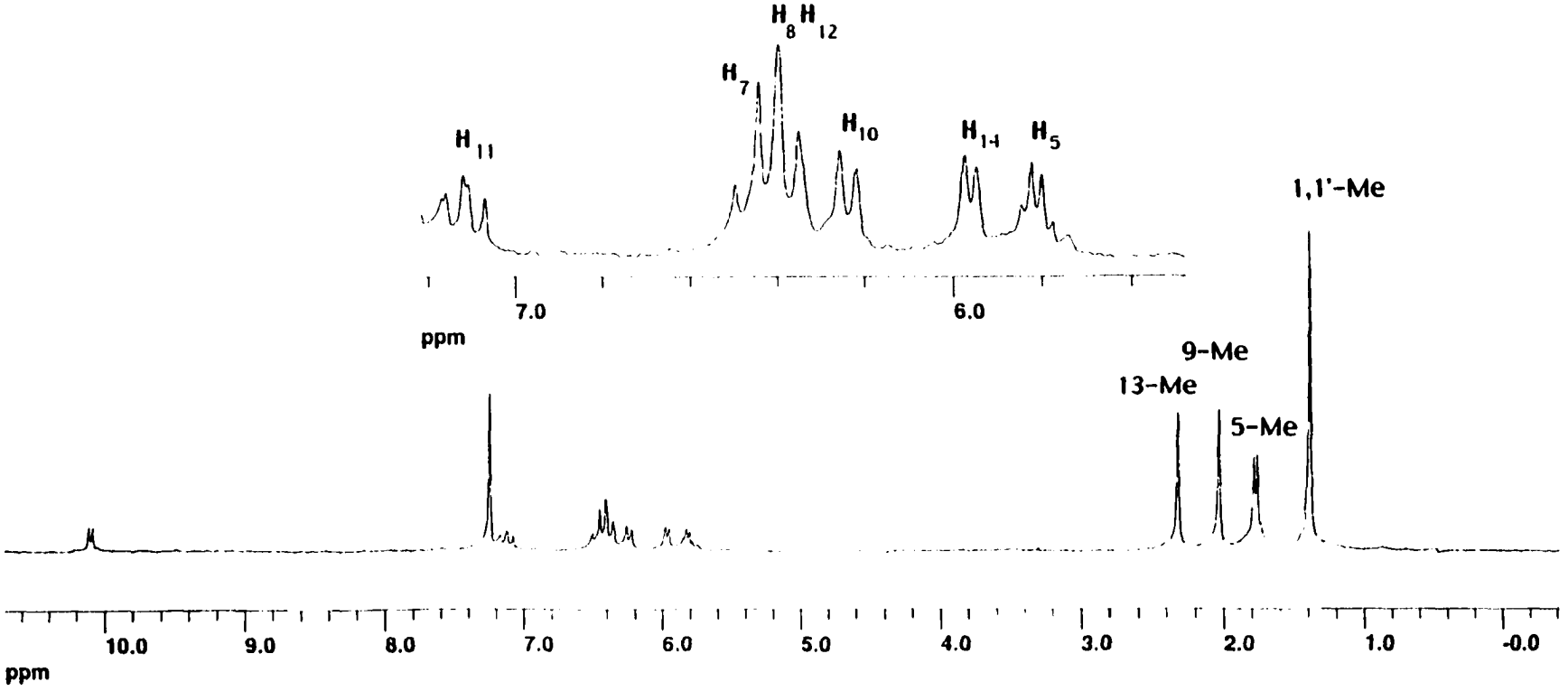

^{1}H NMR spectrum of the key intermediate **10** in $CDCl_3$.

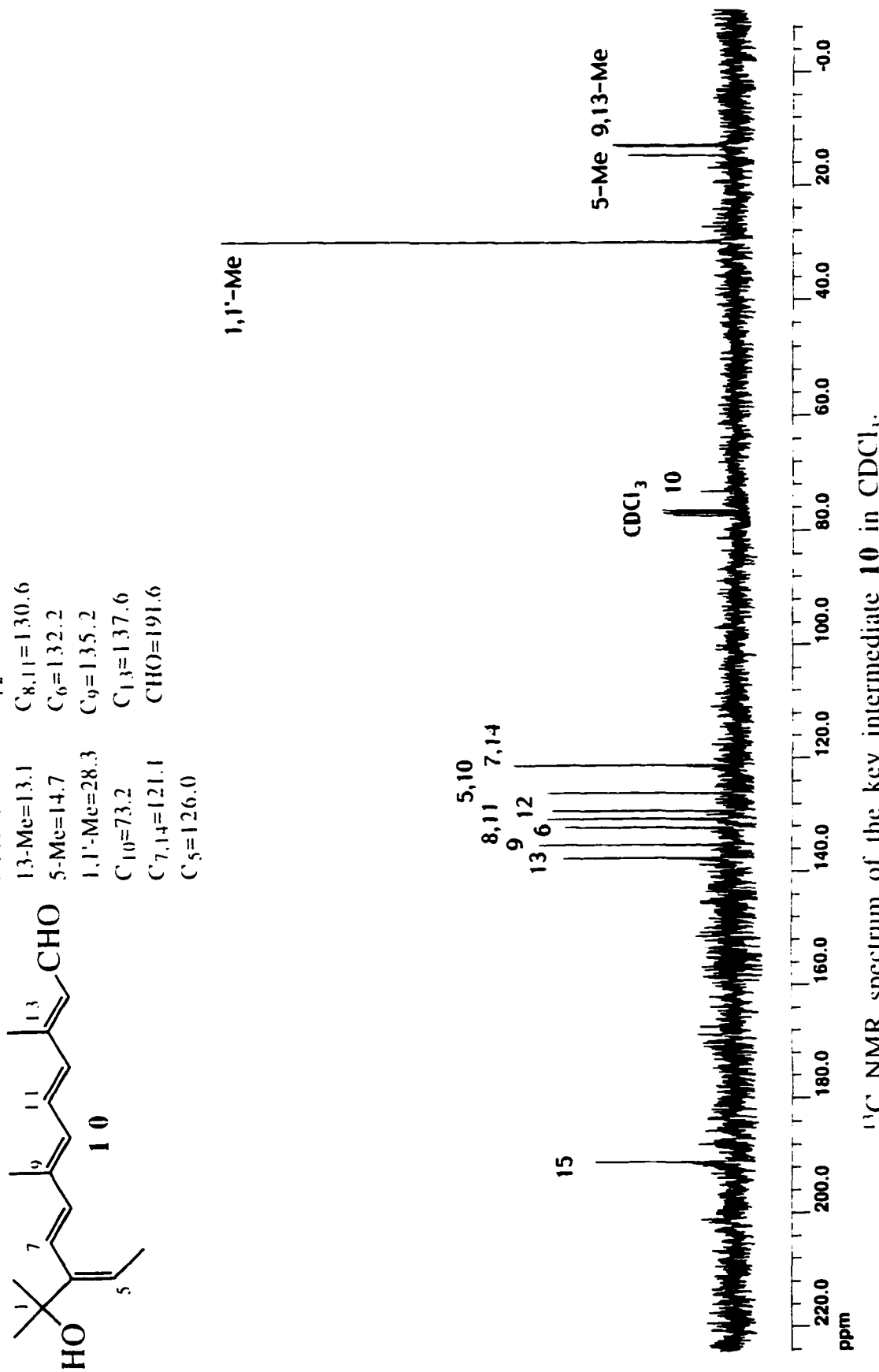

^{13}C NMR spectrum of the key intermediate **10** in $CDCl_3$.

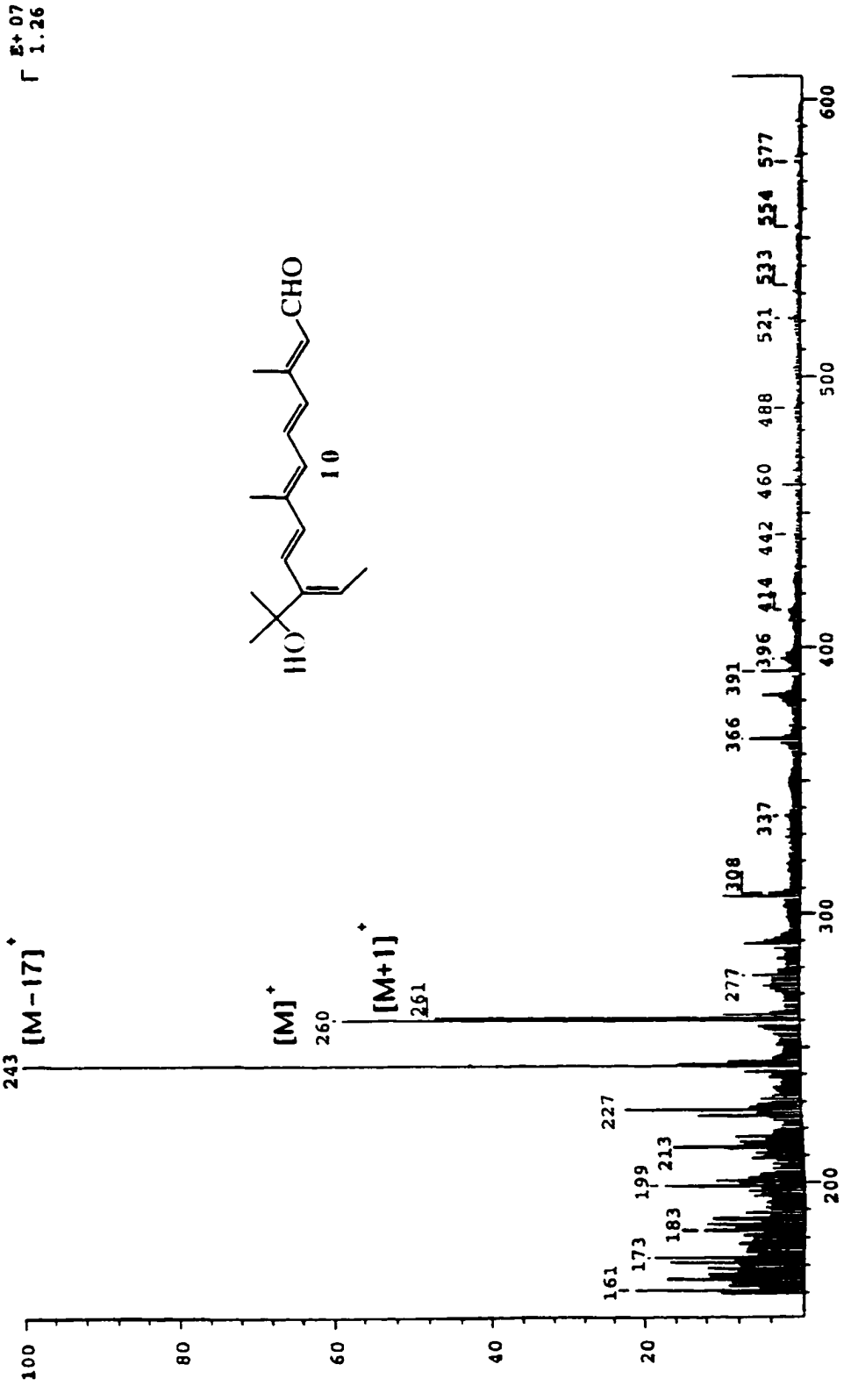

FAB-MS (NBA) spectrum of the key intermediate **10**.

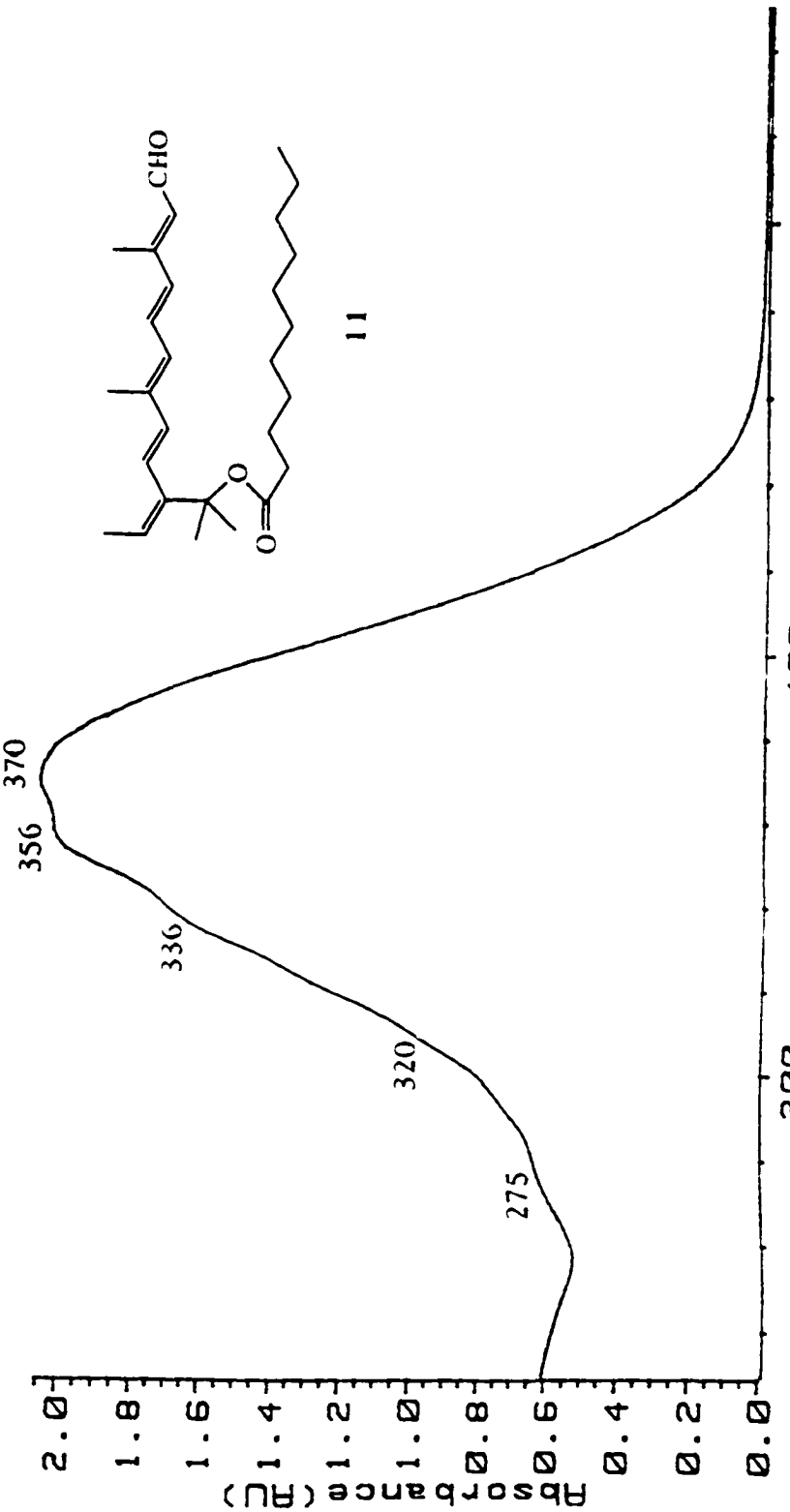

UV-VIS spectrum of the spacer-armed retinal analog **11** in Hexane.

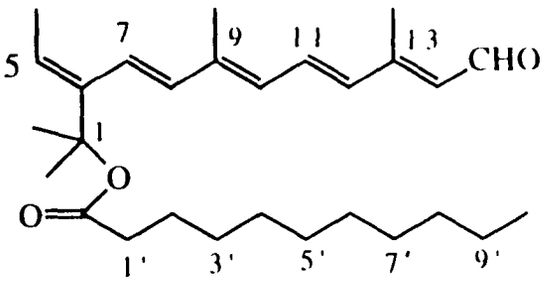

11

H_9=0.85(q, 2H, J= 6Hz)
$H_{2'-8'}$=1.15(br, 14H)
1,1'-Me=1.37(s, 3H)
5-Me=1.75(d, 2H, J=7 Hz)
9-Me=2.02(s, 3H)
13-Me=2.33(s, 3H)
H_1=3.21(t, 2H, J=7 Hz)
H_5=5.79(q, 1H, J=7 Hz)
H_{14}=5.93(d, 1H, J=8 Hz)
H_{10}=6.22(d, 1H, J=10 Hz)
H_{12}=6.36(d, 1H, J=17 Hz)
H_8=6.36(d, 1H, J=17 Hz)
H_7=6.45(d, 1H, J=17 Hz)
H_{11}=7.11(dd, 1H, J=10,17 Hz)
H_{15}=10.07(d, 1H, J=8 Hz)

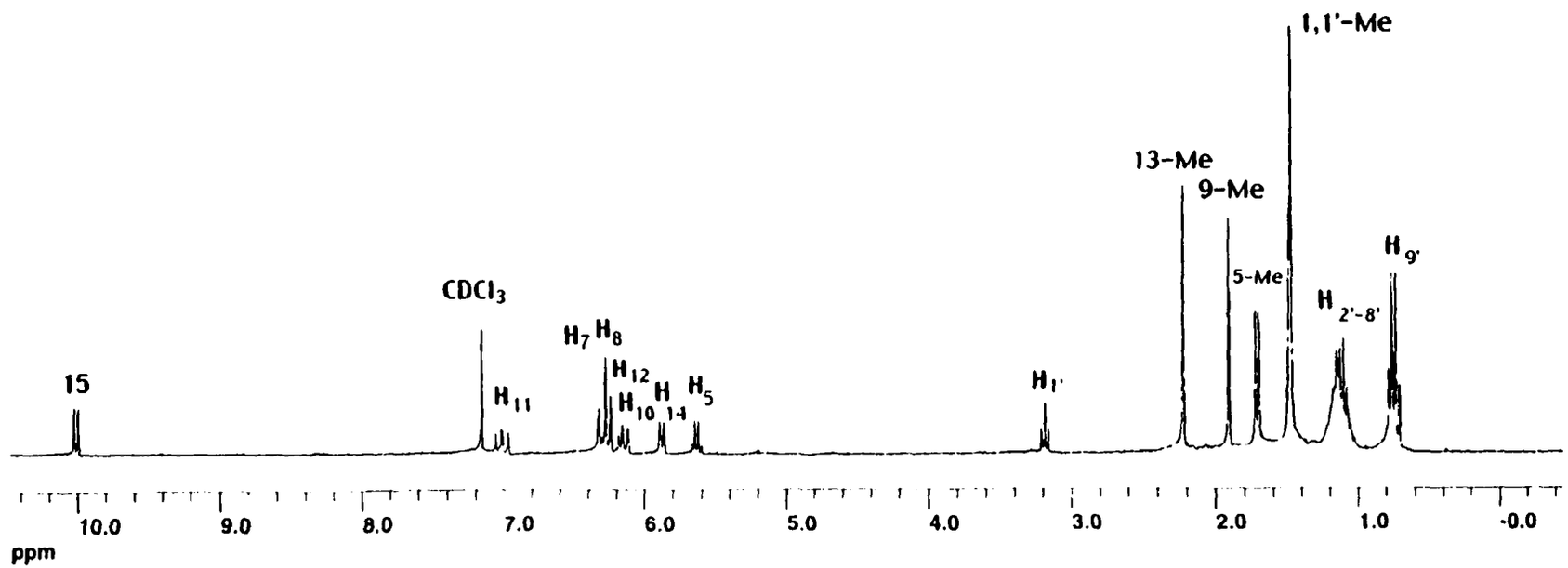

^{1}H NMR spectrum of the spacer-armed retinal analog **11** in $CDCl_3$.

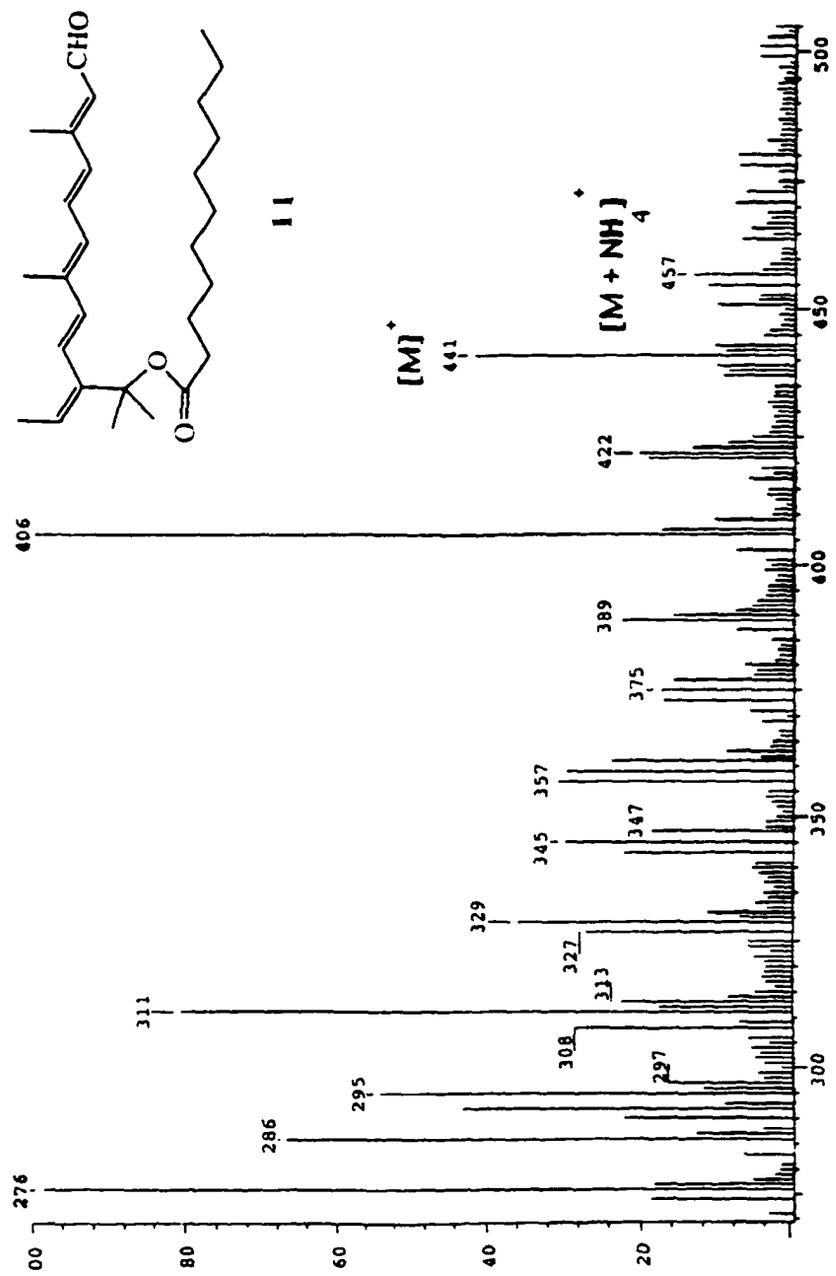

CI-MS (ammonia) spectrum of spcer-armed retinal analog **11**.

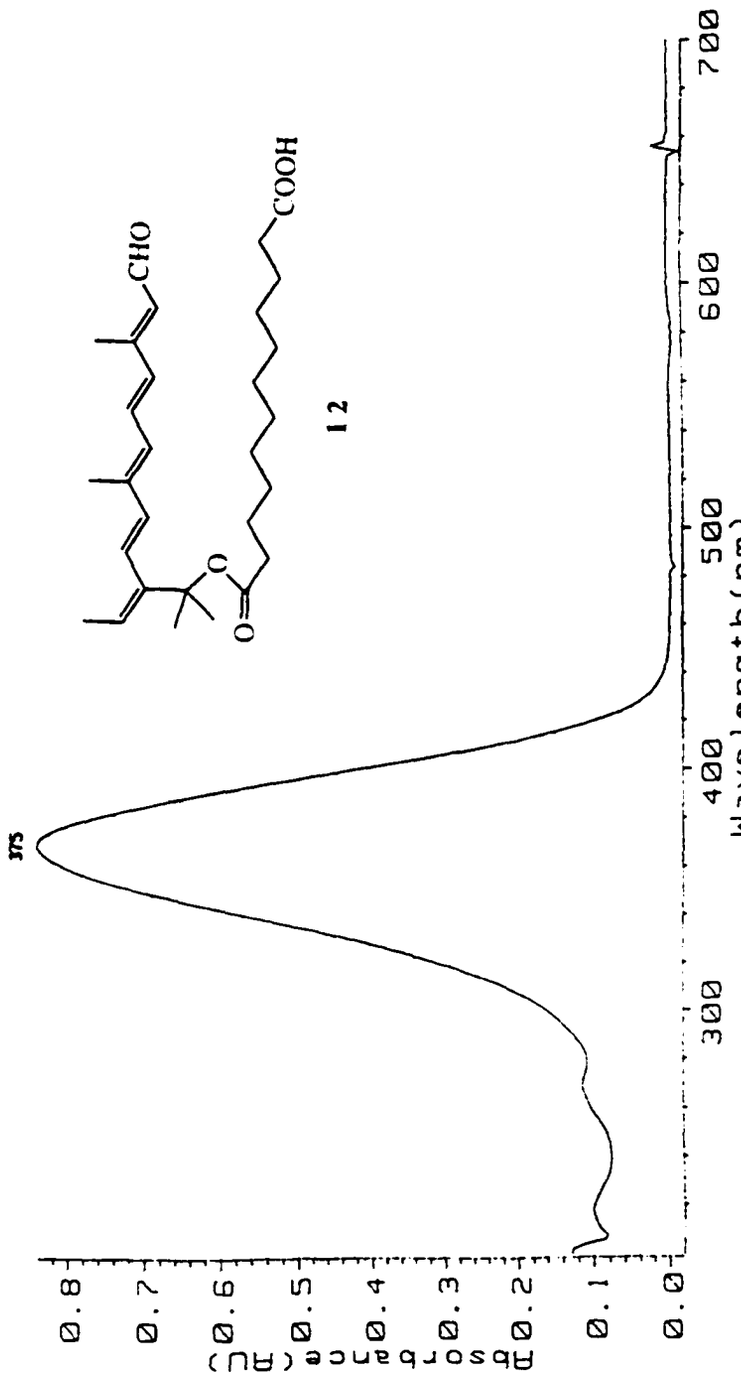

UV-VIS spectrum of the spacer-armed retinal analog **12** in hexane.

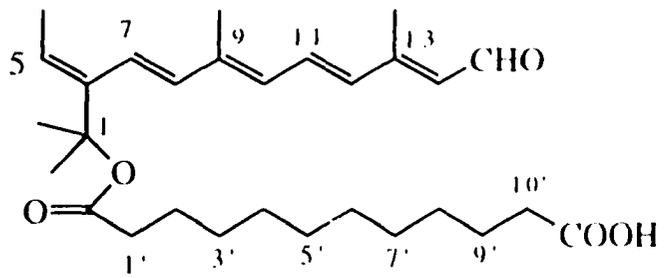

1 2

$H_{9'}$=0.85(q, 2H, J= 6Hz)
$H_{3'-8'}$=1.25(br, 14H)
1,1'-Me=1.37(s, 3H)
$H_{1'}$=1.58(q, 2H, J=7 Hz)
5-Me=1.75(d, 2H, J=7 Hz)
9-Me=2.02(s, 3H)
13-Me=2.33(s, 3H)
$H_{10'}$=2.38(t, 2H, J=7 Hz)
H_5=5.79(q, 1H, J=7 Hz)
H_{14}=5.93(d, 1H, J=8 Hz)
H_{10}=6.22(d, 1H, J=10 Hz)
H_{12}=6.36(d, 1H, J=17 Hz)
H_8=6.36(d, 1H, J=17 Hz)
H_7=6.45(d, 1H, J=17 Hz)
H_{11}=7.11(dd, 1H, J=10,17 Hz)
H_{15}=10.07(d, 1H, J=8 Hz)

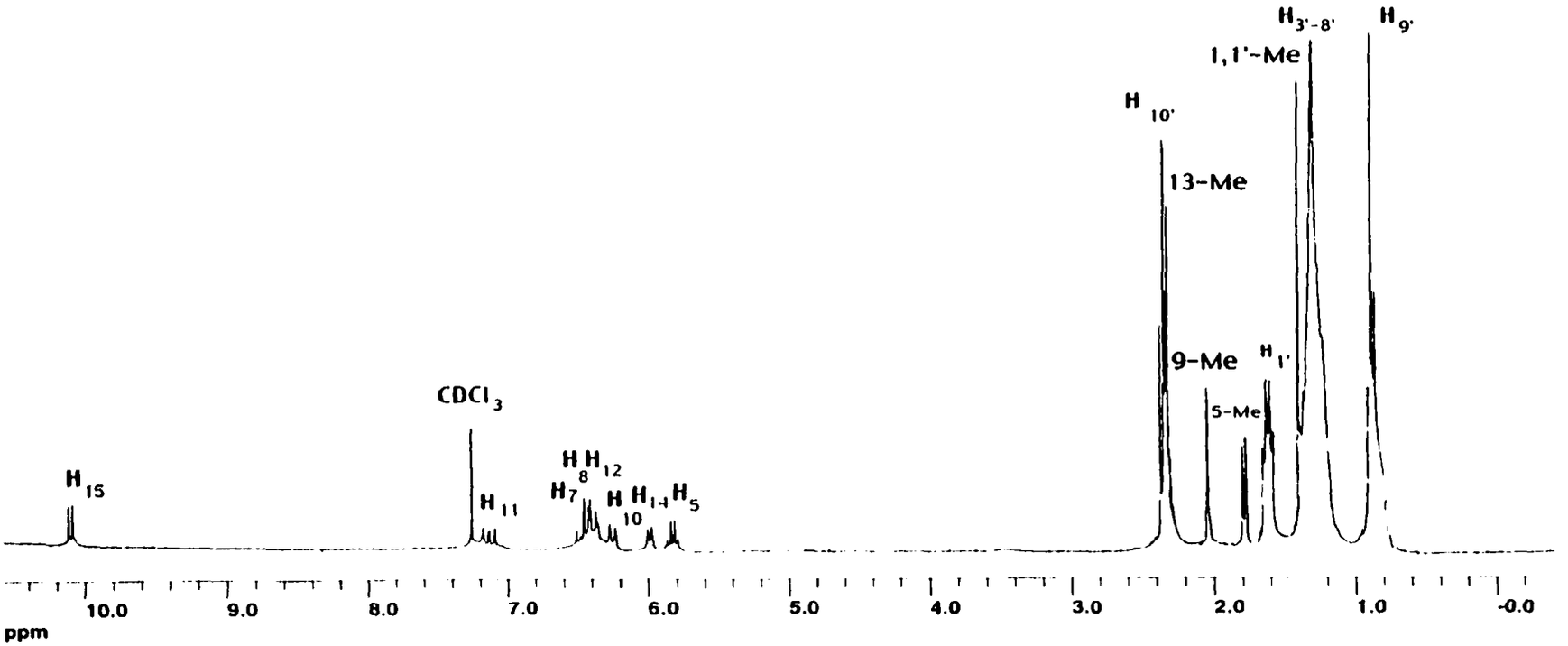

^{1}H NMR spectrum of spacer-armed retinal analog **12** in $CDCl_3$.

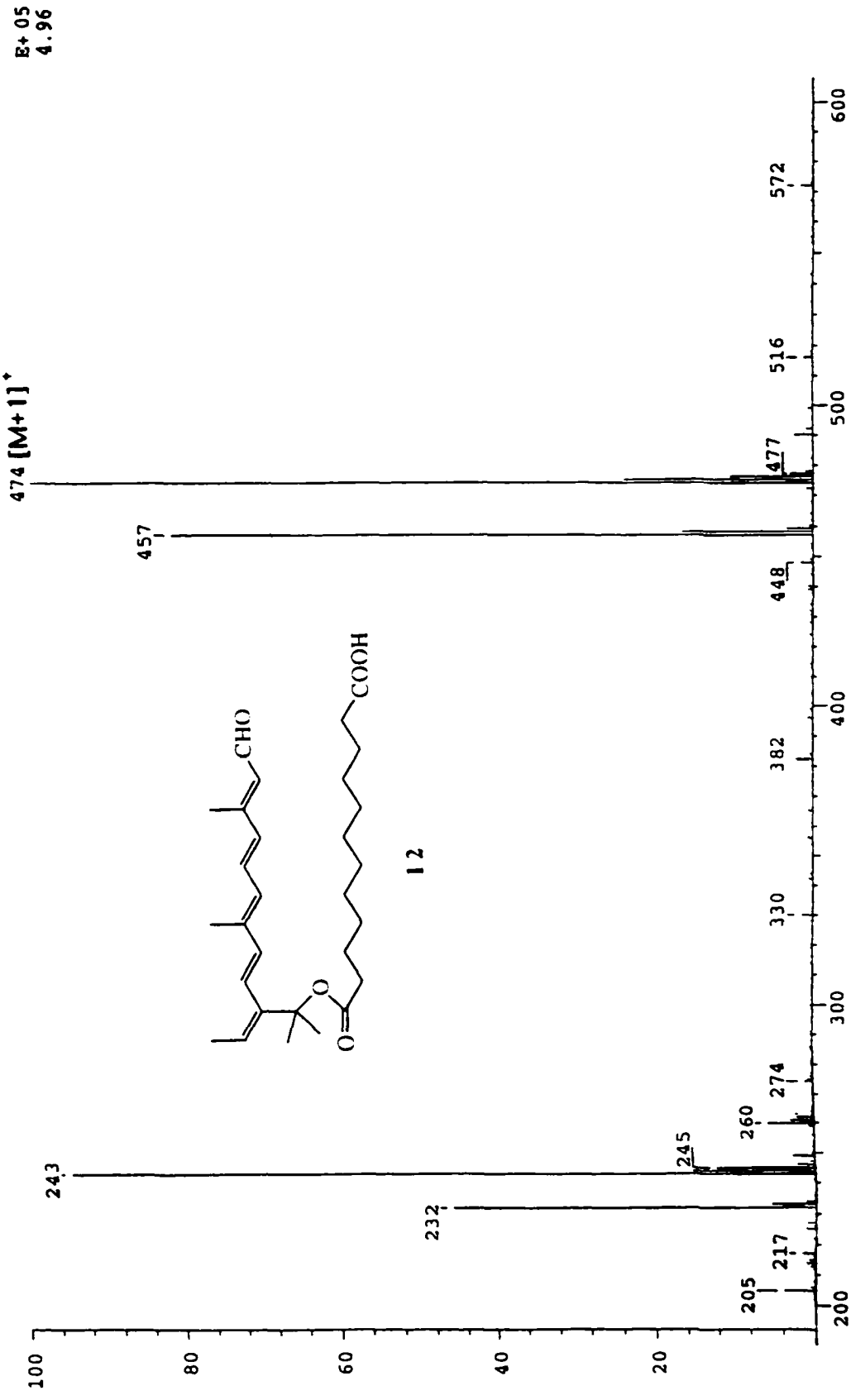

CI-MS spectrum (ammonia) of the spacer-armed retinal analog **12**.

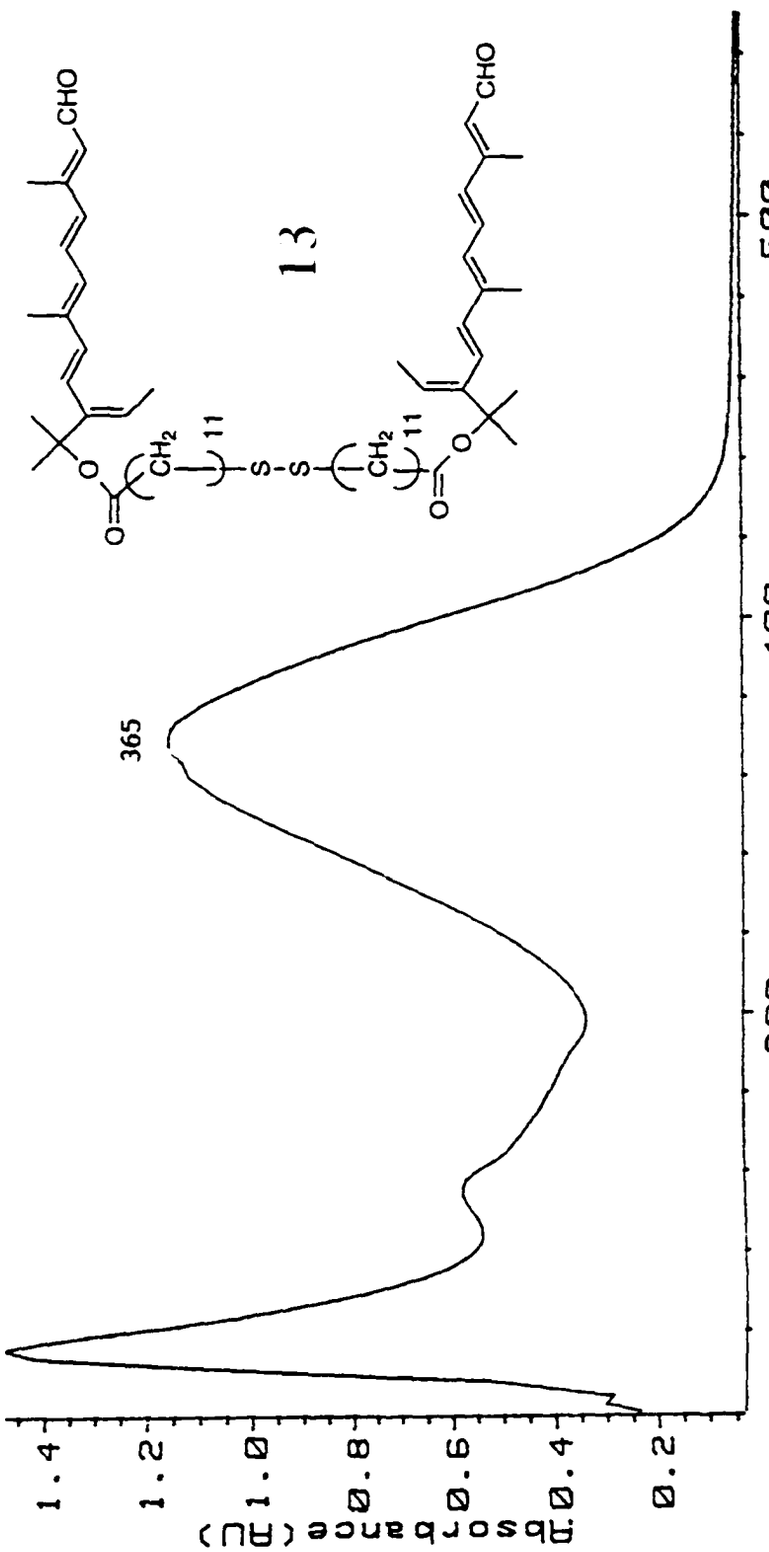

UV-VIS spectrum of the spacer-armed retinal analog **13** in hexane.

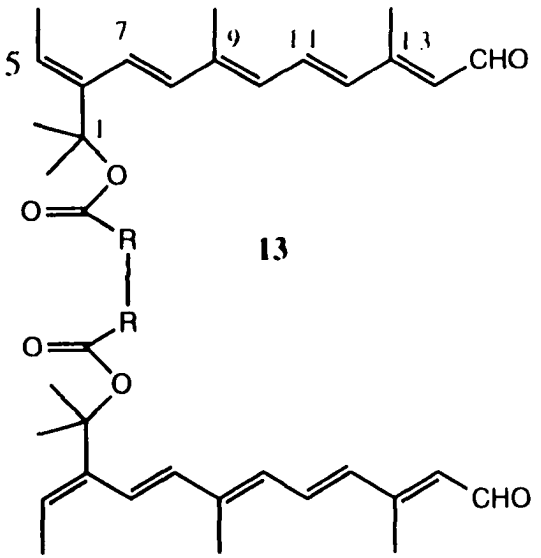

13

$H_{11'}$=0.89(t, 4H, J=8 Hz)
$H_{2'-10'}$=0.89-1.35(m, 18H)
1,1'-Me=1.37(s, 12H)
5-Me=1.76(d, 6H, J=7 Hz)
9-Me=2.02(s, 6H)
13-Me=2.31(s, 6H)
$H_{1'}$=3.01(q, 4H, J=6 Hz)
H_5=5.80(q, 2H, J=7 Hz)
H_{14}=5.95(d, 2H, J=9 Hz)
H_{10}=6.22(d, 2H, J=10 Hz)
H_8=6.36(d, 2H, J=10 Hz)
H_{12}=6.36(d, 2H, J=10 Hz)
H_7=6.45(d, 2H, J=17 Hz)
H_{11}=7.11(d, 2H, J=17 Hz)
H_{15}=10.09(d, 2H, J=9 Hz

R= S 1' 3' 5' 7' 9' 11'

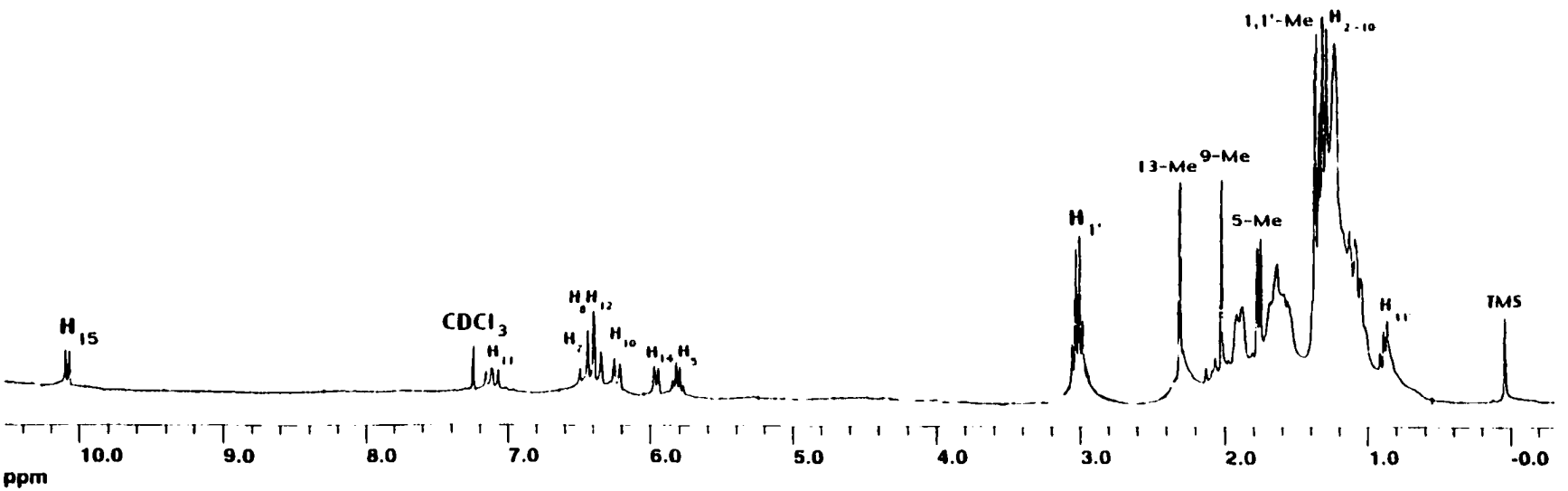

^{1}H NMR spectrum of the spacer-armed retinal analog **13** in $CDCl_3$.

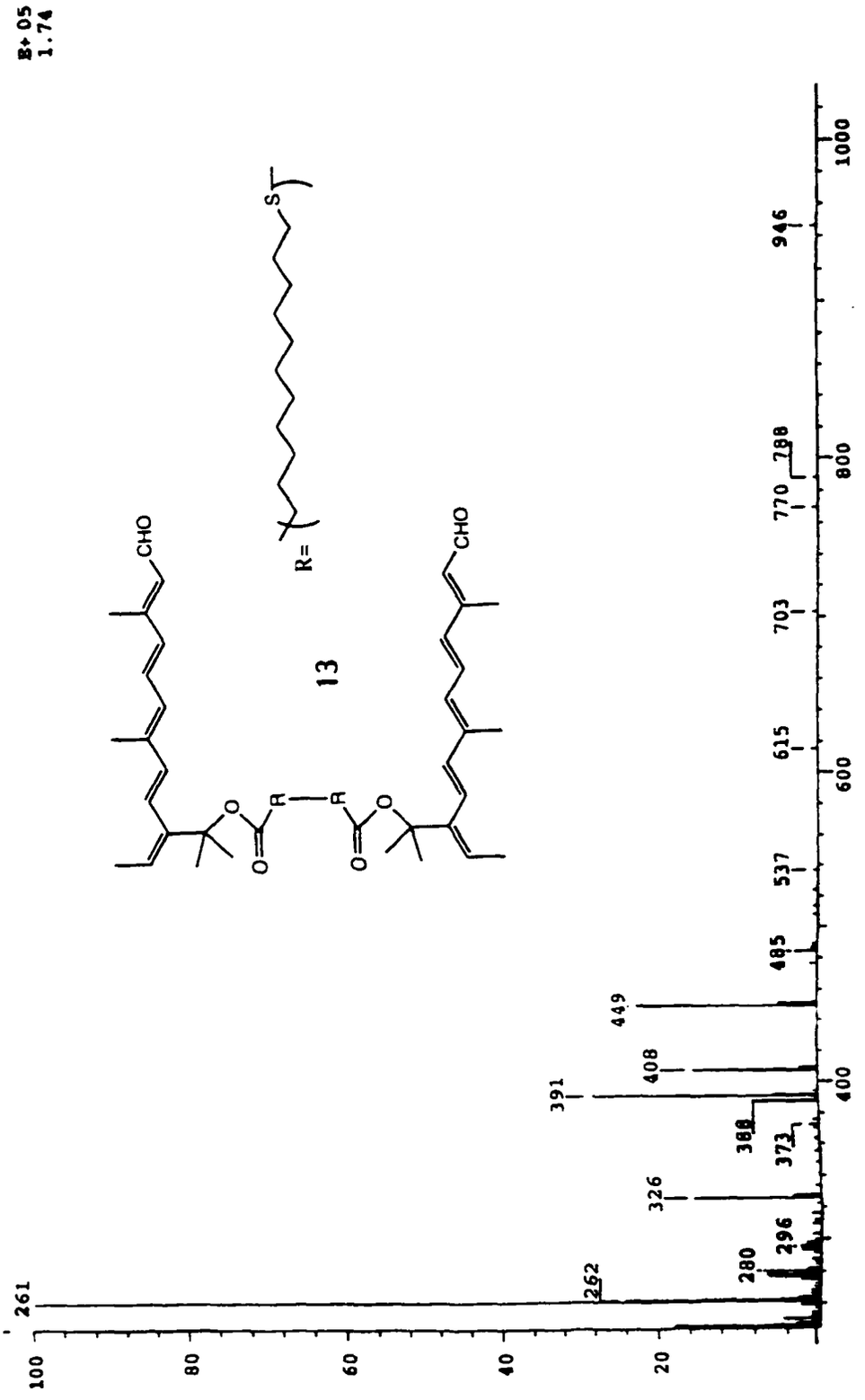

CI-MS (ammonia) spectrum of the spacer-armed retinal analog **13**.

4. REFERENCES

1. D. Oesterhelt and W. Stoeckenius, *Nature New Biol.* **1971**, 233, 149.

2. B.M. Becher and J.Y. Cassim, *Prep. Biochem.*, **1975**, 5, 161.

3. D. Oesterhelt, and W. Stoeckenius, *Proc. Natl. Acad. Sci. USA*, **1973**, 70, 2853.

4. A. Boyer, M. Dery, P. Selles, C. Arbour and F. Boucher, *Biosensors and Bioelectronics*, **1995**, 10, 415.

5. T. Miyasaka, K. Koyama and I. Otoh, *Science*, **1992**, 255, 342.

6. R.R. Birge, *Annu. Rev. Phys. Chem.*, **1990**, 41, 683.

7. D. Oesterhelt, C. Brauchle and N. Hampp, *Q. Rev. Biophys.*, **1991**, 24, 425.

8. V. Balogh-Nair and K. Nakanishi In "*Chemistry and Biology of Synthetic Retinoids*, " M. I. Dawson, W. H. Okamura. Eds., CRC Press, 1990, pp. 147-176.

9. V. Balogh-Nair In "*Biophysical Studies of Retinal Proteins*," T. G. Ebrey, F. Frauenfelder, B. Honig and K. Nakanishi, Eds., University of Illinois Press, 1987, pp.52-57.

10. V. Balogh-Nair, L. Chen and W.-X. Li. *Biophys. J.*, **1988**, 53, 471a.

11. V. Balogh-Nair, L. Chen and W.-X. Li. *Biophys. J.*, **1989**, 55, 255a.

12. V. Balogh-Nair, L. Chen and W.-X, Li. *Biophys. J.*, **1991**, 59, 328a.

12. V. Balogh-Nair, L. Chen and W.-X, Li. *Biophys. J.*, **1991**, 59, 328a.

13. R. Henderson and P.N.T. Unwin, *Nature*, **1975**, 257, 28.

14. H.G. Khorana, G.E. Gerber, W.C. Herlihy, C.P. Gray, R.J. Anderegg, K. Nihei and K. Biemann, *Proc. Natl. Acad. Sci. USA* , **1979**, 76, 5045.

15. Yu. A. Ovchinnikov, N.G. Abdulaev, M.Yu Feigina, A.V. Kiselev and N.A. Lobanov, *FEBS Lett.*, **1979**, 100, 219.

16. R.G. Dunn, J. McCoy, M. Simsek, A. Majumdar, S.H. Chang, U.L. Rajbhandary and H.G. Khorana, *Proc. Natl. Acad. Sci. USA*, **1981**, 78, 6744.

17. (a) D.A. Agard and R.M. Stroud, *Biphys. J.*, **1982**, 37, 589.
(b) J. Trewhella, S. Anderson, R. Fox, E. Gogol, S. Khan, D.M. Engelman and G. Zaccai, *Biophys. J.*, **1983**, 42, 233.
(c) M.P. Heyn, J. Westerhausen, I. Wallat and F. Seiff, *Proc. Natl. Acad. Sci. USA*, **1988**, 85, 2146.

18. K.-S. Huang, R. Radhakrishnan, H. Bayley and H.G. Khorana, *J. Biol. Chem.*, **1982**, 257, 13616.

19. T.W. Kahn and D.M. Engelman, *Biochemistry*, **1992**, 31, 6144.

20. R. Henderson, J. Baldwin, T. Ceska, F. Zemlin, E. Beckmann, and K. Downing, *J. Mol. Biol.*, **1990**, 213, 899.

21. (a) H.D. Lemke and D. Oesterhelt, *FEBS Lett.*, **1981**, 128, 255.
(b) A. Mullen, A.H. Johnson and M. Akhtar, *FEBS Lett.*, **1981**, 130, 187.
(c) H. Bayley, K.-S. Huang, R. Radhakrishnan, A.H. Ross, Y. Takagaki and H.G. Khorana, *Proc. Natl. Acad. Sci. USA*, **1981**, 78, 2225.

22. A. Lewis, J. Spoonhower, R.A. Bogomolni, R.H. Lozier, and W. Stoeckenius, *Proc. Natl. Acad. Sci. USA*, **1974**, 71, 4462.

23. P. Scherrer, W. Stoeckenius, M.K. Mathew, and W. Sperling, In "*Biophysical Studies of Retinal Proteins*," T.G. Ebrey, H. Frauenfelder, B. Honig and K. Nakanishi, eds.), University of Illinois Press, Urbana, p. 206, 1986.

24. B. Aton, A.G. Doukas, R.H. Callender, B. Becher and T.G. Ebrey, *Biochemistry* , **1977**, 16, 2995.

25. (a) K.J. Rothschild and H. Marrero, *Proc. Natl. Acad. Sci.* USA, **1982**, 79, 4045. (b) K. Bagley, G. Dollinger, L. Eisenstein, A.K. Singh and L. Zimanyi, *Proc. Natl. Acad. Sci. USA*, **1982**, 79, 4972.

26. F. Derguini, C. Caldwell, M.G. Motto, V. Balogh-Nair and K. Nakanishi, *J. Am. Chem. Soc.* ,**1983**, 105, 646.

27. P. Dupuis, F.J. Harosi, C. Sandorfy, J.M. Leclercq and D. Vocelle, *Rev. Can. Biol.*, **1980**, 39, 247.

28. G.S. Harbison, J. Herzfeld and R.G. Griffin, *Biochemistry*, **1983**, 22, 1, 29.

29 Y. Cao, G. Varo, M. Chang, B. Ni, R. Needleman and J.K. Lanyi, *Biochemistry*, **1991**, 30, 10972.

30. G.S. Harbison, S.O. Smith, J.A. Pardoen, C. Winkel, J. Lugtenburg, J. Herzfeld, R. Mathies and R.G. Griffin, *Proc. Natl. Acad. Sci. USA*, **1984**, 81, 1706.

31. G.S. Harbison, S.O. Smith, J.A. Pardoen, J.M.L. Courtin, J. Lugtenburg, J. Herzfeld, R.A. Mathies and R.G. Griffin, *Biochemistry*, **1985**, 24, 6955.

32. G.S Harbison, P.P. Mulder, J.A. Pardoen, J. Lugtenburg, J. Herzfeld and R.J. Griffin, *J. Am. Chem. Soc.*, **1985**, 107, 4809.

33. F. Creuzet, A. McDermott, R. Gebhard, K. Van der Hoef, M.B. Spijker-Assink, J. Herzfeld, J. Lugtenburg, M.H. Levitt, and R.G. Griffin, *Science* , **1991**, 251, 783.

34. M.P Heyn, R.J. Cherry and U. Muller, *J. Mol. Biol.*, **1977**, 117, 607.

35. T. Hauss, S. Grzesiek, H. Otto, J. Westerhausen and M.P. Heyn, *Biochemistry*, **1990**, 29, 4904.

36. Leder, R.O., Helgerson, S.L. and Thomas, D.D. *J. Mol. Biol.*, **1989**, 209, 683.

37. J.Y. Huang and A. Lewis, *Biophys. J.*, **1989**, 55, 835.

38. R.A. Mathies, S. Lin, J. Ames and W. Pollard, *Annu. Rev. Biophys. Biophys. Chem.*, **1991**, 20, 491.

39. T.G. Ebrey, R. Becher, B. Mao and P. Kilbridge, *J. Mol. Biol.***1977**, 112, 377.

40. V. Balogh-Nair, J.D. Carriker, B. Honig, V. Kamat, M.G. Motto, K. Nakanishi, R. Sen, M. Sheves, M. Arnaboldi-Tanis, and K. Tsujimoto, *Photochem. Photobiol.*, **1981**, 33, 483.

41. K. Nakanishi, V. Balogh-Nair, M. Arnaboldi, K. Tsujimoto, and B. Honig, *J. Am. Chem. Soc.*, **1980**, 102, 7945.

42. M. Okabe, V. Balogh-Nair and K. Nakanishi, *Biophys. J.*, **1984**, 45, 272a.

43. F. Derguini, D. Dunn, L. Eisenstein, K. Nakanishi, K. Odashima, V.J. Rao, L. Sastry and J. Termini, *Pure & Appl. Chem.*, **1986**, 58, 719.

44. J. Lugtenburg, M. Muradyn-Szweykowska, J. Heeremans, J.A. Pardoen, G.S. Harbison, J. Herzfeld, R.G. Griffin, S.O. Smith and R.A. Mathies, *J. Am. Chem. Soc.*, **1986**, 108, 3104.

45. J.K. Lanyi, *Biochim. Biophys. Acta*, **1993**, 1183, 241.

46. M.S. Braiman, T. Mogi, T. Marti, L.J. Stern, H.G. Khorana and K.J. Rothschild, *Biochemistry*, **1988**, 27, 8516.

47. J. Heberle and N.A. Dencher, *Proc. Natl. Acad. Sci. USA*, **1992**, 89, 5996.

48. K. Gerwert, G. Souvignier and B. Hess, *Proc. Natl. Acad. Sci. USA*, **1990**, 87, 9774.

49. Y. Cao, L.S. Brown, R. Needleman and K. Lanyi, *Biochemistry*, **1993**, 32, 10239.

50. M. Nonella, A. Windemuth and K. Schulten, *Photochem. Photobiol.*, **1991**, 54, 937.

51. I. Logunov and K. Schulten, *J. Am. Chem. Soc.*, **1996**, 118, 9727.

52. G. Varo and J.K. Lanyi, *Biophys. J.*, **1991**, 59, 313.

53. L. Zimanyi, G. Varo, M. Chang, B. Ni, R. Needleman and J. K. Lanyi, *Biochemistry*, **1992**, 31, 8535.

54. R. Sen, R. T. Widlansky, V. Balogh-Nair and K. Nakanishi, *J. Am. Chem. Soc.*, **1983**, 105, 5160.

55. V. Balogh-Nair, C.E. Brathwaite, C.-X. Chen, L. Chen and S. Saba, 10th Internat. Congress on Photobiol., Jerusalem, Israel, Oct. 1988, Abstr. 125.

56. T. Nakayama and H.G. Khorana, *J. Org. Chem.*, **1990**, 55, 4953.

57. W.-D. Ding, A. Tsipuras, H. Ok, T. Yamamoto, M.A. Gawinowicz and K. Nakanishi, *Biochemistry*, **1990**, 29, 4898.

58. R. G. Nuzzo and D. L. Allara, *J. Am. Chem. Soc.*, **1983**,

105, 4481.

59. A. Ullman, Introduction to Ultrathin Films: *From Langmuir-Blodgett Films to Self-Assembly*, Academic Press, Boston, 1991.

60. L.H. Dubois and R.G. Nuzzo, *Annu. Rev. Phys. Chem.*,**1992**, 43, 437.

61. A. Ullman, *Chem. Rev.*, **1996**, 96,1533.

62. G.J. Legget, C.J. Roberts, P.M. Williams, M.C. Davies, , D.E. Jackson and S.J.B. Tendler, *Langmuir*, **1993**, 9, 2356.

63. G. M. Whitesides, D.L. Allara, A.N. Parikh and S.V. Atre, *J. Am. Chem. Soc.*, **1995**, 117, 9529, and references therein.

64. L. Chen, Ph.D. Dissertation, City University of New York, 1993.

65. S.D. Young, C.T. Buse and C.H. Heathcock, *Organic Syntheses* . G. Saucy, Ed., **1984**, 63, 79; C.H. Heathcock, C.T. Buse, W.A. Kleschick, M.C. Pirrung, J. Sohn and J. Lampe, *J Org. Chem.*, **1980**, 45, 1066.

66. J.E. McMurry and W.J. Scott, *Tetrahedron Lett.*, **1983**, 24, 979.

67. W.J. Scott and J.E. McMurry, *Accts. Chem. Res.*, **1988**, 21, 47.

68. W.J. Scott, M.R. Pena, K. Sward, S.J. Stoessel and J.K. Stille, *J. Org. Chem.*, **1985**, 50, 2302.

69. R.F. Heck, *Pure & Appl. Chem.*, **1981**, 53, 2323.

70. E.J. Corey, D. Enders, M.G. Bock, *Tetrahedron Lett.*, **1976**, 7; E.J. Corey and A.G. Myers, *Tetrahedron Lett.*, **1984**, 25, 3559.

72. B. Neises and W. Steglich, *Angew, Chem. Int. Ed. Engl.*, **1978**, 17, 522.

73. A. Hassner, L. Krepski and V. Alexanian, *Tetrahedron*, **1978**, 34, 2069.

74. A. Hassner and V. Alexanian, *Tetrahedron Lett.*, **1978**, 4475.

Part II.

PART II. SYNTHESIS OF ANTIFUNGALS CONTAINING NOVEL PHARMACOPHORES.

1. INTRODUCTION

Once considered a nuisance, fungi are becoming a serious public-health hazard. Epidemiologic studies in the mid-1980s, provided the first evidence that almost 40% of all deaths from hospital-acquired infections are not caused by bacteria or viruses, but by fungi. Over the past decade, the incidence of fungal infections has increased even more dramatically.[1] Although the human immunodeficiency virus (HIV) type 1 epidemic accounts for a large share of this increase, fungi had begun praying on the growing population of patients with impaired immune systems due to cancer chemotherapy, drug treatments with azoles, drugs designed to prevent rejection of transplanted organs, burn patients, and older patients because immune function declines with age. The dearth of effective and safe drugs, the emergence of drug-resistant species, the growing list of pathogens, all contribute to the emerging fungal threat. In the race against this fungal threat, novel strategies are needed to successfully prevent and treat fungal diseases. A new strategy towards the development of antifungals is described below. This strategy is based on the recent discovery of novel antifungal oxidoredox pharmacophores.[2] To generate new types of antifungals, three of these pharmacophores, oxaziridines, metallomacrocycles and nitronyl nitroxides were inserted, by syntheses, into macrocyclic, podand and dendrimeric carrier structures. The antifungal activity of the compounds synthesized is assessed in collaborative studies.

Since the discovery of crown ethers by Pedersen,[3] new ideas about macrocyclic ligand complexation chemistry,[4] host-guest complementary principles,[5] molecular recognition and supramolecular chemistry,[6] have been developed, and thousands of macrocycles have been synthesized. While the crown ethers have enjoyed widespread applications in analytical and separation chemistry, a plethora of macrocyclic compounds now benefits fields as diverse as materials science, biology and medicine. The syntheses of the first poly-oxa crown ethers, macrocyclic polyethers bearing oxygen as donor atoms, was followed by the syntheses of 'thiacrowns', 'azacrowns' and other macrocycles in which one or more types of heteroatoms, such as O, N, S, P, Se, etc. were incorporated as donors into the macrocyclic rings. Cryptands and spherands consisting of one ring, and cavitands that are multi-rings have also been synthesized for different purposes. Among the strategies for obtaining macrocycles, the most useful syntheses include Williamson type nucleophilic substitution and macrocyclization reactions. The two categories of macrocyclizations are 'direct' syntheses in which no template is involved, and 'template' syntheses in which cyclizations with unfavorable entropy factors are promoted by a metal ion. The importance of macrocyclic chemistry cannot be overemphasized: macrocycles and their complexes with a variety of ligands are useful models to study complex processes occurring in biological systems. Thus, the elucidation of the mechanism of photosynthesis and oxygen transport in respiratory systems benefited greatly from studies with model macrocyclic compounds. Studies with macrocyclic host-guest compounds deepened our understanding of how molecular interactions form the basis of the highly specific recognition,

transport and regulation, processes found in biological systems. Prominent examples are substrate binding to receptor proteins, enzymatic reactions, assembly of protein-protein complexes, antigen-antibody association, transcription of the genetic code, and cellular recognition. Further, a number of synthetic macrocycles are potent inhibitors of HIV-1.[7-9] Here, we use the capacity of macrocycles to accommodate multiple pharmacophore units to design antifungal drugs with structures containing up to six units of a novel pharmacophore.[10]

Less effective than macrocycles as to accommodating multiple pharmacophore units, podands are nevertheless attractive pharmacophore carriers because of their comparative ease of synthesis.[2] Thus, before undertaking the syntheses of the more complex macrocyclic structures, podands can be employed to explore the effects of the modification of pharmacophore's structure on the antifungal activity.

Dendrimers are polymers prepared by repetitive branching from a central core. Since the first report of their synthesis,[11] their chemistry has experienced a spectacular development and very recently, dendrimer functionalization has received substantial attention. The numerous applications of dendrimers[12] include redox-active dendrimers useful in electron transfer studies,[13] glycomimetics that present multiple copies of sugar ligands on the surfaces of dendrimers to mimic biological recognition processes,[14] preparation of nanoclusters[15] within dendrimer "nanoreactors," dendrimers with very precise chemical constitution and well-defined molecular structures to generate materials with unique properties,[12]

dendrimeric monolayers useful in the construction of chemical sensor arrays,[16] and dendrimers used for drug delivery.[12] However, before our studies, the application of dendrimers for drug delivery was limited to utilization of their polymeric properties, and all of these applications involved large, (n+1) generation dendrimers. In the present work, a first generation starburst dendrimer structure serves as template for the synthesis of a drug with multiple pharmacophore units and high antifungal activity.

This introduction describes the syntheses of macrocyclic and other carrier structures, and details the syntheses and properties of the novel oxidoredox pharmacophores that led to the development of a new breed of antifungals.

1.1. Synthesis of macrocyclic imines and amides.

1.1.1 Synthesis of macrocyclic imines.

Schiff-base condensations (Scheme 1) have played a prominent role in macrocyclic chemistry, and macrocyclic Schiff bases served as starting materials for some of our target compounds.

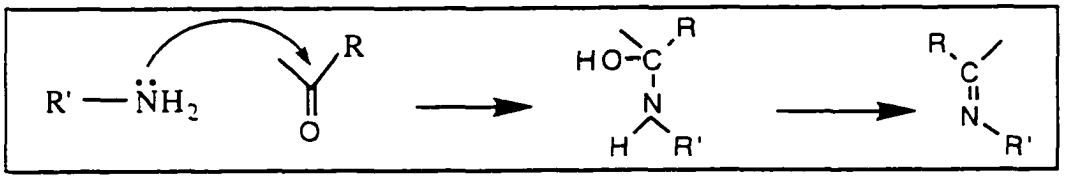

Scheme 1.

Bell and co-workers[17] reported a template directed synthesis of the hexa-aza macrocycle **1**, by condensation of *o*-phenylenediamine with pyridine-2,6-dicarboxaldehyde. Subsequent metal exchange and demetallation steps afforded the metal-free macrocycle, **3**, albeit in

low yield (Scheme 2). Further, NMR and X-ray studies[18] showed that the macrocycle **3** is very flexible and it has poor solubility in organic solvents, hence this type of compound has limited use.

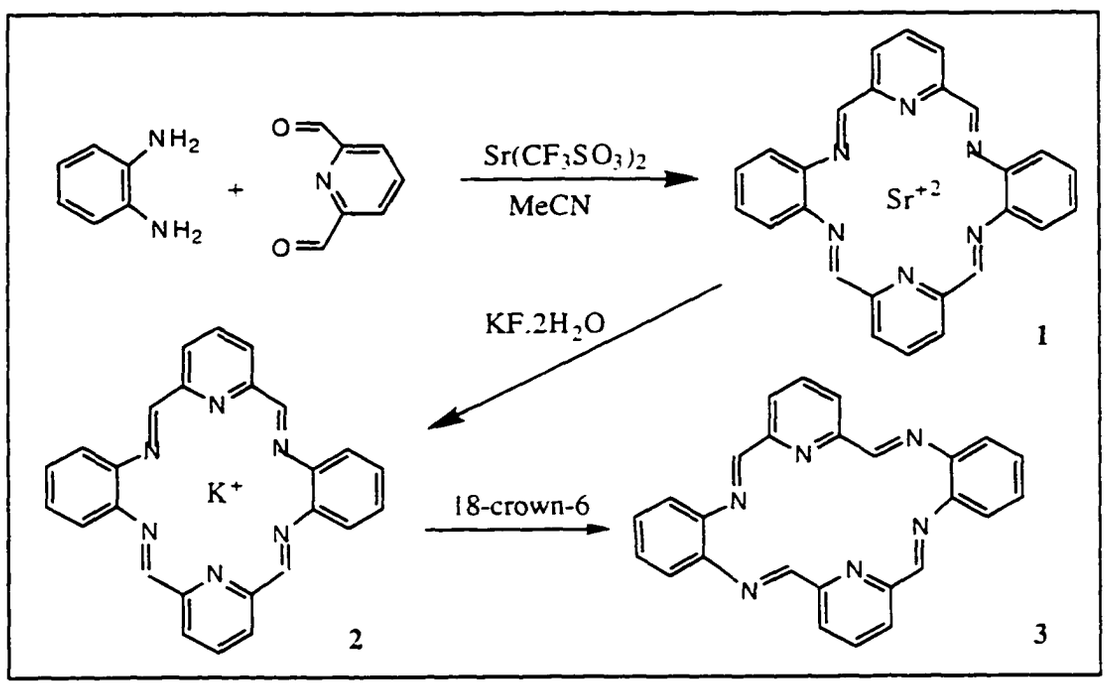

Scheme 2.

Nelson and co-workers developed a simple, one pot synthesis which generated a new group of cryptands of considerable potential.[19-20] Thus, cryptands of the type **4** were synthesized by [3+2] condensations of a series of dicarbonyl compounds with the tripodal amine, tris(2-aminoethyl)amine (Scheme 3). Since the yields of these macrocyclizations was in the range of 45-60%, these syntheses represent a valuable route to a new family of cryptating molecules that have the capacity to act as bi- or tri-nucleating ligands for transition metal ions or may serve as receptors for small organic substrates.

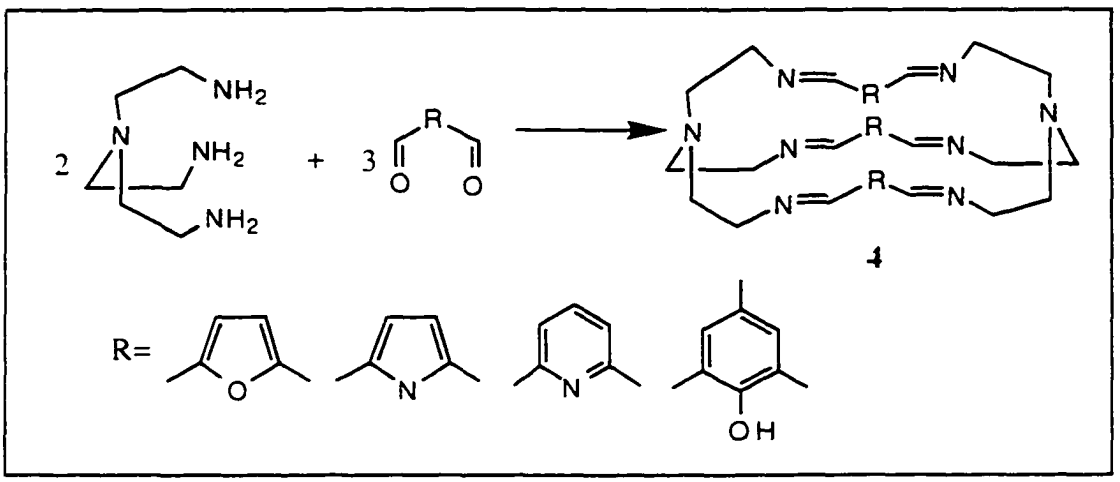

Scheme 3.

Ditopic macropolycyclic ligands yield binuclear cryptates of different types which depend on the nature of binding subunits incorporated in the structures.[20] Lehn and co-workers[21] reported an efficient route to ditopic macrobicyclic ligands, such as **5**, via multiple (amine + aldehyde) condensations. Compared to Nelson's cryptands these macrocycles have much larger cavities and can accommodate two metal ions. Compound **6**, the copper(I) complex of the macrobicyclic

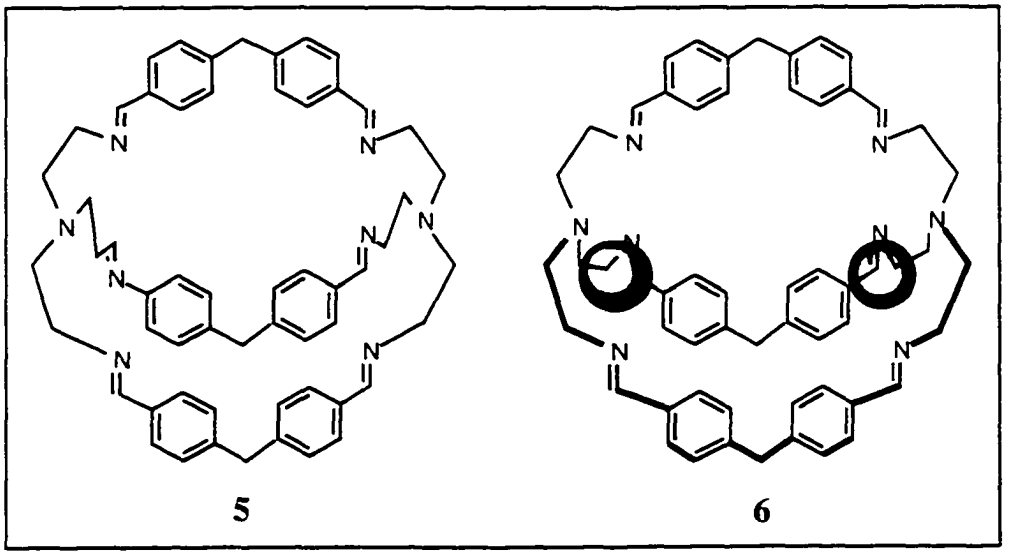

ligand **5**, is a binuclear macrobicyclic cryptate of axial type in which two Cu(I) ions are held inside the cavity, each bound by one of the tripodal (amine, tri-imine) subunits located at the poles of the ligand.

Martell,[22] reviewing the methods of one step [2+2] and [3+2] amine and aldehyde condensations, stressed the importance of the solvent employed. In the synthesis of macrobicyclic cryptands the best yields were obtained using MeOH. Further, successful synthesis of macrocyclic and macrobicyclic Schiff bases by [2+2] or [3+2] condensation of dialdehydes with *bis* or *tris* primary amines requires, in addition to a suitable solvent, a rigid dialdehyde with its carbonyl groups extending toward the bridging position.

The importance of metal complexes of 2,2'-bipyridine in photochemistry, photophysics, and in the splitting of water led to incorporation of multiple 2,2'-bipyridyl units into macrocyclic structures. Thus, two groups have synthesized the macrobicyclic tris-bipyridine ligand **7** by template-free [3+2] condensation of 4,4'-diformyl-2,2'-bipyridine with tris(2-aminoethyl)amine.[23-24]

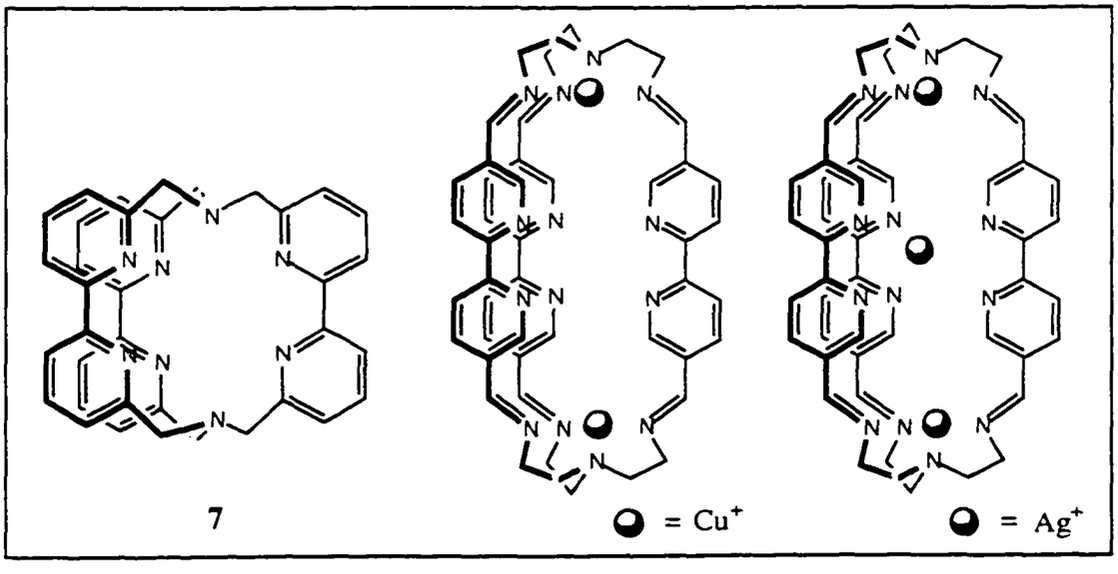

Lehn's group[24] has shown that the tris-bipyridyl ligand **7** is endowed with remarkable complexation properties, readily forming dinuclear bis-Cu(I) and trinuclear tris-Ag(I) complexes in high yields.

1.1.2. Synthesis of macrocyclic amides.

In the early eighties,[25] it was established that deprotonated amide ligands confer thermodynamic stability to Cu(III) and Ni(III) states, and that it is the strong amido-N σ donor capacity that is responsible for the stabilization of these high oxidation states. Since then, driven by the potential applications of stable, highly oxidizing metal centers as catalysts and as models for biological oxidations, a large number of macrocyclic amides was synthesized using either templated or non-templated routes.[26] In the following, only selected examples of tetraamido macrocycles, germain in structural design to the novel antifungal agent **VBN-10**, will be described to illustrate the difficulties encountered in the synthetic methodologies.

Hunter[27] reported the synthesis of the tetraamide macrocycle **8**, using a one-step, [2+2] macrocyclization reaction, albeit in low yield (Scheme 4). In an attempt to improve the yield (10%) of macrocycle **8**, a two step synthesis was developed:[28] The [2+1] condensation product of the diamine with diacid chloride was prepared first, then the podand obtained was reacted further with the diacid chloride to obtain **8**. However, this route yielded three major products; in addition to macrocycle **8**, a cyclic tetramer, **9**, and a [2]-catenane, **10**, were isolated. It is interesting to note that the [2]-catenane, **10**, is locked into a well-defined conformation by a combination of H-bonds and π-π interactions, and it is these interactions that template the formation of the interlocked ring system.

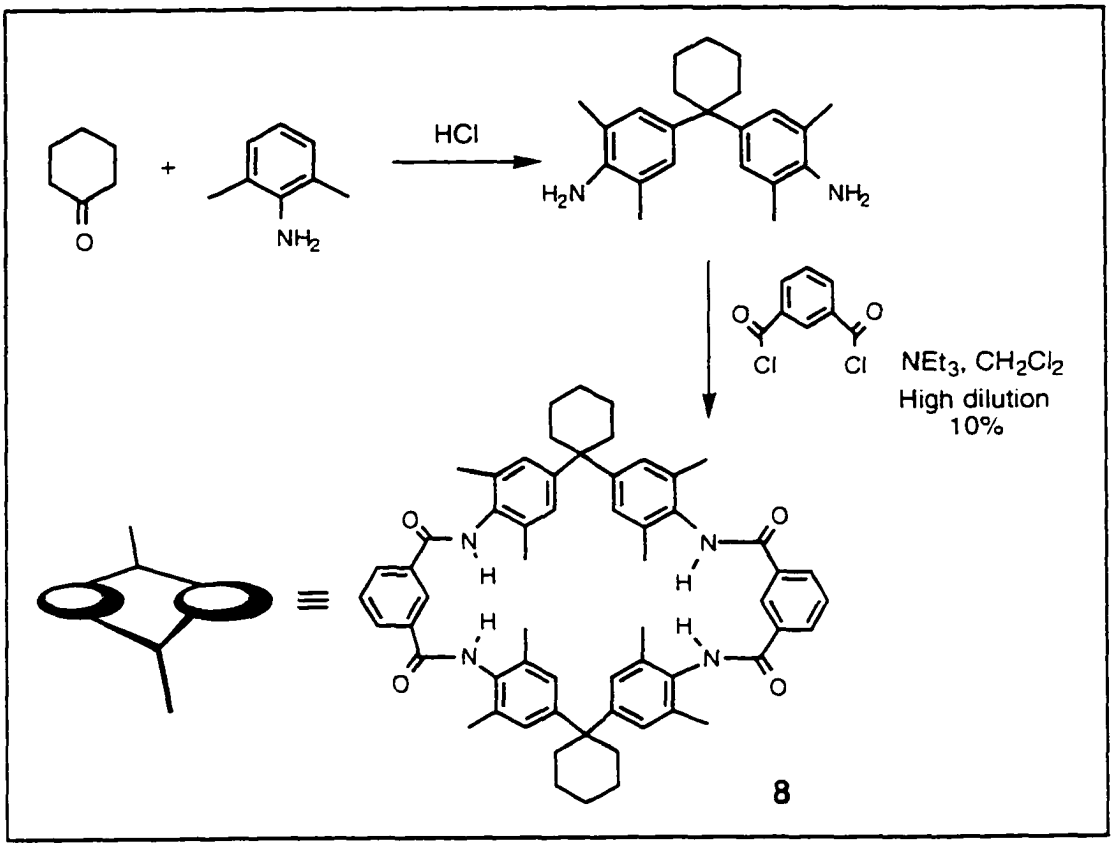

Scheme 4.

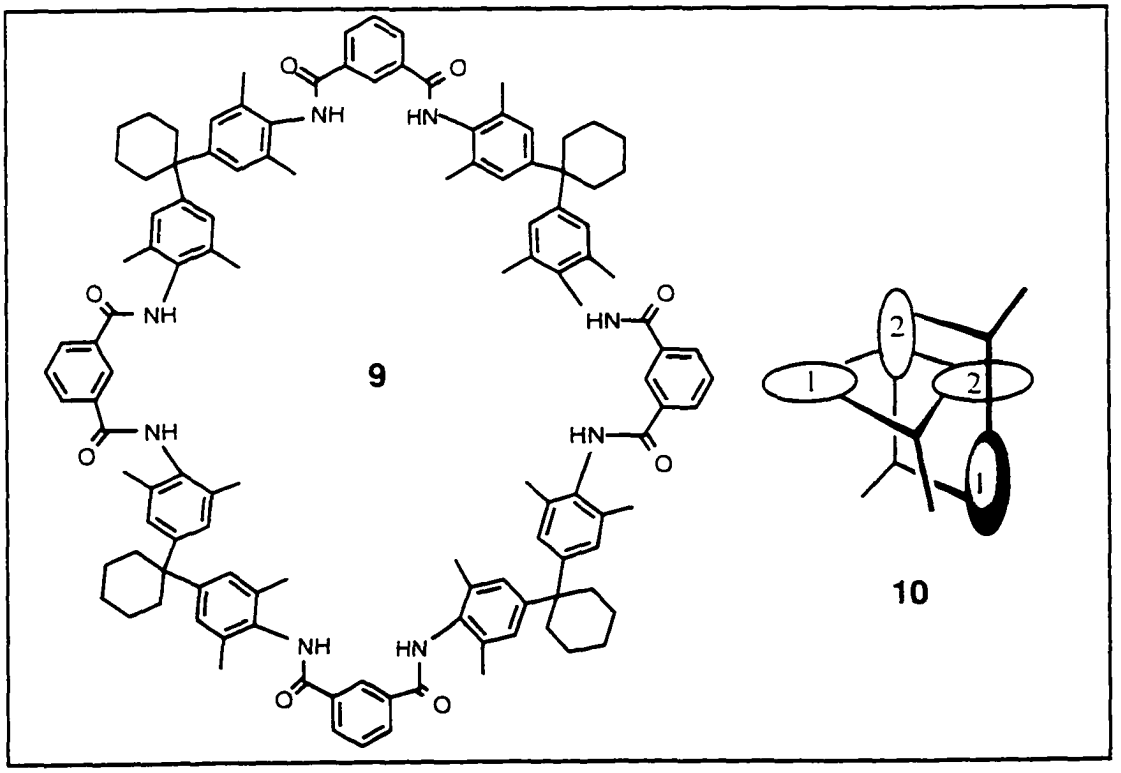

Collins' group[29] succeeded in preparing tetraamide macrocycle **11**, according to the procedures summarized in Scheme 5. The synthesis was not without difficulties. Only after investigating a series of unsuccessful pathways to obtain the diamide diamines (D) did they find that the diazides intermediates (C), not isolated or stored, could be converted reproducibly to the pure diamide diamines (D) in high yields. The macrocyclization reaction of the latter to the tetraamide macrocycles, in 20-30% yields, was accompanied by the concomitant formation of four-membered ring mono- and diimides produced by alternative intramolecular cyclization processes.

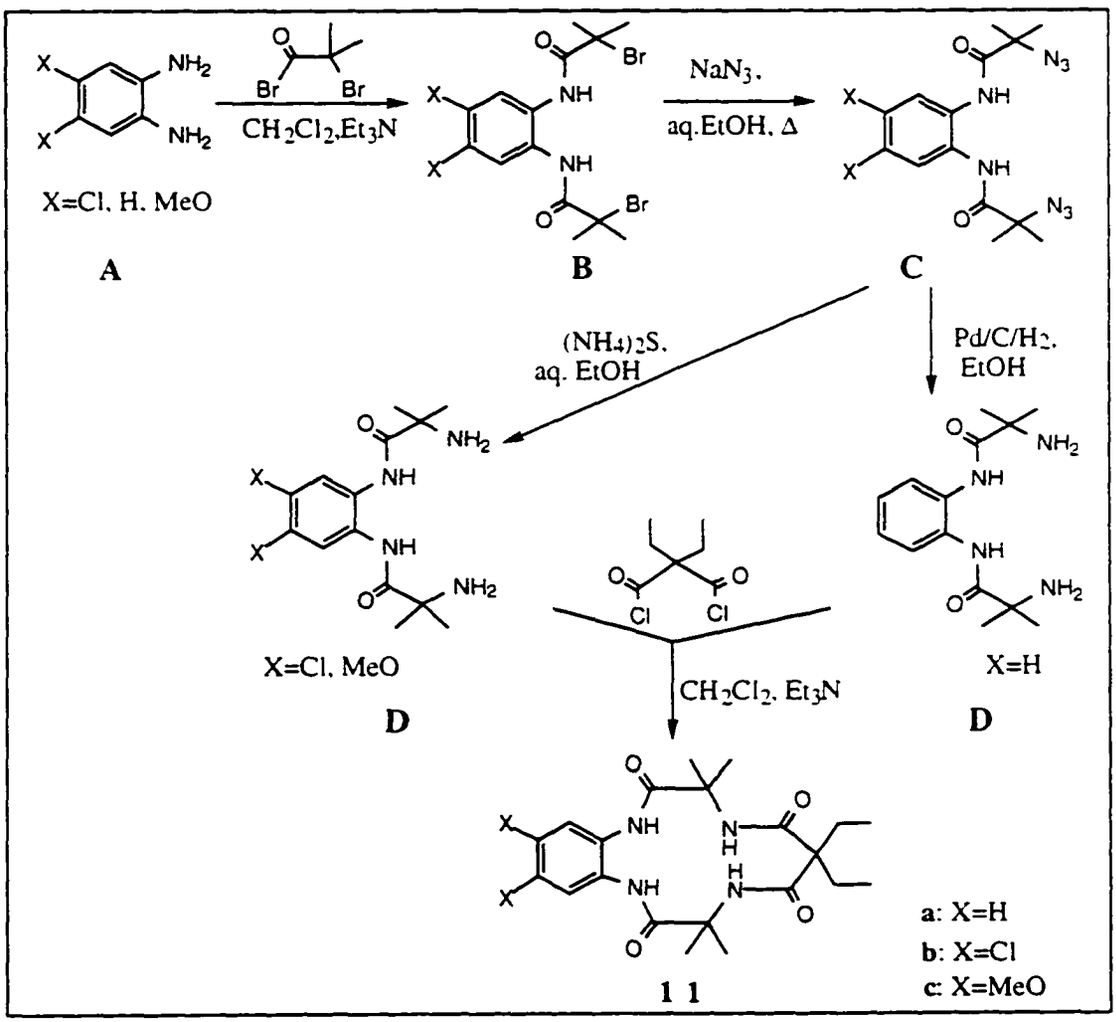

Scheme 5.

1.2. Metal complexes of macrocyclic amides.

Current interest in high valent metal species, such as tervalent nickel and iron(IV), stabilized by macrocyclic ligands stems from their role as oxidation catalysts, DNA cleaving agents, and small molecule mimics of the active sites found in oxidases such as P-450.

Tetraamide macrocycles do not complex metals because the protonated amide does not contain a σ-donating lone pair to lead the coordination process. However, tetradeprotonation affords strongly donating tetraamido-N ligands that are resistant to oxidative destruction. Collins *et al.*[29] developed efficient procedures for metal insertion applicable to metals such as manganese, iron, cobalt, and nickel. To insert metals into polyamide macrocycles it is best to use dry THF as solvent, low temperatures when bases strong enough to decompose THF are employed, strong bases to deprotonate the ligand prior to metal addition, and use divalent metal salts which have some solubility in THF. In this manner, metal insertion into the tetraamide ligands, followed by oxidation, yielded hydrolytically stable complexes, such as **12**[30] and **13**[31] (Scheme 6 and 7).

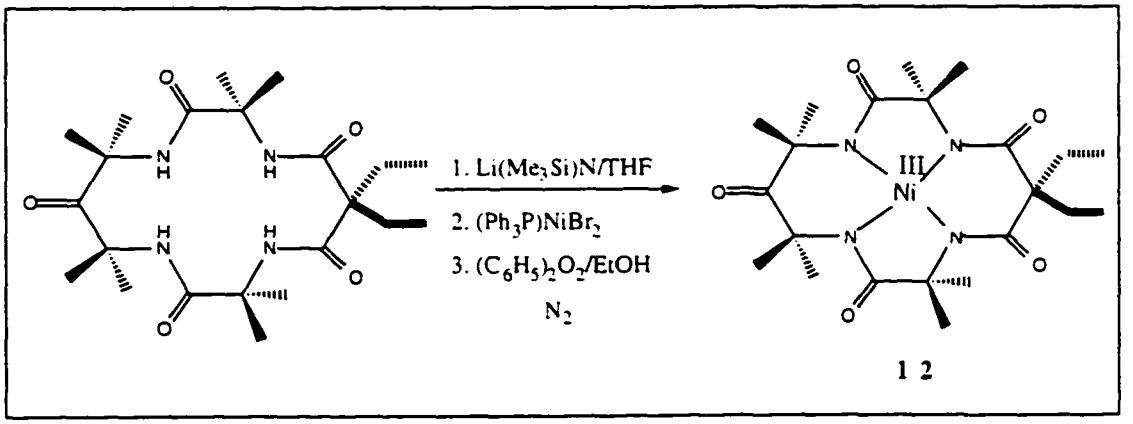

Scheme 6.

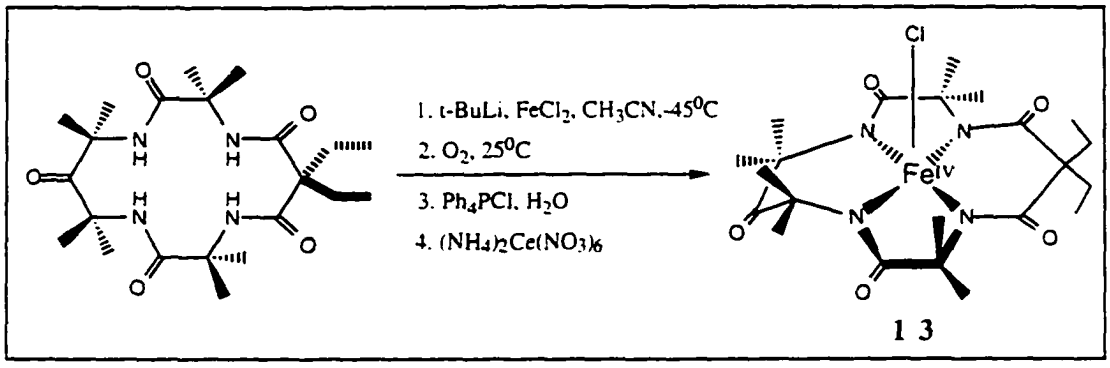

Scheme 7.

1.2.1. DNA cleavage by macrocyclic complexes.

Site-specific recognition and cleavage of DNA using coordination compounds continues to be an area of considerable interest.[32] Ni(II) square planar complexes in the presence of potassium monopersulfate or magnesium monoperoxyphthalate (MMPP), induce guanine-specific modification of single-stranded oligonucleotides leading to strand scission after treatment with base.[33] The postulated mechanism involves direct ligation of nickel to guanine to form the key intermediate, an octahedral nickel(III) species, followed by base oxidation (Scheme 8).[34]

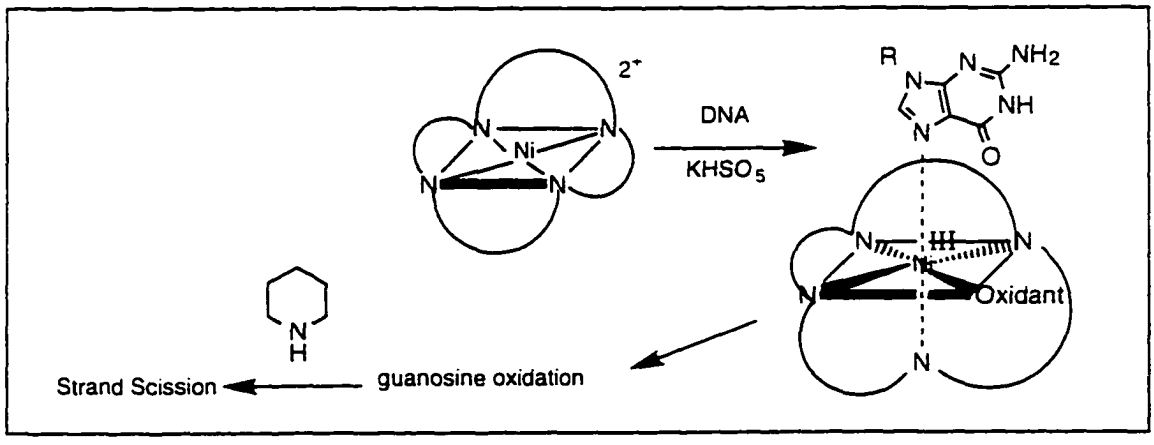

Scheme 8.

Furthermore, systematic studies of the ligand effects using Ni(II) complexes of a series of macrocyclic Schiff base ligands,[34] allowed prediction of features of the complexes that affect their catalytic activity: (1) square-planar Ni(II) complexes are adequate, octahedral ones are not effective; (2) the cavity size of the macrocyclic ligand;[35] (3) the overall charge of the coordination complex, and (4) the redox potential associated with the Ni(II)/Ni(III) redox couple.[36] In addition, the nature of the terminal oxidant is of critical importance: $KHSO_5$ and MMPP were effective as oxidants, but peracetic acid displayed a diminished activity and H_2O_2 with ascorbate was ineffective. The use of molecular oxygen as terminal oxidant is detailed below.

Although reactions of molecular oxygen with Fe(II), Co(II), and Mn(II) peptide complexes were described in the mid-seventies, the first Ni(II)-O_2 complex was reported only a decade later.[37] Furthermore, before this report, the redox potential of Ni(III)/Ni(II) couple was considered too high to permit generation of Ni(III) states by air oxidation. Kimura *et al.*[37] prepared Ni(II)-O_2 complexes, **15a-b**, from dioxopentamines, and apparently these complexes could be activated to yield Ni(III) species, **16a-b**, effective in the oxygenation of aromatic substrates to phenolic products. A series of analogs of **14** were also examined for reactivity with plasmid DNA by Burrow's group.[38] Nickel and O_2-dependent strand scission was observed for complexes of **14a** and **14c**. These ligands immediately form green complexes with Ni^{2+} in water in which only the three amino nitrogens of the macrocycle are coordinated. Raising the pH to about 9 effects amide deprotonation to yield the purple

pentacoordinate complexes, **15**. Exposure to air of compounds**15** converted them to **16** having the hexacoordinate Ni(III) superoxido structures.

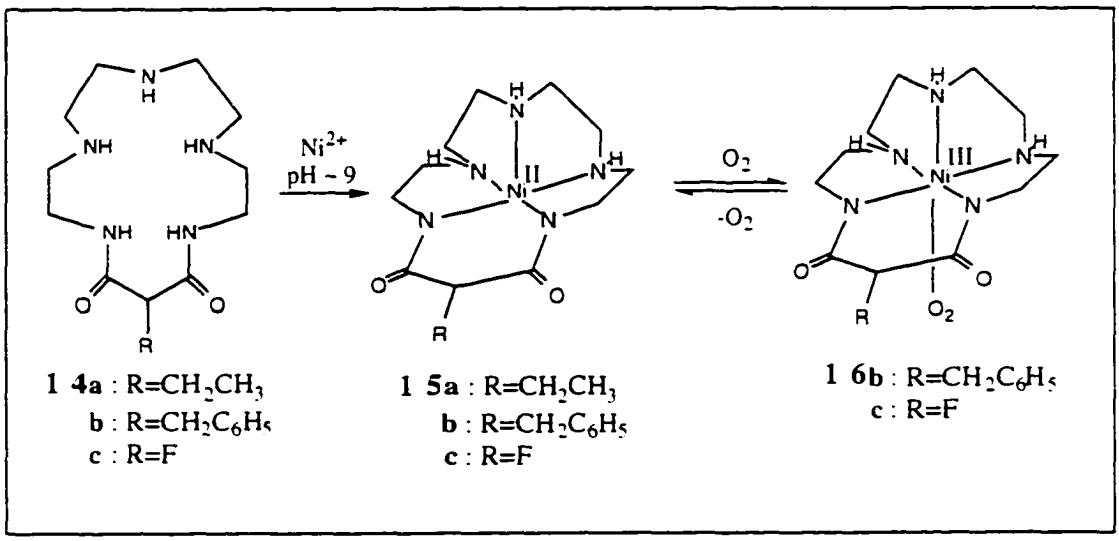

1.2.2. The metallomacrocycle pharmacophore.

Oxygen transfer is among the most important reactions in biology, therefore metal-complex catalyzed transfer of oxygen atoms to organic substrates is of interest in the study of bioorganic mechanisms. Prominent among studies of biomimetic oxygen transfer are metalloporphyrin catalyzed oxidations because of their relationship to enzymatic oxidations with cytochrome P-450. However, a hitherto unexplored aspect of metal-complex catalyzed oxygen transfer is the development of novel antifungal drugs based on the oxidoredox pharmacophore hypothesis.[2] It is in this context that the synthesis and biological evaluation of a nickel containing metallomacrocycle **VBN-10**, an oxygen transfer agent with high antifungal activity, described in Results and Discussion, was undertaken.

Epoxidation of alkenes with terminal oxidants (PhIO, ROOR, NaOCl, etc.) is catalyzed by a variety of square-planar Ni(II) complexes including cyclams and salens.[39-43] In early mechanistic studies[40] an oxygen rebound process was considered most likely (Scheme 9a), and the catalytic activity was tentatively ascribed to an active oxo-nickel(IV) intermediate. When hypochlorite is the terminal oxidant, Hamilton *et al.*[39] proposed that the reactive reagent is the chloroxy radical, ClO•, (Scheme 9b), and that the oxygen transfer in the enzymic reactions of P-450 and related monooxygenases involves Fe(IV)-O•, a high-valent iron-oxygen species. For oxidations with hypochlorite as the terminal oxidant, but with nickel complexes instead of iron as the catalysts, similar mechanisms involving the chloroxy radical were proposed by Burrows (Scheme 10a & 10b).[41] However, in these mechanisms, unprecedented high-valent nickel-oxygen species, (Ni(III)-OCl or Ni(III)-O•) were the putative key intermediates.

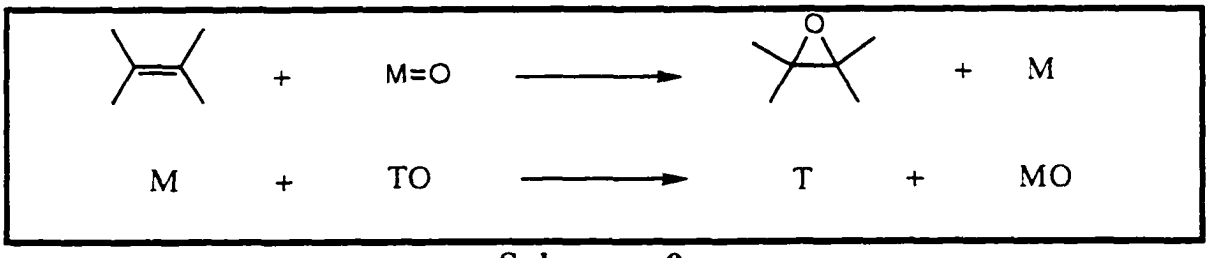

Scheme 9a.

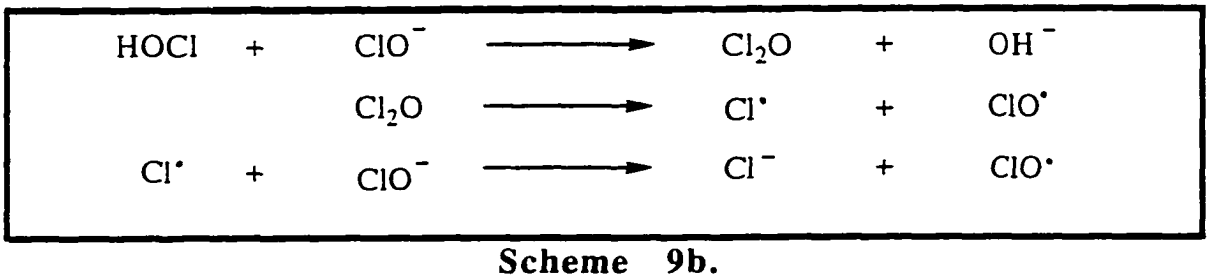

Scheme 9b.

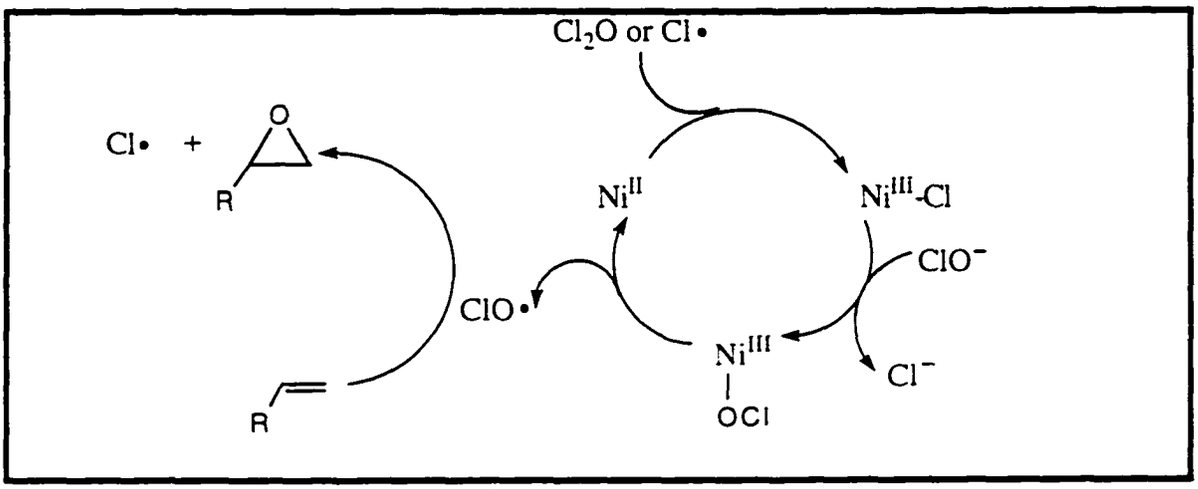

Scheme 10a.

$$LNi^{II} + HOCl \longrightarrow [LNi^{\cdot} - OH]^{+} + Cl^{-} \longrightarrow LNi^{III} - O^{\cdot} + H^{+}$$

$$LNi^{II} + ClO^{-} + H^{+} \longrightarrow LNi^{II}\text{-}O\text{-}Cl\cdots H^{+} \longrightarrow LNi^{III} - O^{\cdot} + HCl$$

Scheme 10b.

Oxidation mechanisms involving hypochlorite as the terminal oxidant are particularly relevant to our studies because stimulated. HOCl-producing neutrophils play a critical role in the immune response and they represent, along with the •NO-producing macrophages, the first line of defense against microorganisms. Thus, in response to fungal attack, the neutrophils' superoxide ($O_2^{\cdot\bullet}$) is dismutated into H_2O_2 which in turn is converted to HOCl by the neutrophils' myeloperoxidase. However, HOCl is not the only important oxidant spewed out by neutrophils. Since its physiological action lasts only ca. three hours, secondary oxidants with longer lifetimes, for instance chloramines, enhance and prolong the microbicidal action. According to the oxidoredox pharmacophore hypothesis,[2] metallomacrocycles could be converted by neutrophils' oxidants to metal-oxo complexes, thereby preserving the oxidizing

equivalent of HOCl in a more effective form to modulate microbicidal action. The antifungal activity of the **VBN-10** metallomacrocycle (see Discussion part) in which nickel is complexed by four deprotonated amide ligands, supports the oxidoredox pharmacophore hypothesis. However, it is not yet possible to ascertain whether interactions with neutrophil components alone accounts for the antifungal effect of **VBN-10**. It is likely that it also forms an adduct with the primary defense molecule of the macrophages, the •NO radical, thereby modulating its concentration and/or transport.

1.3. Oxaziridines.

Oxaziridines were first reported in the mid-fifties.[44-46] and since then extensive investigations of these small heterocycles revealed their unusual reactivity derived from the presence of the strained three-membered ring and a relatively weak N-O bond. Salient features of the chemistry of oxaziridines are, among others, base-induced eliminations, thermal isomerization into nitrones, thermal and photochemical rearrangements to amides, fragmentation with lithium amides (electron transfer reactions), and nitrogen and oxygen transfer reactions.[47-50] Oxaziridines have become widely known because of the synthetic utility of Davis' reagents, the stable and commercially available sulfonyloxaziridines.[51] They are highly successful for sulfur oxidations[52] and have been utilized extensively for the synthesis of chiral α-hydroxycarbonyl compounds.[53] The oxaziridine reagents of Davis along with N-phosphinoyl- and perfluorooxaziridines are

capable of oxygen transfer to olefins, but are not ideal for epoxidation. However, recent rekindling of interest in oxaziridinium salts more reactive than oxaziridines, led to their syntheses in enantiomerically pure form. Lusinchi *et al.*[54] have shown that these enantiomerically pure oxaziridinium salts can be used to achieve catalytic epoxidation of alkenes by Oxone with high enantioselectivities.

Balogh-Nair group's interest in the synthesis of novel oxaziridines stems from their oxygen transferring ability. Already at the time of their discovery, Emmons realized that they are active oxygen compounds, in some respects comparable to organic peroxides, and therefore can be assayed by iodometric procedures. They are members of a class of oxidizing reagents that have their active site oxygens as part of a three-membered ring. The similarity in the structures of metal peroxides, dioxiranes, and oxaziridines suggests that they may have a common mechanism for oxygen transfer, an S_N2-type displacement by the nucleophilic substrate (Z) on the electrophilic oxygen atom (Scheme 11).

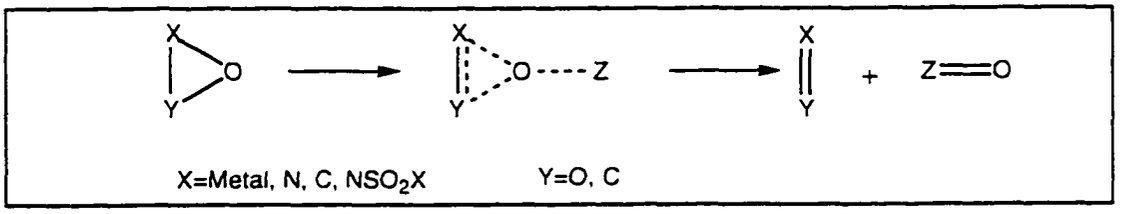

Scheme 11.

The driving force for oxygen transfer in these reagents has been related to relief of ring strain and the enthalpy associated with the formation of double bonds in the products. Oxaziridines, being more

stable than metal peroxides and dioxiranes, are more suitable to study the mechanisms involved in oxygen transfer. According to the oxidoredox pharmacophore hypothesis,[2] because of their ability to transfer oxygen, oxaziridines should display microbicidal action. Previous work in this laboratory led to the syntheses of oxaziridines and sulfonyloxaziridines[10] with high antifungal activities, lending strong support to the oxidoredox pharmacophore hypothesis. This work (Results and Discussion part) represents our continuing efforts to explore the pharmacophore potential of the oxaziridine functionality.

1.3.1. Synthesis and properties of oxaziridines.

The principal routes to N-alkyl and N-aryl oxaziridines[47,48,55] include oxidation of imines, amination of carbonyl compounds, and photochemical isomerization of nitrones. The first of these methods (Scheme 12) is by far the most commonly employed. Many oxidants have been used, peracid oxidation is the most popular, but oxidations with H_2O_2 alone, H_2O_2 with benzoylisocyanate (PhCONHCO-OOH), mixtures of H_2O_2 with nitriles (RC[NH]OOH), H_2O_2-SeO_2, hydroperoxides such as *tert*-amylhydroperoxide with $MoCl_5$ or $Mo(CO)_6$ as catalysts,[56] and transition metal-catalyzed oxidation of imines using molecular oxygen as the terminal oxidant and aldehydes as co-reductants are also known. [57]

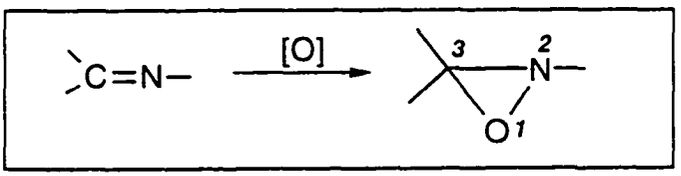

Scheme 12.

The mechanism of the imine peroxy-acid reaction to oxaziridines, contrary to the epoxidation of alkenes, is presumably a stepwise reaction involving protonation of the imine followed by a nucleophilic attack of the basic nitrogen atom on the peroxide bond (Scheme 13). [58-59] Kinetic investigations failed to distinguish between the one-step and two-step mechanisms, but formation of Z/E isomeric mixtures of oxaziridines from sterically definite Schiff bases supports the two-step mechanism.

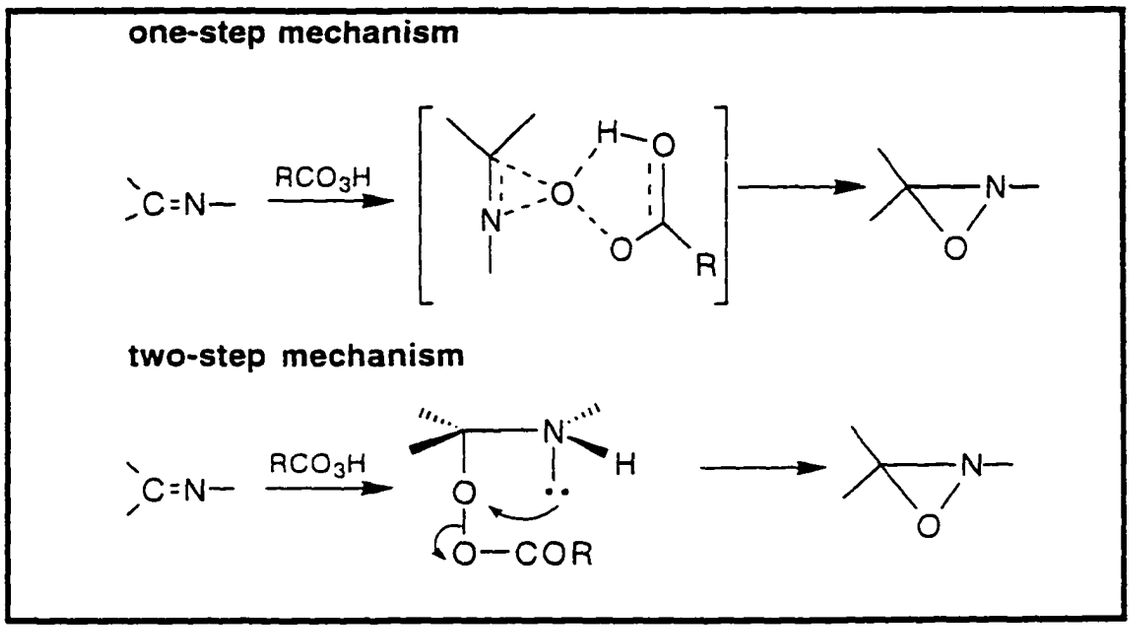

Scheme 13

Peroxy acids used in oxaziridine syntheses include peroxyacetic acid, chiral monopercamphoric acids, perbenzoic acid and *m*-chloroperbenzoic acid (*m*-CPBA), the latter being the most commonly used oxidant. Optically active oxaziridines are usually prepared by oxidation of achiral imines with chiral peracids, by oxidation of chiral imines with achiral peracids, and by oxidation of imines in chiral media. Other methods include treatment of oxaziridines with

brucine, photolysis of nitrones in chiral solvents, and thermal isomerization of oxaziridines in optically active liquid crystals.[60]

The success of the peroxy-acid-imine route to oxaziridines depends on the stability of the parent imine under acidic conditions and on the stability of the oxaziridine product. The thermal stability of oxaziridines varies greatly with substitution pattern. Thus, the 2,2'-di-*tert*-butyl-3,3'-bisoxaziridine decomposes with explosion, while 2,3,3'-trialkylsubstituted oxaziridines are quite stable. The C,N-dialkyl substituted oxaziridines are much less stable than C-aryl,N-alkyloxaziridines. In the case of C-aryl substituted oxaziridines, stability depends on the substituents on the ring nitrogen; among alkyl substituents, the *t*-butyl group has the most stabilizing effect. Electron withdrawing groups attached to the nitrogen further stabilize the C-aryloxaziridines, but these substituents may also have an adverse effect on reactivity and/or biological activity. For instance, N-acyl groups are not suitable for stabilization because they undergo ring enlargement to dioxazoles on heating, and a bis-sulfonyloxaziridine was moderately toxic to Jurkat cells, while the corresponding bis-oxaziridine was completely devoid of toxicity.[8] These considerations, along with other factors, must be taken into account in the design of the oxidoredox hypothesis-based antifungal agents.

Incorporation of a nitrogen atom into a three-membered ring substantially increases the barrier to pyramidal inversion. This increase, from 6-7 Kcal/mol in trivalent amines to 18-20 Kcal/mol in aziridines, is still insufficient, however, to allow isolation of optically active N-alkyl and N-arylaziridines. In oxaziridines, the barrier is

raised to 28-30 Kcal/mol, hence oxaziridines show a remarkable configurational stability about nitrogen. Because oxaziridines do not display inversional epimerization, there are many examples of pairs of isomers that are separable. Thus, a variety of optically active oxaziridines was prepared by oxidation of imines (R_2C=NR') with (+)-monopercamphoric acid (MPCA). Since unsymmetrically substituted imines can exist in both *cis* and *trans* forms, (+)-MPCA oxidation of imines **17** affords *trans*- and *cis*-oxaziridines, **18** and **19**, respectively, which have a diastereomeric relationship.[58-60] The enantiomeric excesses were determined by nmr using chiral solvating agents (CSAs).[61]

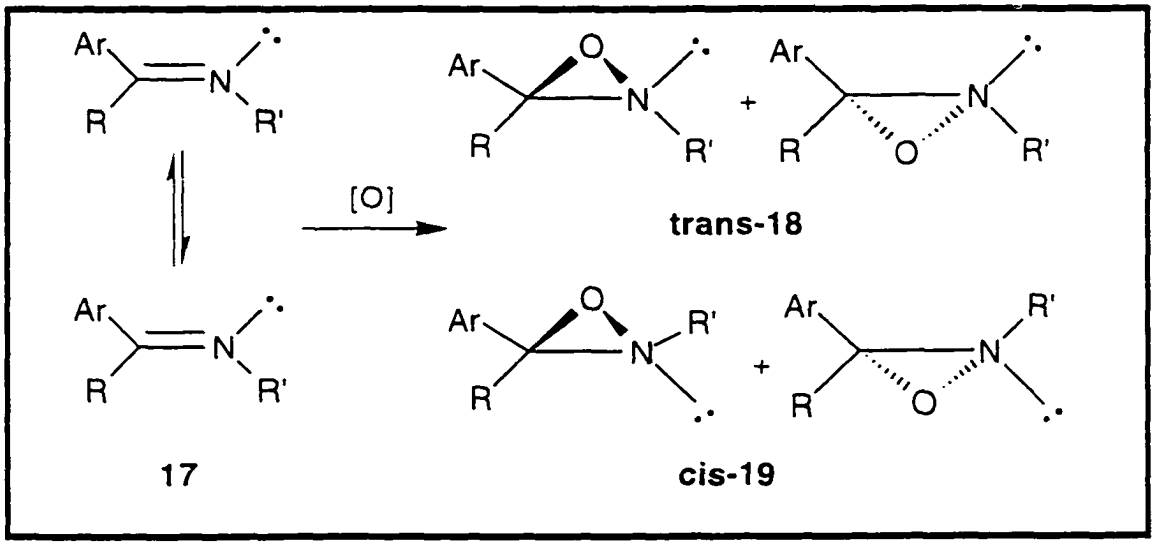

1.3.2. The oxaziridine pharmacophore.

Despite an idea advanced in the early seventies that the critical oxygenating species of flavin oxygenases[62] is an oxaziridine, before Balogh-Nair's studies[10] there were no efforts to explore the pharmacophore potential of the oxaziridine functionality. These oxygenases are unique in that they carry out the only known non-metal-ion requiring oxygen activation reactions in biological systems.

They bind and activate molecular oxygen, ultimately transferring one oxygen atom to substrate and releasing the second as water. Based on mechanistic studies of these enzymes, in 1974 Orf and Dolphin[62] proposed an oxaziridine intermediate as the monooxygenating species, derived by rearrangement of an initial intermediate, 4α-hydroperoxyflavin (Scheme 14). Working with nonenzymatic models, Rastetter *et al.*[63] proposed that a nitroxyl radical derived from Dolphin's oxaziridine (Scheme 14), is a viable candidate for the oxygenating species. However, many other mechanisms were proposed later, not involving the oxaziridine, and these received more attention.[64] The lack of interest in possible biological roles for oxaziridines can be attributed to the fact that at the time of the above mechanistic proposals not much was known about the chemistry of oxaziridines. However, based on prior work of Balogh-Nair's group, we believed that their broad range of reactivities and

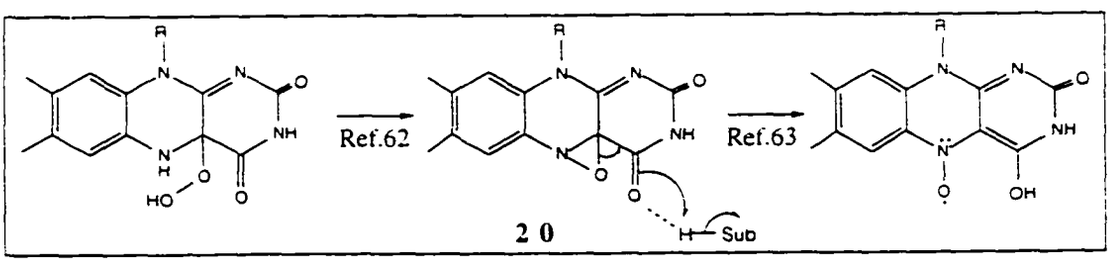

Scheme 14. The putative oxygenating species in flavin monooxygenases.[62-63]

their potential to react with nitrogen and sulfur nucleophiles, ubiquitous in biological systems, make oxaziridines attractive candidates for modulating the oxidoredox processes occurring in phagocytic cells. The antifungal activity of the first series of oxaziridines synthesized and tested against *P. carinii*[65] has demonstrated the potential of this class of compounds and lent support to the oxidoredox pharmacophore hypothesis.[2]

1.4. Nitronyl nitroxides.

Nitroxides constitute a very versatile class of compounds. They are widely used as spin probes and labels in EPR spectroscopy because of their sensitivity to the microenvironment, their mobility, and their high chemical stability.[66] The latter property has made it possible to carry out various reactions without affecting the unpaired electron and to synthesize nitroxides with a great variety of structures. Since their development more than 25 years ago, the availability of a wide variety of chemical structures made nitroxides suitable for a large number of applications in biological systems. Besides their well-established role as probes of proteins' and membranes' structures, important recent applications include their use as contrast agents in nuclear magnetic imaging (MRI) and other *in vivo* nmr techniques. Moreover, nitroxides have provided new ways of measuring metabolism *in vivo*, for instance measuring oxygen concentration in an accurate, nonperturbing way by *in vivo* EPR oximetry.[67] The discovery of the first genuine organic ferromagnet,[68] in 1991, stimulated interest in the application of nitronyl nitroxides in an entirely different area, materials science, where a current topic of interest is the construction of novel organic spin systems that are not available from conventional inorganic materials. Balogh-Nair's interest in nitronyl nitroxides arose from the oxidoredox pharmacophore hypothesis[2] that predicted their microbicidal activity, and this hypothesis is substantiated by the high antifungal activity of the nitronyl nitroxides synthesized in this project.

1.4.1 Synthesis of nitronyl nitroxides.

A versatile series of stable nitroxide free radicals possessing a Δ^2-imidazoline-1-oxyl-3-oxide grouping was synthesized by Ullman in the late sixties and early seventies. [69] Referred to as nitronyl nitroxides (**21**), these compounds can be synthesized by condensation of 2,3-dihydroxyamino-2,3-dimethylbutane with an aliphatic or aromatic aldehyde followed by oxidation of the resulting di-*N*-hydroxy intermediate, **20**, with PbO_2 or $NaIO_4$ (Scheme 15). To improve the properties of spin labels, or to develop novel materials with unusual magnetic properties, numerous nitronyl nitroxides were synthesized, including stable di- and triradicals containing two or three nitronyl nitroxide units in a single molecule (Scheme 16).[70]

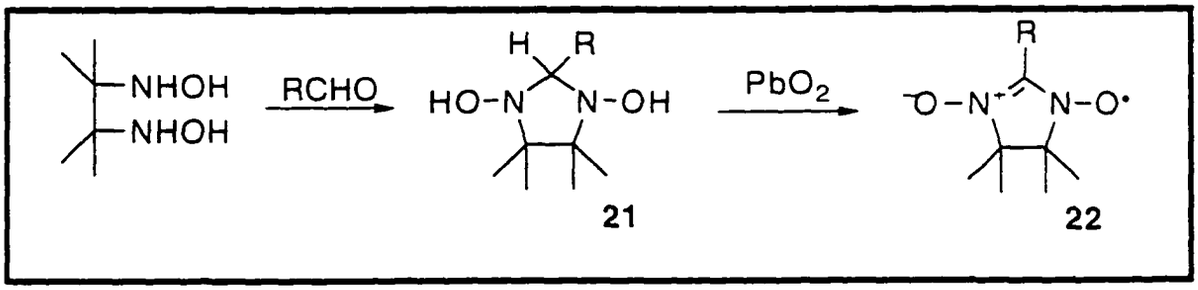

21 22

Scheme 15.

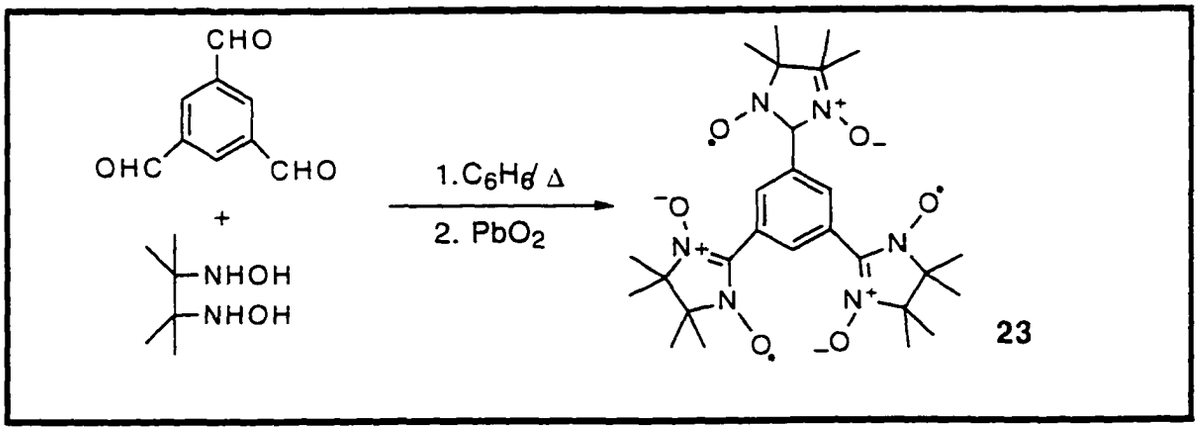

Scheme 16.

1.4.2. The nitronyl nitroxide pharmacophore.

The rationale for selecting nitronyl nitroxides as potential microbicidals is based on consideration of the metabolic pathways antifungal nitrones[71] might undergo according to the oxidoredox pharmacophore hypothesis (Scheme 17).[2]

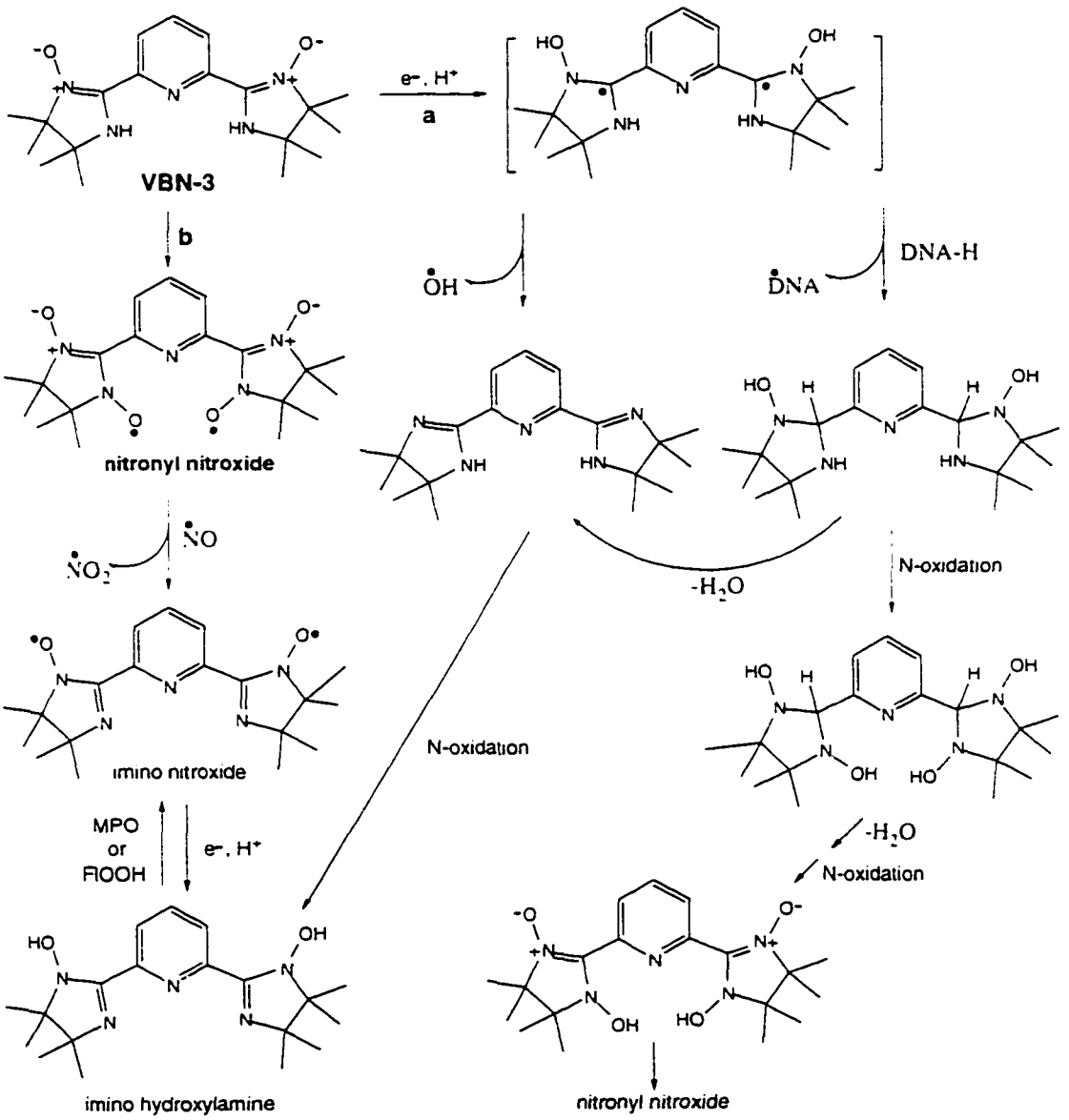

Scheme 17. Pathways postulated for reductive (a), and oxidative (b) activation of the bisnitrone **VBN-3**.[2]

Previous studies have shown that **VBN-3**, a bisnitrone, is highly active against *P. carinii*.[71] Among the several mechanisms by which **VBN-3** could work *in vivo*, two pathways are shown in Scheme 17.[2] According to pathway a, reductive activation would yield the diradical nitronyl nitroxide. This could release two •OH/mol of **VBN-3**, and cause the antifungal effect. DNA damage may also occur as a result of H• abstraction by the diradical initially formed via pathway a. According to pathway b, oxidative activation would yield the nitronyl nitroxide, a diradical. Model experiments showed this radical can be obtained by air oxidation of **VBN-3**, as a crystalline and stable material.[71] *In vivo*, oxidants of neutrophils could accomplish this step. The nitronyl nitroxide should readily react with •NO (from macrophages), since nitronyl nitroxides have been employed to detect •NO in air.[72] The reaction with •NO would yield the imino nitroxide. The imino nitrogen in imino nitroxides has a pronounced basic character, and can be reversibly protonated; the nitroxide is reducible, for example by ascorbate or SH groups, to the corresponding hydroxylamine. The nitronyl nitroxide could also be derived from pathway a, by dehydration/oxidation steps. The bond energy for the OH bond in hydroxylamines is relatively low (~70 kcal/mol), and therefore reoxidation to the nitroxides can be done with a variety of oxidants. *In vivo*, the hydroxylamines could be reoxidized to nitroxides, for example by flavomonooxygenase, by a metal-catalyzed reaction that proceeds through superoxide, or by myeloperoxidase oxidants of the neutrophils. The antifungal activity of the tris-nitronylnitroxide synthesized in this project suggests that it is linked to its ability to undergo pathways a or b (Scheme 17), according to the oxidoredox pharmacophore hypothesis.

2. RESULTS AND DISCUSSION

2.1 Synthesis of oxaziridines.

Emulating biological processes is an attractive strategy for discovering new and better pharmaceutical agents. Thus, oxaziridines are not only of fundamental interest because of their interesting chemistry, they are also important because of their usefulness as P-450 mimics,[10] and their antifungal activity[2] against the pathogens *Pneumocystis carinii* and *Cryptococcus neoformans*. To evaluate the potential of oxaziridines as antifungals, it was necessary to determine how many oxaziridine pharmacophore units a molecule must contain to achieve optimal antifungal activity. Only a few compounds are known to contain more than one oxaziridine unit, and except for the macrobicyclic hexaoxaziridine synthesized by Balogh-Nair' group,[10] none are known to contain more than two. Therefore, a systematic investigation to synthesize compounds with multiple oxaziridine pharmacophore units, such as bis-, tris-, and hexaoxaziridines was undertaken as described below.

2.1.1. Synthesis of bisoxaziridines.

The known bisoxaziridines[47,55,73] (Figure 1) were not deemed suitable as templates for our studies, either because of their lack of stability and/or because of the limited possibilities for appropriate functionalization to enhance pharmacological properties. We selected for synthesis target structures that contain N-alkyl, N-cycloalkyl, and

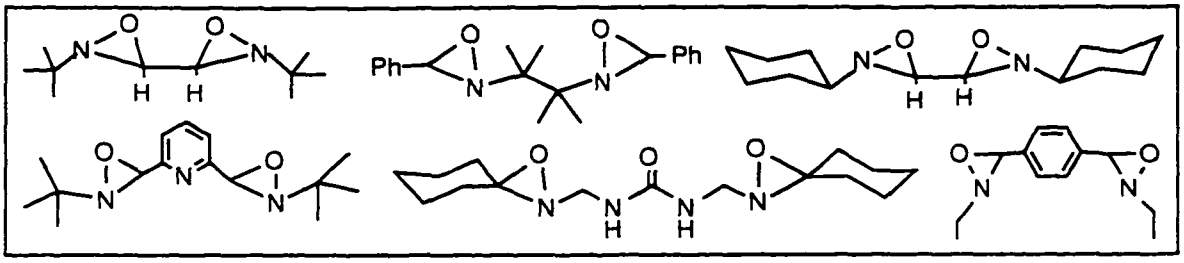

Figure 1. Structures of the known bisoxaziridines.

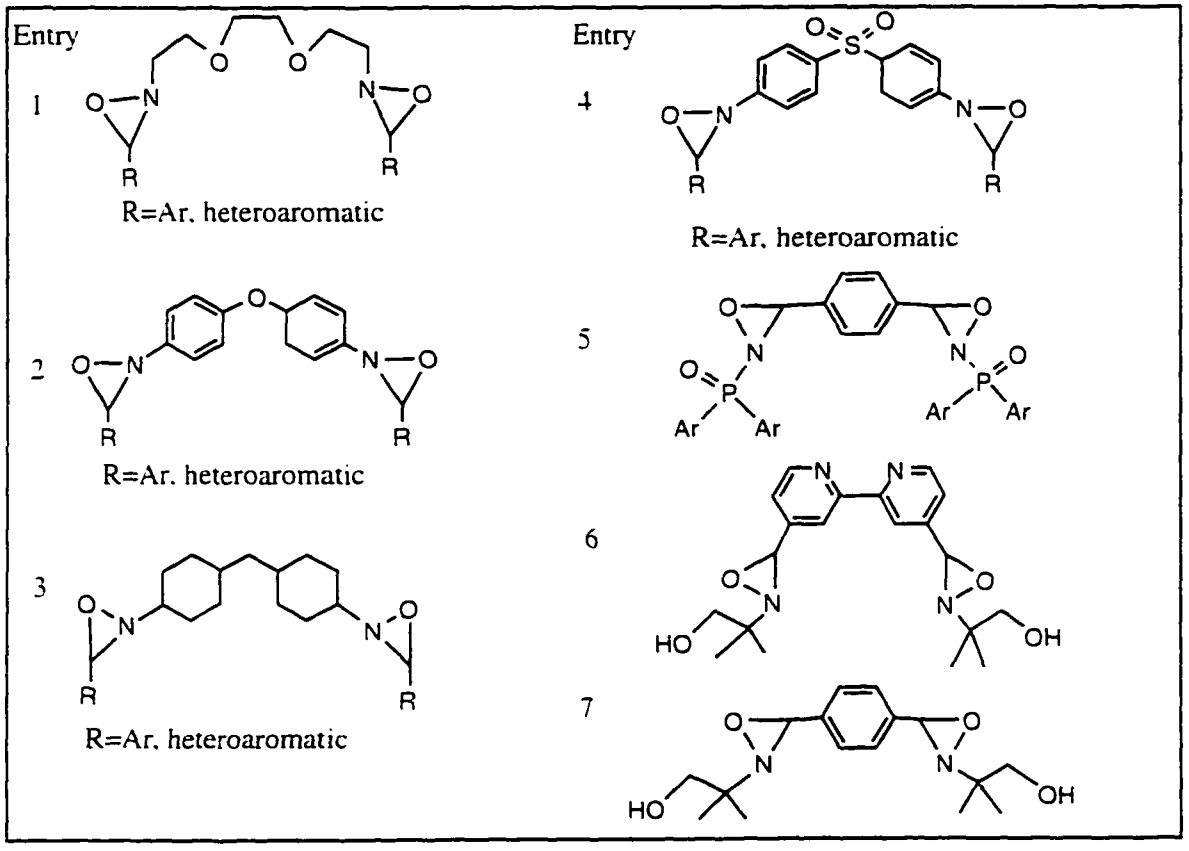

Table 1. Structures of the target bisoxaziridines.

N-aryl substituents on the oxaziridine ring (Table 1). In some of the target structures an electron withdrawing group is attached to the oxaziridine nitrogen to enhance thermal stability and to avoid rearrangements. Unlike known oxaziridines, where stabilization was sought but was not always achieved by an inert N-*tert*-butyl substituent, in the target compounds 6-7 (Table 1) a hydroxymethyl

group attached to the quaternary carbon was used instead. The quaternary carbon was expected to enhance stability by blocking rearrangements, and the hydroxymethyl group should increase water solubility and provide a functionalization site for modulation of biological activity.

Condensation of aldehydes with diamines, or of amines with dialdehydes afforded bisimine precursors which were then oxidized to yield the target bisoxaziridines (Scheme 18).

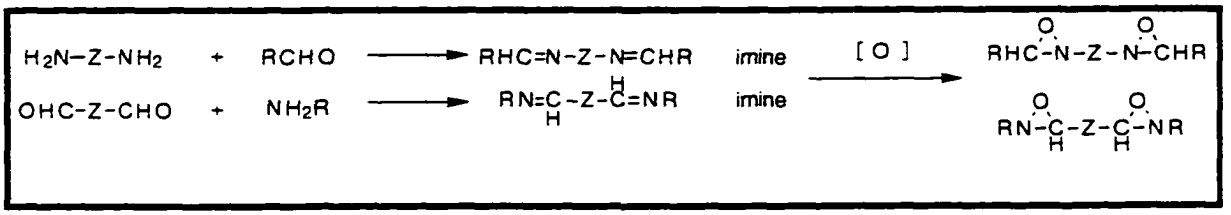

Scheme. 18

Except for entry 16, all bisaldimine intermediates were obtained in good yields by condensations of the amines and aldehydes in anhydrous methanol or acetonitrile either at room temperature or at reflux for 30 minutes (Table 2). The structures of the bisaldimines were confirmed by their CI-MS, ^{1}H and ^{13}C nmr spectra. All the bisaldimines, except the bisdiphenylphosphinoyl imine (entry 16, doublet at 9.35 ppm), had the characteristic signal of the imino protons between 8-9 ppm.

To oxidize the bisaldimines to the target bisoxaziridines, three oxidants *m*-CPBA, Oxone buffered with $KHCO_3$, and dioxirane were employed. Despite varying the reaction conditions for each oxidant, only three of the target bisoxaziridines could be prepared in this manner; entries 1, 4, and 16 (Table 2). However, these three bisoxaziridines were obtained in good to excellent yields by *m*-CPBA

Entry	amine	aldehyde	bisimine (%)	bisoxaziridine (%)	recovered aldehyde (%)
1		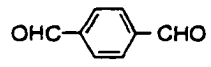	79	91	-
2		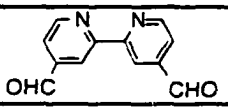	90	-	78
3		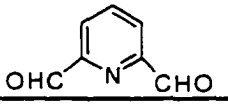	67	-	95
4	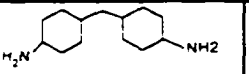	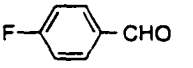	86	52	-
5	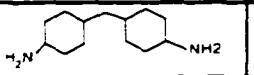	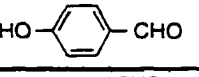	95	-	85
6	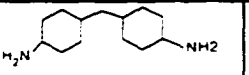	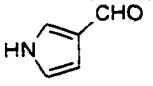	67	-	75
7	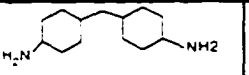	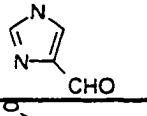	78	-	85
8	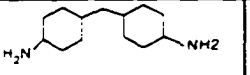	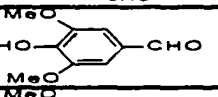	87	-	95
9	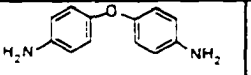	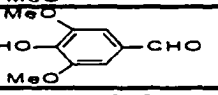	62	-	75
10	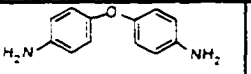	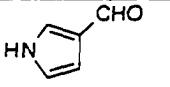	76	-	74
11	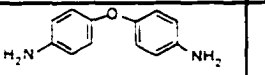	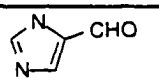	68	-	86
12	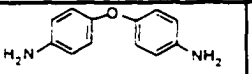	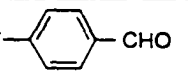	72	-	90
13	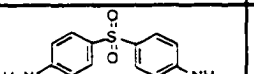	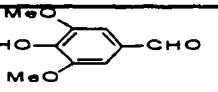	95	-	78
14	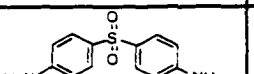	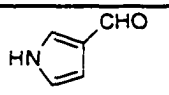	86	-	85
15	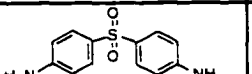	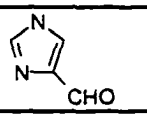	65	-	65
16*	1. NH_2OH 2. PPh_2Cl	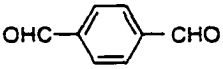	24	77	-

Table 2. Synthesis of bisoxaziridines.

oxidation of the precursor bisimines. The failure to isoilate oxaziridines (entries 2-3, and 5-15) can not be attributed entirely to the failure of the oxidizing agents employed. More likely, the oxaziridines' low stability and propensity to fragment into two or more products is a contributing factor. The stabilizing effect of an N-*tert*-butyl substituent is well-documented; nevertheless, even some of the N-*tert*-butyl substituted oxaziridines are known to decompose spontaneously at room temperature.[55] It was reported that oxaziridines having an N-methylene or an N-methinyl substituent are prone to spontaneous decomposition, decomposition by acids,[45b] and by bases[74] to yield aldehydes, ketones and ammonia (Scheme 19). Nevertheless, an N-methinyl substituted oxaziridine **24** (entry 4, Table 2) was stable, and could be obtained in 52% yield by *m*-CPBA oxidation of its bisimine precursor.

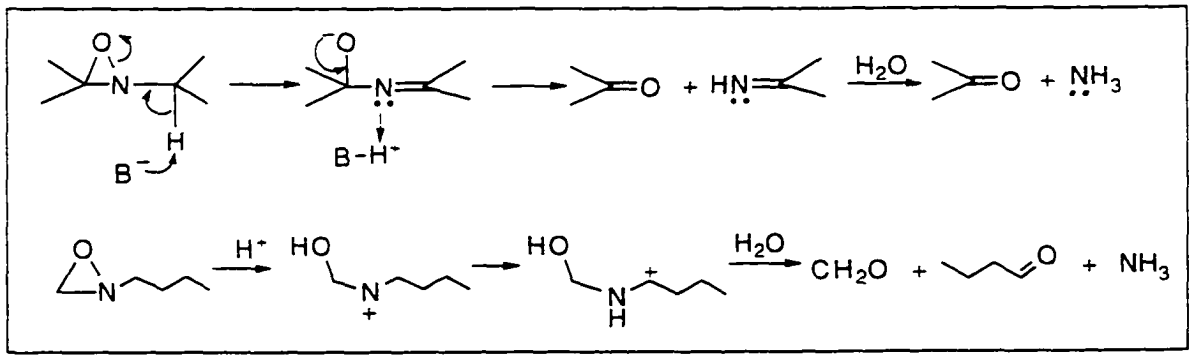

Scheme 19. Decomposition of oxaziridines by acids and bases.[45a,74]

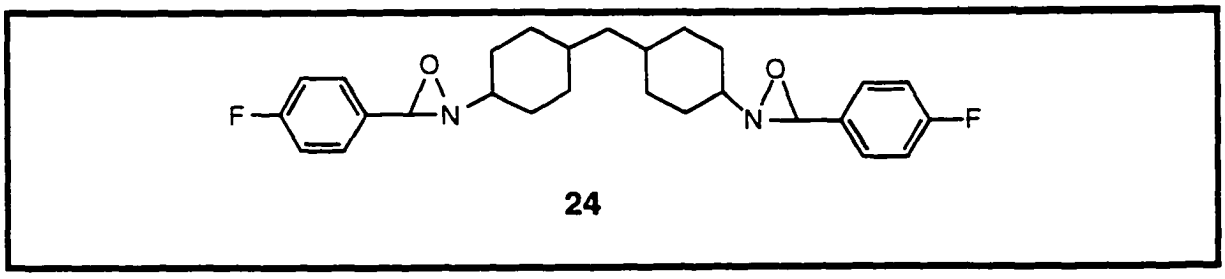

24

The ^{1}H nmr spectrum of bisoxaziridine **24** showed a characteristic peak for the oxaziridine protons at 4.49 ppm (Figure 2). Proton chemical shifts are known to depend on the orientation of adjacent lone pairs of electrons, with protons *trans* to the lone pairs resonating at higher field than those *cis*. Several explanations for the phenomenon have been offered, such as upfield shifts caused by transfer of electron density via the back lobe of the nitrogen lone pair, or by steric factors present when a nitrogen substituent is *cis* to the protons of interest. Alternatively, it has been suggested that the anisotropic character of the nitrogen lone pair causes the protons *cis* to it to shift downfield. Boyd *et. al.*[75] reported that in oxaziridines.

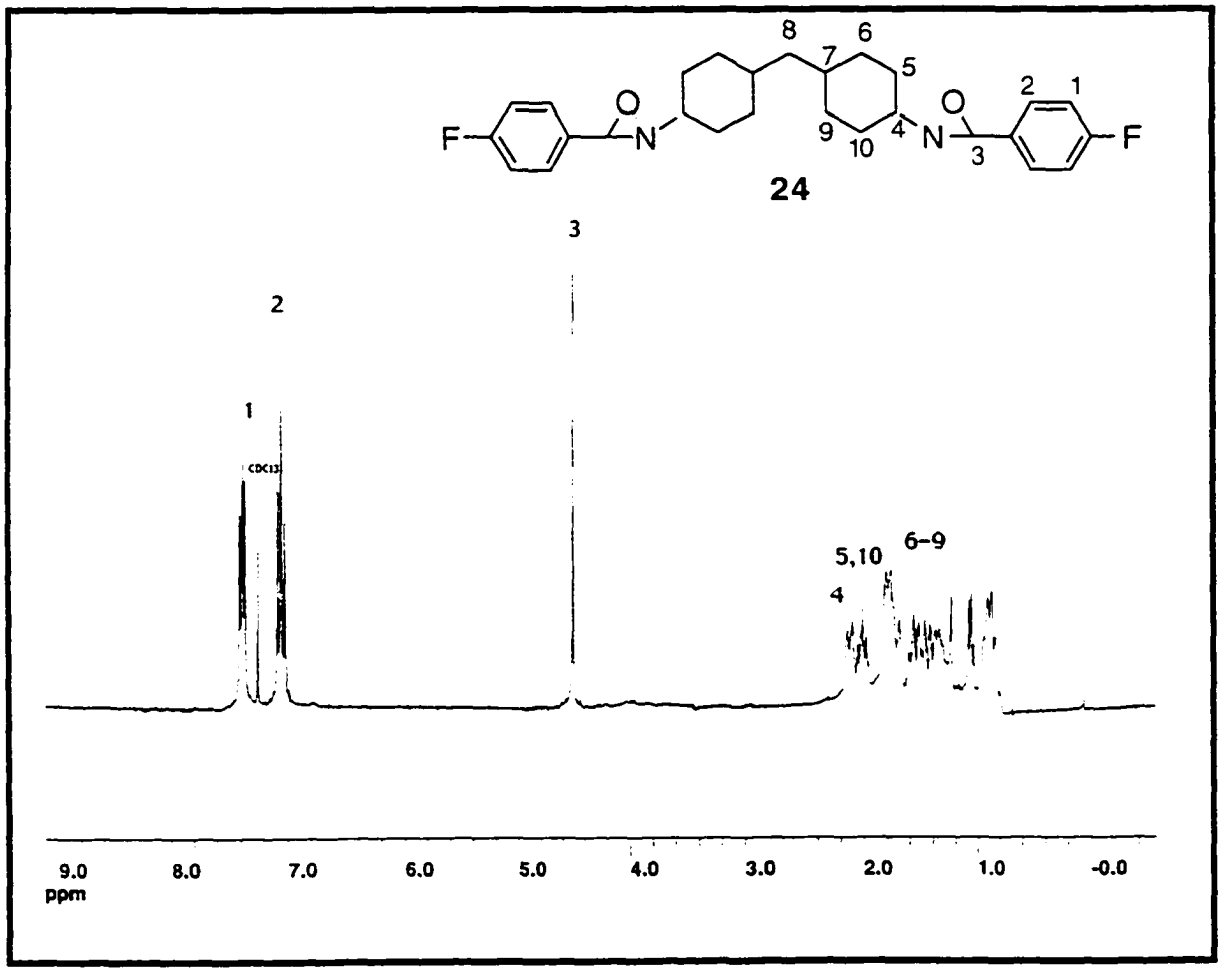

Figure 2. ^{1}H NMR spectrum of bisoxaziridine **24.**

protons *cis* to the lone pair resonate at ca. 5.4 ppm, whereas protons *trans* to it resonate close to 4.7 ppm (Figure 3). Since the oxaziridine protons in bisoxaziridine **24** resonate at 4.49 ppm, *trans* configuration can be assigned to these oxaziridines.

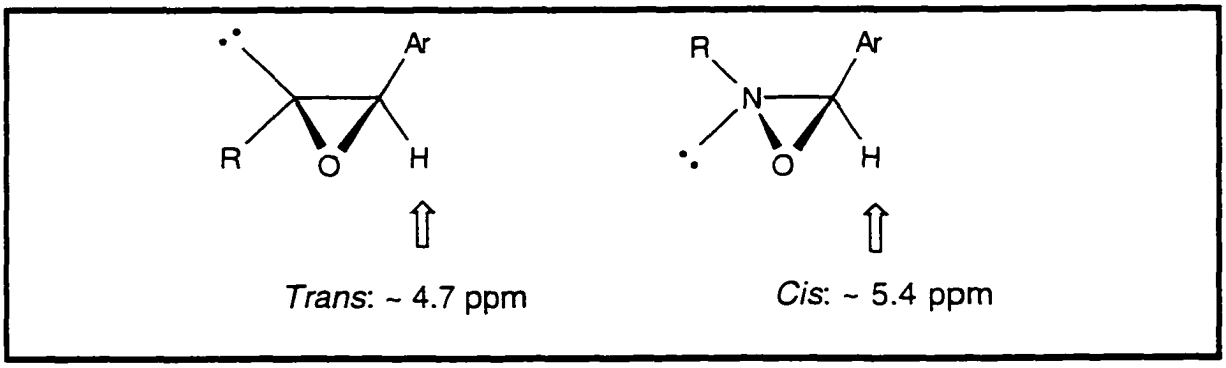

Figure 3. Chemical shifts of the protons in isomeric *trans* and *cis* oxaziridines.[75]

^{13}C Nmr is another diagnostic tool to assign *cis* versus *trans* configuration to oxaziridines:[76] Oxaziridine carbons resonate in the narrow range of 79-84 ppm. Aliphatic carbons *trans* to the nitrogen lone pair in oxaziridines experience a considerable upfield shift relative to *cis* substituents (Figure 4). Moreover, although smaller than the 9 ppm upfield shifts observed for aliphatic carbons, upfield shifts of 3.5 ppm are characteristic of *ipso* carbons *trans* to the nitrogen lone pairs. In agreement with the *trans* geometry assigned to **24**, the oxaziridine carbon resonates at 79.0 ppm, and the *ipso* carbon's signal is at 129.2 ppm (Figure 4). Furthermore, the signals of the oxaziridine protons and carbons both appear as singlets in the ^{1}H and ^{13}C nmr spectra of **24** indicating that the two oxaziridine moieties in **24** have identical, *trans* geometry.

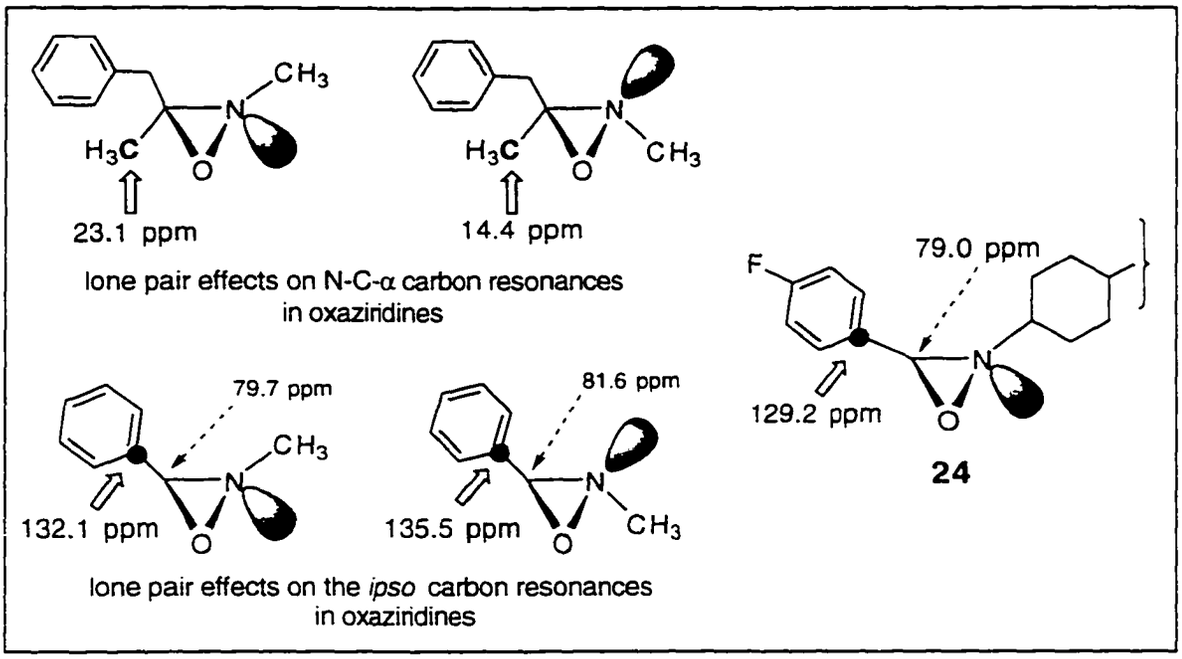

Figure 4. Carbon-13 chemical shifts in *trans* and *cis* oxaziridines.[76]

Like other active oxygen compounds, bisoxaziridine **24** transfers its oxygen atoms to triphenylphosphine quantitatively (Figure 5). Thus,

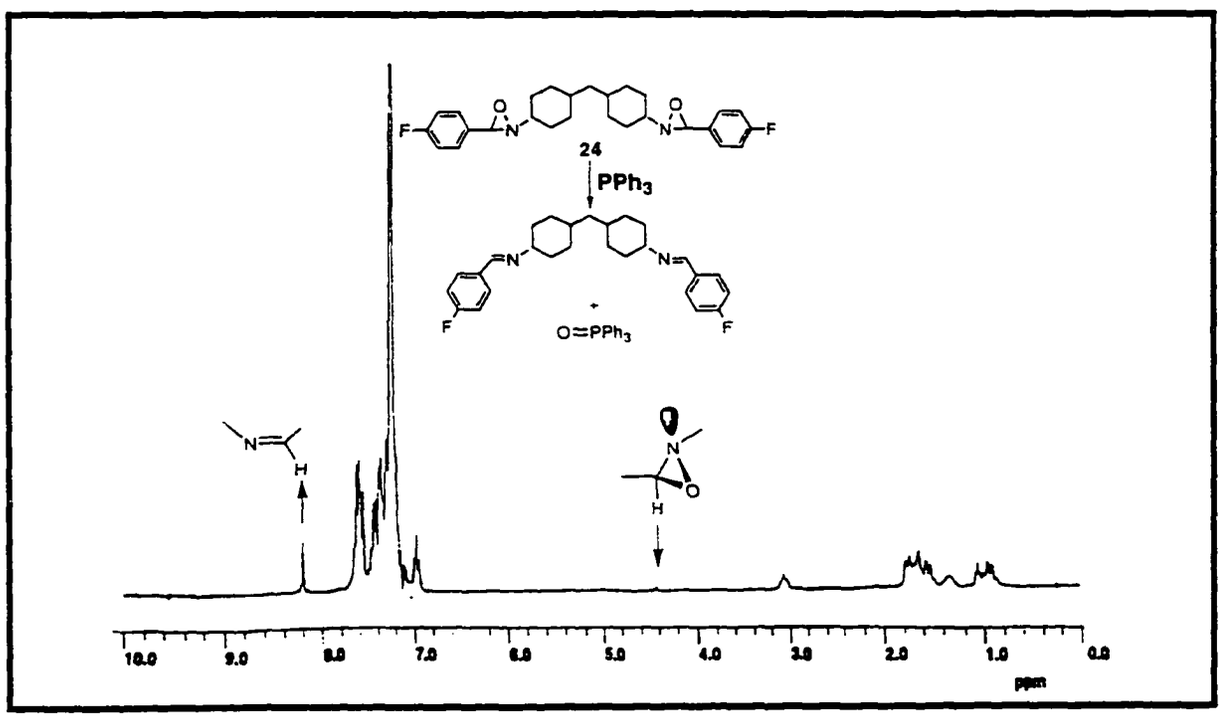

Figure 5. ^1H nmr spectrum of **24** with triphenylphosphine, in $CDCl_3$.

addition of Ph_3P to a $CDCl_3$ solution of **24** led to loss of the oxaziridine protons signal at 4.49 ppm with concomitant appearance of the imine signal at 8.2 ppm.

Mass spectroscopy is especially useful for characterizing oxaziridines because they loose oxygen from their molecular ions.[77] The CI mass spectrum of bisoxaziridine **24** showed the successive loss of two oxygen atoms, yielding fragments at *m/z* 439 and 423, corresponding to 16 mass unit losses from the $[M+1]^+$ ion (Figure 6).

When the bisoxaziridine **24**, homogeneous by tlc, was submitted to hplc analysis, two well separated peaks were observed (Figure 7). The separated peaks had identical mass spectra, and showed the typical loss of 16 mass units characteristic of oxaziridines. Unlike the case of a trisoxaziridine (see section 2.1.2) that consisted of a mixture of rapidly equilibrating conformational isomers, when the separated peaks of **24** were reinjected for hplc analysis, single peaks were observed. This, and the spectral analyses suggested that **24** is a diastereomeric mixture of **24a** and **24b**. Since the diastereomeric mixture was devoid of antifungal activity, preparative hplc separation of the diastereomers was not pursued.

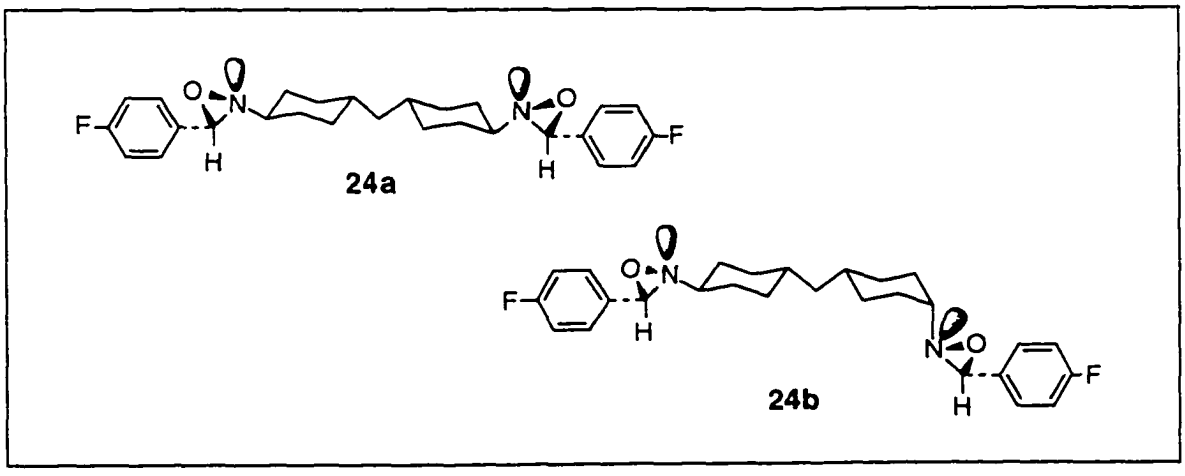

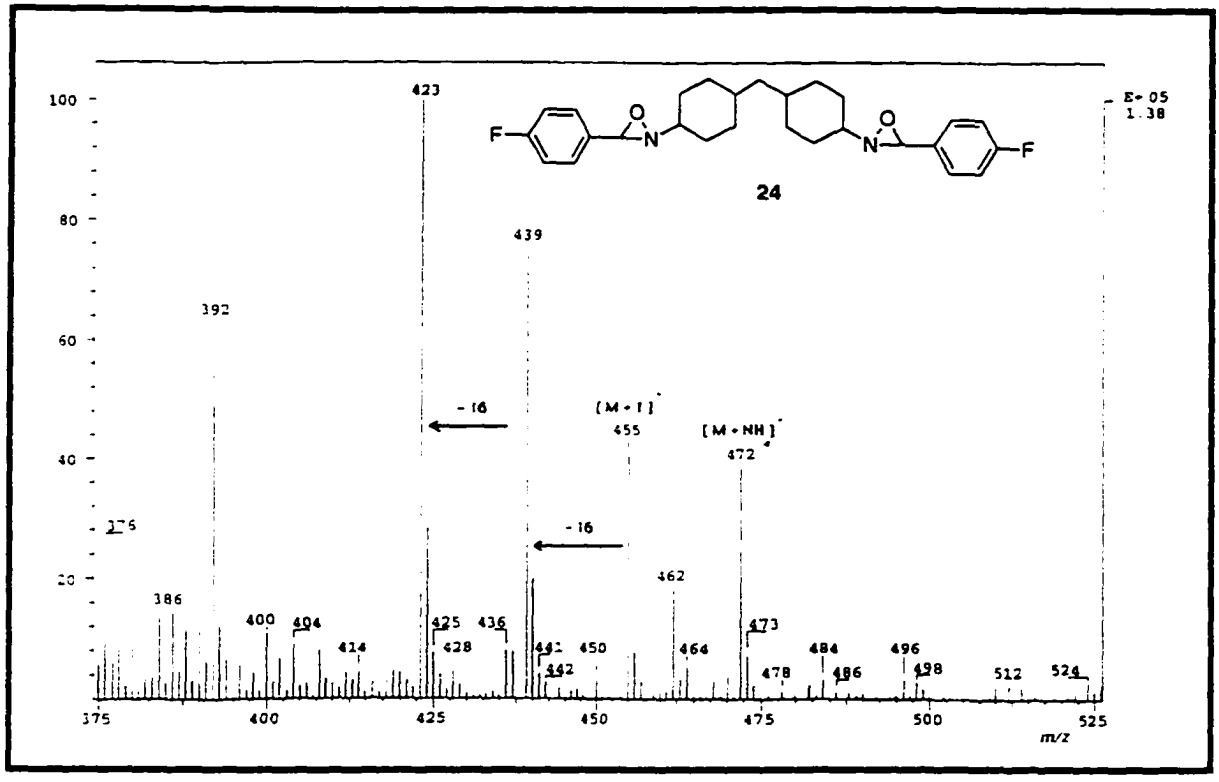

Figure 6. CI-MS (ammonia) of bisoxaziridine **24.**

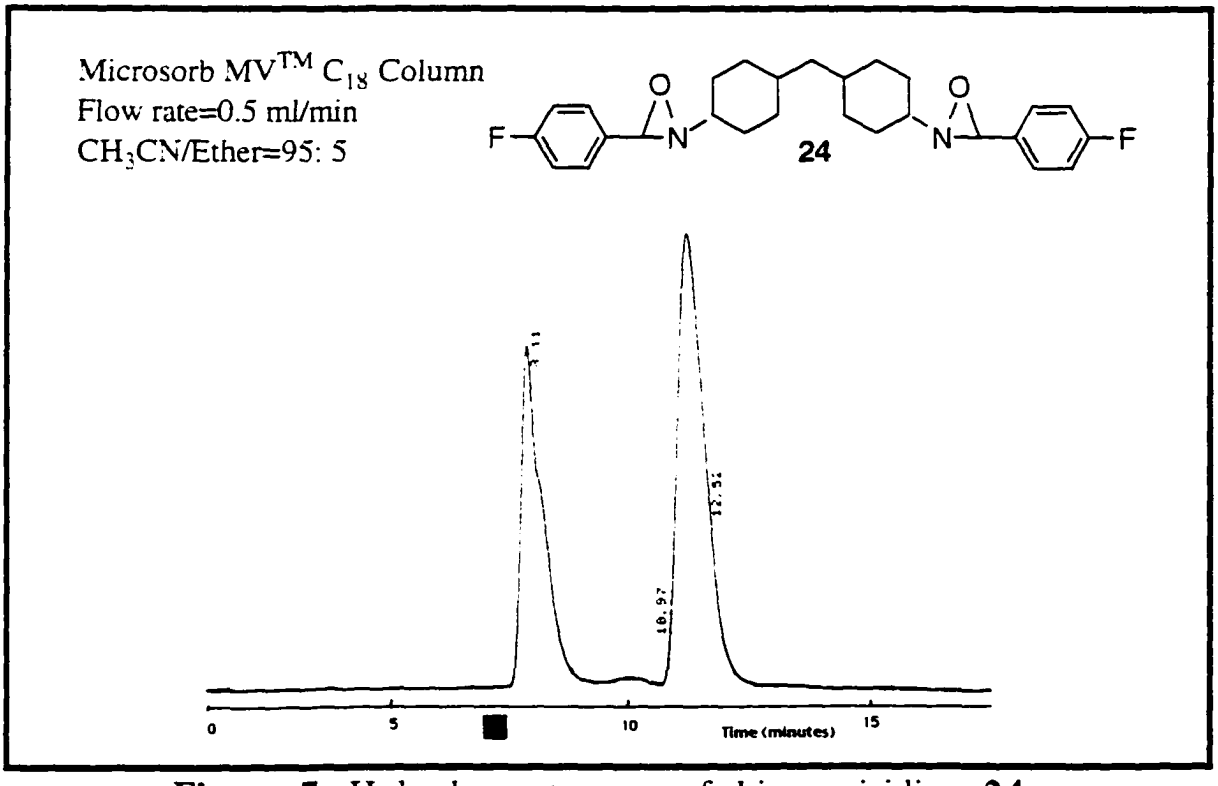

Figure 7. Hpl chromatogram of bisoxaziridine **24.**

The bisoxaziridine **25** was synthesized by condensation of 2-amino-2-methyl-1-propanol with terephthaldicarboxaldehyde, followed by oxidation of the bisimine with *m*-CPBA. Reaction with PPh_3, and the mass spectrum of **25** confirmed the presence of two atoms of active oxygen per molecule. The ^1H nmr spectrum of **25** (Figure 8) showed a singlet for the oxaziridine signal at 4.78 ppm, and the ^{13}C nmr spectrum (Figure 9) showed the oxaziridine carbon resonance at 73.3 ppm, establishing the *trans* geometry of the oxaziridine moieties.

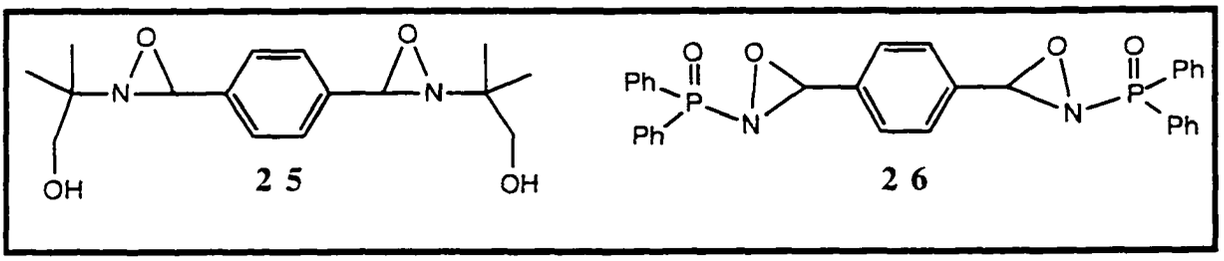

Apart from the highly popular sulfonyloxaziridines, few other types of N-functionalized oxaziridines are known. Until now N-phosphinoyloxaziridines[78-80] were limited to monofunctionalized derivatives, and so the bis-diphenyl phosphinoyloxaziridine, **26**, is the first member of a hitherto unknown class of oxaziridines bearing two oxaziridinyl moieties. Expected to be more alike in reactivity to N-sulfonyloxaziridines than to the N-Alkyl derivatives, **26** was anticipated to be a powerful oxygen transfer agent, and perhaps a better antifungal than the somewhat toxic sulfonyloxaziridines. The bisoxaziridine, **26**, was prepared by Arbuzov type, P^{III} - P^{V} rearrangement[81-82] of the O-diphenylphosphino-oximes to the bis-diphenylphosphinoyl imines, and subsequent biphasic oxidation of

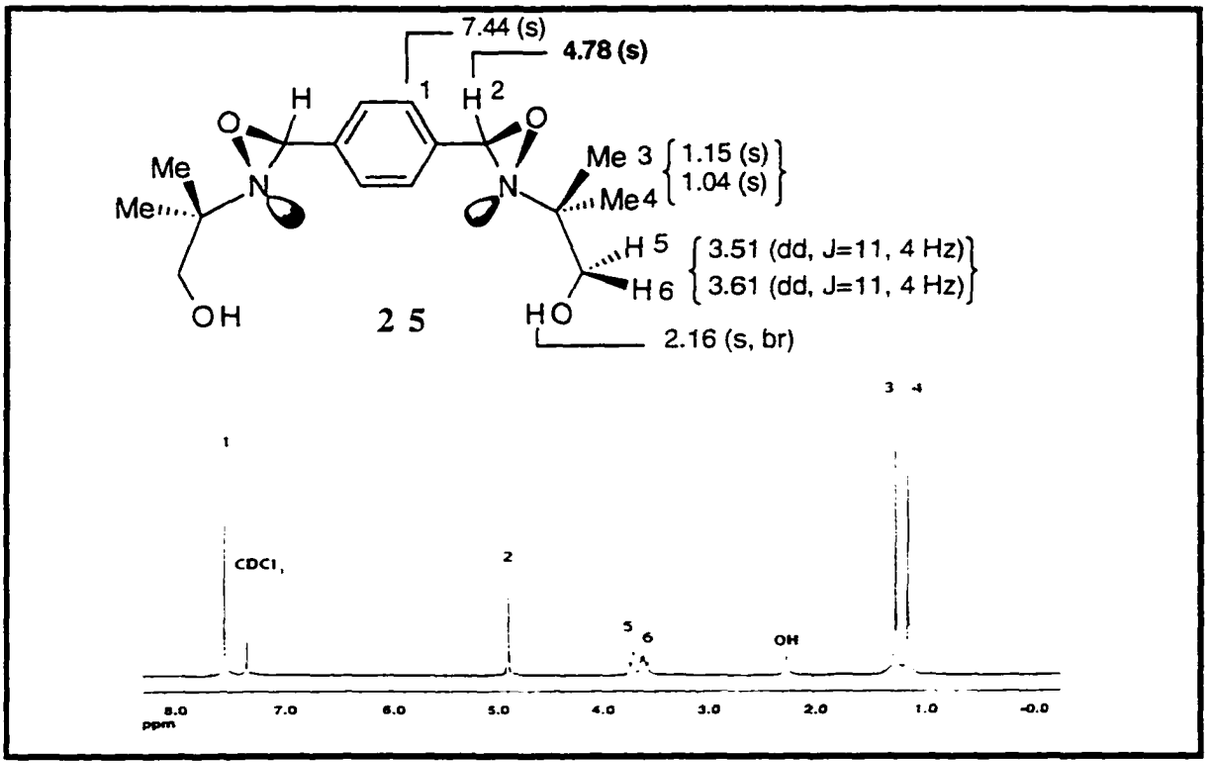

Figure 8. ^{1}H NMR spectrum of bisoxaziridine **25** in $CDCl_3$.

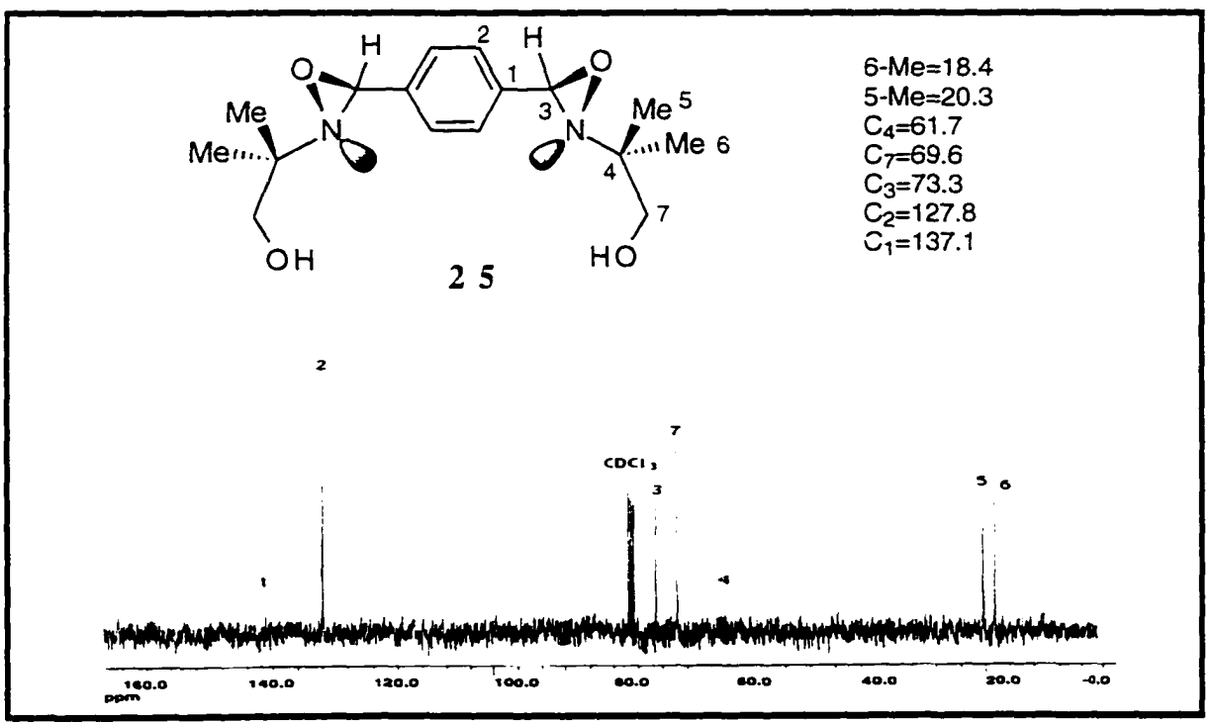

Figure 9. ^{13}C NMR spectrum of bisoxaziridine **25** in $CDCl_3$.

the imines with *m*-CPBA according to Scheme 20.

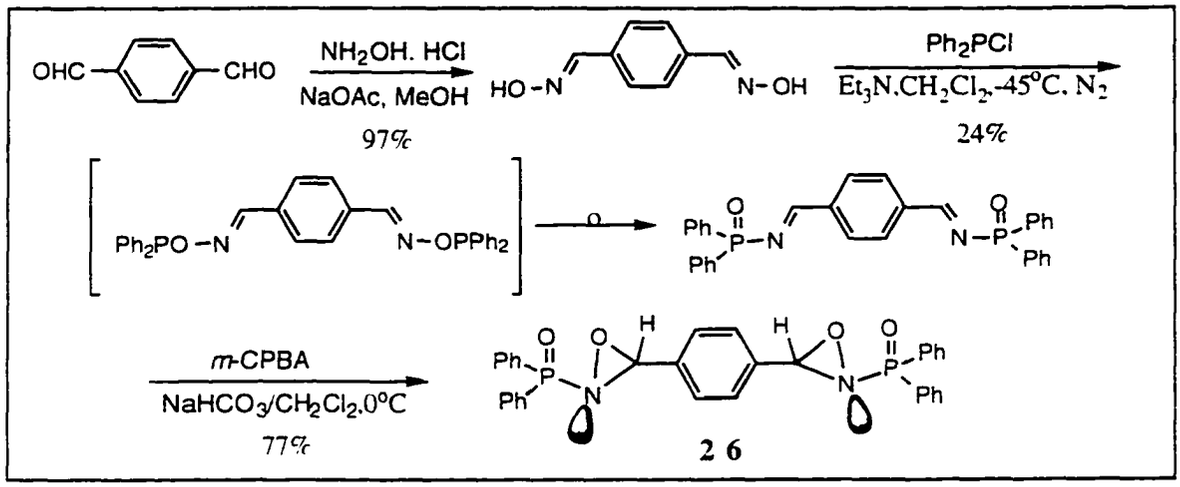

Scheme 20. Synthesis of bis-diphenylphosphinoyloxaziridine, **26.**

The structures of the intermediates, and that of **26**, were ascertained by their ^{1}H, ^{13}C nmr, and CI-MS spectra, and by the transfer of the two active oxygens of **26** to PPh_3. The CI-MS spectrum of **26**, characteristic of oxaziridines, showed sequential loss of two 16 mass units from the molecular ion, corresponding to the loss of two oxygen atoms (Figure 10).

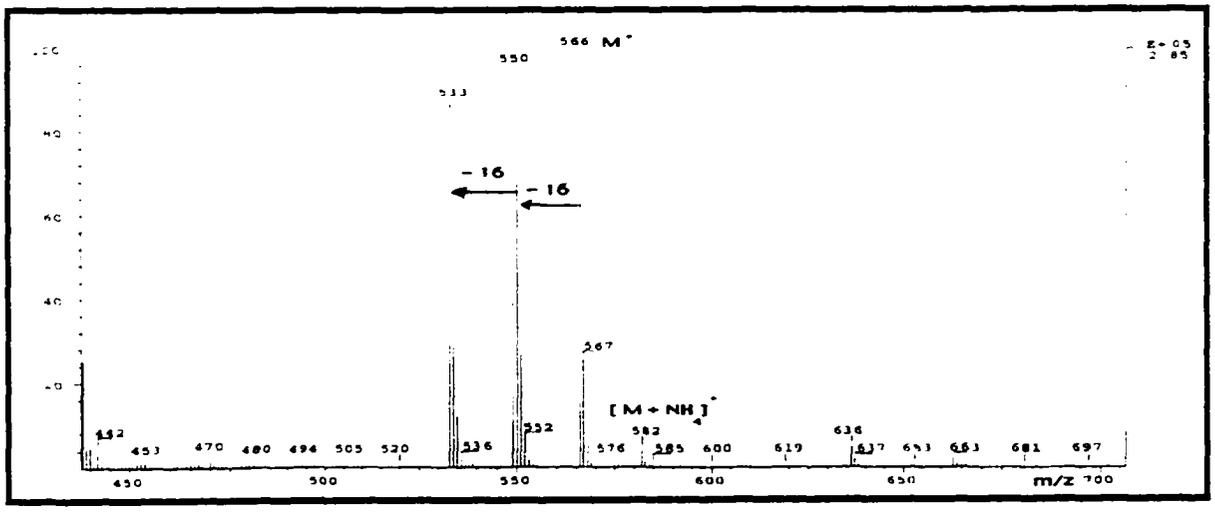

Figure 10. CI-MS (NH_3) spectrum of the bisoxaziridine **26**.

Salient features of the nmr spectrum included the precursor bisimine proton resonance, a doublet at 9.35 ppm, deshielded by the proximity of the diphenylphosphinoyl groups *cis* to them, and characterized by a coupling constant of $^{3}J_{PH}$=31.5 Hz, indicating that the geometry of both imines was *trans*. The signal of the two oxaziridine protons (*cis* to the phosphinoyl moieties), a doublet at 5.65 ppm with a coupling constant of $^{3}J_{PH}$=8 Hz, confirmed the *trans* geometry of the oxaziridine groups.[78]

The bisoxaziridines showed no antifungal activity against *Pneumocystis carinii* at concentrations low enough to predict *in vivo* potential. However, earlier work in this laboratory showed that a hexaoxaziridine was a highly effective antifungal against *P. carinii* in cultures. Therefore, to establish the minimum number of oxaziridine pharmacophore units per molecule that are a prerequisite for antifungal activity, synthesis of oxaziridines containing three pharmacophore units per molecule was undertaken next.

2.1.2 Synthesis of trisoxaziridines.

Since the average molecular weight of most of the useful small molecule drugs is below 1,000, and optimally falls in the range of 500-600,[83] to append several pharmacophore units to a molecule, macrocycles and dendrimers were envisaged as suitable carrier structures. Dendrimers are particularly attractive when the goal is to append identical functionalities (Figure 11). Moreover, a suitably designed dendrimeric core used as pharmacophore carrier prevents high polarity or high lipophilicity of the drug. The high polarity results in poor bioavailability, and high lipophilicity results in slow

excretion. Here, this strategy is employed to append three oxaziridine pharmacophore units to the dendrimeric core, 2,4,6-tris(*p*-formylphenoxy)-1,3,5-triazine, to obtain the trisoxaziridine **28**. To the best of our knowledge compound **28** is the first example of a trisoxaziridine. The 1,3,5-triazine was chosen as the central core of the dendrimer both to facilitate synthesis and to enhance the molecule's drug potential. 1,3,5-Triazines are not toxic, and some triazine derivatives by themselves display fungicidal or antibacterial properties.

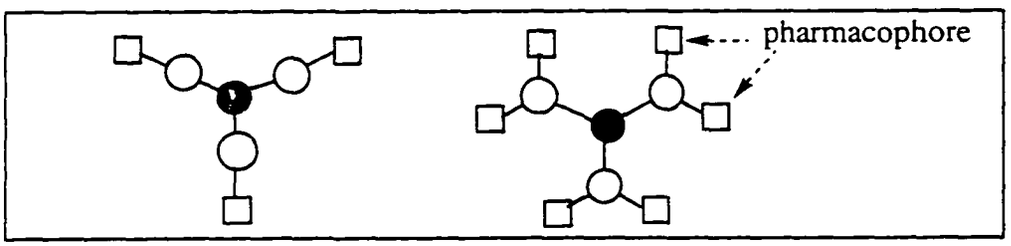

Figure 11. Dendimers appended with multiple pharmacophore units.

Trisoxaziridine **28** was synthesized efficiently, in three steps according to Scheme 21. Reaction of *p*-hydroxybenzaldehyde with cyanuric chloride gave 2,4,6-tris(*p*-formylphenoxy)-1,3,5-triazine in 78% yield.[84] This trialdehyde was then condensed with 2-amino-2-methyl-1-propanol to yield the trisimine **27** in 95% yield. Oxidation of the trisimine **27** with *m*-CPBA in chloroform at room temperature afforded **28** in 91 % yield. This trisoxaziridine, a white powder, can be stored without decomposition at -20°C for several months, and a concentrated solution of it in DMSO (30 mg/ml) is stable for several weeks. The three active oxygens of **28** are transferred to triphenylphosphine rapidly and quantitatively.

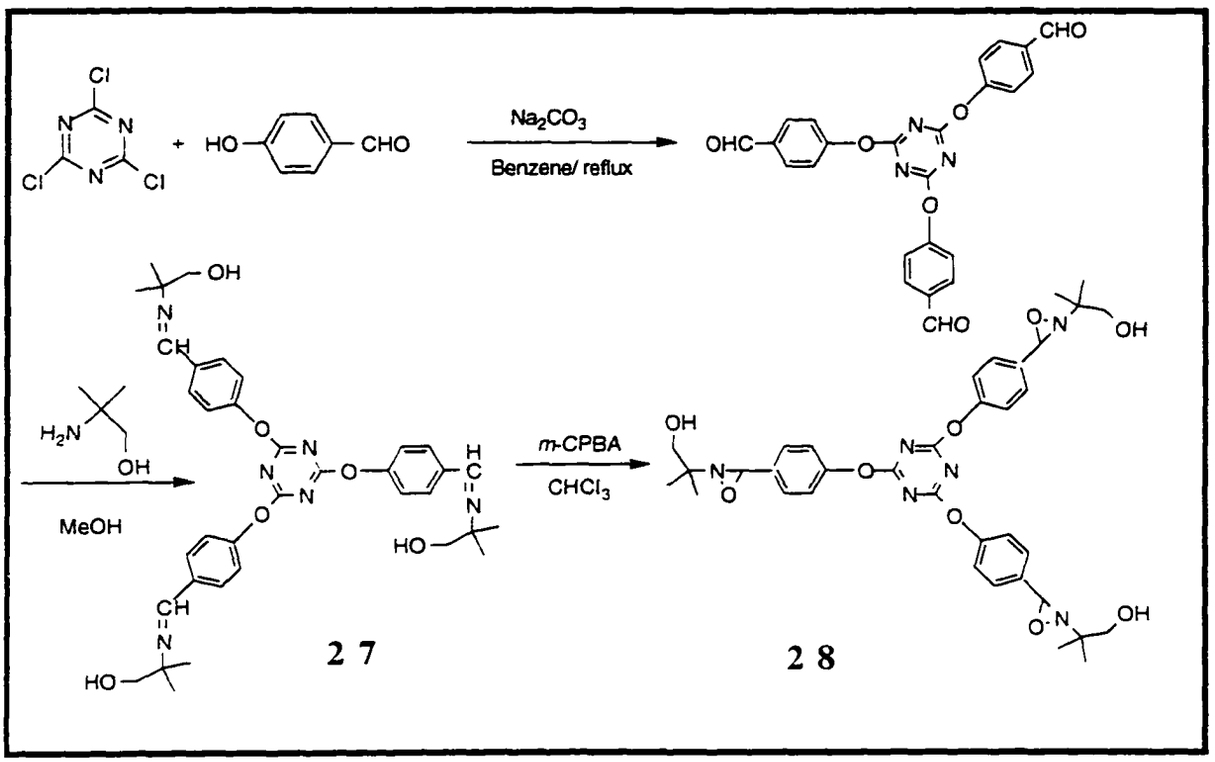

The structures of trisimine **27** and that of trisoxaziridine **28** were assigned on the basis of ^{1}H. and ^{13}C nmr. FT-IR, and MS data. Salient features of the trisimine **27** spectra are the OH and C=N stretching vibrations at 3.399 and 1.643 cm^{-1}, the singlet signal of the imine protons at 8.29 ppm. and the imines' carbon signal at 155.2 ppm (Figure12).

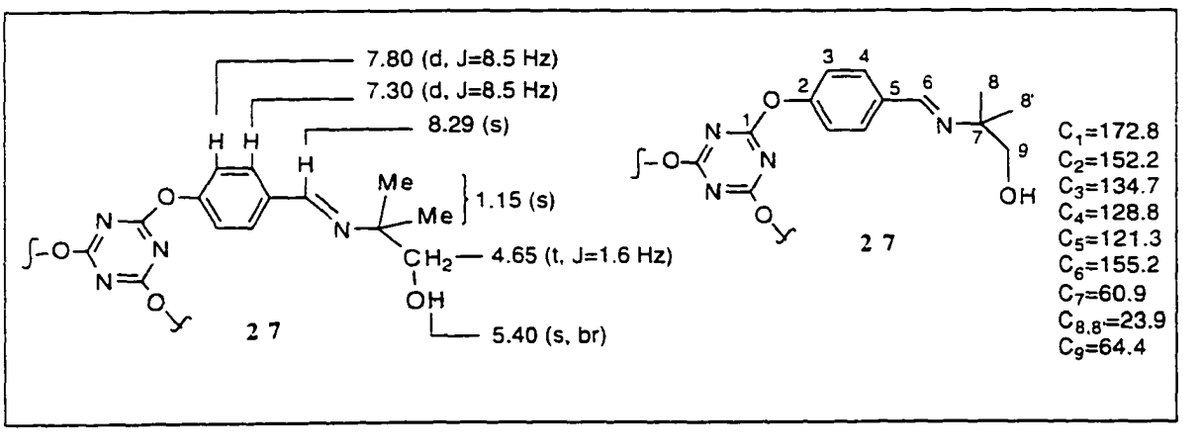

Figure 12. ^{1}H and ^{13}C nmr of the trisimine **27** in DMSO-d_6.

In the ^{1}H nmr spectrum of trisoxaziridine **28** (Figure 13) the signal of the three oxaziridine protons appears as a singlet at 5.03 ppm indicating that the three oxaziridines in **28** have identical, *trans* geometry. Because the *gem*-dimethyl groups are adjacent to a chiral center, their signals appear at slightly different chemical shift values of 1.00 and 1.02 ppm, respectively. The ^{13}C nmr (Figure 14) shows a typical oxaziridine carbon resonance at 66.9 ppm. Unlike the trisimine where the methyl signals have identical chemical shifts, the signals of the methyl carbons adjacent to the chiral nitrogen atom in the trisoxaziridine **28** appear as separate peaks at 14.2 and 18.5 ppm.

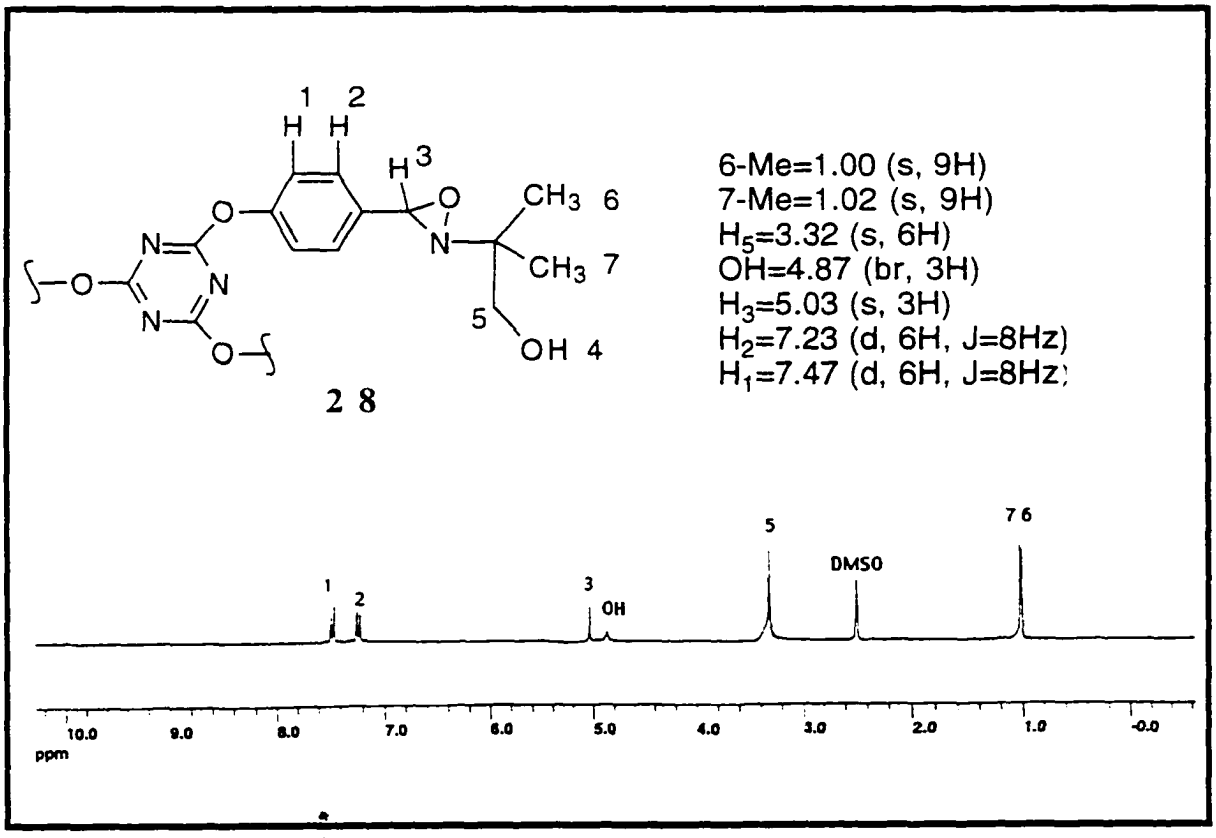

Figure 13. ^{1}H nmr spectrum of the trisoxaziridine **28** in DMSO-d_6.

The FAB mass spectrum of **28** showed the typical fragmentation pattern of oxaziridines, along with fragmentation validating the particular substitution pattern present in **28**. Thus, the fragments at *m/z*=687 $[MH-16]^+$, 671 $[MH-32]^+$, and 655 $[MH-48]^+$ correspond to sequential loss of one, two, and three oxygen atoms from the $[M+1]^+$ ion. The base peak at *m/z*=616 represents the fragment $[MH-87]^+$ probably of structure $RC{\equiv}O^+$ formed by loss of one of the three oxaziridinyl moieties - $NC(CH_3)_2CH_2OH$ - appended to the core. Losses of two $[MH-(2 \times 87)]^+$ and three oxaziridinyl moieties $[MH-(3 \times 87)]^+$ were also observed, as well as peaks resulting from demethylations and dehydrations. The presence of three active oxygens in **28** was corroborated by quantitative transfer of the oxygen atoms to PPh_3.

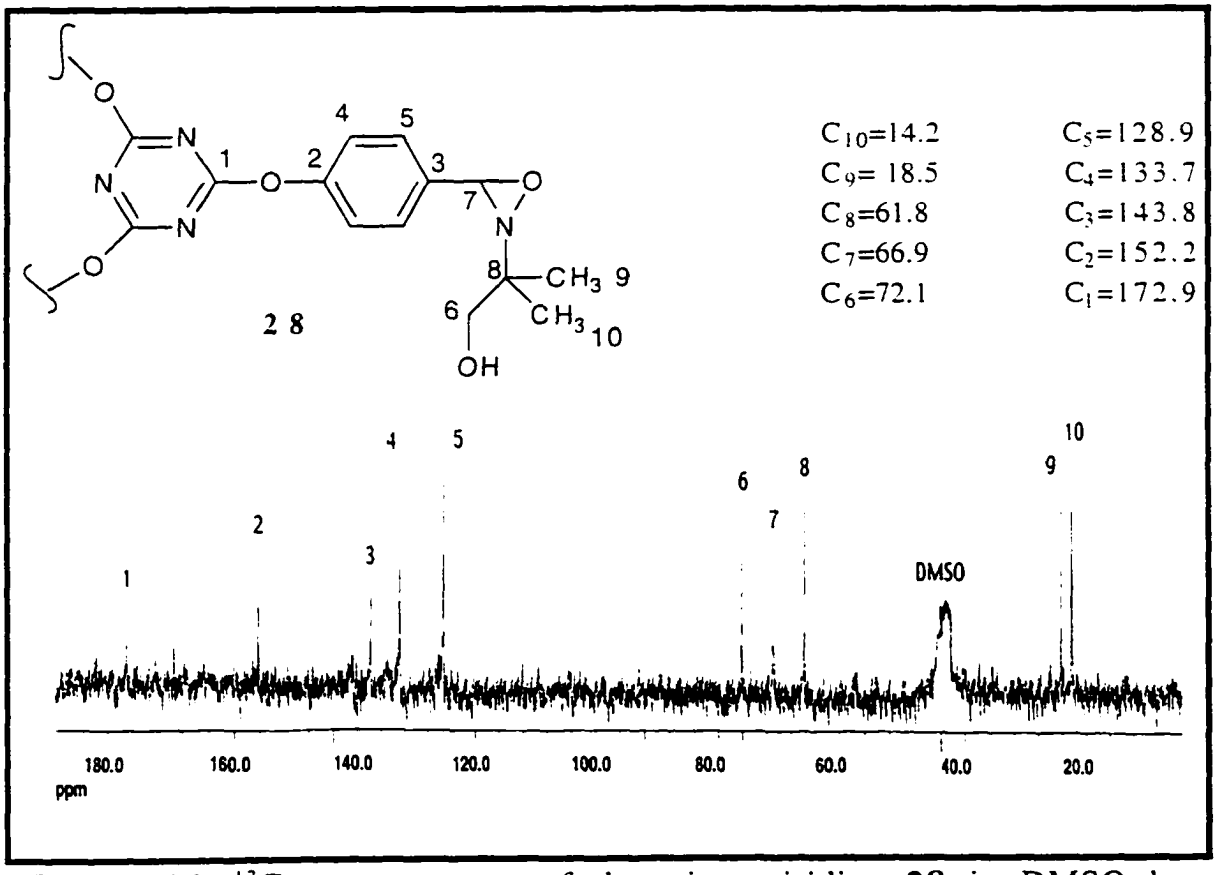

Figure 14. ^{13}C nmr spectrum of the trisoxaziridine **28** in DMSO-d_6.

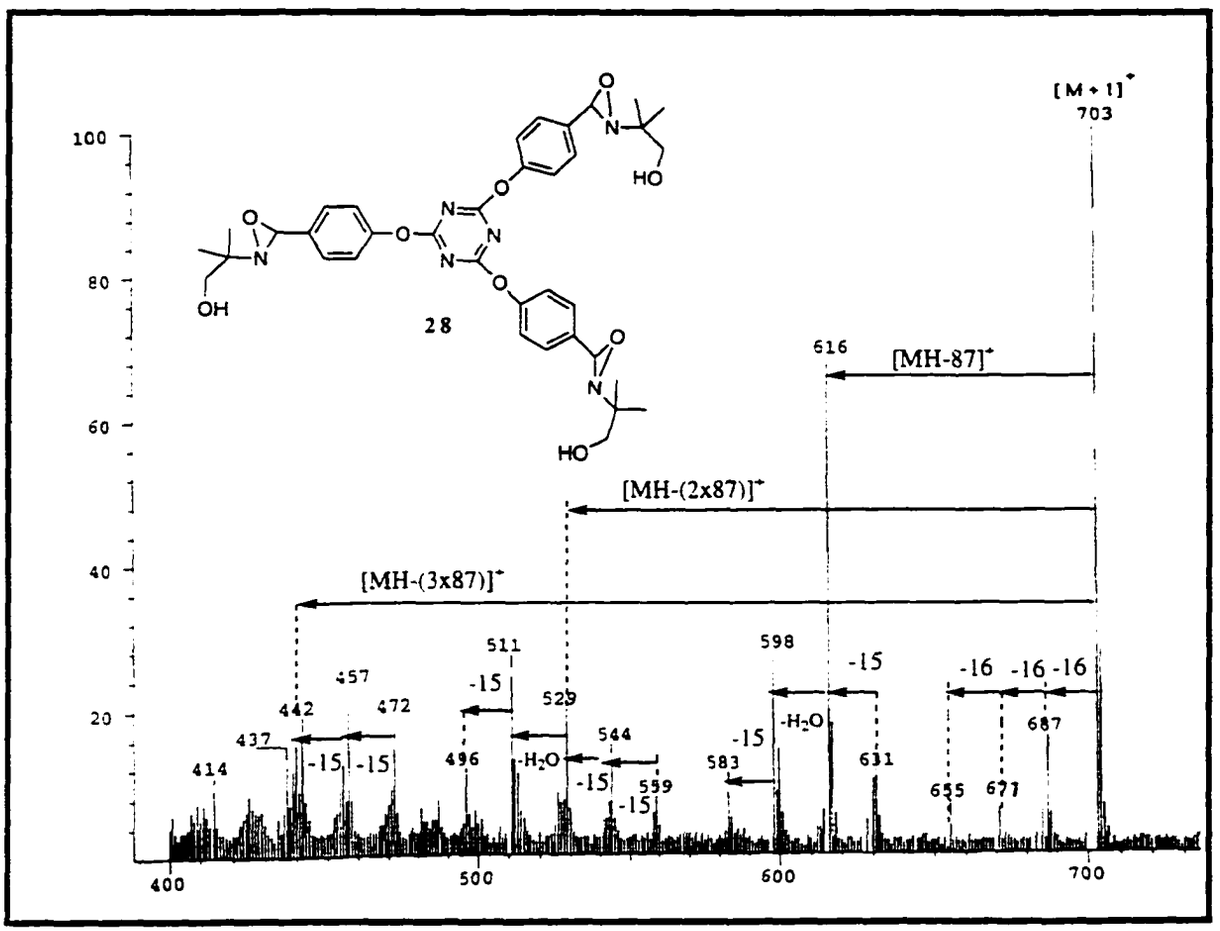

Figure 15. FAB (NBA) mass spectrum of the trisoxaziridine **28**.

Unlike bisoxaziridines **24-26** which display antifungal effects only at concentrations far exceeding the useful range, trisoxaziridine **28** was active against *P. carinii* at a concentration of 25 µg/ml. Over a period of seven days of incubation with *P. carinii* cultures, **28** caused ca. 50% reduction of the number of tropozoites compared to the control (Figure 16). This demonstrated that the number of oxaziridine pharmacophore units per molecule is a critical factor for modulation of antifungal activity. Therefore, to enhance the level of activity so that complete inhibition of *P. carinii* reproduction is achieved at concentrations of less than 10 µg/ml, synthesis of drug

candidates containing six oxaziridine pharmacophore units per molecule was undertaken.

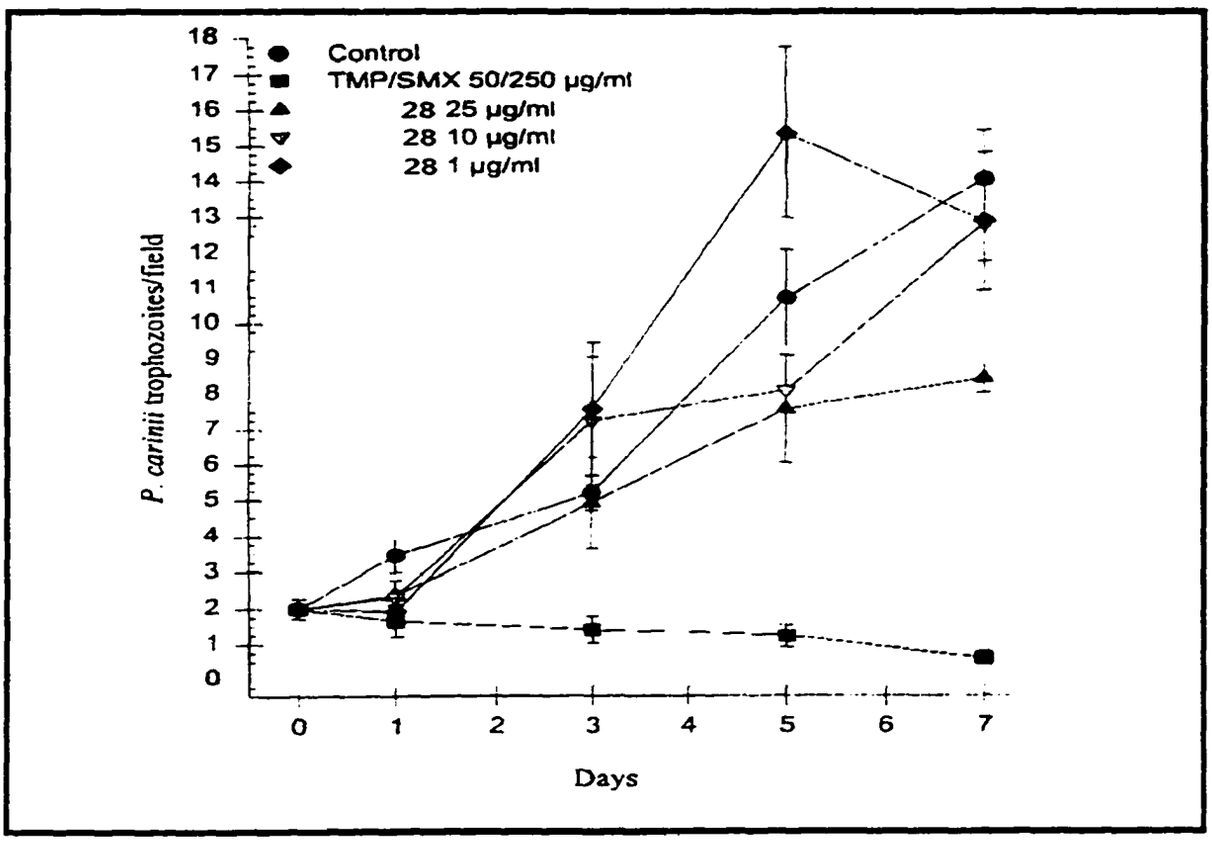

Figure 16. Inhibition of the growth of *Pneumocystis carinii* by the antifungal trisoxaziridine **28**.

2.1.3. Synthesis of macrocyclic oxaziridines.

Since the oxaziridine pharmacophore was unknown prior to the studies of Balogh-Nair *et al.*,[10] in the first attempt to establish its usefulness against *Pneumocystis carinii*, a macrocyclic compound, **30**, containing several oxaziridine units, was synthesized in 1992.[10] This macrobicyclic hexaoxaziridine, the first macrocycle containing oxaziridine moieties, was highly active against *Pneumocystis carinii* in cultures at concentrations of <1 µg/ml.[2] The high level of antifungal activity warranted *in vivo* testing of the compound

requiring gram amounts of the material. However, due to the low yield of ca. 10% in the first synthesis of **30** (Scheme 21, step b), the compound was available only in milligram amounts.

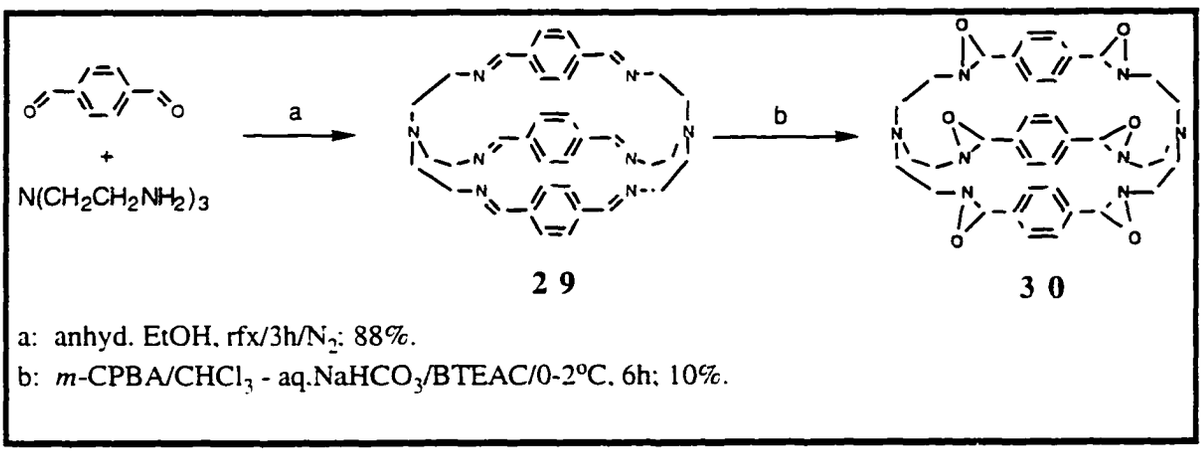

Scheme 21. Synthesis of the macrobicyclic hexaoxaziridine, **30**.[10]

To obtain adequate amounts of **30** for *in vivo* studies the synthesis was scaled-up, and the reaction conditions were modified, as described in the Experimental Section, to afford the hexaoxaziridine, homogeneous by hplc, in 35% yield. Moreover, it was necessary to determine the configurations of the six oxaziridine moieties in **30**, and so nmr experiments were carried out to establish the stereochemistries as described in the following section.

2.1.3.1. Stereochemistry of the macrocyclic oxaziridine, 30.

In principle, in the absence of diastereofacial selectivity, the peracid attacks on the six prochiral C=N bonds in **29** could have led to a complex mixture of diastereomeric products. Thus, *m*-CPBA could have attacked the six imine bonds from both the "endo" face and the "exo" face leading to *E* and *Z* oxaziridine isomers, ***E*-30/*Z*-30** (Figure 17), in addition to the numerous other possible

diastereomeric products. However, in agreement with ^{1}H and ^{13}C nmr data and hplc analysis (single peak in several solvent systems), compound **30** was obtained as a single diastereomer, indicating that the reaction proceeds with high diastereofacial selectivity. While it is possible that other diastereomers were formed, but could not be isolated because of their facile decomposition (since the yield was only 35%), molecular modeling showed that the rigid structure of macrocyclic imine **29** will favor attack by the peracid from the *exo* face of the six stereoelectronically equivalent imines. The ^{1}H and ^{13}C nmr spectra were in agreement with the rigid structure, and the presence of six identical, stereoelectronically equivalent, *trans* imine bonds in the hexaimine **29** (Figures 18 and 19).

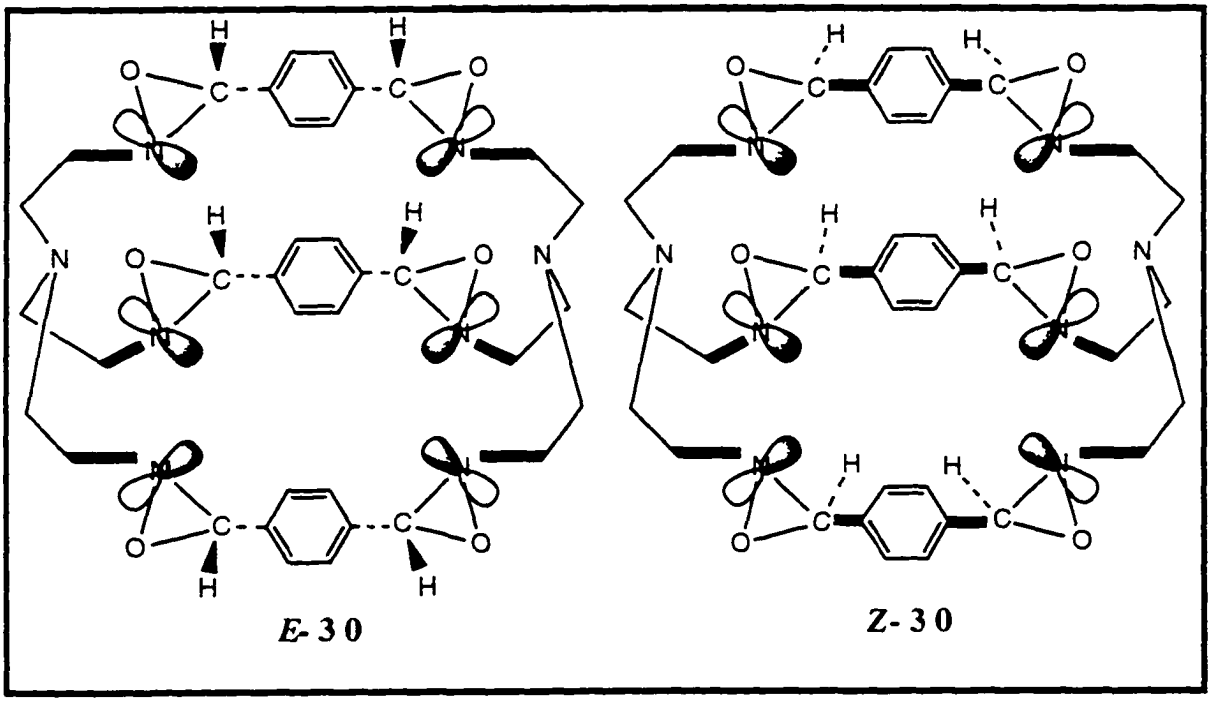

Figure 17. Postulated diastereomeric products ***E*30/*Z*30**.

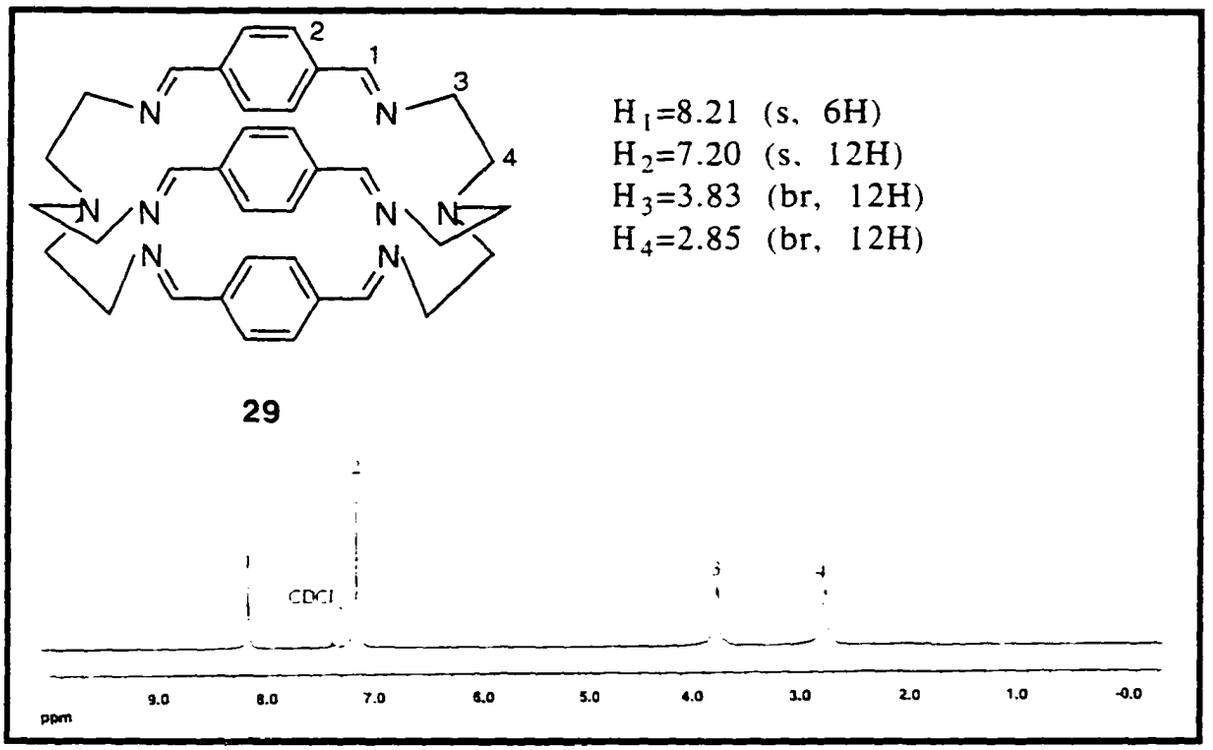

Figure 18. ^{1}H NMR spectrum of the macrocyclic imine **29** in $CDCl_3$.

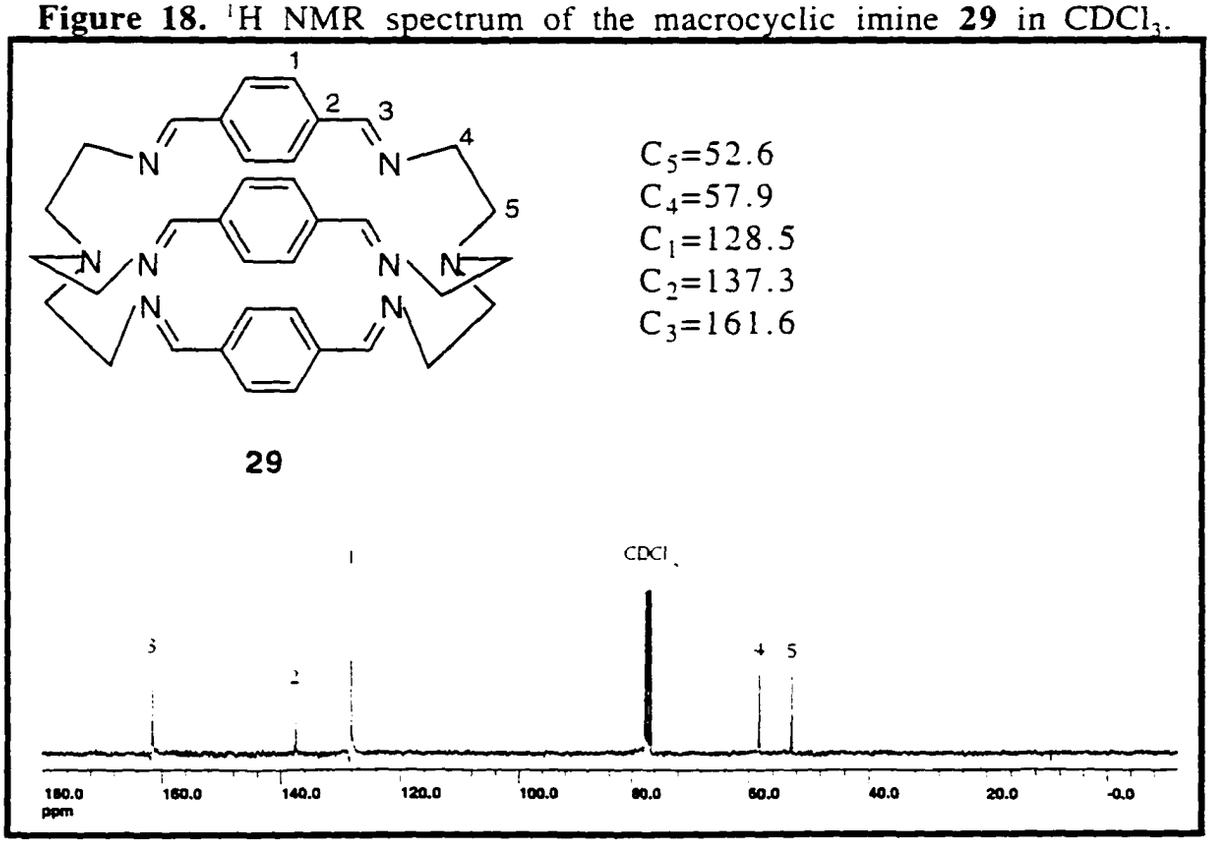

Figure 19. ^{13}C NMR spectrum of the macrocyclic imine **29** in $CDCl_3$.

The ^{1}H nmr spectrum of **30** showed only one signal, a singlet, for the oxaziridine protons, at δ 4.67 ppm (Figure 20). This indicated that the six oxaziridine protons are magnetically equivalent, and that each of these protons is *anti* to the nitrogen lone pairs (Figure 21). This suggested that the peracid attacks on the imine bonds occurred from the *exo* faces, and that each oxaziridine in the macrocycle was an *E* isomer. The aromatic rings' protons also gave only one signal, a singlet at δ 6.95 ppm, and the diastereotopic methylene protons gave four anisochronous, well resolved signals at room temperature. This data indicated that **30** has a rigid, highly symmetric structure, with a three-fold axis of symmetry.

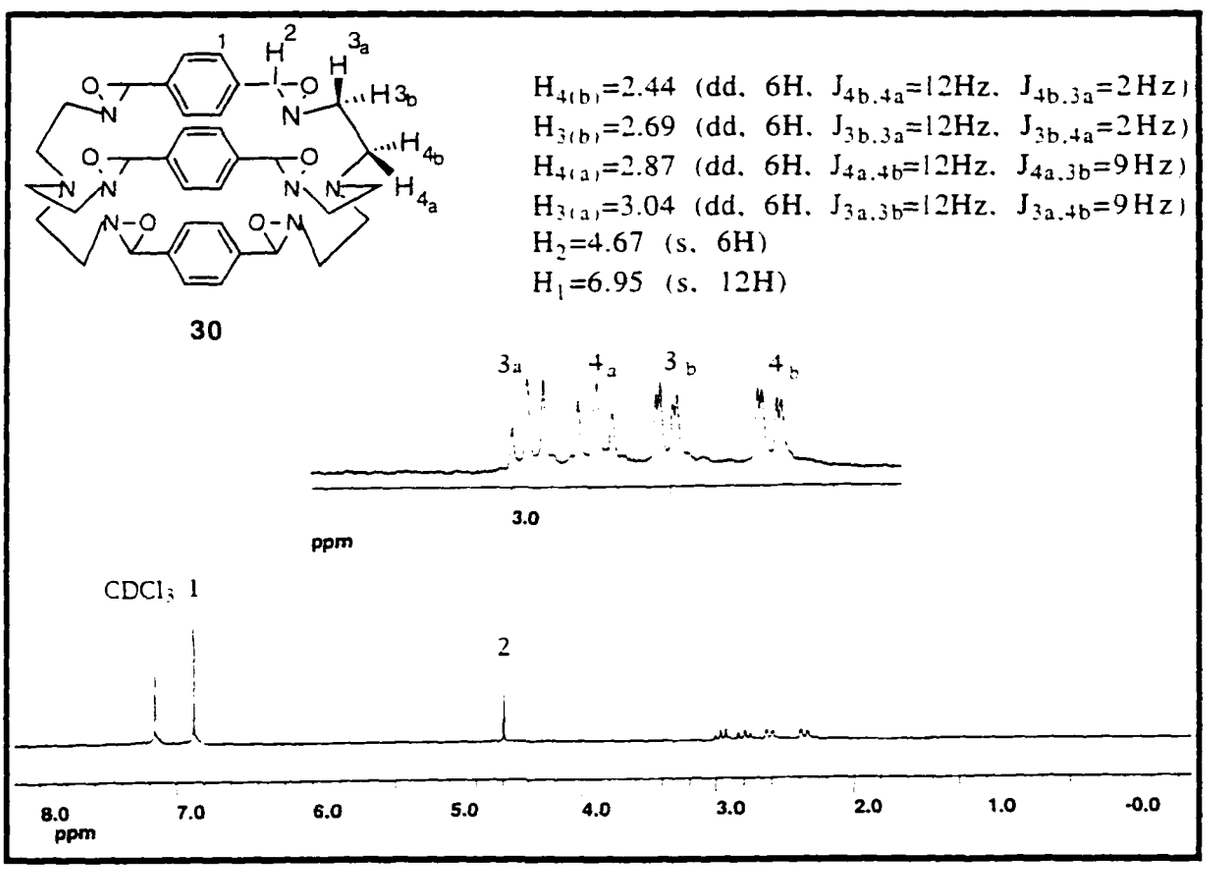

Figure 20. ^{1}H NMR spectrum of the macrocyclic oxaziridine **30**.

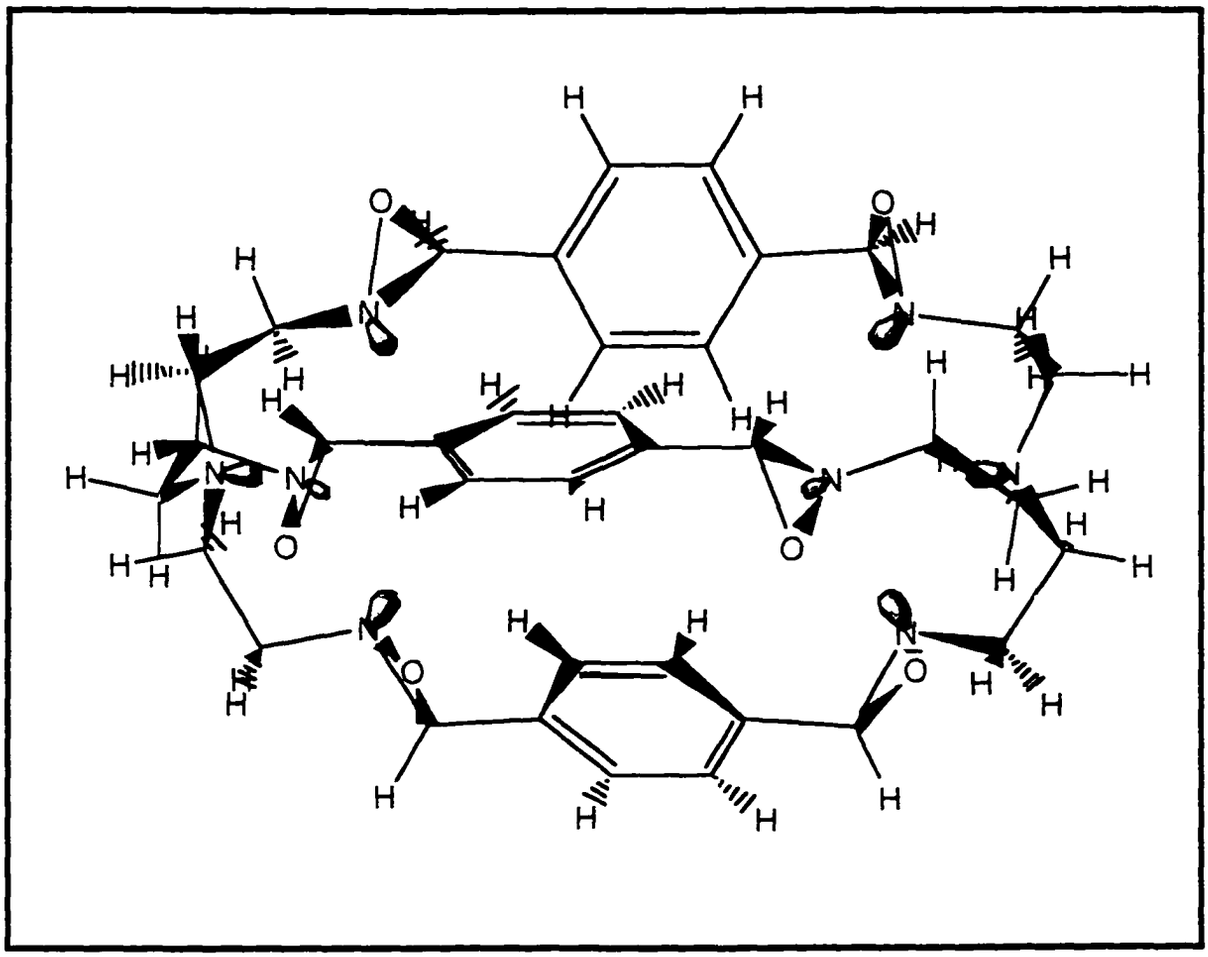

Figure 21. 3D structure of hexaoxaziridine **30** by Macromodel[85] showing the *E* stereochemistry of the oxaziridine rings and the "*endo*" orientation of all nitrogen lone pairs.

The rigid, highly symmetrical 3D structure obtained using the program Macromodel[85] was further supported by the ^{13}C nmr spectrum of **30** consisting of only five peaks. Thus, all the six stereoelectronically equivalent oxaziridine carbons resonate at 80.1 ppm, and the carbons within each group of the two sets of aromatic and the two sets of methylene carbons have identical chemical shifts (Figure 22).

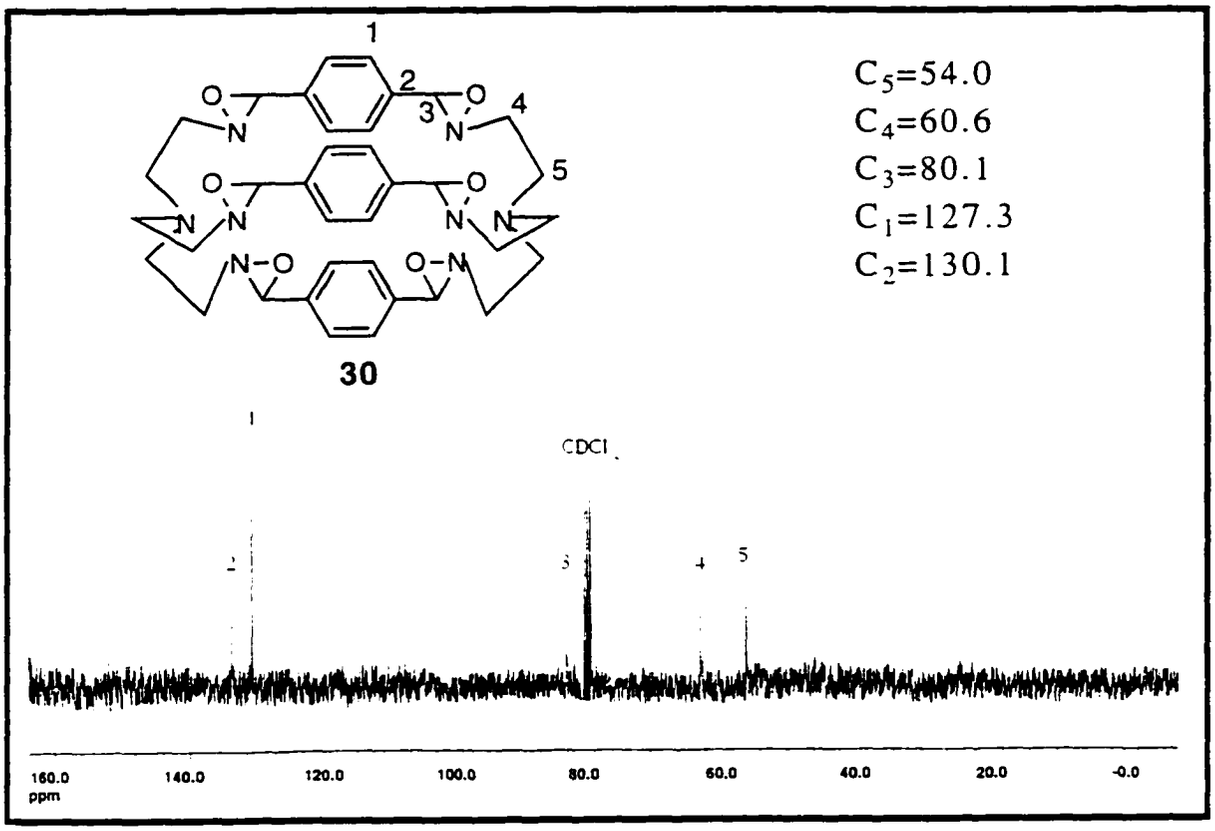

Figure 22. ^{13}C NMR spectrum of the macrocyclic oxaziridine **30**.

There are no known stereoselective reactions of oxaziridines which convert them to compounds of established stereochemistry. and there are few X-ray studies on oxaziridines. For these reasons. spectroscopic studies have been directed towards developing methods for ascertaining their absolute configuration and enantiomeric composition. The ^1H nmr methods employed for this purpose include the use diamagnetic chiral solvating agents (CSA) and chiral lanthanide shift reagents (CLSR).[86-87] The latter class contain paramagnetic metals chelated to organic ligands that disperse the chemical shifts of the enantiomers more efficiently than do chiral solvating agents. However, this advantage of producing greater shift values is often offset by the line broadening caused by paramagnetic

relaxation, and by formation of 2:1 or higher substrate-CLSR complexes, thereby interfering with interpretation of the data. Perfluoroalkyl-arylcarbinols, one example of the chiral solvating agents, has two relatively acidic hydroxyl and methine protons which can take part in hydrogen bonding interactions with substrates to form short-lived, diastereomeric chelate-like solvates, represented by structures **A** and **B** in Figure 23. In these structures, B_1 and B_2 are

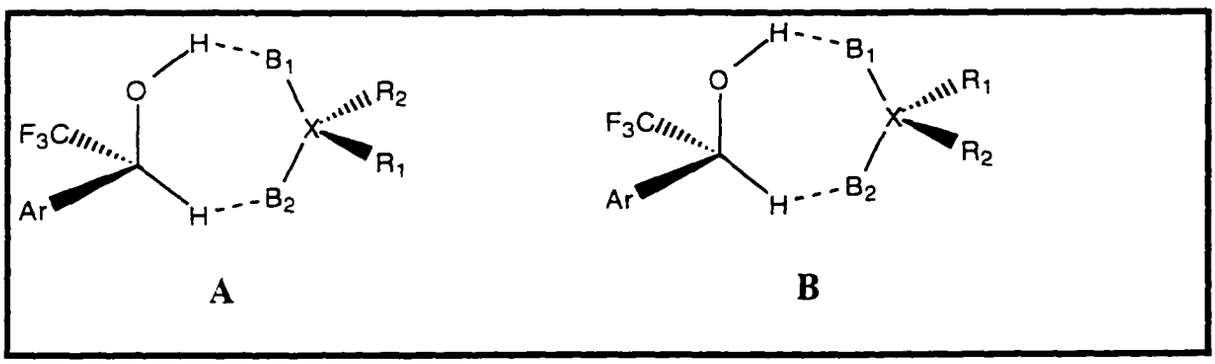

Figure 23.

primary and secondary basic sites on the chiral substrate to be analyzed, and X is the chiral center. Once chelate formation has taken place, the R substituents on the enantiomers experience differential shielding from the aryl ring in structures **A** and **B**. Thus, R_1 is shielded in **A** while the other enantiomer has its R_1 substituent barely affected by the aryl ring in **B**. The converse is true for the enantiotopic R_2 group, resulting in the opposite observed senses of nonequivalence. The enantiomeric composition can be determined from the integrated peak intensities, or more conveniently from the peak heights in some instances, e.g., in the case of the hexaoxaziridine **30** discussed below.

The study of a series of oxaziridines[87] revealed that in unhindered oxaziridines, the nitrogen acts as B_1 site and the oxygen acts as B_2 site, even though steric effects by bulky substituents can switch the primary hydrogen bonding site to oxygen (Figure 24, **A** to **B**). In addition, C-aryl substituents can further complicate interpretation of the spectral nonequivalence, since chelation, as shown in Figure 24 (**C** and **D**), might also occur.

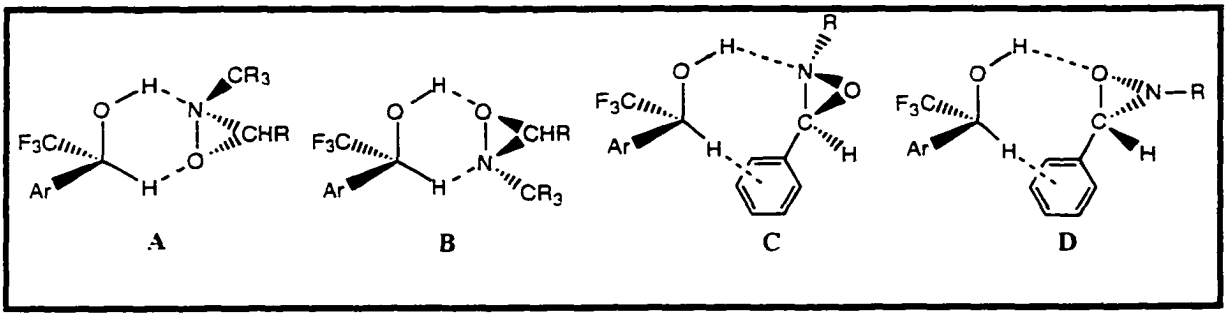

Figure 24.

A modification of the Pirkle and Rinaldi method[87] was employed to determine the configuration of the six oxaziridine units in **30**. Addition of exactly one equivalent of (R)-(-)2,2,2,-trifluro-1-(9-anthryl)ethanol or its (S)-isomer (the CSAs) to **30** in both experiments resulted in split signals of equal intensity of the oxaziridine protons, with one half of each signal shifted upfield (from 4.67 to 4.77 ppm). The addition of one equivalent of an equimolar mixture of the (R) and (S) shift reagents to **30** gave only one signal, shifted upfield (Figure 25, top spectrum). The aromatic protons' signal at 6.95 ppm experienced changes paralleling those seen with the oxaziridine protons, and the signals of the methylene protons were also split upon addition of the (R)- or the (S)-CSA, suggesting that chelates of the type C (Figure 24) are the most significant

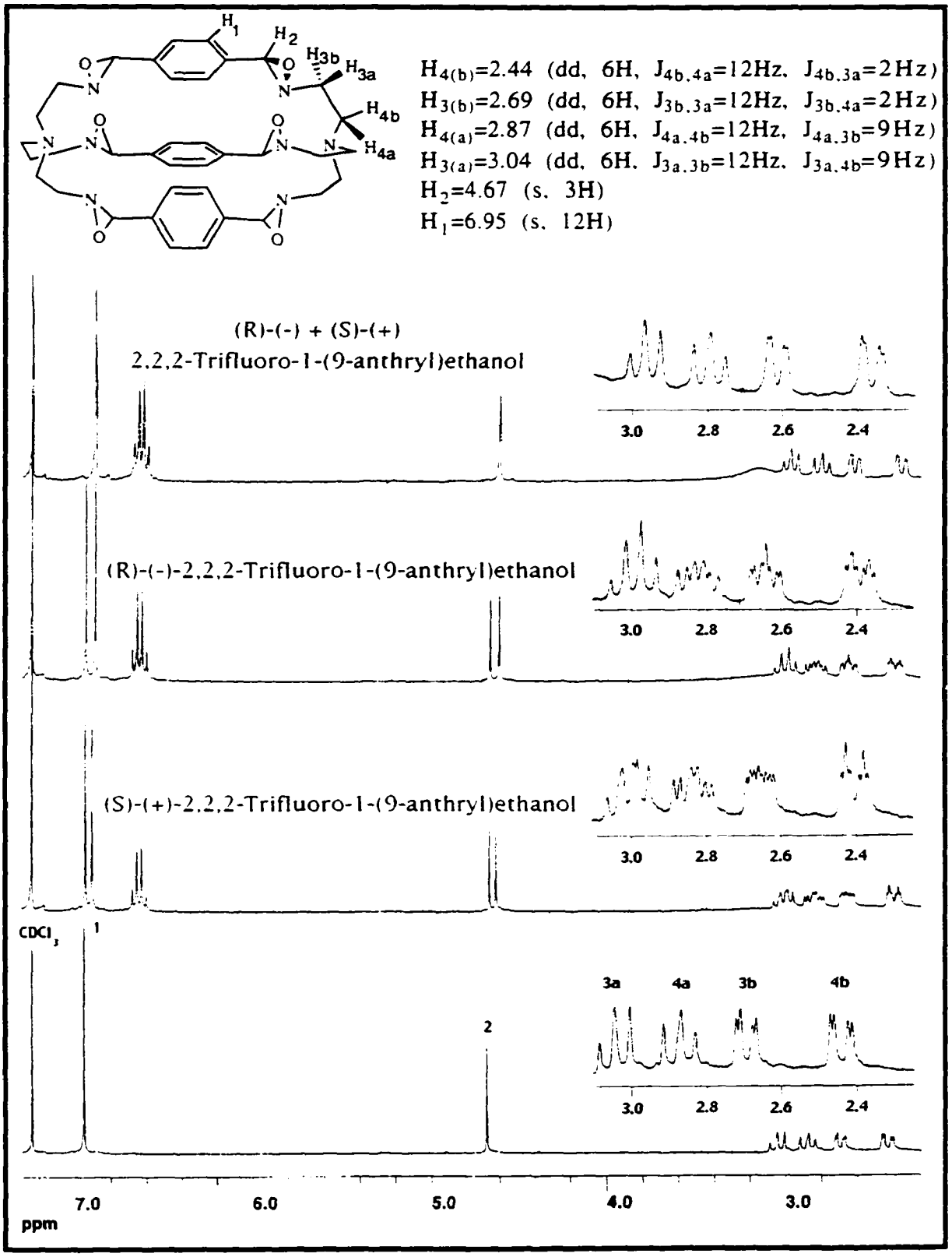

Figure 25. ^{1}H NMR spectrum of the diastereomeric chelates of macrocyclic oxaziridine **30** with the nmr shift reagent (R)-(-)- and (S)-(+)-2,2,2-Trifluoro-1-(9- anthryl)ethanol in $CDCl_3$.

contributors to the shifts. Since the relative intensities of the asynchronous resonances resulting from the interaction **30** with the (+)- and the (-)-CSAs showed a ratio of 1:1, the results indicate that **30** encompasses (R,R) and (S,S) oxaziridines in a ratio of 1:1. The molecule has a three-fold symmetry axis along the two bridgehead nitrogen atoms, and a plane orthogonal to it, to encompass the three identical enantiomeric sets of (R,R) and (S,S) oxaziridines. As expected, hexaoxaziridine **30** had no optical rotation, further supporting the assigned structure (Figure 26).

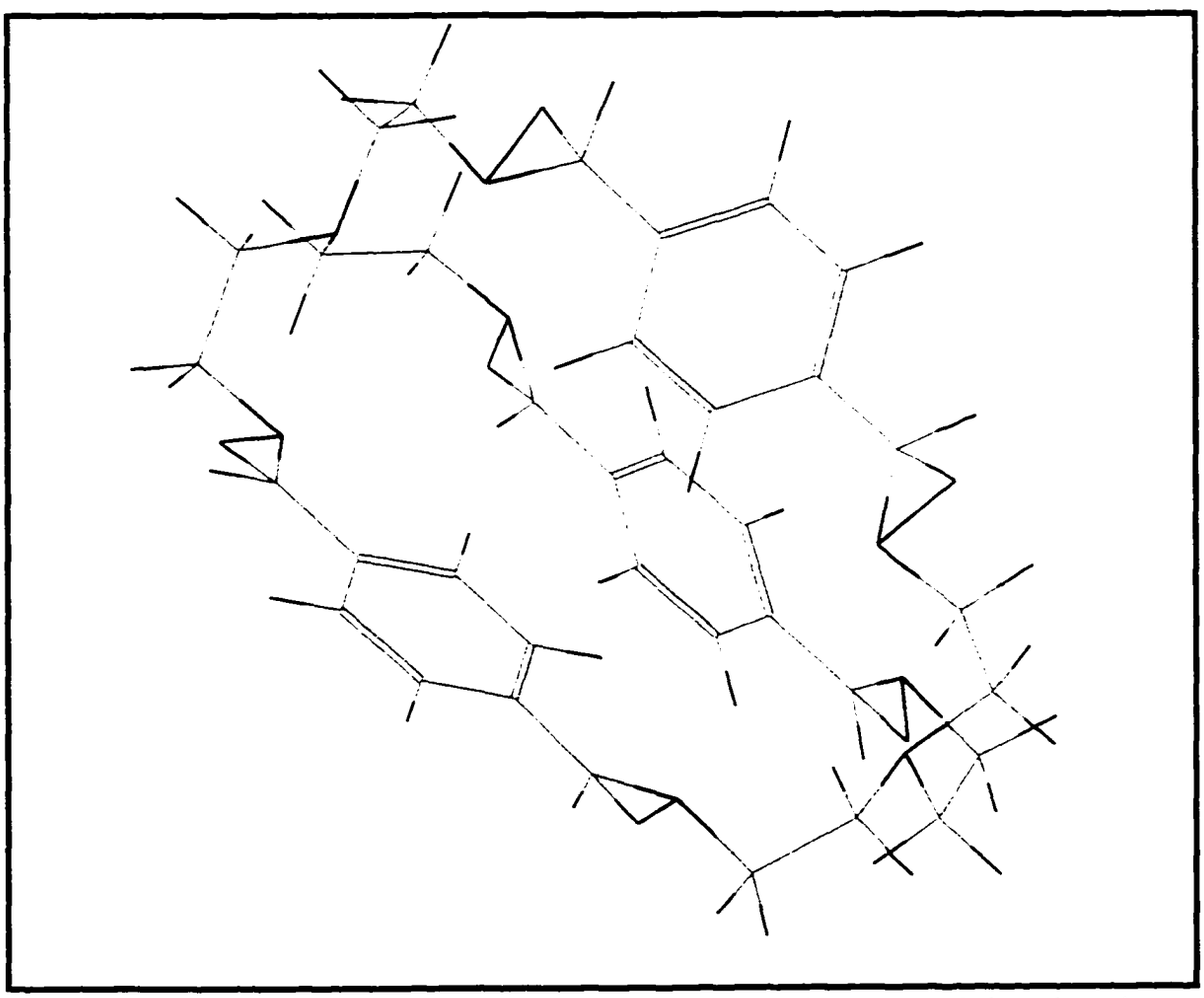

Figure 26. Structure of hexaoxaziridine **30** (Macromodel) showing the two enantiomeric sets of (R,R) and (S,S) oxaziridines.

For X-ray studies, crystals of **30** were grown by slow diffusion of ether into a saturated methylene chloride solution of the oxaziridine at -20°C over a period of several weeks. Although single crystals could be obtained in this manner (Figure 27), they were not of suitable quality for X-ray studies as determined by the group of Professor Jon Clardy at Cornell University.

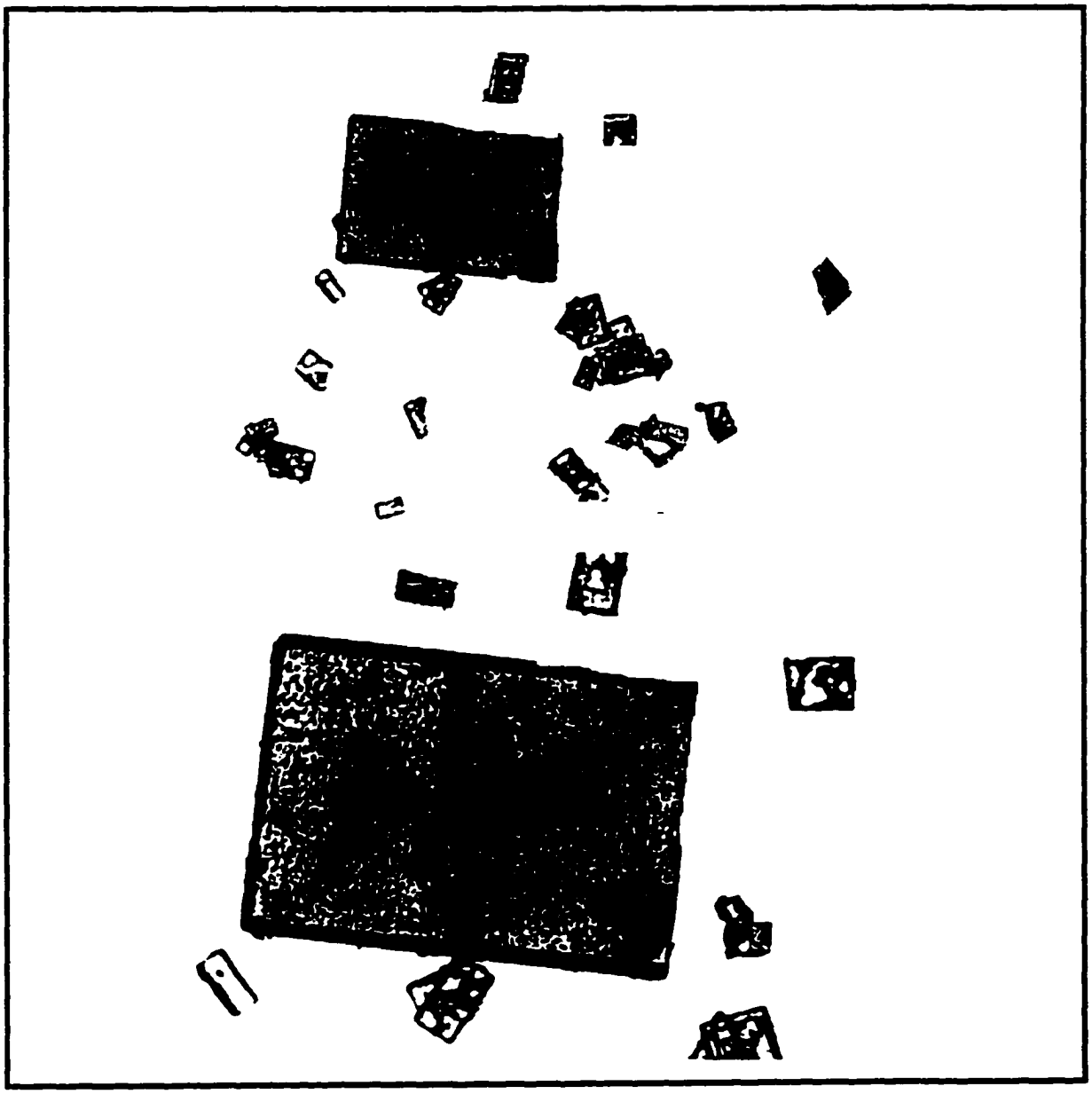

Figure 27. Single crystals of oxaziridine **30** (magnification:1x150).

2.1.3.2. Synthesis and oxidation of a tris(2,2'-bipyridine cryptand.

The very low solubility of hexaoxaziridine **30** in water prevented its intraperitoneal delivery to mice, and when it was given orally, mixed with peanut butter, its rapid decomposition rendered it useless *in vivo*. These studies were conducted by Professor Marilyn S. Bartlett' s group at the Indiana University Medical School. The cryptand, **31**, having symmetry properties similar to that of the hexaimine **29**, was considered an attractive starting material for synthesis because the hexaoxaziridine derived from it, having three bipyridyl moieties, was expected to have better water solubility than **30**. Moreover, it was envisaged that the water solubility of the hexaoxaziridine derived from **31** might be increased even further if the six bipyridine nitrogens in **31** could be oxidized to the polar N-oxide derivatives.

The cryptand **31** was synthesized by template-free [3+2] condensation of 4,4'-diformyl-2,2'-bipyridine with tris(2-aminoethyl)amine in 70% yield[88] (Scheme 22). However, instead of the reported four step synthesis, the 4,4'-diformyl-2,2'-bipyridine was prepared by a shorter route, in two steps,[89] and the macrocyclization was carried out in MeOH instead of the THF[88a] or CH_3CN[88b] employed by Beer *et al.* In our hands, using THF led to a polymeric material, and no [3+2] macrocyclization product could be isolated. The structure of **31** was confirmed by ^1H nmr and FAB-MS (Figure 28a and 28b).

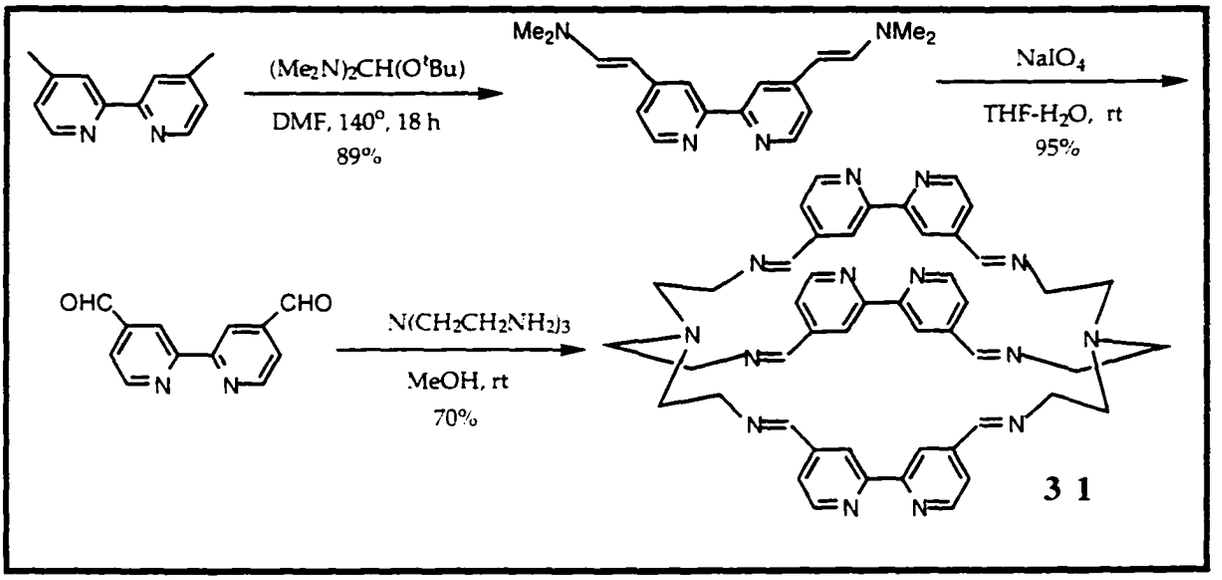

Scheme 22.

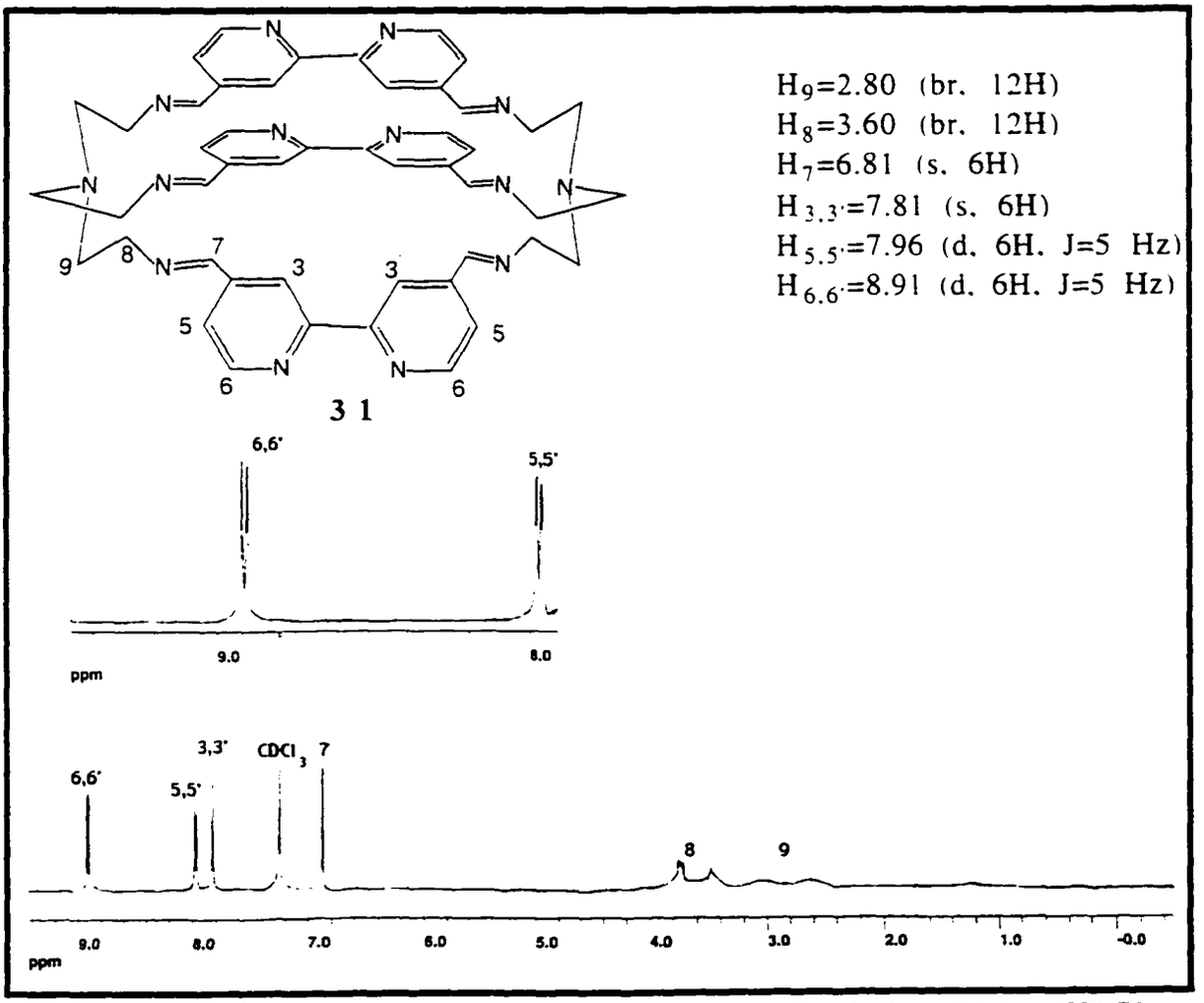

Figure 28a. ^{1}H nmr spectrum of the macrocyclic imine **31** in $CDCl_3$.

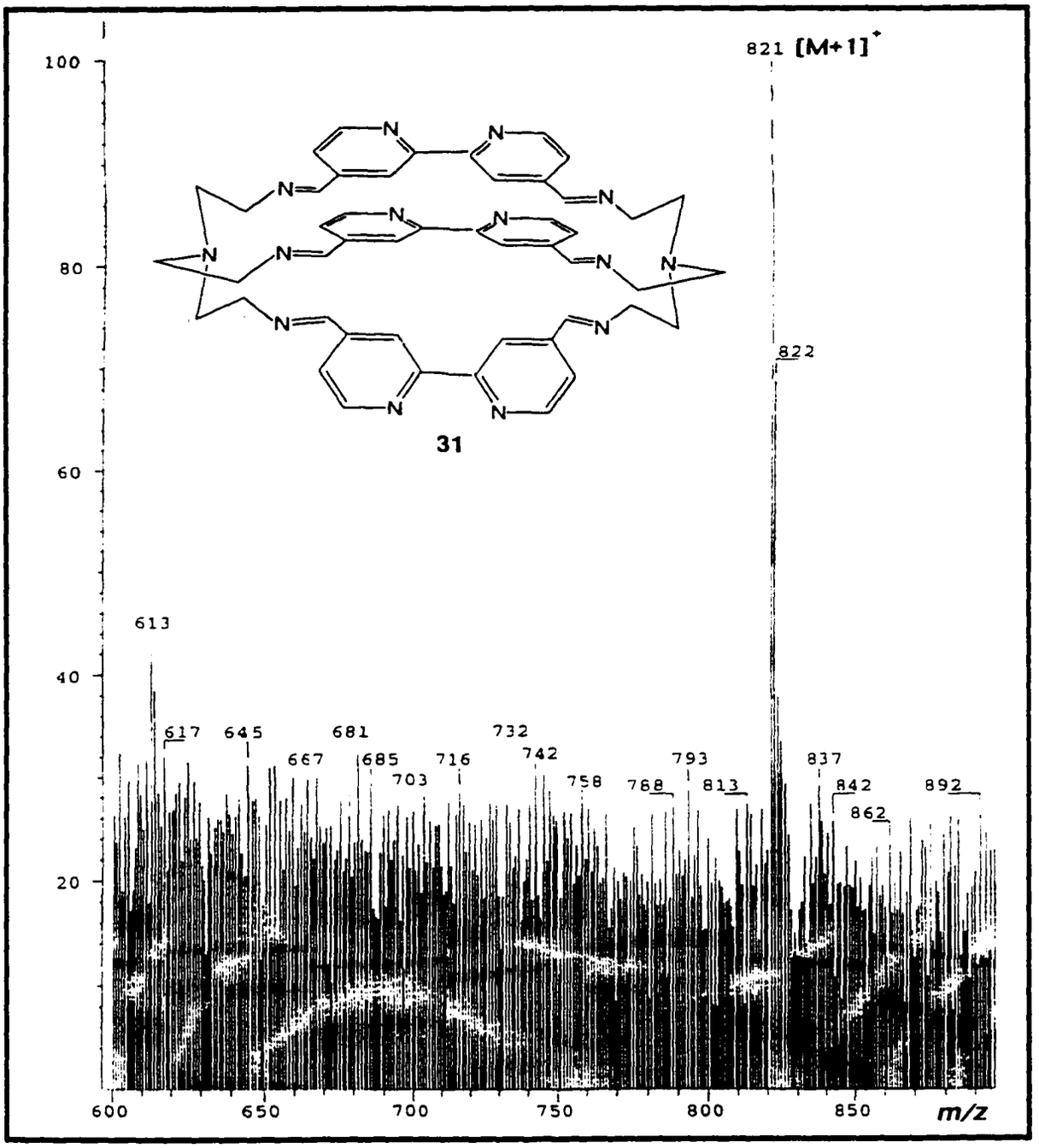

Figure 28b. FAB (NBA) mass spectrum of the macrocyclic imine **31**.

Attempted oxidation of **31** with *m*-CPBA in $CHCl_3$ at various temperatures (27°C, -20°C, and -78°C), or in aqueous $NaHCO_3/CHCl_3$, with or without phase transfer agent, failed to yield the desired

hexaoxaziridine as did Oxone. Thus, despite the numerous attempts to oxidize hexaimine **31** to a hexaoxaziridine, the only major product isolated from these reactions was the decomposition product, 4,4'-diformyl-2,2'-bipyridine. It is likely that the low stability of the oxaziridine is the major cause of these failures. However, the stability and/or the conformational flexibility of the hexaimine might also contribute to the problem. As indicated by the unresolved methylene peaks in its ^{1}H nmr spectrum (Figure 28a), unlike the hexaimine **29** the rigid precursor of the hexaoxaziridine **30**, hexaimine **31** is a much more flexible molecule.

2.2. Synthesis of a macrocyclic amide - Ni^{II} complex, 33.

The macrocyclic amide, **32**, and its Ni(II) complex, **33**, were first synthesized by C.E. Brathwaite in this laboratory.[10] The *in vitro* antifungal activity of **33** was found comparable to that of the drug currently in use against *P. carinii*, and so we required a large scale synthesis of this compound. Therefore, ca. 10 grams of macrocyclic amide **32**, hitherto available only in milligram amounts, was prepared following the route established previously.[10] It was converted into **33** following a novel route (Scheme 23). The macrocyclic amide, **32**, was deprotonated with lithium bis(trimethylsilyl)amide at low temperature, and the Ni(II) was inserted using $(Ph_3P)_2NiBr_2$. Deprotonation prior to nickel insertion was necessary because the protonated amide does not contain a σ-donating lone pair to lead the coordination process.

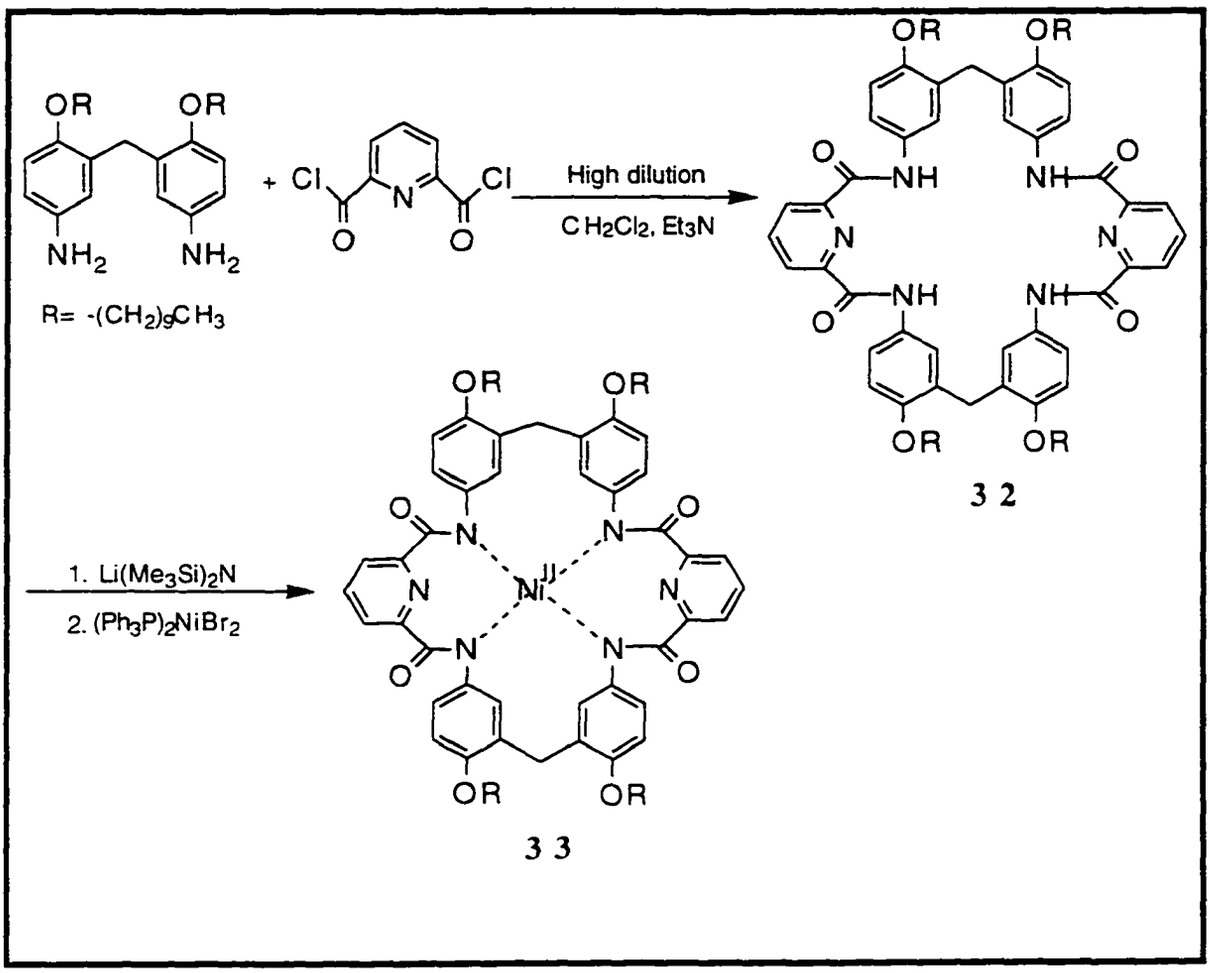

Scheme 23.

The UV and MS spectra of the macrocyclic amide **32** were identical with those reported earlier,[10] as were the UV spectrum of the Ni(II) complex, **33**, which showed an absorption band at 366 nm and an [M+Ni] ion at *m/z* 1340 in the FAB-MS confirming the presence of the nickel in **33**. The FTIR spectrum of tetraamido macrocycle **32** showed the expected amide bands (Figure 29). The FTIR spectrum of the Ni(II) complex **33** showed bands for the deprotonated amides (Figure 30a) and, in addition, a band for the metal-nickel vibration at 540.9 cm^{-1} (Figure 30b).

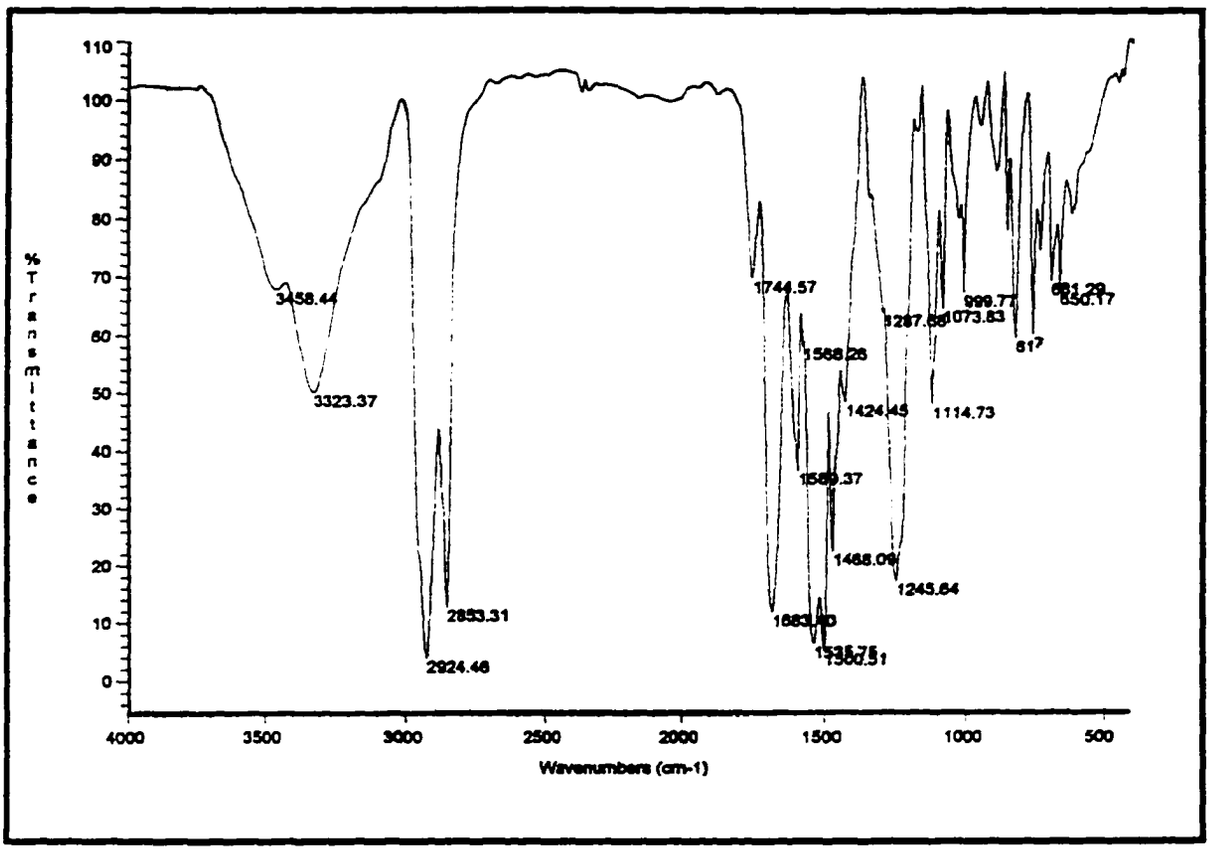

Figure 29. FTIR (KBr) spectrum of the macrocyclic amide **32**.

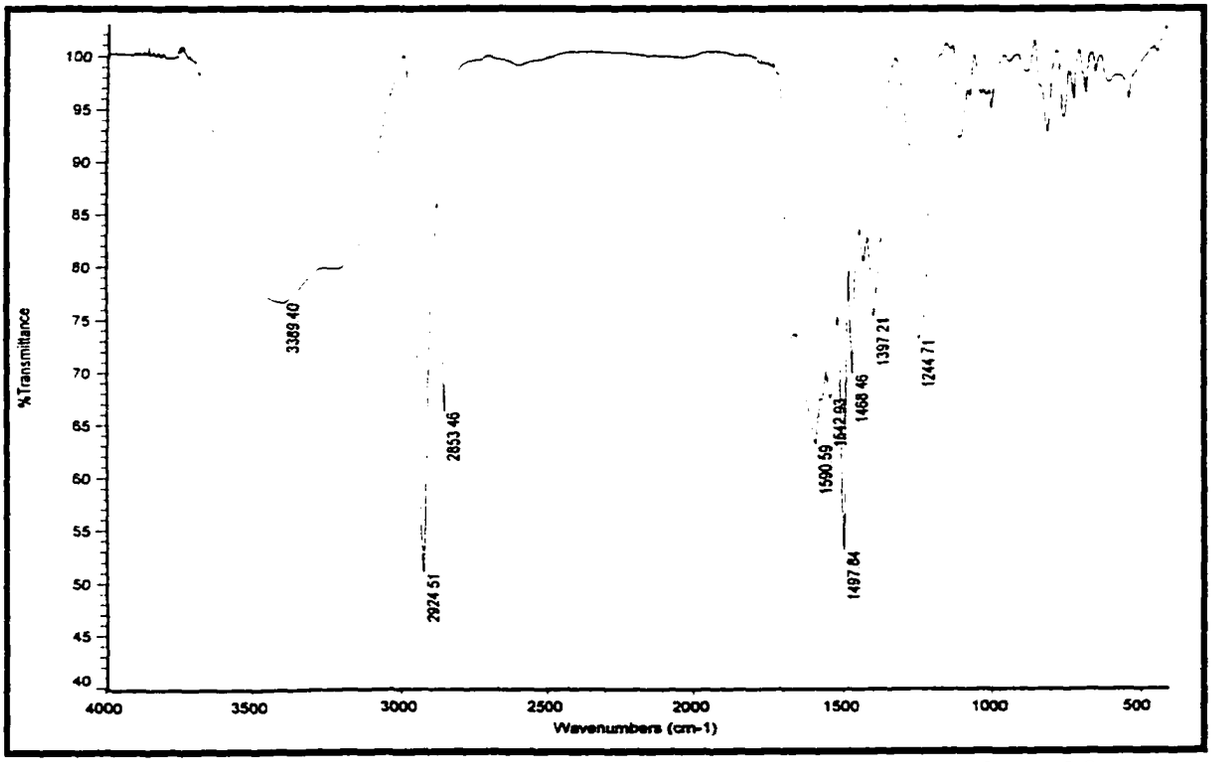

Figure 30a. FTIR (KBr) spectrum of the Ni(II) complex, **33**.

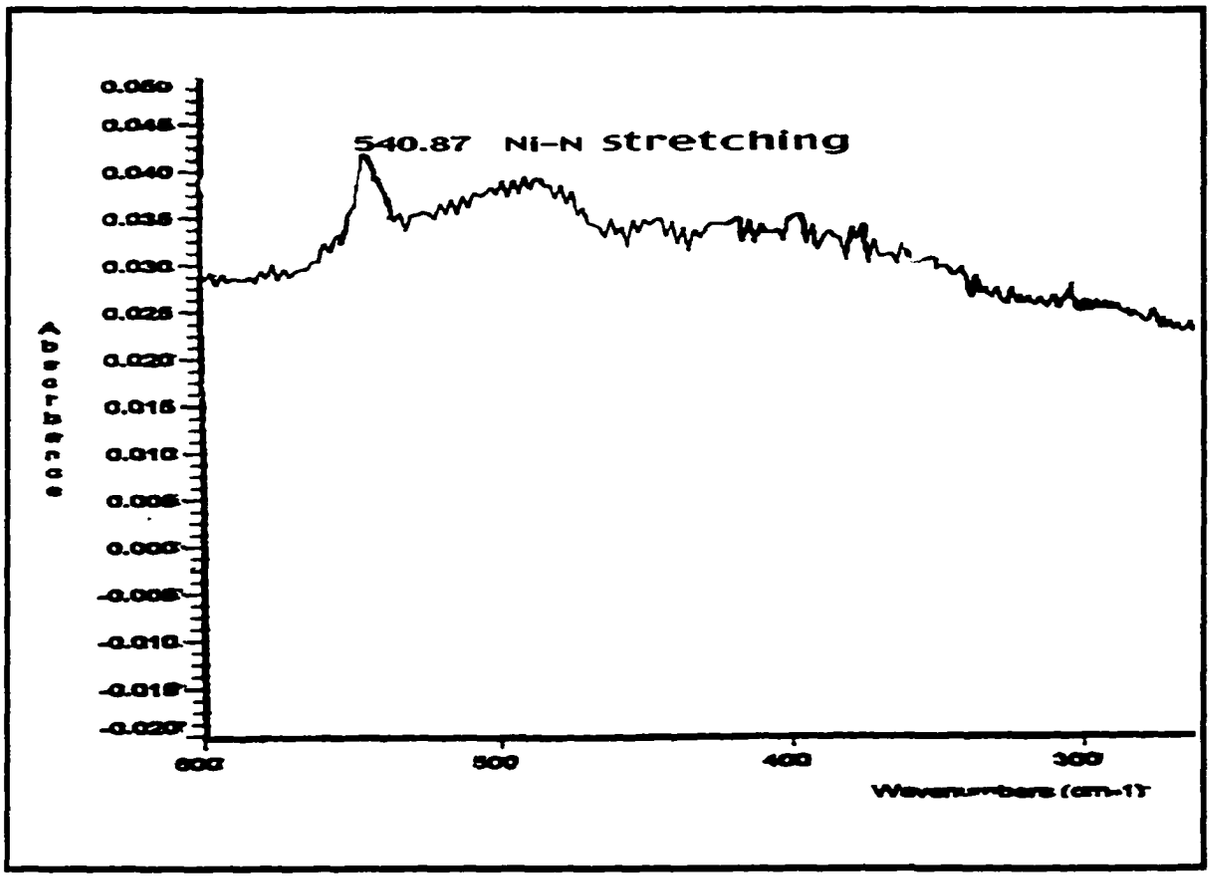

Figure 30b. Far-FTIR (dry film on polyethylene) spectrum of the Ni(II) complex, **33**.

In vivo studies in mice to determine the efficacy of the nickel complex against the opportunistic pathogen *P. carinii* are in progress at the testing laboratories of the National Institutes of Health.

2.3. Synthesis of tris(nitronyl nitroxide), 36.

Since the dendrimer **28** containing a 1,3,5-triazine core appended with oxaziridinyl pharmacophores (Section 2.1.2.) showed promising antifungal activity, and was not toxic, we used this same core to synthesize the tris(nitronyl nitroxide) **36** (Scheme 24).

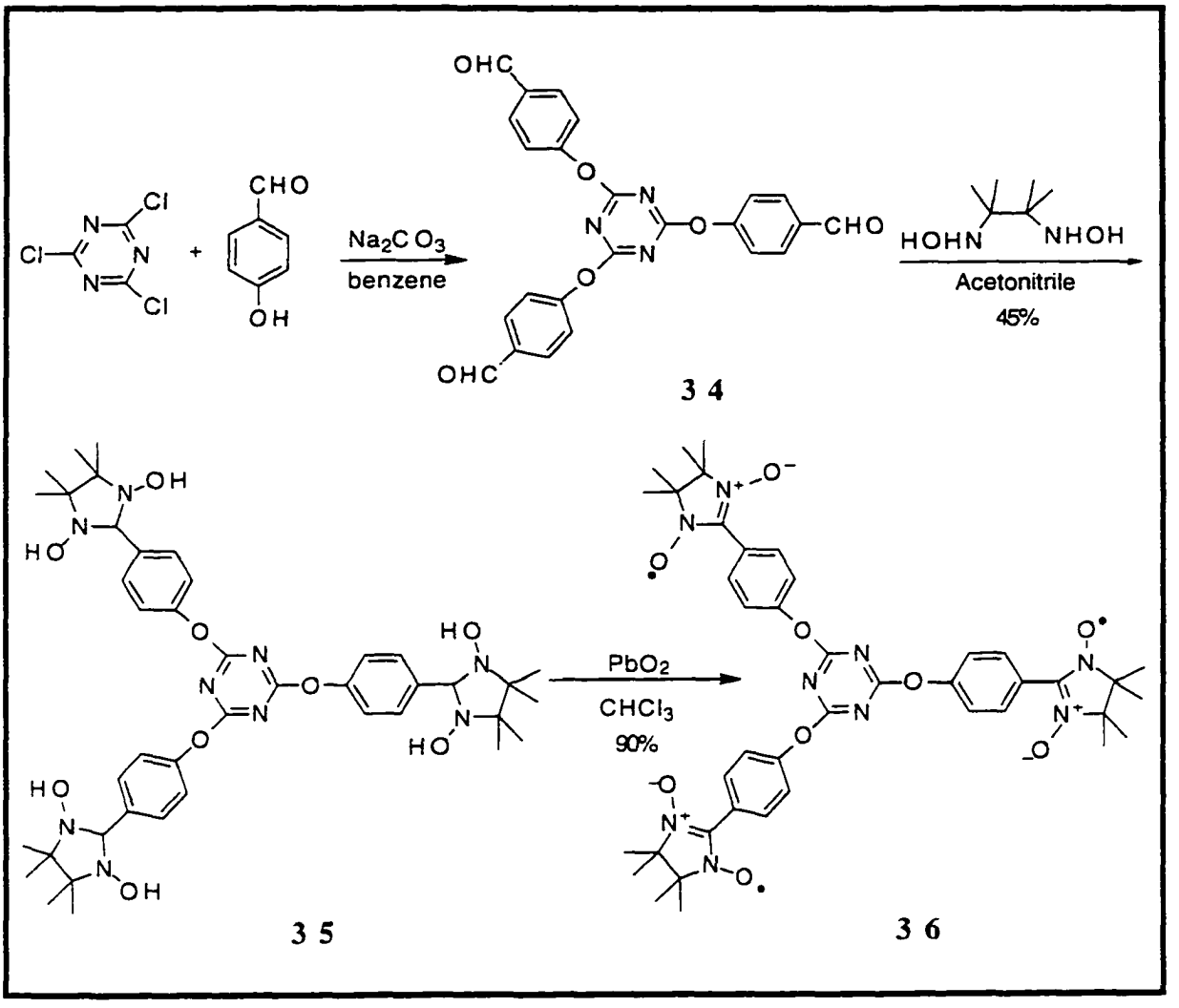

Scheme 24.

Condensation of the trisaldehyde[84] **34** with 2,3-dihydroxyamino-2,3-dimethylbutane gave a colorless tris(di-*N*-hydroxy) intermediate, **35**, which was oxidized with PbO_2 to afford the tris(nitronyl nitroxide) **36** in excellent yield. The triradical **36**, obtained as deep-blue colored microcrystalline material, was stable at room temperature for several months. It had limited solubility in water, <2 mg/ml, but was very soluble in DMSO (34 mg/ml) so it could be tested against *P. carinii* in cultures at both low and at high concentrations.

HPLC analyses showed that the tris(nitronyl nitroxide **36** consisted of a mixture of conformers in equilibrium. When either of the two major HPLC peaks was separated, then reinjected for analysis, an identical pattern of peaks with the same intensity ratios was seen as had been obtained prior to the separation of the peaks. Moreover, each peak had identical FAB-MS (Figure 31). Although the FAB mass spectrum of **36** did not show molecular ion at *m/z* 822, it displayed a fragmentation pattern in agreement with the assigned structure.

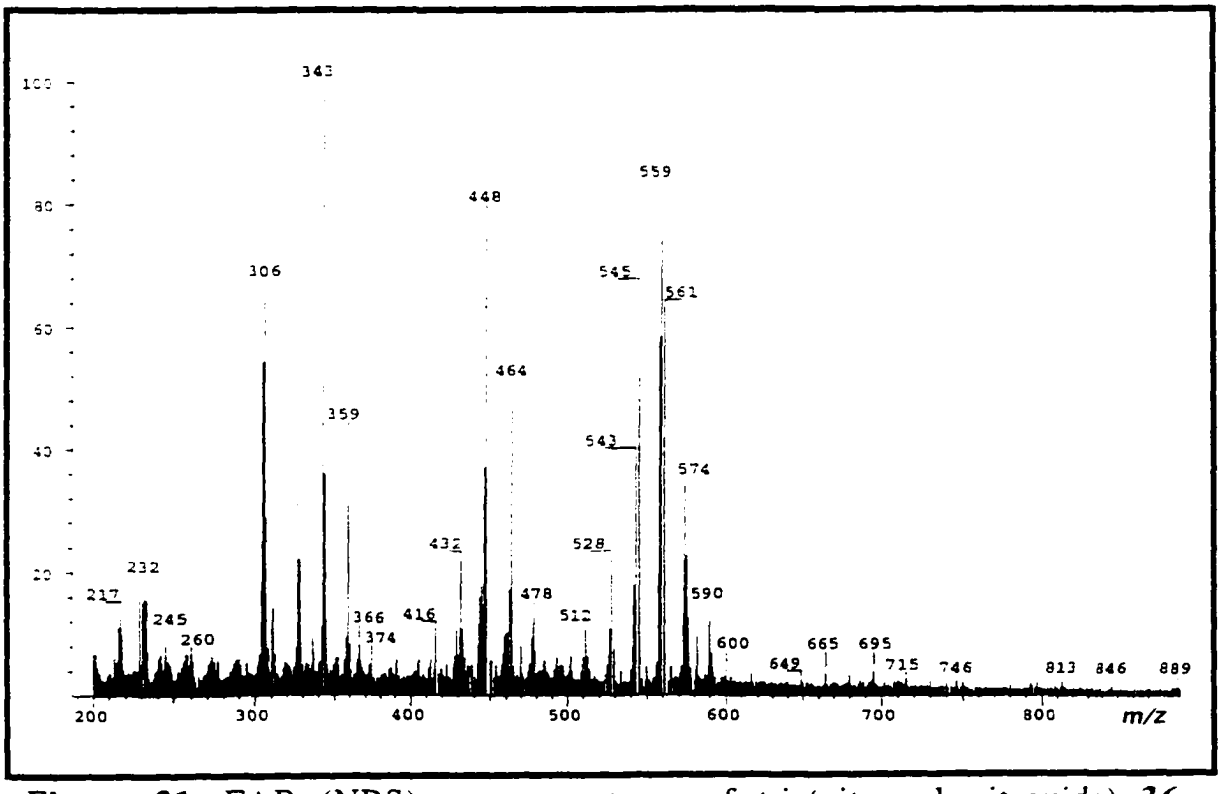

Figure 31. FAB (NBS) mass spectrum of tris(nitronyl nitroxide) **36**.

The main fragmentation pathway *a* (Scheme 25), involves cleavage of the O - phenyl ether bond and consecutive losses of two of the three phenylnitronyl nitroxides attached to the triazine ring giving the ions at *m/z* 590 and 358. The latter releases a methyl radical to

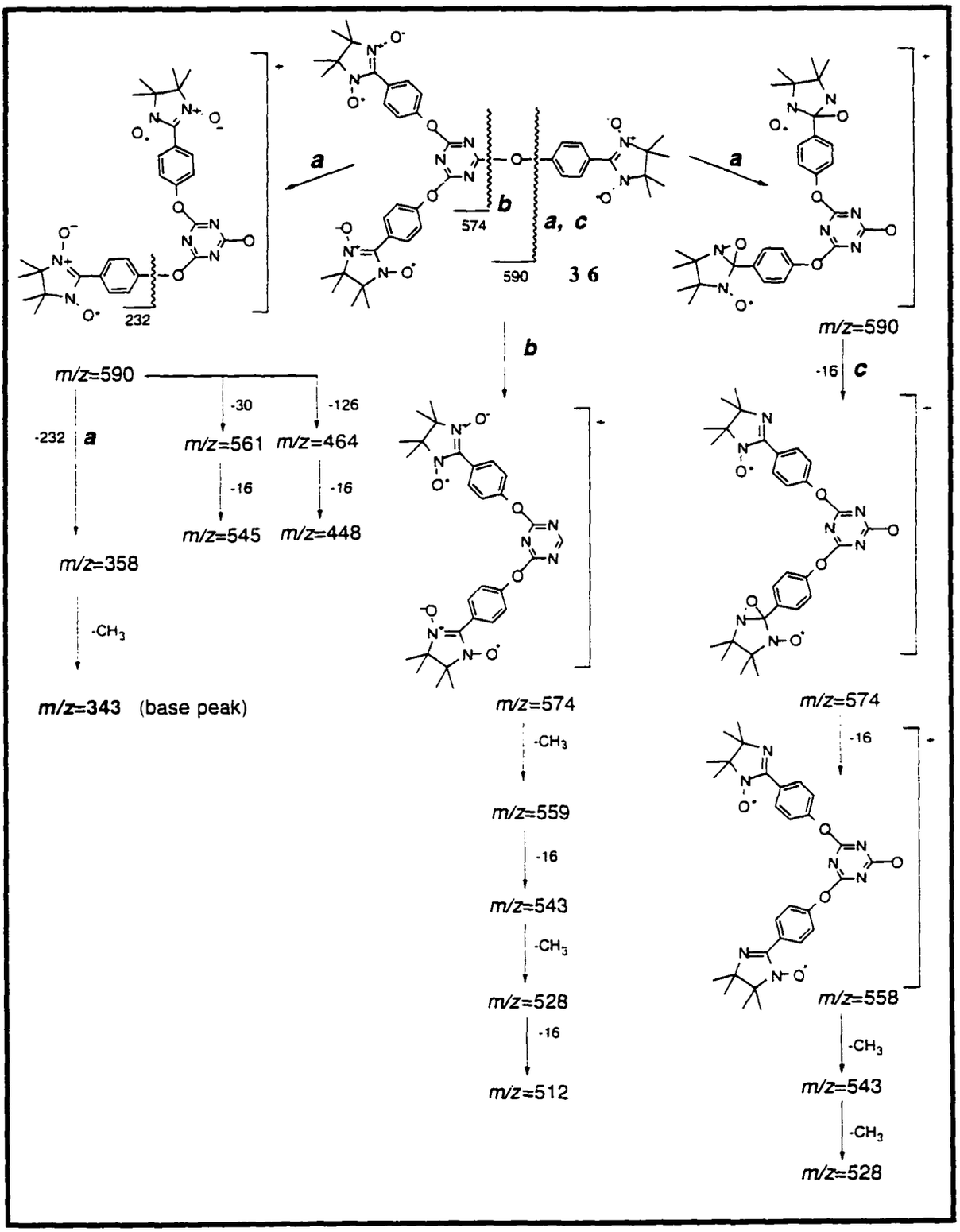

Scheme 25.

yield the base peak at m/z=343. In pathway *b*, cleavage of the triazine-O bond yields the m/z=574 ion. Subsequent loss of a methyl, an oxygen, a methyl, and again an oxygen atom accounts for the ions at m/z=559, 543, 528, and 512. In pathway *c*, as in *a*, the 590 ion is formed first. It then loses two oxygens and a methyl radical to yield ions at m/z=574, 558, 543, and 528. Unlike in pathway *a*, here the 590 ion has an oxaziridinyl nitroxide structure, accounting for the consecutive losses of the 16 mass units. Because nitrones are not active oxygen compounds, to account for the losses of 16 mass units from 574, one could invoke the cyclization of the nitronyl moieties to oxaziridines. However, the loss of 16 mass units in nitrones are of no diagnostic value. Their intensity is strongly dependent not only on the structure of the nitrone, but also on the experimental measuring conditions, so it can range from <1% to close to 100% of the base peak's intensity. From the sparse evidence so far available, aromatic N-oxides do lose an oxygen atom to an appreciable extent, but nonaromatic N-oxides do not share this propensity for oxygen ejection. Loss of N-O$^{\bullet}$ followed by loss of oxygen from the m/z=591 peak accounts for the fragments seen at m/z=561 and 545. The peaks at m/z 464 and and 448 could result from fragmentation of the nitronyl nitroxide ring and subsequent loss of a16 mass unit.

Triradical **36** had a broad, long wavelength absorption band at 598 nm, typical of nitroxides,[69] and bands at 362 and 252 nm in the UV corresponding to the conjugated nitrones and the aromatic moieties, respectively (Figure 32).

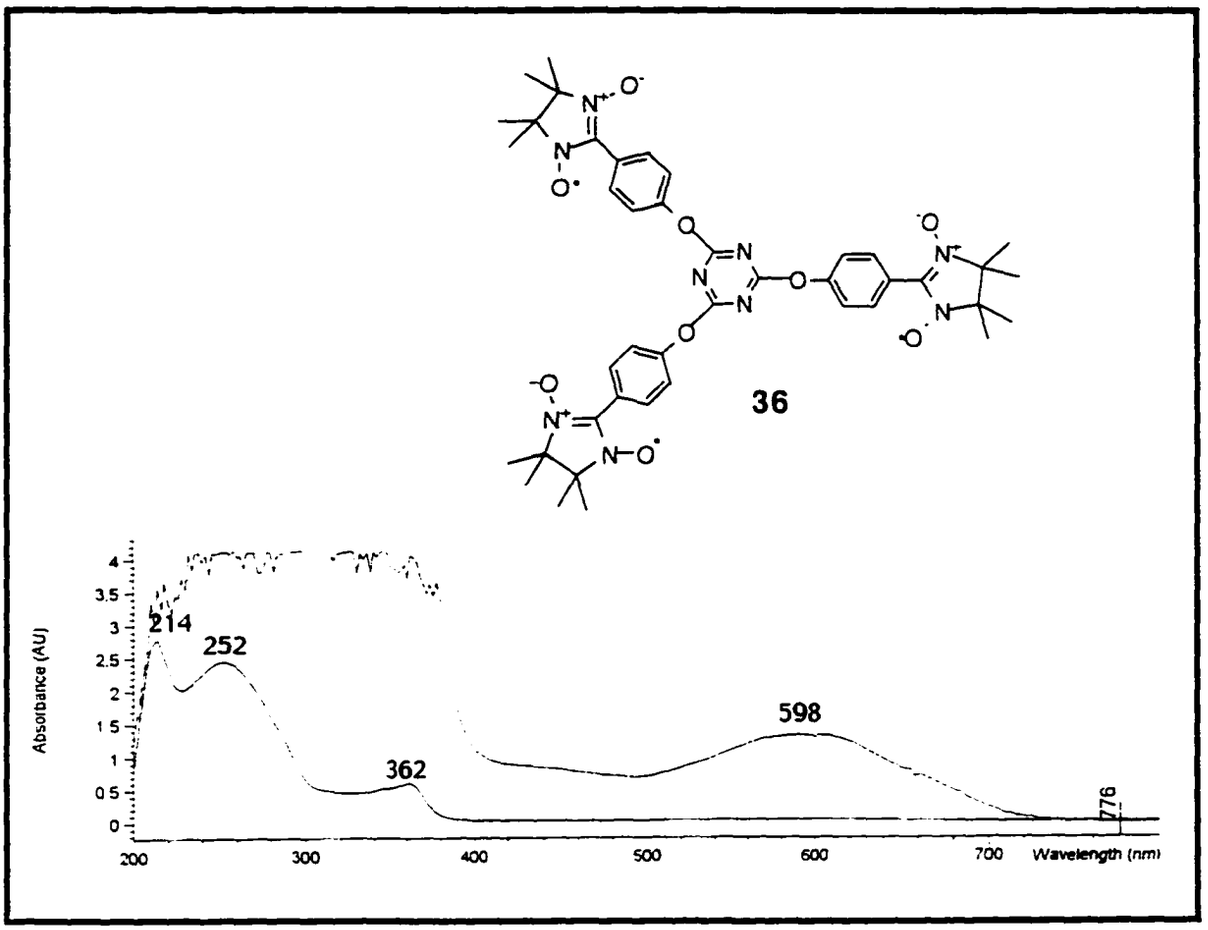

Figure 32. UV-VIS spectrum of the tris(nitronyl nitroxide) **36** in methanol at two different concentrations.

To facilitate spectral analysis of **36**, a paramagnetic species, it was reduced with methylhydrazine to the corresponding tris(N-hydroxy) derivative **37**. The UV-VIS spectrum of **37** (Figure 33) showed disappearance of the nitroxide band at 598 nm, and a slight red shift of the nitrone band, from 362 to 368 nm. Moreover, the latter band had a more pronounced fine structure, with maxima at 368 and shoulders at 345 and 371 nm. This indicates a more rigid structure having more extensive planarity of the phenyl rings with the five membered rings containing the nitrone groups.

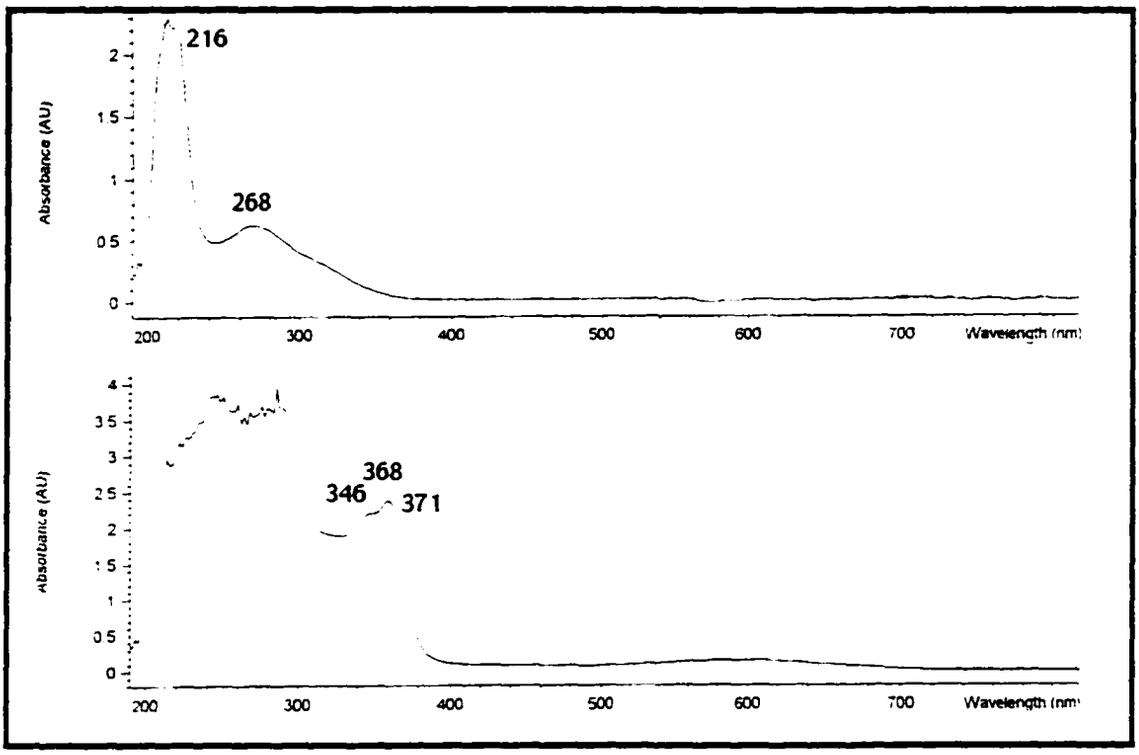

Figure 33. UV-VIS spectrum of the reduction product **37** in methanol at two different concentrations.

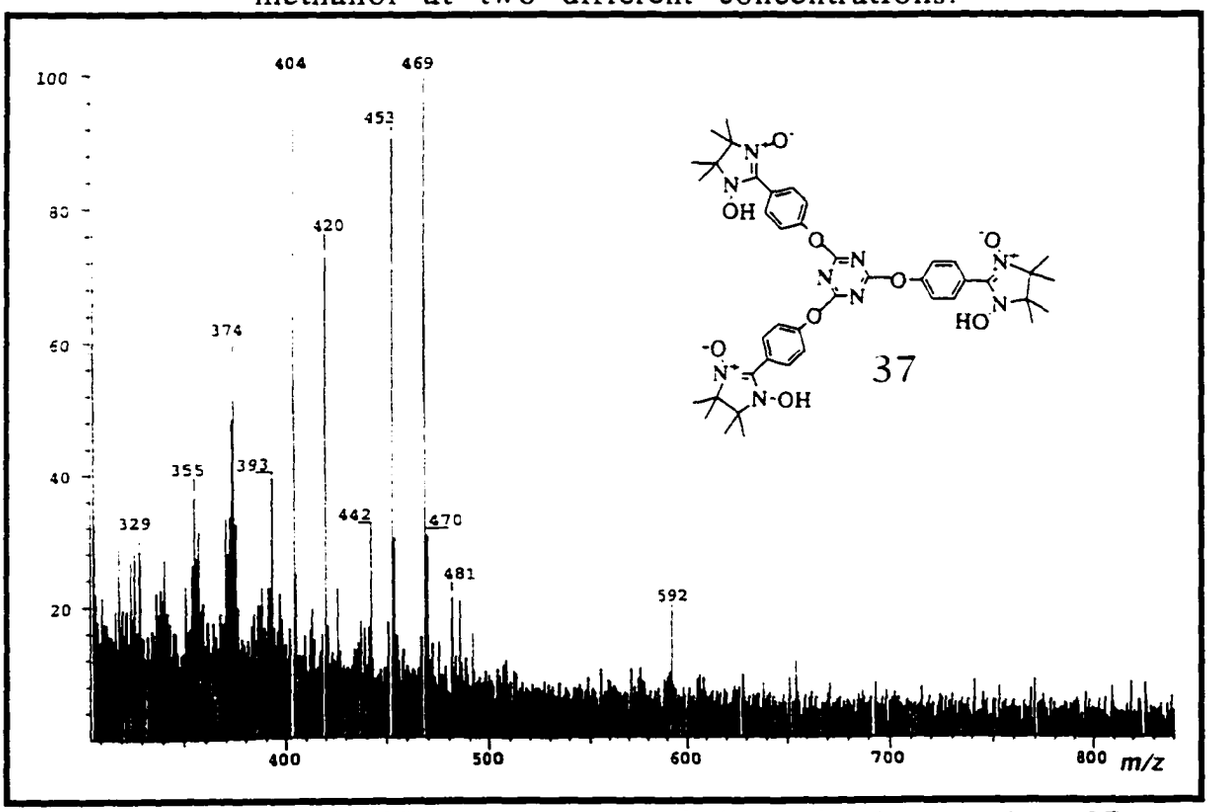

Figure 34. FAB-MS (NBA) spectrum of the reduction product **37**.

The FAB mass spectrum of **37** (Figure 34), as was the case with **36**, lacked a molecular ion, but showed a fragmentation pattern confirming the structure. Noteworthy is that cleavage of the O - Phenyl bond in **37** gave a fragment at *m/z*=592, two mass unit higher than the fragment resulting from the same cleavage in **36**, thereby confirming reduction of the N-O• to N-OH groups.

HPLC analysis of the reduction product **37** (Figure 35) showed

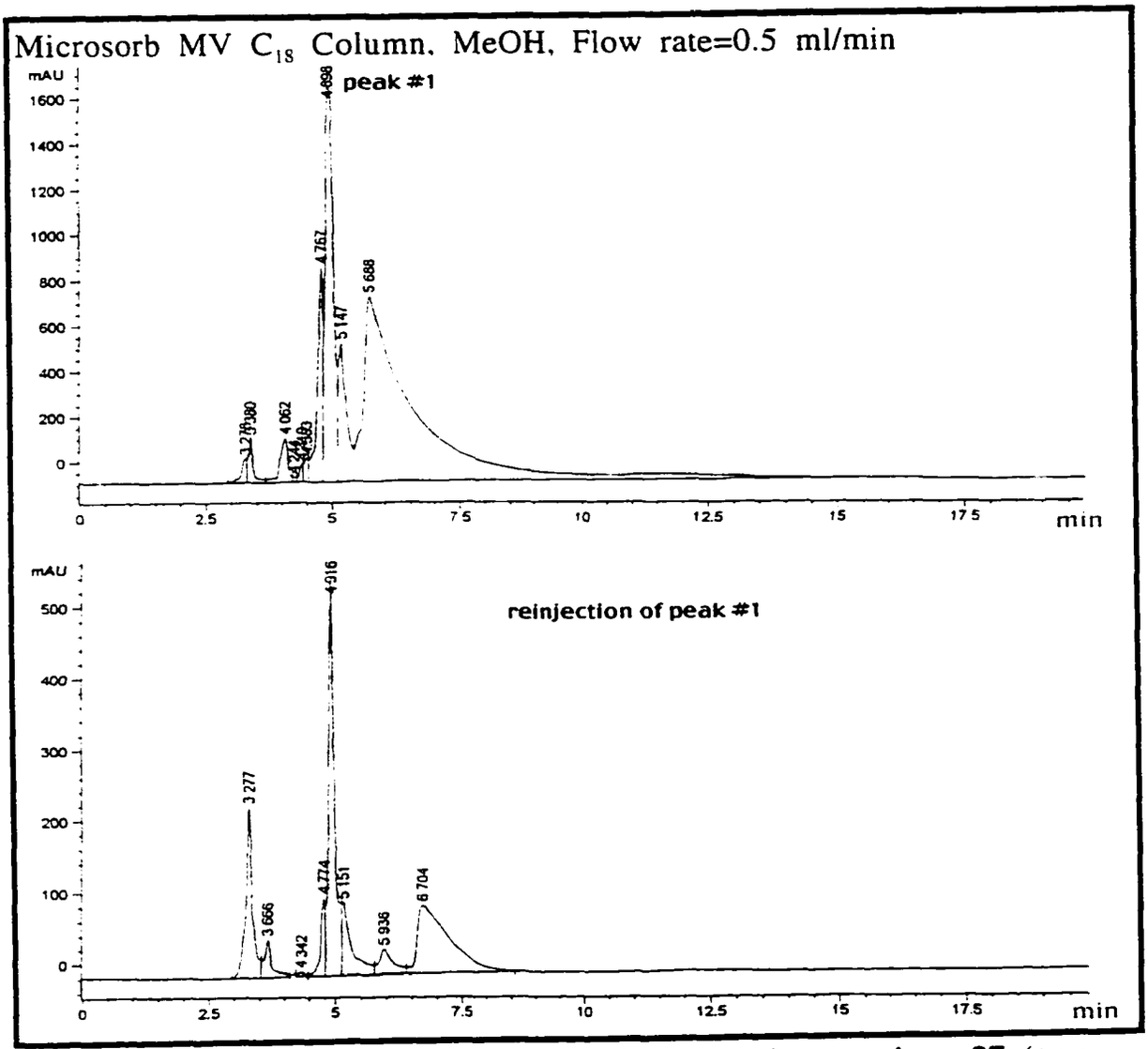

Figure 35. Hpl chromatogram of the reduction product **37** (top panel), and chromatogram of the reinjected peak #1 (bottom panel).

the presence of conformers at equilibrium, similar to that seen in the case of the tris-radical **36**.

Because of the excessive paramagnetic line-broadening, the ^{1}H nmr spectrum of **36** could not be used to confirm its structure. However, *in situ* reduction to the N-hydroxy derivative **37**, achieved by adding methylhydrazine to the nmr sample until the blue color of the radical disappeared, afforded a ^{1}H nmr spectrum that indirectly confirmed the structure of **36**. To optimize separation of the signals, the reduction product was solubilized in a mixture of DMSO-d_6/benzene-d_6 (85:15) (Figure 36a).

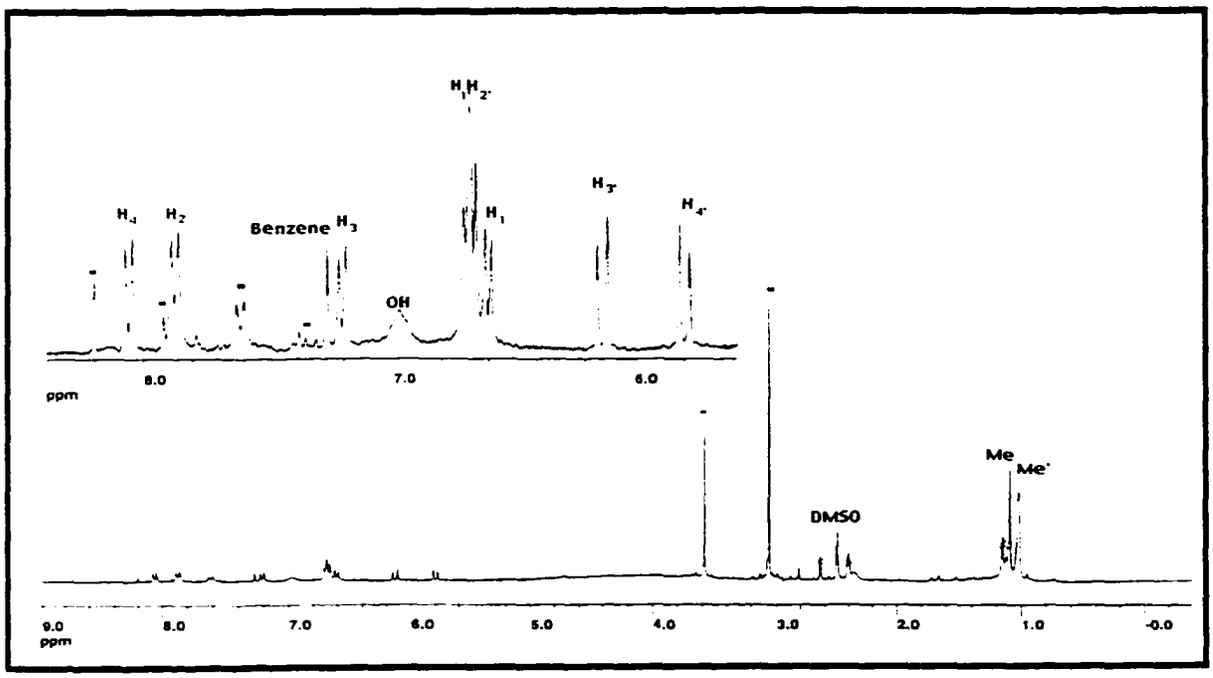

Figure 36a. ^{1}H nmr spectrum of the reduction product **37/37'** in DMSO-d_6 - benzene-d_6.

In addition to an as yet unidentified minor conformer (peaks shown by *), the ^{1}H nmr spectrum confirmed the presence of two distinct, major conformers in **37**, each stabilized by a network of hydrogen

bonds (Figure 36b). In conformer **37** the hydrogen bonds are among the three N-OH groups, whereas in conformer **37'** hydrogen bonding of the nitrone's $=N^{+}-O^{-}$ groups with the N-OH groups that stabilize the structure.

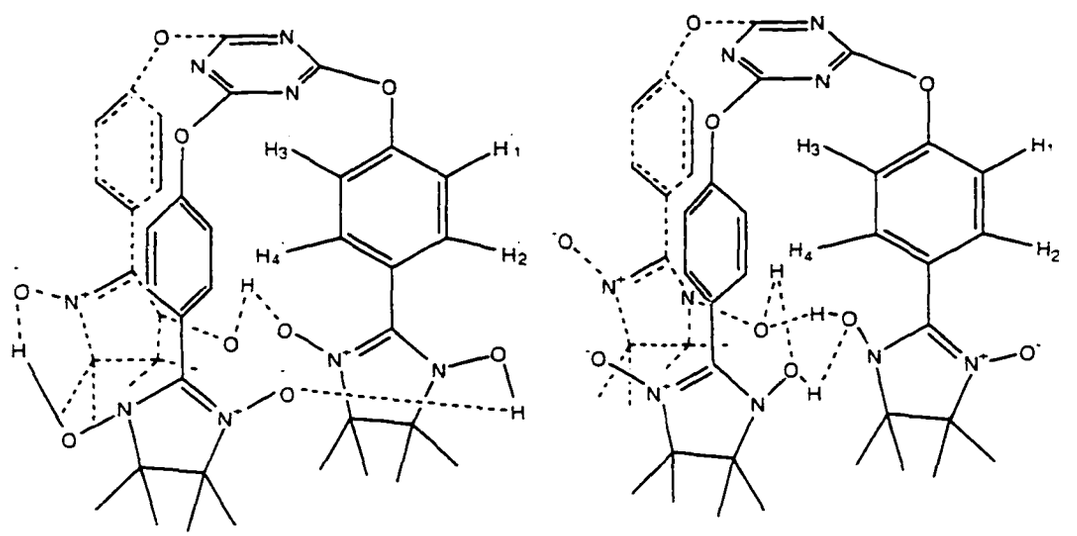

37'

Me'=1.02 (br, 32H)
H_4=5.80 (d, 3H, J=12 Hz)
H_3=6.13 (d, 3H, J=12 Hz)
H_2=6.66 (d, 3H, J=8 Hz)
H_1=6.68 (d, 3H, J=8 Hz)
OH=6.97 (br, 3H)

37

Me=1.09 (br, 32H)
H_1=6.60 (d, 3H, J=8 Hz)
OH=6.97 (br, 3H)
H_3=7.21 (d, 3H, J=8 Hz)
H_2=7.87 (d, 3H, J= 8Hz)
H_4=8.05 (d, 3H, J=8 Hz)

Figure 36b. Proton chemical shifts of the hydrogen bonded conformers **37/37'** in DMSO-d_6 - benzene-d_6.

The ^{13}C nmr spectrum of the reduction product showed two distinct sets of carbons thereby confirming the presence of the two major conformers, **37** and **37'** (Figure 37).

Molecular modeling using MACSPARTAN Plus (Wavefunction Inc., Irvine, CA) showed that each of the hydrogen bonded major conformers has a three-fold axis of symmetry and can achieve a tent-like structure as shown for conformer **37** (Figure 38a). The hydrogen bonds among the N-OH groups in **37** are longer (~3.6 Å, Figure 38b) than the hydrogen bonds in **37'** (~3.0 Å, Figure 38c) formed by the nitrone groups' oxygen (=N^+-O^-) with the N-OH groups, suggesting that the latter conformer is more stable.

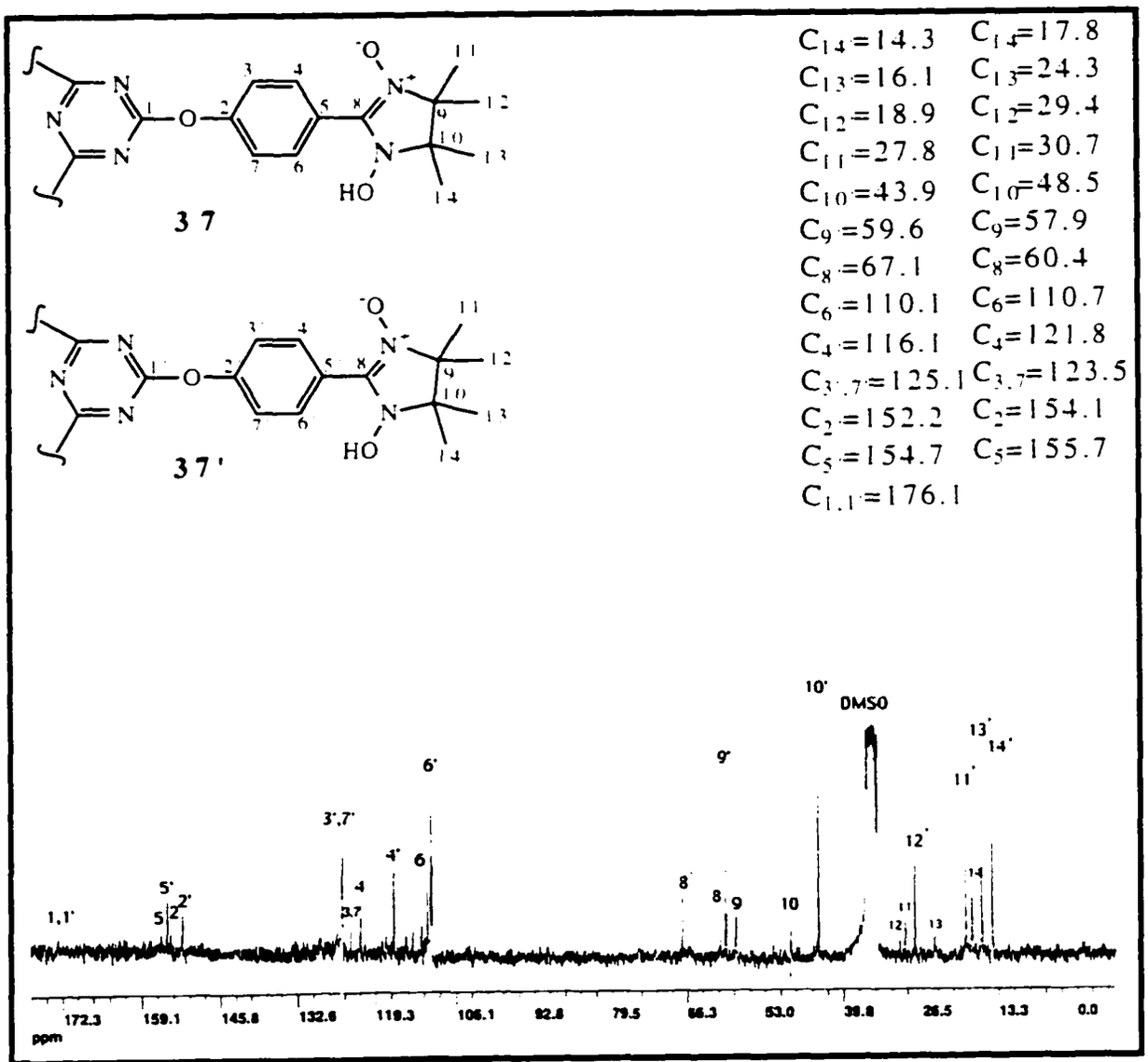

Figure 37. ^{13}C nmr spectrum of the reduction product **37/37'** in DMSO-d_6.

Figure 38a. MACSPARTAN Plus representation of the hydrogen-bonded conformer **37**, side view.

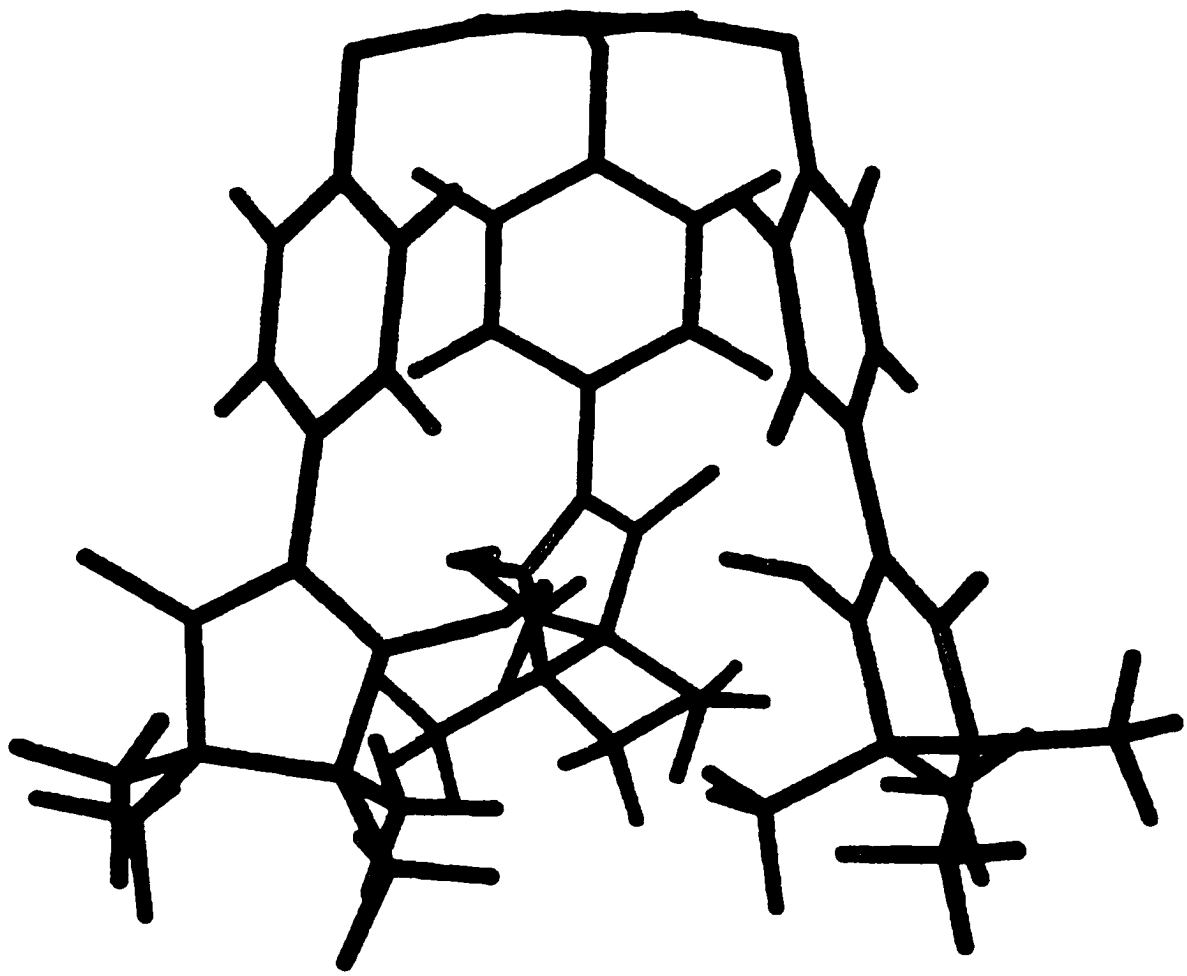

Figure 38b. MACSPARTAN Plus representation of the hydrogen-bonded conformer **37**, top view.

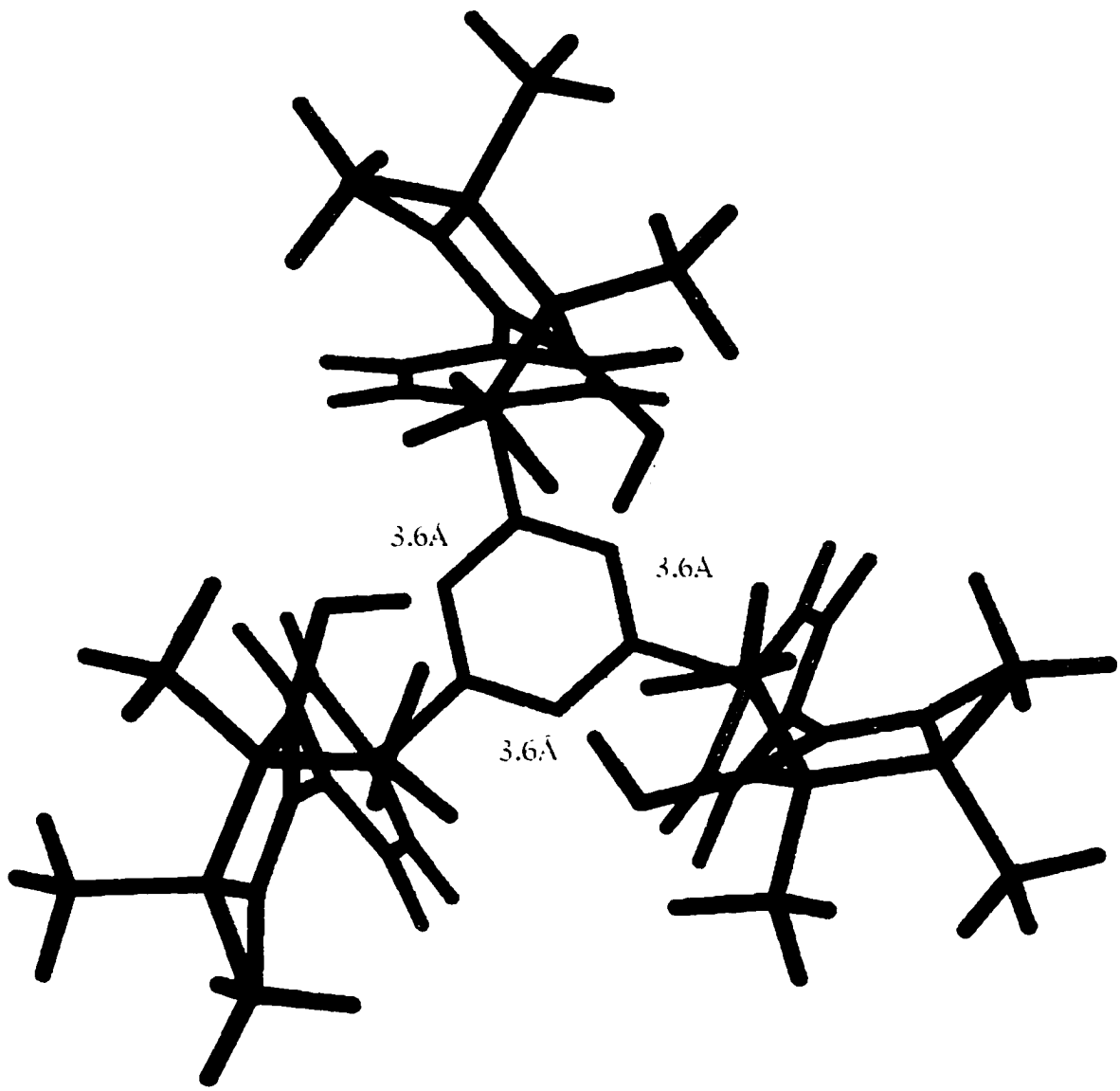

Figure 38c. MACSPARTAN Plus representation of the hydrogen-bonded conformer **37'**, top view.

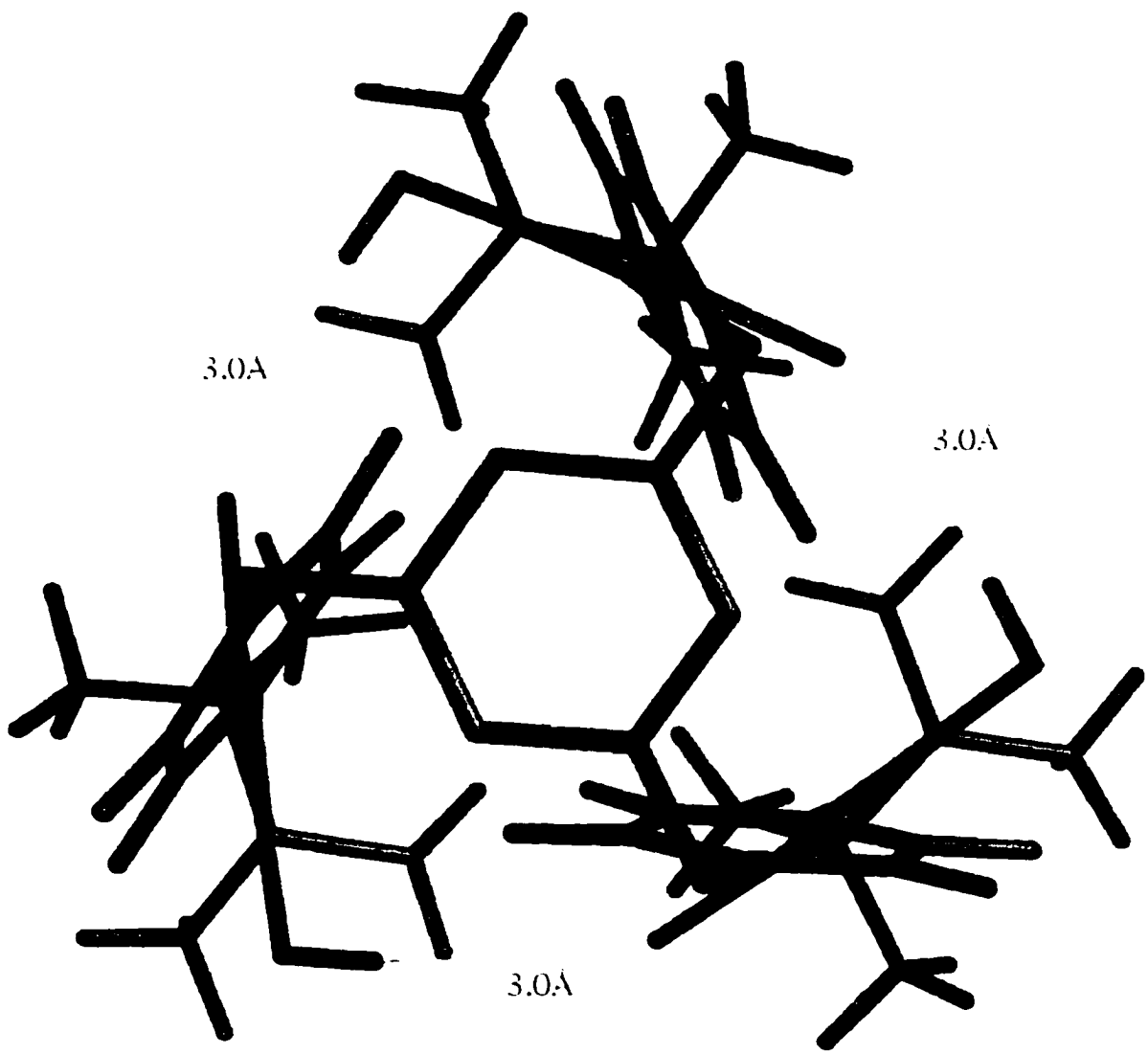

Figure 39 shows that the activity of the triradical **36** against *Pneumocystis carinii* at a concentration of 1 μg/ml is comparable to that of TMP/SMX, the drug in current use, and at 10 or 25 μg/ml **36** is better. These results confirm the hypothesis of drug action as outlined in Scheme 17 (Introduction), and they demonstrate that a minimum of three pharmacophore units/molecule is needed to achieve optimal antifungal activity.

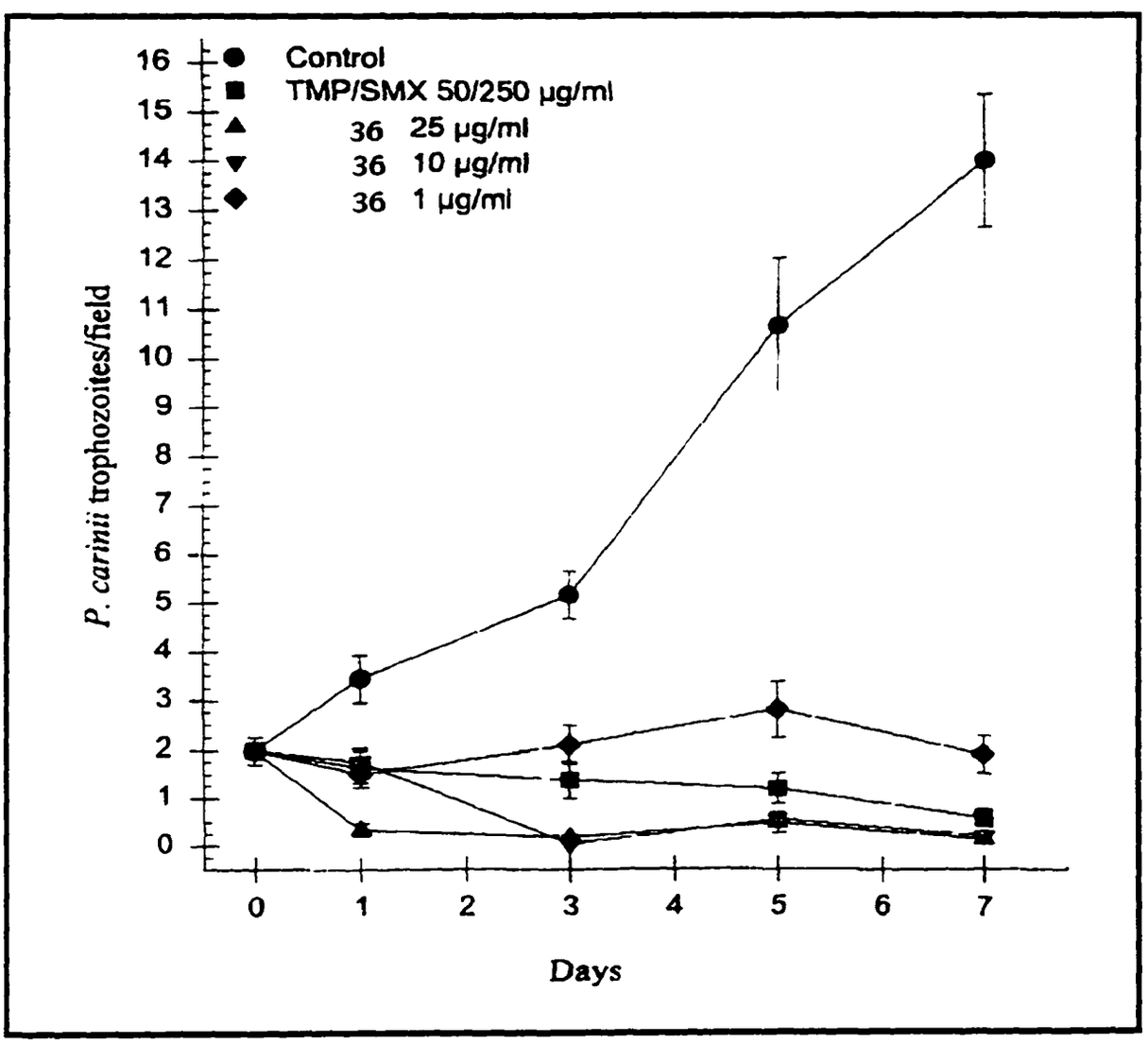

Figure 39. Inhibition of the growth of *P. carinii* by the antifungal tris(nitronyl nitroxide), **36**.

2.4. Conclusion.

Three bisoxaziridines, **24-26**, were synthesized in good yields by *m*-CPBA oxidation of the corresponding bisimines. Substitution of the oxaziridine nitrogen with a quaternary carbon, or with an electron withdrawing group enhanced the oxaziridine's stability. The bisoxaziridines showed only modest activity in the antifungal assays against *Pneumocystis carinii*.

A dendrimer-based trisoxaziridine, **28**, and a macrobicyclic hexaoxaziridine, **30**, were synthesized in good yields in multistep syntheses. Antifungal testing in collaborative studies established that at least three oxaziridine units per molecule are necessary to achieve high levels of antifungal activity.

A Ni(II) macrocyclic amide complex, **33**, with antifungal properties was synthesized, demonstrating the usefulness of the metallomacrocycle pharmacophore.

A dendrimer-based tris(nitronyl nitroxide), triradical **36**, was synthesized efficiently, and its structure was confirmed by the spectral data of its reduction product. Its antifungal activity was equivalent to that of the current drug lending strong support to the oxidoredox pharmacophore hypothesis.

4. EXPERIMENTAL

General techniques

Nuclear magnetic resonance (^{1}H and ^{13}C) spectra were recorded on a Bruker NR300 MHz instrument. Chemical shifts are reported as δ values from tetramethylsilane. Ultraviolet-visible spectra were recorded on a Hewlett-Packard HP8452A fast-scan UV/VIS diode array spectrophotometer. Infrared spectra were measured on a Nicolet Magna 750 FT-IR spectrophotometer as KBr pellets. Electron impact, chemical ionization and fast atom bombardement mass spectra (EI-MS, CI-MS, and FAB-MS) were obtained with a Finnegan Mat SSQ70 instrument. The matrix for FAB mass spectra was *m*-nitrobenzyl alcohol (NBA) or glycerol. Crystals of the macrocyclic bisoxaziridine **30** were visualized using an Olympus PM-10AK microscope.

All air and/or moisture-sensitive reactions were carried out in flame-dried glassware under nitrogen atmosphere, using standard syringe/septum techniques. Anhydrous solvents and air-sensitive reagents used were purchased from Lancaster and Sigma-Aldrich Inc. Reactions were monitored by thin layer chromatography (TLC) on Polygram Sil G UV-254 plates and preparative TLC was carried out on Analtech silica gel GF glass plates. The spots were visualized by UV light at 254 and/or 365 nm. Flash column chromatography[90] (FCC) was carried out on silica gel (Merck, grade 60, 230-400 mesh), and high performance liquid chromatography (HPLC) was performed by using using a Hewlett-Packard 1100 chromatograph equipped with Chem Station and a DAD UV/VIS detector. The analytical column used was: Rainin Microsorb-MV C_{18}, 5μ, 4.6 mm x 25 cm.

Synthesis of the bisoxaziridine (24).

To a stirred solution of 4-fluorobenzaldehyde (5.8 g, 47 mmol) in anhydrous methanol (100 ml), 4,4'-Diamino-dicyclohexylmethane (5 g, 23.5 mmol) dissolved in anhydrous methanol (100 ml) was added slowly at rt, then the mixture was refluxed under an inert atmosphere for 2 h. After cooling to rt, the white precipitate which has formed was filtered off under suction, was washed with methanol twice, and dried under vacuum, to give 10 g of the bisimine precursor of **24** (86% yield).

Mp. 169-172°C.

^{1}H NMR ($CDCl_3$): δ 8.62 (s, 2H, N=CH), 7.69 (dd, 4H, J=9, 2 Hz, ArH), 7.06 (dd, 4H, J=9, 2 Hz, ArH), 1.80-0.88 (m, 22H).

To a solution of the above bisimine (2g, 4.7 mmol) in chloroform (40 ml), cooled in an ice bath , a cold solution of *m*-CPBA (2.23 g, 9.4 mmol) in chloroform (40 ml) was added, and the mixture was stirred at 0-2° for 2 h. The mixture was washed successively with cold, 10% aq $NaHSO_3$ (40 ml), 5% aq K_2CO_3 (40 ml), and then water (2 x 25 ml). The solvent was removed under reduced pressure until product began to precipitate. The solid that had precipitated was filtered, dried in vacuum at rt to give 1.12 g bisoxaziridine **24** as a white powder (52% yield). HPLC analysis on a Rainin Microsorb-MV™ C_{18} column, flow rate 0.5 ml/min, eluting with acetonitrile/ether (95:5) showed that **24** was a mixture of two diastereomers with retention times of 8.11 and 12. 52 min respectively.

Mp. 76°C.

^{1}H NMR ($CDCl_3$): δ 7.37 (dd, 4H, J=9, 2 Hz, ArH), 7.04 (dd, 4H, J=9, 2 Hz, ArH), 4.49 (s, 2H, oxaziridine-H), 2.20-0.88 (m, 22H).

^{13}C NMR ($CDCl_3$): δ 165.3 (aromatic-CF), 115.3 (aromatic-C), 129.2 (aromatic-C) (*ipso*-C), 129.3, 79.0 (Oxaziridine-C), 70.4, 44.27, 31.6, 31.5, 31.3, 31.1, 28.96.

UV-VIS (MeOH): 224, 248 nm.

FAB-MS (NBA):*m/z*=472 $[M+NH_4]^+$, 455 $[M+1]^+$, 439 $[MH-16]^+$, 423 $[MH-(2x16)]^+$.

Synthesis of the bisoxaziridine (25).

A solution of terephthaldicarboxaldehyde (1.34 g, 10 mmol) and 2-amino-2-methyl-1-propanol (2.3 g, 25 mmol) in anhydrous methanol (20 ml) was refluxed for 30 min. After cooling the reaction mixture to rt, the white precipitate was filtered off, and was dried in vacuum at rt for 3 h. The crude product was crystallized from chloroform-acetonitrile (2:1) to give 2.2 g of the bisimine precursor of **25** (79% yield).

^1H NMR (DMSO-d_6): δ 8.33 (s, 2H, N=CH), 7.79 (s, 4H), 3.32 (s, 4H), 2.2 (s, br, 2H), 1.16 (s, 12H).

FTIR (KBr): 3175, 2967, 1636 (C=N), 1567, 1473, 1379, 1304, 1284, 1180, 1064 $cm.^{-1}$

CI-MS (NH_3): *m/z*=277 $[M + 1].^+$

A solution of the above bisimine (2.76 g, 10 mmol) and *m*-CPBA (6.69 g, 28.2 mmol) in chloroform (40 ml) was stirred at rt for 4 h. The reaction mixture was washed successively with 10% aq $NaHSO_3$ (20 ml), 5% aq K_2CO_3 (20 ml), and finally with water (2 x 20 ml). After drying ($MgSO_4$) and filtering, the solvent was removed using a rotary evaporator at rt, to give 2.2 g of bisoxaziridine **25** (70% yield).

^{1}H NMR ($CDCl_3$): δ 7.44 (s, 4H, ArH), 4.78 (s, 2H, oxaziridine-H), 3.61 (dd, 2H, J=11, 4 Hz, CH_2), 3.51 (dd, 2H, J=11, 4 Hz, CH_2), 2.16 (s, br, 2H, OH), 1.15 (s, 6H, Me), 1.04 (s, 6H, Me).

^{13}C NMR ($CDCl_3$): δ 138.1 (aromatic-**C**H), 127.3 (aromatic-**C**), 73.3 (oxaziridine-**C**), 69.5 (**O**CH_2), 61.7 (N-**C**), 20.3 (**C**H_3), 18.4 (**C**H_3).

Synthesis of bis-diphenylphosphinoyloxaziridine (26).

To a stirred mixture of terephthaldicarboxaldehyde (13.4 g, 0.1 mol), NaOAc (89 g, 0.66 mol) and methanol (150 ml), cooled to 0°C, hydroxylamine hydrochloride (15.28 g, 0.22 mol) was added in small portions. The reaction mixture was stirred for an additional hour at 0°C, then at rt for 2 h. Water (150 ml) was added, and the mixture was allowed to stand at rt overnight. The solid was collected by filteration to afford 14.24 g of the bis-oxime (97% yield).

M.p. 76°C.

^{1}H NMR (CD_3OD): δ 4.80 (br, 2H, OH), 7.51 (s, 4H, Ar-H), 8.00 (s, 2H, CH=N).

A 50 ml of three necked, round-bottomed flask was equipped with a magnetic stirrer, thermometer, and a pressure-equalizing dropping funnel attached to a nitrogen inlet. The flask was charged with the above bisoxime (0.6 g, 3.65 mmol), triethylamine (1 ml, 7.3 mmol) and anhydrous CH_2Cl_2 (20 ml), and the mixture was cooled to -45°C. Chlorodiphenylphosphine (1.38 ml, 7.3 mmol) was added dropwise over a period of one hour, then the mixture was allowed to warm to rt, and the solid was filtered. The organic layer was dried (Na_2SO_4), and the solvent stripped. The product was crystallized from benzene/ether (10:1) to give 0.5 g of the bis(N-phosphinoyl imine) (24% yield).

M.p. 120-122°.

^{1}H NMR ($CDCl_3$): δ 7.47 (m, 10H, Ar-H), 7.88 (m, 10H, Ar-H), 8.11 (s, 4H, Ar-H), 9.35 (d, 2H, $^3J_{PH}$=31.5 Hz, CH=N).

To a mixture of bis(N-phosphinoyl imine) (500 mg, 0.94 mmol), chloroform (100 ml) and saturated aq. $NaHCO_3$ (40 ml), *m*-CPBA (5.7 g, 1.88 mmol) in chloroform (20 ml) was added dropwise at 0-2°C, and the mixture was stirred for 2 h. After washing with cold solutions of 10% aq. $NaHSO_3$ and 5% aq. K_2CO_3, the organic layer was separated and stripped to about half of its volume. Ether was then added, and the resulting white precipitate was filtered and dried in vacuum to give 400 mg of the bis(N-phosphinoyloxaziridine) **26** (77% yield).

^{1}H NMR ($CDCl_3$): δ 5.67 (d, 2H, $^3J_{PH}$=8 Hz, oxaziridine-H), 7.40 (m, 10H, Ar-H), 7.80 (m, 10H, Ar-H), 8.12 (s, 4H, Ar-H).

CI-MS (NH_3): *m/z*=584 $[M + NH_4]^+$, 566 $[M]^+$, 550 $(M-16)^+$, 534 $[M-(2x16)]^+$.

Synthesis of the trisimine (27).

To a solution of 2,4,6-tris(*p*-formylphenoxy)-1,3,5-triazine (4.41 g, 0.01 mol) in anhydrous methanol (100 ml), 2-amino-2-methyl-1-propanol (2.89 g, 0.032 mol) was added and the mixture was stirred at rt for 20 h. The white precipitate was filtered, washed with methanol (2 x 20 ml), and dried under vacuum to give 6.57 g of the trisimine **27** (100% yield).

^{1}H NMR (DMSO-d_6): δ 8.29 (s, 3H, N=CH), 7.80 (d, J=8.5 Hz, 6H), 7.30 (d, 6H, J=8.5 Hz,), 5.4 (br, 3H), 4.65 (t, J=1.6 Hz), 1.15 (s, 18 H).

^{13}C NMR (DMSO-d_6): δ 172.8, 155.2, 152.2, 134.7, 128.8, 121.3, 64.4, 60.9, 23.9.

FTIR (KBr): 3399.1, 2967.4, 2929.0, 2869.2, 1643.1, 1606.5, 1573.0, 1504.1, 1467.1, 1371.3, 1299.5, 1208.2, 1061.6, 1016.0, 848.8, 803.2 cm^{-1}.

Synthesis of the trisoxaziridine (28).

To a solution of trisimine **27** (0.3 g, 0.46 mmol) in chloroform (25 ml), *m*-CPBA (0.4 g, 2.3 mmol) was added in one batch and the mixture was stirred at rt for 3 h. The reaction mixture was washed successively with 5% aq sodium thiosulfate solution (5 ml), 10% aq $NaHCO_3$ (5 ml), then with water (2 x 5 ml). The organic layer was dried ($MgSO_4$), filtered, then ether was added (15 ml) until a white precipitate formed. After keeping the suspension at -20°C overnight, the precipitate was filtered to give 0.3 g of trisoxaziridine **28** (91% yield).

^1H NMR (DMSO-d_6): δ 7.47 (d, 6H, J=8 Hz), 7.23 (d, 6H, J=8 Hz), 5.03 (s, 3H), 4.87 (br, 3H.), 3.32 (s, 6H), 1.02 (s, 9H), 1.00 (s, 9H).

^{13}C NMR (DMSO-d_6): δ 172.9, 152.2, 143.8, 133.7, 128.9, 72.1, 66.9, 61.8, 18.5, 14.2.

FTIR (KBr): 3434.9, 2974.1, 1572.9, 1509.2, 1371.2, 1212.8, 1055.6 cm^{-1}.

FAB-MS (NBA): *m/z*=703 $[M+1]^+$, 687 $[M-16]^+$, 671 $[M-(2x16)]^+$, 655 $[M-(3\ x16)]^+$, 616 $[MH-87]^+$, 529 $[MH-(2x87)]^+$, 442 $[MH-(3x87]^+$.

Synthesis of the macrobicyclic imine (29).

A 100 ml, three-necked, round-bottomed flask was equipped with a magnetic stirrer, a condenser, and a pressure equalizing dropping funnel attached to a nitrogen inlet. The flask was charged with tris(2-aminoethyl)amine (0.292 g, 2 mmol) and anhydrous methanol

(50 ml), then terephthaldicarboxaldehyde (0.402 g, 3 mmol) in anhydrous methanol (50 ml) was added in one portion with stirring, and the mixture was refluxed under nitrogen atmosphere for 3 h. The reaction mixture was allowed to stand overnight at rt and the insoluble materials were filtered through a sintered glass funnel of medium porosity. The filtrate was reduced to half of its volume, then water was added (10 ml) slowly with stirring until a white precipitate formed. The precipitate was filtered through a sintered-glass funnel of medium porosity and was washed with water (2 x 5 ml) then dried in vacuum for 12 h, at rt to give 0.61 g of the macrobicyclic imine **29**, as a white powder (92% yield).

Mp:>300°C (dec.)

^{1}H NMR ($CDCl_3$): δ 8.21 (s, 6H, HC=N), 7.20 (s, 12H, ArH), 3.83 (br 12H, CH_2), 2.85 (br, 12H, CH_2)

^{13}C NMR ($CDCl_3$): δ 161.6 (C=N), 137.3 (Ar), 128.5 (Ar), 57.9 (CH_2), 52.6 (CH_2).

FTIR (KBr): 3387.8, 1642.9, 1456.5, 1438.5, 1381.9, 1303.1, 1077.8, 1033.9, 908.4, 832.2 cm^{-1}.

FAB-MS (glycerol): *m/z*=587 [M+1].$^+$

Synthesis of macrobicyclic oxaziridine (30).

A 1000 ml round-bottomed flask was equipped with a magnetic stirrer and a pressure equalizing dropping funnel. The flask was charged with the macrobicyclic imine **29** (2 g, 3.4 mmol) dissolved in $CHCl_3$ (200 ml), saturated aq $NaHCO_3$ (100 ml) and 6 g BTEAC (6 g). The mixture was cooled to 0-2°C, and a solution of *m*-CPBA (8 g, 25 mmol) in $CHCl_3$ (200 ml) was added dropwise with stirring over a

period of10 min. The reaction mixture was stirred for an additional 6 h at 0-2°C, then the layers were separated. The organic layer was washed successively with 10% aq $NaHSO_3$ (100 ml), 5% aq K_2CO3 (100 ml) then water (2 x 100 ml), then ether was added to the organic layer until a white precipitate formed. It was filtered and dried in vacuum for 8 h at rt to give 0.93 g of the macrobicyclic oxaziridine **30,** as a white powder (40% yield).

^1H NMR ($CDCl_3$): δ 6.95 (s, 12H, ArH), 4.67 (s, 6H, oxaziridine-H), 3.04 (dd, 6H, J=12, 9 Hz, CH_2), 2.87 (dd, 6H, J=12, 9 Hz, CH_2), 2.69 (dd, J=12, 2 Hz, CH_2), 2.42 (dd, J=12, 2 Hz, 6H, CH_2).

^{13}C NMR ($CDCl_3$): δ 130.1 (Ar-**C**H), 127.3 (Ar-**C**), 80.1 (oxaziridine-**C**), 60.6 (O-N**C**), 54.0 (N**C**).

FTIR (KBr): 2952.1, 2814.2, 1444.6, 1353.2, 1300.9, 807.3 cm^{-1}.

FAB-MS (NBA): *m/z*=683 $[M+1]^+$.

Synthesis of 4,4'-dienamine-2,2'-bipyridine (Scheme 22).[89]

A 25 ml three-necked, round-bottomed flask was equipped with a thermometer, a magnetic stirrer, and a condenser attached to a nitrogen inlet. The flask was charged with 4,4'-Dimethyl-2,2'-bipyridine (1 g, 5.4 mmol), *tert*-butoxybis(dimethylamino)methane (4.7 ml, 22.7 mmol), and anhydrous DMF (5 ml) and the mixture was heated for 18 h at 140°. After this had been cooled to rt, water was added (50 ml) and the mixture was extracted with CH_2Cl_2 (5 x 15 ml). The organic layers were dried ($MgSO_4$), concentrated, then ether was added to precipitate 1.12 g (89%) of 4,4'-Dienamine-2,2'-bipyridine which was used directly in the next step.

^1H NMR ($CDCl_3$): δ 8.33 (d, 2H, J=5.5 Hz, 6,6'-ArH), 8.10 (d, 2H J=2Hz, 3,3'-ArH), 7.19 (d, 2H, J=14 Hz, CH=), 6.93 (d,d, 2H, J=5.5 Hz, 5,5'-

ArH). 5.07 (d, 2H, J=14 Hz, CH=), 2.86 (s, 12H, Me), 2.86 (s, 12H, NMe_2).

Synthesis of 4,4'-Diformyl-2,2'-bipyridine (Scheme 22).[89]

To a solution of 4,4'-dienamine-2,2-bipyridine (1.43 g, 4.8 mmol) in THF (20 ml), an aqueous solution of $NaIO_4$ (8 g, 37.4 mmol) was added dropwise at rt and the reaction mixture was stirred for 12 h. The insolubles were removed by filtration and washed with THF (50 ml). The solvent was removed under reduced pressure and dichloromethane (60 ml) was added. The organic layer was washed twice with saturated aq $NaHCO_3$ and once with water, dried ($MgSO_4$), and evaporated to dryness to give 0.97 g of 4,4'-Diformyl-2,2'-bipyridine (98 % yield).

^1H NMR ($CDCl_3$): δ 10.18 (s, 2H, CHO), 8.94 (d, J=5 Hz, 2H, 6,6`-ArH), 8.87 (d, J=1.5 Hz, 2H, 3,3`-ArH), 7.76 (dd, J=5 and1.5 Hz, 2H, 5,5`-ArH).

Synthesis of macrobicyclic bipyridine (31).

A 25 ml three-necked, round-bottomed flask was equipped with a magnetic stirrer, a thermometer, and a pressure-equalizing dropping funnel attached to a nitrogen inlet. The flask was charged with a solution of 4,4`-diformyl-2,2`-bipyridine (0.1g, 0.47 mmol) in anhydrous THF (5 ml), then tris(2-aminoethyl)amine (0.07 g, 0.49 mmol) in anhydrous THF (5 ml) was added dropwise, under an inert atmosphere. The reaction mixture was stirred for 12 h at rt. The yellow precipitate was filtered, dissolved in chloroform (10 ml), and the solution was stirred for 18 h at rt. The insolubles were removed

by filtration, the filtrate was concentrated under reduced pressure, and then THF (5 ml) was added until a white precipitate formed. The suspension was kept at -20°C overnight, then it was filtered to give 0.15 g macrobicyclic bipyridine **31** (38% yield), as a white solid.

^{1}H NMR ($CDCl_3$): δ 8.91(d, 6H, J=5 Hz, 6,6'-ArH), 7.94 (dd, 6H, J=1, 5 Hz, 5,5'-ArH), 7.81 (s, 6H, 3,3'-ArH), 6.85 (s, 6H, CH=N), 3.79 (m, 12H, N=CH-CH_2), 2.80 (m, 12H, CH_2-N).

^{13}C NMR ($CDCl_3$): δ 159.8 (C=N), 150.3 (C_2), 156.5 (C_3), 131.5 (C_4), 134.3 (C_5), 121.3 (C_6), 58.3 (C-C=N), 53.3 (C-N).

FAB-MS (NBA): *m/z* =821 $[M+1]^+$.

Synthesis of Macrocyclic amide (32).

2,2'-Methylenebis(4-nitrophenol):

p-Nitrophenol (27.8 g, 0.02 mol) and 5 ml of water were placed into a 500 ml of three-necked flask equipped with a mechanical stirrer and a condenser, and the mixture was heated to 75°C in an oil bath. To this, conc. H_2SO_4 (24 ml) and 37% aq formaldehyde (0.12 mol, 10 ml) were then added. The temperature was kept beween 120°-130°C for 2 h until the product separated into a pale yellowish semi-solid mass and a clear supernatant liquid. The solid was filtered off and dissolved in 100 ml of 4% aq. NaOH. The dark red solution was filtered, and 5M HCl was added to the filtrate until a pale yellow precipitate formed and the color of the solution turned pale yellow (pH=2-3). The precipitate was filtered, washed with 1000 ml of water, and dried at 110°C, to give 28 g of 2,2'-Methylenebis(4-nitrophenol), a pale yellow powder (95% yield).

Mp: 268°C.

^{1}H NMR ($CDCl_3$): δ 11.26 (s, 2H, -OH), 8.03 (d, 2H, J=8 Hz, 5,5'-ArH), 7.94 (s, 2H, 3,3'-ArH), 6.97 (d, 2H, J=8 Hz, 6,6'-ArH), 3.90 (s, 2H, CH_2).

^{13}C NMR ($CDCl_3$): δ 199.3 (C_4), 176.9 (C_1), 164.3 (C_3), 163.3 (C_5), 161.6 (C_2), 152.6 (C_6), 66.8 (CH_2).

FTIR (KBr): 3331.2, 1591.1, 1518.6, 1486.8, 1331.7, 1281.3, 1090.8, 836.5, 821.9, 752.3, 640.9 cm^{-1}.

CI-MS (CH_4): *m/z*=291 $[M+1]^+$.

2,2'-methylenebis(4-nitrophenyl decylether):

A 500 ml three-necked, round-bottomed flask was equipped with a magnetic stirrer, condenser and a nitrogen inlet. The flask was charged with of 2,2'-methylene bis(4-nitrophenol) (5.8 g, 20 mmol), 1-bromodecane (8.86 g, 40 mmol), anhydrous K_2CO_3 (11.04 g, 80 mmol) and anhydrous DMF (150 ml). The mixture was stirred at 65°C for 48 h. After cooling to rt, the mixture was filtered through a sintered-glass funnel. The residue was washed with 200 ml of ethanol. The combined filtrates were concentrated under reduced pressure. The bright yellow solid was isolated by trituration in 20 ml of ethanol. The solid was dried in vacuum at rt for 16 h to give 9.60 g of 2,2'-methylenebis(4-nitrophenyl decylether) as a yellow powder (84% yield).

^{1}H NMR ($CDCl_3$): δ 8.08 (d, 2H, J=3Hz, 3,3'-ArH), 8.05 (dd, 2H, J=10, 3 Hz, 5,5'-ArH), 6.82 (d, 2H, J=10 Hz, 6,6'-ArH). 4.00 (t, 4H, J=6 Hz, -CH_2-O) , 3.95 (s, 2H, Ar-CH_2-Ar), 1.84 (q, 2H, J=7 Hz, 9'-CH_2), 1.15-1.61 (m, 14H, 2'-8'-CH_2), 0.86 (t, 3H, J=7 Hz, 10'-CH_3).

2,2'-methylenebis(4-aminophenyl decylether):

To a stirred solution of 2,2'-methylene bis(4-nitrophenyldecylether) (4 g, 7 mmol) in a mixture of THF (100 ml), ethanol (200 ml) and

water (50 ml), NH_4Cl (2 g, 40 mmol) and activated Zn dust (5 g) were added and the mixture was kept at 50°C for 30 min. After an additional hour of stirring at rt, the mixture was filtered on a celite pad and the residue was washed with ethanol (100 ml). The solvents were removed at reduced pressure and the dark brown solid was dried in vacuum for 16 h at rt to give 4.46 g of 2,2'-methylene bis(4-aminophenyl decylether) (98% yield).

^1H NMR (DMSO-d_6): δ 6.62 (d, 2H, J=8 Hz, 6,6'-ArH), 6.32 (dd, 2H J=8, 2 Hz, 5,5'-ArH), 6.18 (s, 2H, 3,3'-ArH), 4.44 (s, 2H, Ar-CH_2-Ar), 3.75 (t, 2H, J=6 Hz, 1'-CH_2), 1.59 (q, 2H, J=7 Hz, 9'-CH_2), 0.9-1.6 (m, 14H, 2'-8'-CH_2), 0.83 (t, 3H, J=7 Hz, 10'-CH_3).

Macrocyclic amide (**3 2**):

A 1000 ml three-necked, round-bottomed flask was equipped a magnetic stirrer, a condenser, a pressure-equalizing dropping funnel attached to a nitrogen inlet. The flask was charged with of 2,2'-methylenebis(4-aminophenyl decylether) (4 g, 2.6 mmol), anhydrous CH_2Cl_2 (500 ml) and dry triethylamine (2 ml). To this, a solution of 2,6-pyridinedicarbonylchloride (1.26 g, 6.2 mmol) in 50 ml of anhydrous CH_2Cl_2 was added dropwise, at rt, and the mixture was stirred for 16 h at rt. Methanol (600 ml) was then added, and the CH_2Cl_2 was removed under reduced pressure at rt until the dark brown product began to precipitate. The product was dried in vacuum at rt for 16 h to give 1.8 g the macrocyclic amide **32** (44% yield).

^1H NMR ($CDCl_3$): δ 8.05 (t, 2H, J=9 Hz, H_a), 8.38(d, 2H, J=9 Hz, H_b), 9.22 (s, 4H, H_c), 7.64 (d, 4H, J=9 Hz, H_d), 6.93(d, 4H, J=9 Hz, H_e), 7.02 (s, 4H, H_f), 3.35-3.39 (br, 4H, H_g, $H_{l'}$), 1.8-0.84 (m, 2'-9'CH_2&10'CH_3).

FTIR (KBr): 3389.4, 1590.6, 1397.2 $cm.^{-1}$

CI-MS (NH_3): m/z=1282 $[M]^+$.

Synthesis of the Ni(II) complex of macrocyclic amide (33).

A 500 ml three-necked, round-bottomed flask was equipped with a magnetic stirrer, a condenser and a pressure-equalizing dropping funnel attached to a nitrogen inlet. The flask was charged with the macrocyclic amide **32** (3 g, 2.34 mmol) dissolved in anhydrous THF (200 ml), and a 1M solution of $Li(Me_3Si)_2N$ in THF (10ml) was added. The mixture was stirred for 15 min at rt, then $(Ph_3P)_2NiBr$ (1.8 g, 2.4 mmol) was added and the mixture was stirred for an additional 20 min at rt. Removal of the solvent under reduced pressure at rt gave a dark brown powder of the Ni(II) complex of macrocyclic amide. It was washed once with CH_2Cl_2 (50 ml) and twice with water. The brown powder was dried in vacuum for 16 h at rt to give 3.86 g of **33** (98% yield).

UV (MeOH): 366 nm

Far-FTIR (polyethylene film): 540 cm^{-1} (Ni-N stretching).

CI-MS (NH_3): m/z=1338 $[M + Ni]^+$.

Synthesis of 2,4,6-tris(*p*-formylphenoxy)-1,3,5-triazine (34).

Cyanuric chloride (1.2 g, 6.5 mmol) and *p*-hydroxybenzaldehyde (3.2 g, 26.2 mmol) were added to a stirred suspension of Na_2CO_3 (10 g) in benzene (100 ml), and the mixture was refluxed for 20 h. After cooling, the solid was removed by filtration and was washed twice with hot ethyl acetate. The filtrate was extracted with 10% aq Na_2CO_3 twice and with water once. The combined organic layers

were dried (Na_2SO_4) and concentrated to give a white precipitate that was collected by filtration to afford 2.1 g of **34**, as a white powder (78% yield).

FTIR (KBr): 2833, 1702, 1567, 1361, 1211, 842, cm^{-1}.

^1H NMR ($CDCl_3$): δ 10.0 (s, 3H), 7.92 (d, 6H, J=8.5 Hz), 7.32 (d, 6H, J=8.5 Hz).

^{13}C NMR ($CDCl_3$): δ 122.2, 131.3, 134.5, 155.7, 173.2 (N=**C**), 190.6 (**C**=O).

FAB-MS (NBA): *m/z*=442 $[M + 1]^+$.

Synthesis of tris(nitronyl nitroxide) (36).

A mixture of 2,4,6-Tris(*p*-formylphenoxy)-1,3,5-triazine (0.32 g, 0.72 mmol) and N,N'-Dihydroxy-2,3-diamino-2,3-dimethylbutane (0.32 g, 2.2 mmol) in anhydrous acetonitrile (50 ml) was stirred for 4 h at rt. The white precipitate was filtered, washed with acetonitrile (20 ml), and dried in vacuum to yield 0.28 g of **35** (45% yield). A solution of this crude tris(di-N-hydroxy) compound **35** (0.16 g, 0.19 mmol) in a mixture of chloroform (15 ml) and methanol (5 ml) was then stirred with PbO_2 (1.5 g, 11.6 mmol) at rt for 5 h. The mixture was filtered through a celite pad and the filtrate was concentrated. The tris(nitronyl nitroxide) was purified by FCC, eluting with ethyl acetate/methanol (5:1) to give 0.2 g of **36** (33% yield), as deep blue crystals.

M.p 350° (dec.)

λ_{max} (MeOH): 214, 252, 362 (nitrone), 598 (nitronyl nitroxide) nm.

FTIR (KBr): 3188, 2982, 1593 (triazine ring), 1481, 1366 (N-O· stretching), 1218, 1171 cm^{-1}.

FAB-MS (glycerol): *m/z*=590 [M-232]$^+$, 358 [M-(2 x 232)]$^+$, 343 [M-(2 x 232)-15],$^+$ 574, 558, 543, 528, 512, 464, 448, 432, 416.

Hydrazine reduction[91] of tris(nitronyl nitroxide) (36) to the hydroxylamine (37).

To a solution of the tris(nitronyl nitroxide) **36** in anhydrous methanol (15 ml), methylhydrazine (38 mg, 0.83 mmol) was added and the mixture was stirred at rt until the deep blue color of the radical **36** changed to yellow-brown (ca.15 min.). Evaporation of the solvent under reduced pressure at 50°C gave a yellow-brown oil that was purified by FCC eluting with methanol/ether (10:3) to give 160 mg of the hydroxylamine **37** (95% yield). HPLC analysis on a Microsorb MV C18 column, eluting with methanol showed the sample to be a mixture of conformational isomers, **37** and **37'**, in addition to minor, unidentified products.

m.p. 136°C.

λ_{max} (MeOH): 216, 268, 346(sh), 368, 371 (sh) nm.

Samples for ^{1}H nmr measurements were prepared by dissolving 2.5 mg of compound **37** in 0.4 ml of DMSO and adding 2 drops (ca. 0.06 ml) of benzene-d_6) to it.

^{1}H NMR (DMSO-d_6-benzene-d_6):

37: δ 1.09 (br, 36H, Me), 6.60 (d, 3H, J=8 Hz, 1-H), 6.97 (br, 3H, OH), 7.21 (d, 3H, J=8 Hz, 3-H), 7.26 (s, benzene-H), 7.87 (d, 3H, J=8 Hz, 2-H), 8.05 (d, 3H, J=8 Hz, 4-H).

37': δ 1.02 (br, 36H, Me'), 5.80 (d, 3H, J=12 Hz, 4'-H), 6.13 (d, 3H, J=12 Hz, 3'-H), 6.66 (d, 3H, J=8 Hz, 2'-H), 6.68 (d, 3H, J=8 Hz, 1'-H), 6.97 (br, 3H, OH), 7.26 (s, benzene-H).

^{13}C NMR (DMSO-d_6):

37: δ 17.8 (C_{14}), 24.3 (C_{13}), 29.4 (C_{12}), 30.7 (C_{11}), 48.5 (C_{10}), 57.9 (C_9), 60.4 (C_8), 110.7 (C_6), 121.8 (C_4), 123.5 ($C_{3,7}$), 154.1 (C_2), 155.7 (C_5).
37': δ 14.3 ($C_{14'}$), 16.1 ($C_{13'}$), 18.9 ($C_{12'}$), 27.8 ($C_{11'}$), 43.9 ($C_{10'}$), 59.6 ($C_{9'}$), 67.1 ($C_{8'}$), 110.1 ($C_{6'}$), 116.1 ($C_{4'}$), 125.1 ($C_{3',7'}$), 152.2 ($C_{2'}$), 154.7 ($C_{5'}$).

FAB-MS (NBS): m/z=592 $[M-232]^+$, 481, 469, 453, 420, 404, 393, 374.

4. REFERENCES

1. N.M. Ampel, *Emerging Infectious Diseases*, **1996**, 2, 109.

2. V. Balogh-Nair, Oxidoredox Suppression of Fungal Infections by Novel Pharmacophores, In "*Advances in Bioorganic Chemistry*, "J.K. Snyder and R. Cooper, Eds., Marcel Dekker, 1998, in press.

3. C. J. Pedersen, *J. Am. Chem. Soc.*, **1967**, 89, 2495.

4. C. J. Pedersen, *Angew. Chem. Int. Ed. Engl.*, **1988**, 27, 1021.

5. D. J. Cram, *Angew. Chem. Int. Ed. Engl.*, **1988**, 27, 1009.

6. J. M. Lehn, *Angew. Chem. Int. Ed. Engl.*, **1988**, **27**, 90.

7. E. DeClercq, N. Yamamoto, R. Pauwels, M. Baba, D. Schols, H. Nakashima, J. Balzarini, Z. Debyser, B.A. Murrer, D. Schwartz, D. Thornton, G. Bridger, S. Fricker, G. Henson, M. Abrams and D. Picker, *Proc. Natl. Acad. Sci. USA*, **1992**, 89, 5286.

8. V. Balogh-Nair, C. E. Brathwaite, C. X. Chen and J. Vargas, *Cell. & Mol. Biol.* **1995**, **41**, S9-14.

9. V. Balogh-Nair, R.W. Finberg *et al.*, unpublished results.

10. C. E. Brathwaite, C. X. Chen and V. Balogh-Nair, *Indian. J. Chem.*, **1992**, 810.

11. E. Buhleier, W. Wehner and F. Vogtle, *Synthesis*, **1978**, 155.

12. G.R. Newcome, C.N. Moorefield and F. Vogtle, *Dendritic Molecules: Concepts, Synthesis and Perspectives*, VCH, Weinheim, Germany, 1996.

13. C. M. Cardona and A.E. Kaifer, *J. Am. Chem. Soc.*, **1998**, 120, 4023.

14. D. Zanini and R. Roy, *J. Org. Chem.*, **1998**, 63, 3486.

15. M. Zhao, L. Sun and R.M. Crooks, *J. Am. Chem. Soc.*, **1998**, 120, 4877.4877.

16. R.M. Crooks and A.J. Ricco, *Acc. Chem. Res.*, **1998**, 31, 219.

17. T. M. Bell and F. Guzzo, *J. Chem. Soc. Chem. Commun.*, **1978**, 760.

18. M. G. B. Drew, J. de O. Cabral, M. F. Cabral, F.S. Esho and S. M. Nelson, *J. Chem. Soc. Chem. Commun.*,**1979**, 1033.

19. D. MacDowell and J. Nelson, *Tetrahedron Lett.*,**1988**, 29, 385.

20. V. McKee, M. R. J. Dorrity, J. F. Malone, D. Marrs and J. Nelson, *J. Am. Soc. Chem. Commun.*, **1992**, 383.

21. J.-M. Lehn, *Pure & Appl. Chem.*, **1980**, 52, 2441.

22. D. Chen, A. E. Martell, *Tetrahedron*, 1991, **47**, 6895.

23. O. Kocian, R. J. Mortimer and P. D. Beer, *Tetrahedron. Lett.*, **1990**, 31, 5069.

24. J. de Mendoza, E. Mesa, J.-C. Rodriguez-Ubis, P. Vazquez, F. Vogtle, P.-M. Windscheif, K. Rissanen, J.-M Lehn, D. Lilienbaum and R. Ziessel, *Angew. Chem. Int. Ed. Engl.*, **1991**, 30.1331.

25. D.W. Margerum, *Pure Appl. Chem.*, **1983**, 55, 23.

26. T.J. Collins, *Acc. Chem. Res.*, **1994**, 27, 279.

27. C. A. Hunter, *J. Chem. Soc., Chem. Commun.*, **1991**, 749.

28. C. A. Hunter, *J. Am. Chem. Soc.*, **1992**,114, 5303.

29. T. J. Collins, R. D. Powell, C. Slebodnick and E. S. Uffelman, *J. Am. Chem. Soc.*, **1991**, 113, 8419.

30. T. J. Collins, T. R. Nichols, E. S. Uffelman, *J. Am. Chem. Soc.*, **1991**, 113, 4708.

31. K. L. Kostka, B. G. Fox, M. P. Hendrich, T. J. Collins, C. E. F. Rickard, L. J. Wright and E. Munck, *J. Am. Chem. Soc.*, **1993**, 115, 6746.

32. A. M. Pyle, J. K. Barton, In "*Progress in Inorganic Chemistry: Bioinorganic chemistry*", S.J. Lippard, Ed. JohnWiley, New York,

1990, Vol. 38, pp. 413-417.

33. X. Chen, S. E. Rokita, C. J. Burrows, *J. Am. Chem. Soc.*, **1991**, 113, 5884.

34. J. G. Muller, X. Chen, A. C. Dadiz, S. E. Rokita, C. J. Burrows, *J. Am. Chem. Soc.*, **1992**,114, 6407.

35. N. Jubran, D. Meyerstein, J. Koresh and H. Cohen, *J. Chem. Soc. Dalton Trans.*, **1986**, 2509.

36. A. Buttatava, L. Fabbrizzi, A. Perotti, A. Poggi, G. Poli and B. Seghi, *Inorg. Chem.*, **1986**, 25, 1456.

37. E. Kimura, R. Machida and M. Kodama, *J. Am. Chem. Soc.*, **1984**, 106, 5497.

38. C. C. Cheng, S. E. Rokita and C. J. Burrows, *Angew. Chem. Int. Ed. Engl.*, **1993**, 32, 277.

39. H. E. Fonouni, S. Krishnan, D. G. Kuhn and G. A. Hamilton, *J. Am. Chem. Soc.*, **1983**, 105, 7672.

40. J. D. Koola and J. K. Kochi, *Inorg. Chem.*, **1987**, 26, 908.

41. H. Yoon, T.R. Wagler, K.J. O'Connor and C. J. Burrows, *J. Am. Chem. Soc.*, **1990**, 112, 4568.

42. J. F. Kinneary, T. R. Wagler and C. J. Burrows, *Tetrahedron Lett.*, **1988**, 29, 877.

43. T. R. Wagler and C. J. Burrows, *Tetrahedron Lett.*, **1988**, 29, 5091.

44. H. Krim, *British Patent* 743940; **1953**; *Chem. Abstr.*, **1957**, v265.

45. (a) W. D. Emmons, *J. Am. Chem. Soc.*, 1956, **78**, 6208.
(b) W. D. Emmons, *J. Am. Chem. Soc.*, 1957, **79**, 5739.

46. L. Horner and E. Jurgens, *Chem. Ber.*, 1957, **90**, 2184.

47. E. Schmitz, *Adv. Heterocycl. Chem.*, 1979, **24**, 63.

48. E. Schmitz in *Comprehensive Heterocyclic Chemistry*, Vol. 7, Part 5, W. Lwowski, Ed., Pergamon Press, Oxford, 1984, p. 195.

49. F.A. Davis and A.C. Shepard, *Tetrahedron*, **1989**, 45, 5703.

50. M. Newcomb and R.A. Reeder, *J. Org. Chem.*, **1980**, 45, 1489.

51. F. A. Davis, J. Lamendola, Jr., U. Nadir, E. W. Kluger, T. C. Sedergran, T. W. Panunto, R. Billmers, R. Jenkins, Jr., I. J. Turchi, W. H. Waston, J. S. Chen and M. Kimura, *J. Am. Chem. Soc.*, **1980**, 102, 2000; F.A. Davis, L.C. Vishwakarma, J.M. Billmers and J. Finn, *J. Org. Chem.*, **1984**, 49, 3241.

52. F.A. Davis, S.G. Lal and H. D Durst, *J. Org. Chem.*, **1988**, 53, 5004.

53. F.A. Davis and B.-C. Chen, *Chem. Rev.*, **1992**, 92, 919.

54. L. Bohe, G. Hanquet, M. Lusinchi and X. Lusinchi, *Tetrahedron Lett.*, **1993**, 34, 7271; P.C.B. Page, G.A., Rassias, D. Bethell and M.B. Schilling, *J. Org. Chem.*, **1998**, 63, 2774.

55. W. Rundel in "*Methoden der organishen Chemie*", J. Houben, Th. Weyl and E. Muller, Eds., Vol. X, Part 4, Thieme, Stuttgart, 1968, p.449.

56. G.A. Tolstikov, U.M. Jemilev, V.P. Jurjev, F.B. Gershanov and S.R. Ravikov, *Tetrahedron Lett.*, **1971**, 2807.

57. L. Martiny and K.A. Jorgensen, *J. Chem. Soc. Perkin I*, **1995**, 699.

58. V. Madan and L.B. Clapp, *J. Am. Chem. Soc.*, **1969**, 91, 6078

59. M. Buciarelli, A. Forni, I. Moretti and G. Torre, *J. Chem. Soc. Perkin II*, **1977**, 1339.

60. D. R. Boyd and R. Spratt, *J. Chem. Soc.* (C), **1969**, 2650.

61. F.A. Davis and R.H. Jenkins, Jr., In "Asymmetric Synthesis," J.D. Morrison and J.W. Scott, Eds., Academic Press, 1984, p. 322.

62. H.W. Orf and D. Dolphin, *Proc. Natl. Acad. Sci. USA*, **1974**, 71, 2646.

63. W.H. Rastetter, T.R. Gadek, J.P. Tane and J.W. Frost, *J. Am. Chem. Soc.*, **1979**, 101, 2228.

64. T.C. Bruice, In "*Mechanistic Principles of Enzyme Activity*," J.F. Liebman and A. Greenberg, Eds., VCH Publishers, New York, 1988, Chapter 8, p. 315.

65. C.X. Chen, Ph.D. Dissertation, 1995.

66. N. Kocherginsky and H.M. Schwartz, *Nitroxide Spin Labels. Reactions in Biology and Chemistry*, CRC Press, 1995.

67. G. Sosnovsky, N.U.M. Rao, S.W Li and H.M. Schwartz, *J. Org. Chem.*, **1989**, 54, 3667.

68. M. Kinoshita, P. Turek, M. Tamura, K. Nozawa, D. Shiomi, Y. Nakazawa, M. Ishikawa, M. Takahashi, K. Awaga, T. Inabe and Y. Maruyama, *Chem. Lett.*, **1991**, 1225.

69. J. H. Osiecki and E. F. Ullman, *J. Am. Chem. Soc.*, **1968**, 90, 1078; D. G. B. Boocock, R. Darcy and E. F. Ullman, *J. Am. Chem. Soc.*, **1968**, 90, 5945 and 6873; E. F. Ullman and D. G. B. Boocock, *J. Chem. Soc. Chem. Commun.*, **1969**, 1161; E. F. Ullman, L. Call and J. H. Osiecki, *J. Org. Chem.*, **1970**, 35, 3623; E. F. Ullman, J. H. Osiecki, D. G. B. Boocock and R. Darcy, *J. Am. Chem. Soc.*, **1972**, 94, 7049.

70. L. Dulog and J. S. Kim, *Angew. Chem. Int. Ed. Engl.*, **1990**, 29, 415; A. Izuoka, M. Fukada, T. Sugawara, M. Sakai and S. Bandow, *Chem. Lett.*, **1992**, 1627; A. Izuoka, M. Fukada, R. Kumai, M. Itakura, S. Hikami and T. Sugawara, *J. Am. Chem. Soc.*, **1994**, 116, 2609.

71. V. Balogh-Nair and C.-X Chen, Submitted for publication in *J. Am. Chem. Soc.*, 1998.

72. J.S. Nadeau and D.G.B. Boocock, *Anal. Chem.*, **1977**, 49, 1672.

73. J. Mlochowski, E. Kubicz, K. Kloc, M. Mordarski, W. Peczynska and L. Syper, *Liebigs. Ann. Chem.*, **1988**, 455.

74. D.R. Boyd, P.B. Coulter, R. Hamilton, N.T. Thompson, N.D. Sharma and M.E. Stubbs, *J. Chem. Soc. Perkin Trans. I*, **1985**, 2123.

75. W.B. Jennings, D.R. Boyd, C.G. Watson, E.D. Becker, R.B. Bradley and D.M. Jerina, *J. Am. Chem. Soc.*, **1972**, 94, 8501.

76. G.J. Jordan and D.R. Crist, *Org. Magn. Reson*, **1977**, 9,372.

77. G.G. Spence, E.C. Taylor and O. Buchardt, *Chem. Rev.*, **1970**, 70, 231.

78. D. R. Boyd, W. B. Jennings, R. M. McGuckin, M. Rutherford, and B. M. Saket. *J. Chem. Soc., Chem. Commun.*, **1985**, 582.

79. D. R. Boyd, J.F. Malone, R.M. McGuckin, W. B. Jennings, M. Rutherford and B. M. Saket, *J. Chem. Soc. Perkin II*, **1988**, 1145.

80. W.B. Jennings and S.P. Watson and D.R. Boyd, *Tetrahedron Lett.*,**1989**, 30, 235.

81. C. Brown, R.F. Hudson, A. Maron and K.A.F. Record, *J. Chem. Soc. Chem. Commun.*, **1976**, 663.

82. B. Krzyzanowska and W.J. Stec, *Synthesis*, **1978**, 521; **1982**, 270.

83. Burger's Medicinal Chemistry and Drug Discovery, Vol. 1: Principles and Practice, M.E. Wolff, Ed., 5th Edition, John Wiley, 1995.

84. D.C. Tahmasebbi and T. Sasaki, *J. Org. Chem.*, **1994**, 59, 679.

85. W.C. Still, Columbia University, Macromodel, Version 1996.

86. W.H. Pirkle and P.L. Rinaldi, *J. Org. Chem.*, **1977**, 42, 3217.

87. W.H. Pirkle and P.L. Rinaldi, *J. Org. Chem.*, **1978**, 43, 4475.

88. (a) O. Kocian, R.J. Mortimer and P.D. Beer, *Tetrahedron Lett.*, **1990**, 31, 5069;

(b) P.D. Beer, O. Kocian, R.J. Mortimer and P. Spencer, *J. Chem. Soc. Chem. Commun.*, **1992**, 602.

89. P. Dupau, T. Renouard and H.Le Bozec, *Tetrahedron Lett.*, **1996**, 37, 7503.

90. W.C. Still, M. Kahn and A. Mitra, *J. Org. Chem.*, **1978**, 43, 2923.

91. T.D. Lee and J.F.W. Keana, *J. Org. Chem.*, **1975**, 40, 3145.

IMAGE EVALUATION
TEST TARGET (QA-3)

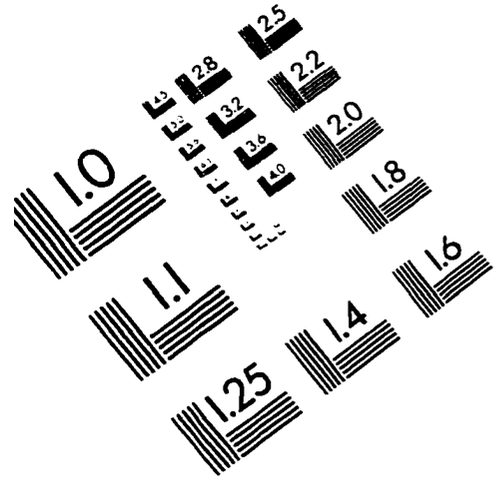

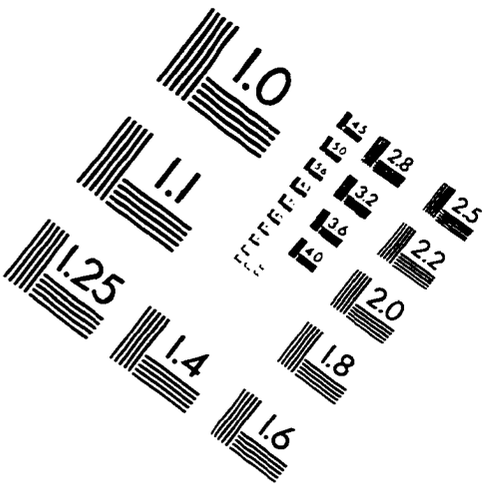

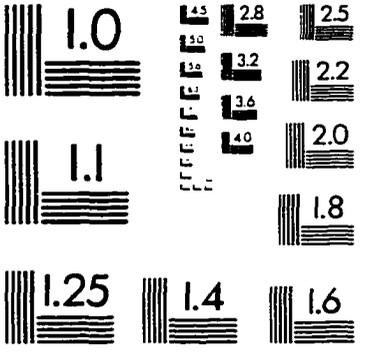

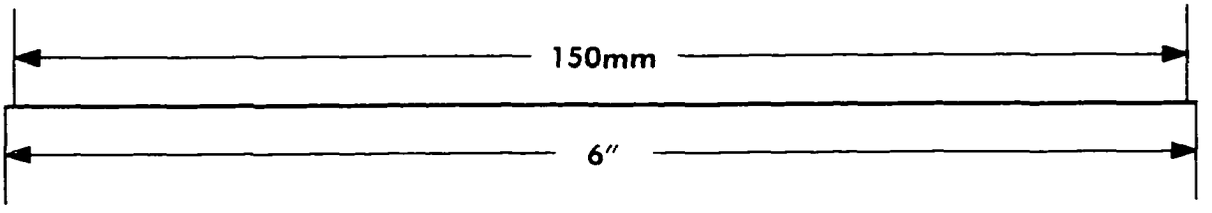

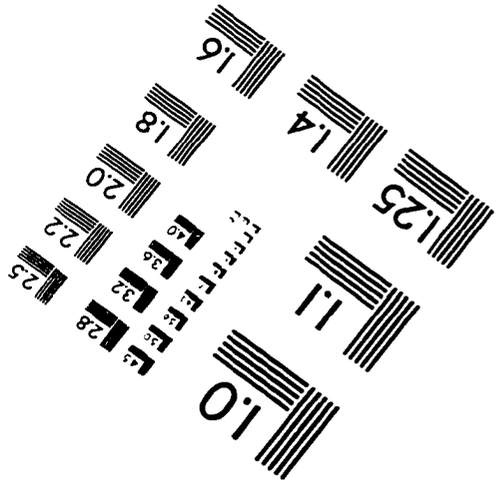

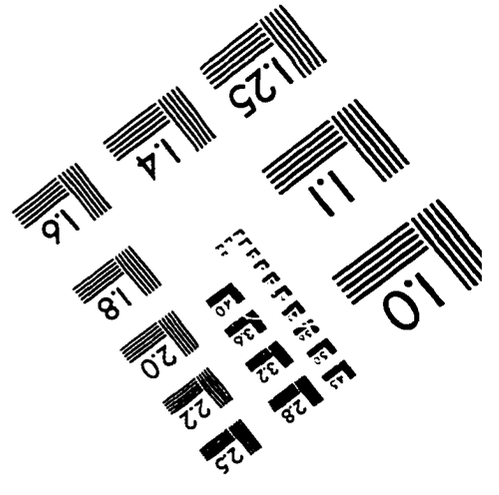

APPLIED IMAGE, Inc
1653 East Main Street
Rochester, NY 14609 USA
Phone: 716/482-0300
Fax: 716/288-5989